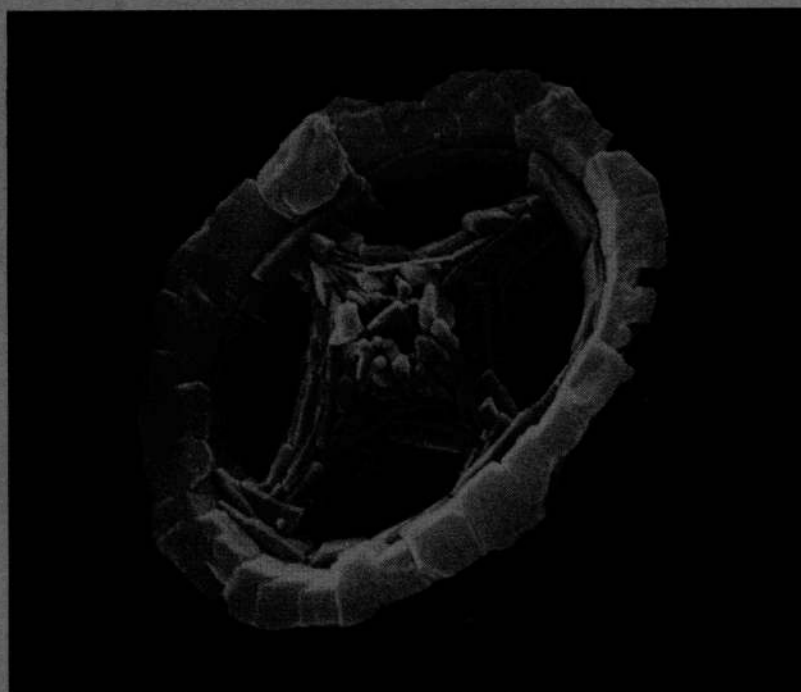


SPECIAL PAPERS IN PALAEOLOGY · 38

**Taxonomy, evolution,
and biostratigraphy of
late Triassic–early
Jurassic calcareous
nannofossils**



THE PALAEOONTOLOGICAL ASSOCIATION

PRICE £30

SPECIAL PAPERS IN PALAEOLOGY NO. 38

TAXONOMY, EVOLUTION, AND
BIOSTRATIGRAPHY OF LATE
TRIASSIC-EARLY JURASSIC
CALCAREOUS NANNOFOSSILS

BY

PAUL RICHARD BOWN

with 15 plates and 19 text-figures

THE PALAEOLOGICAL ASSOCIATION
LONDON

NOVEMBER 1987

© The Palaeontological Association, 1987

TAXONOMY, EVOLUTION AND
BIOSTRATIGRAPHY OF LATE
TRIASSIC-EARLY JURASSIC
CALCAREOUS NANNOFOSSILS

BY RICHARD BORN

WITH 12 PLATES AND 10 FIGURES

THE PALAEOZOOLOGICAL ASSOCIATION
LONDON

Printed in Great Britain

CONTENTS

	<i>page</i>
ABSTRACT	5
INTRODUCTION	5
MATERIAL AND TECHNIQUES	7
COCCOLITH MORPHOLOGY AND DESCRIPTIVE TERMINOLOGY	7
TAXONOMY	11
SYSTEMATIC PALAEOLOGY	12
Family ZYGODISCACEAE Hay and Mohler, 1967	12
<i>Archaeozygodiscus</i> Bown, 1985	13
<i>Crepidolithus</i> Noël, 1965	13
<i>Tubirhabdus</i> Rood, Hay and Barnard, 1973	18
<i>Zeugrhabdotus</i> Reinhardt, 1965	20
Family PARHABDOLITHACEAE BOWN, 1987	21
<i>Crucirhabdus</i> Rood, Hay and Barnard, 1973	22
<i>Diductius</i> Goy, 1979	24
<i>Mitrolithus</i> Deflandre, 1954	26
<i>Parhabdolithus</i> Deflandre, 1952	30
<i>Timorella</i> gen. nov.	34
<i>Bucanthus</i> gen. nov.	35
Family STEPHANOLITHACEAE Black, 1968	36
<i>Stradnerlithus</i> Black, 1971	36
Family MAZAGANELLACEAE fam. nov.	37
<i>Mazaganella</i> gen. nov.	38
<i>Triscutum</i> Dockerill, 1987	39
Family BISCUTACEAE Black, 1971	40
<i>Biscutum</i> Black in Black and Barnes 1959	41
<i>Discorhabdus</i> Noël, 1965	47
<i>Sollasites</i> Black, 1967	50
Family CALYCVLACEAE Noël, 1973	53
<i>Calyculus</i> Noël, 1973	54
<i>Carinolithus</i> Prins in Grün <i>et al.</i> 1974	56
Family PODORHABDACEAE Noël, 1965	59
<i>Axopodorhabdus</i> Wind and Wise in Wise and Wind 1976	60
<i>Ethmorhabdus</i> Noël, 1965	61
Family WATZNAUERACEAE Rood, Hay and Barnard, 1971	61
<i>Lotharingius</i> Noël, 1973	62
<i>Bussonius</i> Goy, 1979	70
INCERTAE SEDIS	72
<i>Conusphaera</i> Trejo, 1969	72
<i>Orthogonoides</i> Wiegand, 1984	74

Family SCHIZOSPHAERELLACEAE Deflandre, 1959	76
<i>Schizosphaerella</i> Deflandre and Dangeard, 1938	76
<i>Prinsiosphaera</i> Jafar, 1983	80
Family THORACOSPHAERACEAE Schiller, 1930	82
<i>Thoracosphaera</i> Kamptner, 1927	82
EARLY EVOLUTIONARY HISTORY OF CALCAREOUS NANNOFOSSILS	83
BIOSTRATIGRAPHY	105
PROVINCIALISM	110
CONCLUSIONS	113
ACKNOWLEDGEMENTS	114
REFERENCES	114
APPENDIX: Classification and Species Index	118

ABSTRACT. Structural analysis of Triassic and Lower Jurassic calcareous nannofloras using the scanning electron microscope has revealed five major coccolith lineages, each defined by characteristic rim structures. The evolutionary and taxonomic importance of rim structure underlies the classification presented, which is set as far as possible within an evolutionary framework. One new order, Watznaueriales; one new family, Mazaganellaceae; three new genera, *Mazaganella*, *Bucanthus*, and *Timorella*; fourteen new species, *Crepidolithus granulatus*, *Mitrolithus lenticularis*, *Timorella cypella*, *Bucanthus decussatus*, *Mazaganella pulla*, *M. protensa*, *Biscutum planum*, *B. grandis*, *B. intermedium*, *Discorhabdus criotus*, *Calyculus depressus*, *Bussonius leufuensis*, *Lotharingius primigenius*, and *L. imprimus*; and two new subspecies, *Parhabdolithus liasicus liasicus* and *P. l. distinctus* are described and discussed. A comprehensive evolutionary scheme has been developed and the processes and patterns of coccolith evolution evaluated. A new biostratigraphic zonation scheme for north-west Europe based upon calcareous nannofossils is formulated with eight zones and eleven subzones. Mediterranean and Pacific assemblages revealed a marked provincialism in the Lower Jurassic. A Tethyan Realm (Mediterranean-Tethys) was characterized by abundant *Mitrolithus jansae* (Sinemurian-Lower Toarcian) and the earlier first occurrence of many taxa. Pacific-Tethys information, while still limited, includes assemblage features distinct from those of the Mediterranean and north-west Europe.

INTRODUCTION

THE late Triassic-early Jurassic time interval represents a particularly important period for calcareous nannofossils. It includes their earliest known occurrences in the Triassic of Tethys, rapid expansion in terms of both abundance and diversity, and subsequent colonization of the adjacent epicontinental seas. During this time the coccolithophorid algae became established as the dominant calcareous nannofossil group and formed an increasingly important component of marine phytoplankton. The coccolithophorids increased from three species in the Rhaetian to over fifty species in the Toarcian; by Pliensbachian times six major family groups had appeared from which all later Mesozoic developments can be traced.

This time interval despite its recognized significance has remained relatively poorly known, with only approximately thirty pertinent studies. The bulk of this published work has concentrated on taxonomy (e.g. Deflandre 1954; Noël 1965, 1973; Rood *et al.* 1973; Grün *et al.* 1974; Goy 1981) and biostratigraphy (e.g. Stradner 1963; Prins 1969; Barnard and Hay 1974; Hamilton 1982). Ideas concerning the early evolution of calcareous nannofossils is limited to papers by Prins (1969) and Jafar (1983), and palaeobiogeographic information is severely restricted by the eurocentric nature of almost all the research. The presence of calcareous nannofossils and coccoliths in the Upper Triassic has only recently been successfully demonstrated by Moshkovitz (1982), Jafar (1983), and Bown (1985) working on material from the Austrian and German Alpine region.

The results presented here form part of a major initiative at University College London under the supervision of Dr A. R. Lord which has followed the publication of the generalized *Stratigraphical Index of Calcareous Nannofossils* (Lord 1982), itself a synthesis of earlier project work. The aim is to establish a greater understanding of all aspects of early and mid-Mesozoic calcareous nannofossils. This entire period has lacked the quantity and quality of work which has especially characterized the study of Tertiary calcareous nannofloras.

This paper presents a coherent taxonomy including detailed descriptions and illustrations of all observed taxa. The classification employed benefited greatly from detailed scanning electron microscopy and from an improved evolutionary understanding of nannofossils, particularly coccoliths, for this interval. A comprehensive evolutionary scheme is proposed utilizing the recognition of discrete coccolith rim structure groups and the lineages they define. The processes and patterns of coccolith evolution during this part of their history are also described and discussed. A new calcareous nannofossil biostratigraphic zonation scheme is proposed for north-west Europe and the need for separate biozonations in Mediterranean-Tethys and Pacific-Tethys is discussed.



TEXT-FIG. 1. Location of study sections. **Triassic**: *Alpine*—Weissloferbach, Fischerwiese, Kandelbachgraben, Pass Lueg, Picolbach, Öfenbach, Lehenmühlengraben. *North-west European*—St Audries Slip, Lavernock, Larne. **Lower Jurassic**: *Britain*—BGS Mochras Borehole, BGS Trunch Borehole, Hock Cliff, Yorkshire Coast, Skye and Raasay. *South Germany*—Trimeusel, Ballrechten, Badenweiler, Unterstürmig, Ebersdorf. *Netherlands (boreholes)*—Oldenzaal 4, Zweelo 1, Boeikop 1. *Mediterranean-Tethys sections*—Brenha (Portugal), Djebel Zaghouan (Tunisia), Longobucco (South Italy), DSDP Site 547. (*Pacific-Tethys sections*—Timor, Picun Leufu (Argentina), Queen Charlotte Islands (Canada) were also studied.)

The final section summarizes present knowledge of Lower Jurassic nannofloral distribution including the recognition of nannofloral provinces.

MATERIAL AND TECHNIQUES

Nannofloral assemblages from thirty-four sections covering the entire Triassic-early Jurassic time interval were studied (text-fig. 1). Triassic material was collected from Austria, southern West Germany, northern Italy, and Britain with nannofossils found only in the Alpine sections. Lower Jurassic material came from twenty-four sections in Britain, West Germany, Holland, Portugal, Italy, Tunisia, off-shore Morocco, Timor, Argentina, and Canada. The north-west European sections supplemented previously published nannofossil data, while the extra-European material allowed the evaluation of nannofossils and their distribution in completely unstudied areas. Further details of study sections have been deposited with the British Library, Boston Spa, Yorkshire, UK, as Supplementary Publication No. SUP 14031 (67 pages). Nannofossil range charts for the Mochras and Brenha sections are given in text-figs. 2 and 3.

Standard techniques for nannofossil preparation were employed (see e.g. Taylor and Hamilton, p. 11, *in* Lord 1982) with both smear and concentrated preparation slides viewed in the light microscope. When the nannofossils were rare and/or when the preparation was intended for scanning electron microscopy, centrifuging was used to 'clean' and concentrate the assemblages. The centrifuge spin speeds of Medd (1971, p. 822) yielded the most successful concentrations for the small size range nannofossils typical of this period, preserved in predominantly argillaceous rocks. Routine biostratigraphical observation and assemblage counting was carried out with a Carl-Zeiss Mark II photomicroscope using both phase-contrast illumination and cross-polarized light. A JEOL T-200 scanning electron microscope was used for detailed analysis of nannofossil ultrastructure. The tilt and swivel mechanism allowed the observation of the same specimen in plan and side views. In addition, the easy production of stereo-pair micrographs further aided the determination of three-dimensional relationships between the external structural components. The combination of information concerning crystallographic organization of elements displayed in the light microscope, with high resolution and 3-D images of surface details in the scanning electron microscope, provided the optimum amount of information for both taxonomic and evolutionary study.

All slide material and photographic negatives are deposited in the collections of the Postgraduate Unit of Micropalaeontology, University College London. Conventionally, photographic negatives are used as 'types', and catalogue numbers cited here refer to film and frame numbers, e.g. UCL-2074-23 is frame 23 of film 2074.

COCCOLITH MORPHOLOGY AND DESCRIPTIVE TERMINOLOGY

Coccoliths are the constituent components of a complete cell-wall covering known as a coccosphere. In all present-day coccolithophorids the individual coccolith consists of three component parts; the organic baseplate, organic matrix, and crystal elements of calcium carbonate. Only the latter component is preserved in the fossil record. Those coccoliths formed external to the cell wall from unmodified rhombohedral units of calcite are called holococcoliths (reported from the Middle Jurassic to the present day), whereas those formed internally and composed of organically controlled crystals are termed heterococcoliths. Further information concerning living coccolithophorids can be found in syntheses by Tappan (1980) and Hibberd (1980).

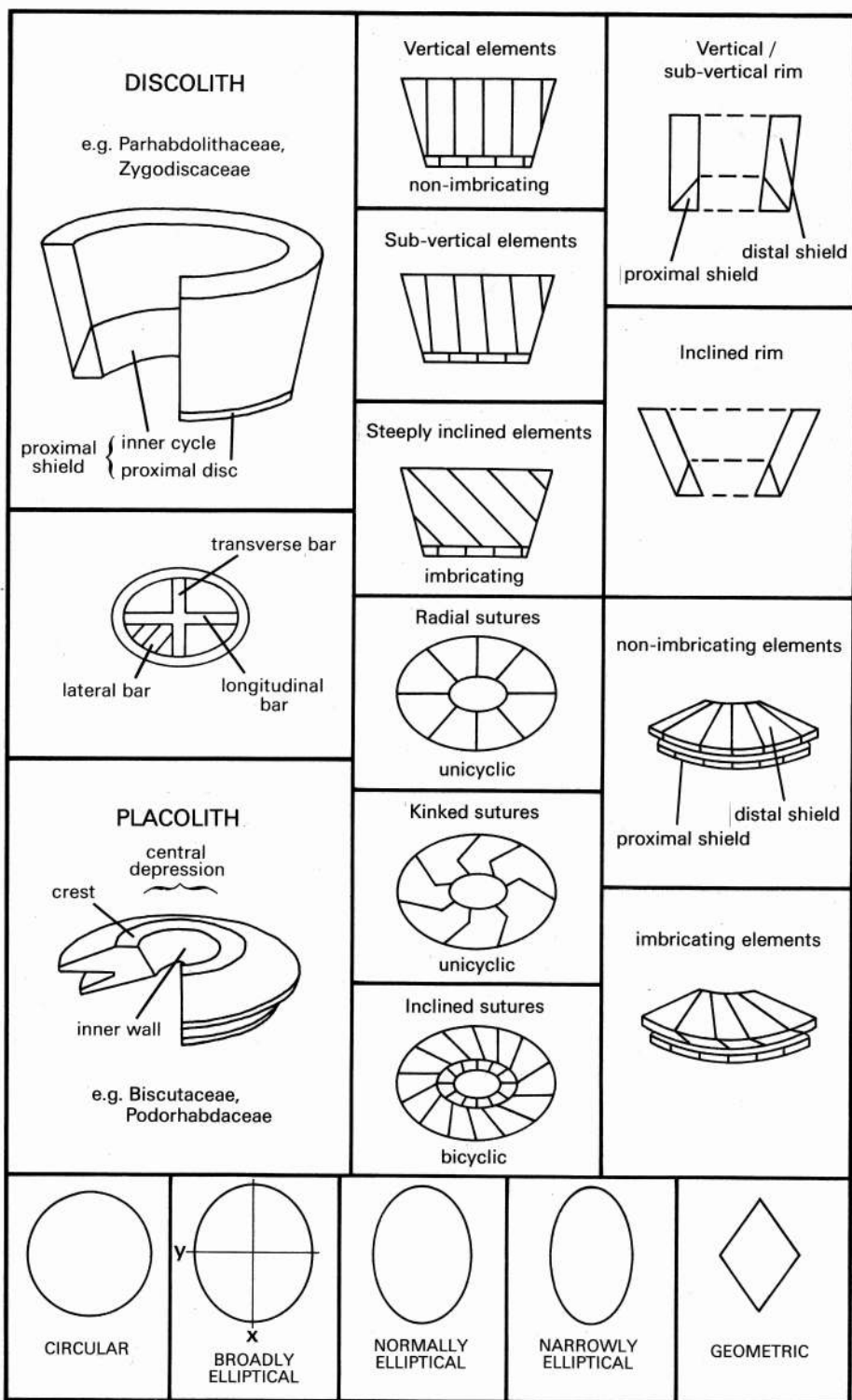
Coccolith morphology generally takes the form of an elliptical or circular **ring** of calcite elements, enclosing a central space which can be filled by a variety of **bars**, **crosses**, **grills**, and **spines**. The terms **normally**, **narrowly** and **broadly elliptical**, **circular**, and **geometric** are used to describe coccolith shape (text-fig. 4; Black 1972, p. 13). The marginal ring is termed the **rim** and the enclosed inner space, the **central area**. A rim may consist of one or more rings of elements and when concentric rings occur in the same plane these are called **cycles**; when rings are superimposed on each other in different planes these are termed **shields**. The shield thought to be closest to the cell wall is termed **proximal** and the shield furthest from the cell wall is termed **distal**.

Within the wide variety of heterococcolith morphology, two major groups predominate: the discoliths and placoliths. Discoliths were the earliest type of coccolith to appear, in the late Triassic, and consist of a relatively thin, vertical or steeply sloping rim (= wall). The rim is usually constructed from unicyclic distal and proximal components joined along a sloping boundary (text-fig. 4). It is considered appropriate to term these components shields as they are disposed in a proximal and distal position and appear to be analogous to the distinctly separate proximal and distal components (shields) of the later placolith coccoliths. The distal

LOWER SINEMURIAN	UPPER SINEMURIAN	LOWER PLIENS-BACHIAN			UPPER PLIENS- BACHIAN		LOWER TOARCIAN	UPPER TOARCIAN	LOWER BAJO- CIAN	AMMONITE ZONE SPECIES
		jamesoni	ibex	davoiei	margaritulus	spinatum				
										<i>C. crassus</i>
										<i>C. plienschachensis</i>
										<i>C. primulus</i>
										<i>M. elegans</i>
										<i>M. jansae</i>
										<i>P. liasicus distinctus</i>
										<i>S. punctulata</i>
										<i>T. patulus</i>
										<i>O. hamiltoniae</i>
										<i>P. liasicus liasicus</i>
										<i>P. marthae</i>
										<i>B. novum</i>
										<i>P. robustus</i>
										<i>C. granulatus</i>
										<i>B. finchii</i>
										<i>B. grandis</i>
										<i>L. hauffii</i>
										<i>L. sigillatus</i>
										<i>B. prinsii</i>
										<i>D. ignotus</i>
										<i>L. barozi</i>
										<i>M. lenticularis</i>
										<i>S. lowei</i>
										<i>B. dubium</i>
										<i>Calyculus</i> sp. indet.
										<i>Z. erectus</i>
										<i>C. superbus</i>
										<i>D. criotus</i>
										<i>B. intermedium</i>
										<i>A. atavus</i>
										<i>C. cavus</i>
										<i>B. depravatus</i>
										<i>C. magharensis</i>
										<i>D. constans</i>
										<i>D. patulus</i>
										<i>W. britannica</i>
										<i>Triscutum</i> sp. indet.

TEXT-FIG. 3. Stratigraphic distribution of calcareous nannofossils from Brenha, Portugal. The section is composed of marl and limestone in the Sinemurian and clay and marl in the Pliensbachian and Toarcian.

The sixty-nine samples studied all yielded abundant and well-preserved nannofossil assemblages.



TEXT-FIG. 4. Morphological terminology for discolith and placolith coccoliths.

shield is made up of tall elements which may be **vertical (non-imbricating)** or **inclined (imbricating)**. In proximal and side view the proximal shield appears as a thin disc. However, in distal view its vertical extension appears as an inner cycle to the distal shield. The placolith structure first occurs in the Sinemurian and consists of two or more thin, wide shields separated by a gap and connected by a shared central **inner wall**. When three shields form the placolith rim the terms **distal**, **intermediate**, and **proximal** are employed. The component elements of the shields may be vertical or inclined in side view and radial or twisting in plan view. The terms **inclination** and **precession** have been used to describe the deviation from radially arranged elements (and the sutures along which they are joined), the former by Hay *et al.* (1966, p. 383) for imbricate coccoliths, and the latter by Black (1972, p. 16) for non-imbricate coccoliths. Imbrication is termed **dextral** when overlapping occurs in a clockwise direction and **sinistral** when overlapping occurs in an anticlockwise direction.

TAXONOMY

Calcareous nannofossils are a heterogeneous group of very small fossils, usually taken as below 25 μm in size. The most important group consists of calcified scales of prymnesiophycean algae (= coccoliths), which dominate modern marine phytoplankton, whereas most other groups are extinct and of uncertain biological affinity (= nannoliths). The commonly used term calcareous nannoplankton strictly refers to living forms where a pelagic mode of life can be demonstrated.

Classification of calcareous nannofossils is necessarily based upon the morphology of individual parts of a (presumed in some cases) composite cell-wall covering. The study of living coccolithophorids has shown that coccoliths are a fairly reliable guide to biological relationships within the group. In most cases individual coccoliths reflect the morphology of the entire coccosphere. However, exceptions are observed in the form of polymorphic coccospheres. Such coccospheres are usually dimorphic and one of the two coccolith morphs is subordinate in number and restricted to specialized positions on the coccosphere, e.g. around flagellar bases. Other examples show the two coccolith morphs forming 'exathecal' layers at different levels via flaring appendages. A second type of dimorphism is exemplified by the well-known *Coccolithus pelagicus* (Wallich) Schiller which bears two entirely different coccospheres during its life cycle. While the palaeontological difficulties raised by such dimorphism are not in dispute, it now appears that these examples are not typical of the coccolithophorids as a whole and may have been even rarer in their early history. If we remain aware of these problems highlighted by the extant counterparts then features such as dimorphism can be recognized in the fossil record using stratigraphical considerations and the occasional intact coccospheres. Such phenomena by no means negate attempts to produce a biological classification or to understand evolutionary patterns.

The classification of nannofossils has generally been purely morphological. No fixed weighting of morphological characters has been applied and the taxonomy is often inconsistent and incoherent. To some extent this has been caused by a lack of detailed knowledge of nannofossil structure, particularly before 1954 when only light microscope observation was available. The development of transmission and scanning electron microscopes has greatly aided the observation of nannofossil structure, but the morphology is still poorly understood and generally inadequately reflected in taxonomy. Comprehensive classifications have recently been presented by Hay (1977), Tappan (1980), and Perch-Nielsen (1985), but with very little discussion of higher taxonomic divisions and the taxonomic significance of coccolith structures, an exception being Verbeek (1977, p. 71). The classification adopted here is based upon conclusions drawn from detailed structural observations and particularly the assumption that coccolith rim structure is the morphological feature of fundamental evolutionary and taxonomic significance. The recognition of discrete morphological groups characterized by distinct rim structures in these earliest coccolithophorids provides a framework from which it is possible to produce a coherent classification. The potential for rationalizing coccolith taxonomy and classification throughout the geological column, having observed the principles in the earliest and relatively undiversified representatives, is of great significance for the group. In addition, this morphological classification is viewed within an

evolutionary context in an attempt to reflect true biological relationships. The taxonomic divisions and the morphological features employed in their discrimination are as follows:

Order—generalized morphology of the rim, e.g. placolith, discolith, or multi-tiered, and the general organization of the individual elements within the rim, e.g. imbrication and orientation of suture lines.

Family—shape and organization of the rim elements, together with the width and nature of the central area.

Genus—detailed rim features and general central area structures.

Species—detailed central area structures.

Many Lower Jurassic taxa have been widely cited but are in fact often poorly defined, described, and illustrated. The taxonomy presented here therefore includes detailed descriptions together with SEM and LM photographs for each species encountered during the study. Emendments to original diagnoses have been made where necessary. Translations are included for German and French diagnoses. Dimensions are given as ranges observed in the present work but holotype information is also given in brackets. The following abbreviations are used: L, rim length; W, rim width; RH, rim height; SH, spine height; LM, light microscope; SEM, scanning electron microscope; p-c, phase contrast; c-p, crossed polars. The term 'occurrence' is used for stratigraphical distribution data gained in the present work, and 'range' for data acquired from published sources. Where two catalogue numbers are given for a holotype they refer to different views of the same specimen.

SYSTEMATIC PALAEOLOGY

Division PRYMNESIOPHYTA Hibberd, 1976

Class PRYMNESIOPHYCEAE Hibberd, 1976

Order EIFFELLITHALES Rood, Hay and Barnard, 1971

Diagnosis. 'Coccoliths with a simple marginal area consisting solely of a double cycle of elements; the 2 cycles are superimposed in such a way that they appear as a single cycle in most proximal and distal views, a suture being visible only on the inner surface of the cirlet, facing the central area. Central area structures are variable, consisting of a cross, bar, or more complex feature which may be surmounted by a spine' (Rood *et al.* 1971, p. 248).

Remarks. Coccoliths of the Eiffellithales have a tall rim composed of two shields; a high distal shield and a thin proximal shield which may have distal extensions seen as an inner cycle to the distal shield. The two shields are usually joined along a sloping surface (text-fig. 4). The distal shield may be composed of elements which are imbricating or non-imbricating.

Included families. Eiffellithaceae, Parhabdolothaceae, Rhagodiscaceae, Zygodiscaceae.

Family ZYGODISCACEAE Hay and Mohler, 1967

Diagnosis. 'Coccoliths consisting of an elliptical ring composed of strongly imbricate laths or tabulae and an open central area spanned by an I-, X-, or H-shaped structure symmetrical about the short axis of the ellipse. Rim dextrogyre in distal view between cross polarizers' (Hay and Mohler 1967, p. 1532).

LM characteristics. Elliptical rim of variable thickness, high, with two cycles—an outer dark cycle and an inner bright cycle (p-c and c-p) crossed by four thin isogyres (c-p). In side view the proximal and distal components are joined along a sloping boundary, the triangular cross-section of the proximal shield is prominent.

Remarks. The use of this family is based upon the assumption that Mesozoic loxolith coccoliths gave rise to the similarly structured Tertiary forms which typify the Zygodiscaceae.

Included genera. *Archaeozygodiscus*, *Crepidolithus*, *Tubirhabdus*, *Zeugrhabdotus* (also see Perch-Nielsen, 1985, pp. 406-409).

Range: Upper Triassic to Oligocene.

Genus ARCHAEOZYGODISCUS Bown, 1985

Type species. *Archaeozygodiscus koessenensis* Bown, 1985.

Diagnosis. 'Elliptical coccoliths possessing a loxolith structured rim imbricating in an anticlockwise direction with an inner cycle of tangential and overlapping laths' (Bown 1985, p. 32).

Remarks. *Archaeozygodiscus* is unique in displaying sinistral imbrication in its distal shield as opposed to the dextral imbrication which all other Mesozoic loxolith coccoliths possess.

Archaeozygodiscus koessenensis Bown, 1985

Plate 1, figs. 1-3; Plate 12, figs. 1 and 2

1985 *Archaeozygodiscus koesseni* Bown, p. 32, pl. 1, figs. 1-3.

Diagnosis. 'A species of *Archaeozygodiscus* with the short axis of the ellipse spanned by a bar constructed from a number of calcite elements. The centre of the bar has a circular hole which may or may not be a spine base' (Bown 1985, p. 32).

Description. An extremely small, elliptical coccolith with a loxolith rim composed of a relatively broad and high distal shield with twenty-two to twenty-six elements imbricating sinistrally. The proximal shield forms a thin basal disc of around twenty subsquare elements with a distal extension forming an inner cycle to the distal shield. The proximal shield is spanned in the minor axis by a broad bar with a central hole.

Dimensions. L: 1.7-3.2 (1.9) μm , W: 1.0-2.1 (1.4) μm , RH: 0.4-0.7 μm .

Remarks. The significance of sinistral rim imbrication is unknown but this species is nevertheless considered the precursor of the Jurassic loxolith lineage. *A. koessenensis* is distinguished from *Zeugrhabdotus erectus* and *Tubirhabdus patulus* by its smaller size and sinistral rim imbrication.

Occurrence. Fischerwiese, Rhaetian; Weissloferbach, Rhaetian.

Genus CREPIDOLITHUS Noël, 1965

Type species. *Crepidolithus crassus* (Deflandre, 1954) Noël, 1965.

Diagnosis. 'Elliptical coccolith, like a massive disc, more or less swollen, with heightened constituent rim elements which form a marginal rim, composed of vertical or subvertical rhombohedral calcite elements, placed side by side, lying on a floor of horizontal calcite lamellae' (Noël 1965, p. 84).

Remarks. *Crepidolithus* is a genus characterized by large coccoliths possessing high, blocky, and broad rims. It is unusual in that it includes a number of species which appear to display variation in the degree of rim element inclination, from subvertical to steeply inclined. However, the majority of specimens within the taxon possess typical loxolith rim types and thus the genus is included in the Zygodiscaceae. *Crepidolithus* is restricted in range to the Jurassic but very similar coccoliths occur in the Maastrichtian and Palaeocene genus *Neocrepidolithus*. The non-concurrent ranges of the two genera appear to preclude any close relationship.

Crepidolithus cavus Prins ex Rood, Hay and Barnard, 1973

Plate 1, figs. 4 and 5; Plate 12, figs. 3 and 4

1969 *Crepidolithus cavus* Prins, pl. 1, fig. 4c (non fig. 4a-b) (nom. nud.).

1973 *Crepidolithus cavus* Prins ex Rood et al., p. 375, pl. 2, fig. 5.

- 1974 *Crepidolithus impontus* Prins and Zweili in Grün *et al.*, pp. 310–311, pl. 2, figs. 1–3.
 1979 *Crepidolithus impontus* Prins and Zweili; emend. Goy in Goy *et al.*, p. 39, pl. 2, fig. 2.
 1981 *Crepidolithus impontus* Prins and Zweili; Goy, pp. 28–29, pl. 6, figs. 2–8; pl. 7, fig. 1; text-fig. 5.
 1984 *Crepidolithus cavus* Prins ex Rood *et al.*; Crux, fig. 11 (7, 8); fig. 14 (3, 4).
 non 1974 *Crepidolithus cavus* Prins ex Rood *et al.*; Barnard and Hay, pl. 1, fig. 2; pl. 4, fig. 2.

Original diagnosis. 'A species of *Crepidolithus* with a bridge in the minor axis of the elliptical central area' (Rood *et al.* 1973, p. 375).

Emended diagnosis. 'A species of *Crepidolithus* with a wall composed of distinctly inclined and overlapping calcite laths. The central area is occupied by a delicate bridge aligned along the short axis of the ellipse; the middle of the bridge supports a slender spine' (Goy 1979, p. 39).

Description. A large elliptical loxolith coccolith with a relatively narrow and high distal shield composed of around thirty-four steeply inclined, dextrally imbricating laths. The proximal shield is composed of about thirty elements with distal extensions which line the inner surface of the distal shield for three-quarters of its height. The broad central area of the proximal shield is spanned by a delicate bar, aligned along the minor axis of the ellipse, supporting a central, slender spine, never rising higher than the distal wall and often broken.

Dimensions. L: 5.0–8.0 (5.2) μm , W: 3.0–5.5 (3.3) μm , RH 1.5–3.5 μm .

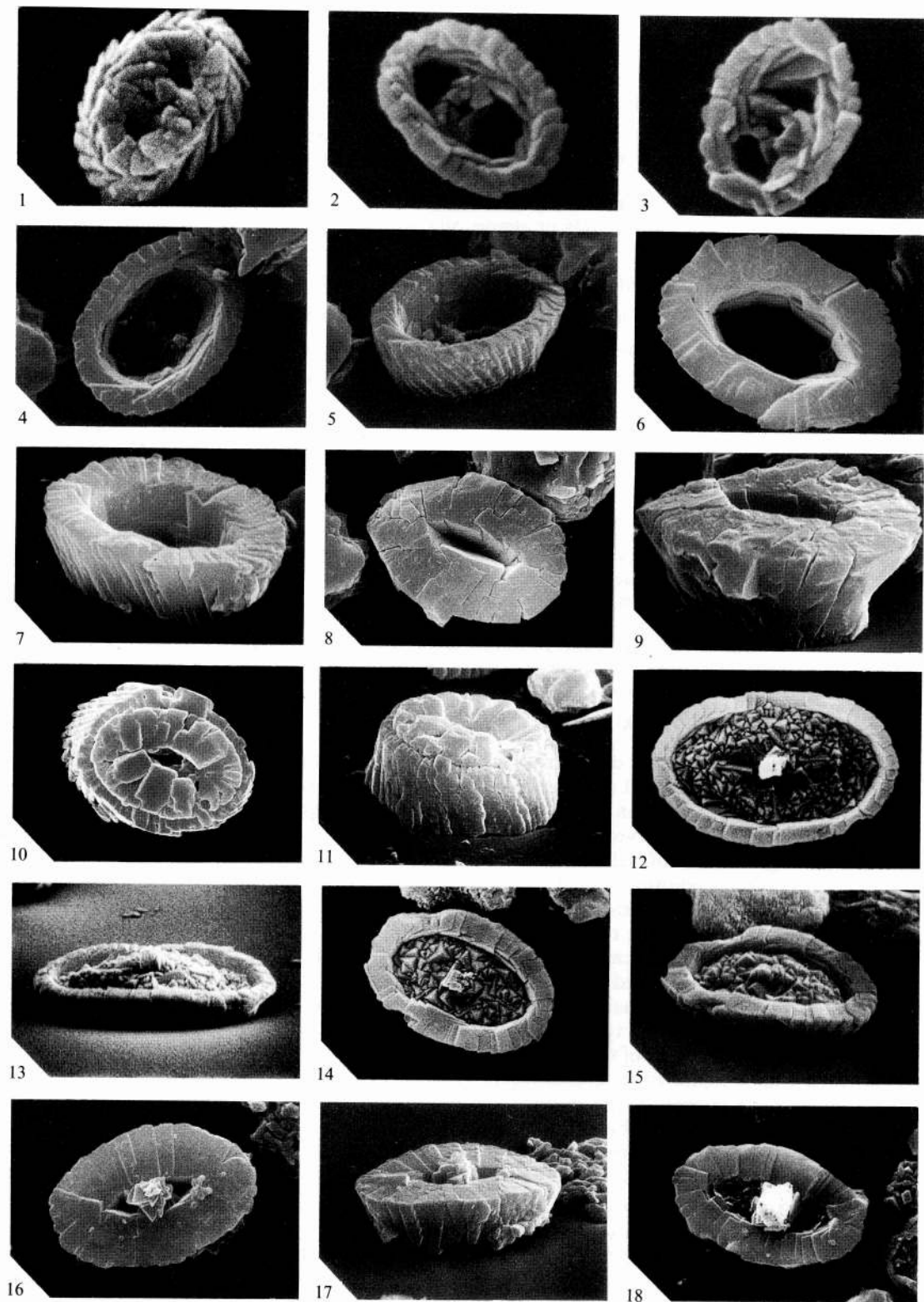
Remarks. First named informally by Prins (1969) the species was validated by Rood *et al.* (1973). Grün *et al.* (1974, p. 311) considered the holotype proposed by Rood *et al.* (1973) to be a specimen of *Parhabdololithus marthae* and instead proposed a new name *C. impontus*. Goy (1979, 1981) made no comment on the name *C. cavus* but emended the diagnosis of Grün *et al.* which was based only on specimens in proximal view and thus lacked any information concerning the spine. The holotype of Rood *et al.* (1973) is here considered valid, possessing a high imbricating wall, a thin bar, and a slender spine, quite unlike *P. marthae*. Thus *C. impontus* is considered a junior synonym of *C. cavus*, however the diagnosis of Goy (1979) is precise and complete and preferred to that of Rood *et al.* (1973).

C. cavus displays little morphological variation. However, overgrowth is common and the bar and spine are often destroyed. Under the light microscope *C. cavus* usually appears as a large, narrow rim with a wide vacant central area and two nodes at either end of the minor axis of the ellipse. Steep element inclination in the distal shield is always present, i.e. a typical loxolith rim structure.

C. cavus is distinguished from *C. crassus* and *C. plienschachensis* by its narrower rim, broader central area, and delicate bar and spine. *C. cavus* is larger than *Z. erectus* and *T. patulus* with a much higher rim and finer bar and spine.

EXPLANATION OF PLATE I

- Figs. 1–3. *Archaeozygodiscus koessenensis* Bown, 1985. Weissloferbach, *marshi* zone (E13b). 1, proximal view, UCL-2117-4, $\times 15\ 700$. 2, distal view, UCL-2040-33, $\times 17\ 500$. 3, distal view, UCL-2040-29, $\times 16\ 200$.
 Figs. 4 and 5. *Crepidolithus cavus* Prins ex Rood *et al.* 1973. Unterstürmig, Lower Toarcian (U6). 4, distal view, UCL-2036-3, $\times 6000$. 5, oblique view of fig. 4, UCL-2036-2, $\times 6700$.
 Figs. 6–11. *C. crassus* (Deflandre, 1954) Noël, 1965. 6, distal view, UCL-1916-24, Mochras, *ibex* Zone (M339), $\times 6300$. 7, oblique view of fig. 6, UCL-1916-23, $\times 6350$. 8, distal view, UCL-1940-18, Mochras, *rariostatum* Zone (M285), $\times 4300$. 9, oblique view of fig. 8, UCL-1940-20, $\times 6200$. 10, proximal view, UCL-2290-15, Badenweiler, *variabilis* Zone (BAD2), $\times 4100$. 11, oblique view of fig. 10, UCL-2290-14, $\times 4100$.
 Figs. 12–15. *C. granulatus* sp. nov. Brenha, *ibex* Zone (3531). 12, holotype, distal view, UCL-2178-35, $\times 6100$. 13, oblique view of fig. 12, UCL-2178-34, $\times 6150$. 14, isotype, distal view, UCL-2170-4, $\times 5450$. 15, oblique view of fig. 14, UCL-2170-3, $\times 6000$.
 Figs. 16–18. *C. plienschachensis* Crux, 1985. 16, distal view, UCL-2072-25, Timor, mid-Pliensbachian, $\times 4800$. 17, oblique view of fig. 16, UCL-2072-26, $\times 4800$. 18, distal view, UCL-2177-29, Brenha, Upper Sinemurian (6040), $\times 4000$.



BOWN, *Archaeozygodiscus*, *Crepidolithus*

Occurrence. Badenweiler, *bifrons* Zone to *aalensis* Zone; Ballrechten, *bifrons* Zone to *levesquei* Zone; Brenha, *variabilis* Zone to Middle Jurassic; Mochras, *spinatum* Zone to *levesquei* Zone; Trimeusel, *tenuicostatum* Zone to *levesquei* Zone; Unterstürmig, Lower Toarcian.

Range. *jamesoni* Zone to *tenuicostatum* Zone (Prins 1969), *jamesoni* Zone to *tenuicostatum* Zone (Barnard and Hay 1974), Lower Toarcian (Grün *et al.* 1974), *oxynotum* Zone to *opalinum* Zone (Aalenian) (Crux 1984), Lower Toarcian (Goy 1979, 1981).

C. cavus was not found lower than the *spinatum* Zone in the present study and earlier ranges for this species are thought to be misidentification or sample contamination.

Crepidolithus crassus (Deflandre, 1954) Noël, 1965

Plate 1, figs. 6–11; Plate 12, figs. 5 and 6

1954 *Discolithus crassus* Deflandre in Deflandre and Fert, p. 144, pl. 15, figs. 12 and 13; text-fig. 49.

1965 *Crepidolithus crassus* (Deflandre); Noël, pp. 85–91, pl. 2, figs. 3–7; pl. 3, figs. 1–5; text-figs. 17–21.

1973 *Crepidolithus crucifer* Rood *et al.*, pl. 2, fig. 4.

1974 *Crepidolithus crucifer* Rood *et al.*; Barnard and Hay, pl. 1, fig. 5.

1981 *Crepidolithus crassus* (Deflandre); Goy, pp. 26–27, pl. 5, figs. 8–11; pl. 6, fig. 1.

non 1971 *Crepidolithus crassus* (Deflandre); Rood *et al.*, pl. 2, fig. 7.

Diagnosis. 'A typical *Crepidolithus*' (Noël 1965, p. 88).

Description. *C. crassus* is a species which displays considerable morphological variation. It consists of a broad, high, elliptical rim with a vacant central area often reduced to a lenticular slit. The distal shield forms a high wall and is constructed from around thirty subvertical to steeply inclined elements. The width of this wall may vary; the broader the wall, the narrower the central area. The proximal shield is formed from fifteen to twenty-five rectangular elements which constitute a thin basal disc which may be open or closed. The proximal shield distal extension forms an inner cycle to the distal shield for about half its height. The central area lacks any organized bars, crosses, or spines.

Dimensions. L: 5.0–9.0 (8.2) μm , W: 3.5–5.5 (5.5) μm , RH: 2.0–4.5 μm .

Remarks. *C. crassus* is a large distinctive coccolith, common throughout its range in the Lower Jurassic and extremely resistant to diagenetic dissolution. It appears that the coarse blocky nature of the rim structure forms an ideal nucleation site for diagenetic calcite and much of the morphological variation observed is thought to be due to overgrowth. Thus, *C. crassus* may survive diagenetic reorganization of calcite at the expense of other, more delicate, components of the assemblage and this is confirmed by its occurrence in highly impoverished assemblages with only one or two other resistant forms (e.g. Moshkovitz and Ehrlich 1976b, where only *C. crassus* and *Schizosphaerella punctulata* are recovered from numerous Israeli sections).

Variability in element imbrication is observed in the distal shield of this species. However, the majority of specimens observed possessed strongly inclined rim elements. *C. crassus* specimens illustrated in the literature usually have at least subvertical and slightly inclined elements if not steeply inclined elements more typical of the loxolith structure group.

The first occurrence datum of *C. crassus* is generally reported in the Upper Sinemurian. However, in the Hock Cliff samples small *Crepidolithus* specimens resembling *C. crassus* first appear in the *semicostatum* Zone (Lower Sinemurian). Its earliest appearance in the Tethyan area is at least Lower Sinemurian in the Brenha section.

C. crassus is distinguished from *C. pliensbachensis* by its larger size and vacant central area and from *C. granulatus* by its taller, broader rim and closed central area.

Occurrence. Badenweiler, *bifrons* Zone to *aalensis* Zone; Ballrechten, *bifrons* Zone to *levesquei* Zone; Brenha, Lower Sinemurian to Middle Jurassic; DSDP Site 547, Sinemurian to Lower Toarcian; Longobucco, Lower Pliensbachian to Lower Toarcian; Mochras, *oxynotum* Zone to *levesquei* Zone; Timor, mid-Pliensbachian; Trimeusel, *tenuicostatum* Zone to *levesquei* Zone; Trunch, *oxynotum* Zone to *jamesoni* Zone; Tunisia, Upper Pliensbachian to Toarcian; Unterstürmig, Lower Toarcian.

Range. *jamesoni* Zone to *tenuicostatum* Zone (Prins 1969), *raricostatum* Zone to *tenuicostatum* Zone (Barnard and Hay 1974), *oxynotum* Zone to *opalinum* Zone (Aalenian) (Crux 1984).

Crepidolithus granulatus sp. nov.

Plate 1, figs. 12–15; Plate 12, figs. 7 and 8

- 1969 *Crepidolithus crassus* (Deflandre, 1954) Noël, 1965; Prins, pl. 1, fig. 5C.
 1977 *Ethmorhabdus* aff. *E. gallicus* Noël, 1965; Hamilton, pl. 1, figs. 4–6.
 1984 *Crepidolithus crassus* (Deflandre); Crux, fig. 11 (2).

Diagnosis. A species of *Crepidolithus* which possesses a relatively low rim, narrow to moderately thick, and composed of elements which may be subvertical to steeply inclined; the central area is wide and completely filled with a floor of granular calcite rhombs. A small central boss or pore may also be present.

Description. A normally elliptical coccolith with a low distal shield of variable thickness surrounding a wide central area. The distal shield is constructed from thirty to forty elements which may be subvertical to steeply inclined. The proximal shield has not been observed in detail but takes the form of a thin basal disc with little or no distal extension. The large central area is completely filled by numerous, small, roughly equidimensional calcite rhombs; a small central boss or pore may be present.

Dimensions. L: 5.5–6.3 (6.2) μm , W: 3.6–4.0 (4.0) μm , RH: 0.5–1.1 (0.7) μm , RW: 0.3–0.9 (0.4) μm .

Derivation of name. From Latin *granulum*, grain.

Holotype. UCL-2178-35, UCL-2178-34 (Pl. 1, figs. 12 and 13).

Isotype. UCL-2170-3, UCL-2170-4 (same specimen).

Type locality. Brenha, Portugal.

Type level. *davoei* Zone.

Occurrence. Brenha, Upper Sinemurian to *davoei* Zone; DSDP Site 547, Upper Sinemurian; Mochras, *ibex* Zone to *margaritatus* Zone.

Range. Lower Sinemurian to Toarcian (Hamilton 1977).

Crepidolithus plienschachensis Crux, 1985 emend.

Plate 1, figs. 16–18; Plate 2, figs. 1–3; Plate 12, figs. 9 and 10

- 1965 *Parhabdololithus liasicus* Deflandre, 1952; Noël, pl. 4, fig. 7.
 1969 *Bidiscorhabdus ocellatus* Prins, pl. 2, fig. 7A (*non* 7B) (*nom. nud.*).
 1984 *Crepidolithus ocellatus* Crux, p. 181, fig. 11 (3, 5, ?6); fig. 14 (5, 6, 7) Homonym.
 1985 *Crepidolithus plienschachensis* Crux, p. 31.

Original diagnosis. 'A species of *Crepidolithus* with a bridge forming spine base' (Crux 1984, p. 181).

Emended diagnosis. An elliptical coccolith with a broad rim constructed from subvertical to vertical elements and a narrow lenticular central area from which a low spine protrudes.

Description. A species of *Crepidolithus* with a broad blocky distal shield constructed from around thirty vertical or subvertical elements. The central area is a lenticular slit through which a low spine protrudes. The proximal shield is a thin basal disc which may have a distal extension. The spine is usually no more than twice the height of the rim.

Dimensions. L: 5.5–8.0 (5.8) μm , W: 3.5–5.0 (3.9) μm , RH: 1.5–2.0 μm , SH: 1.8–4.4 μm .

Remarks. The original name of *C. ocellatus* was preoccupied and the replacement name of *C. plienschachensis* given (Crux 1985). *C. plienschachensis* is differentiated from *C. crassus* by its low

spine, from *C. cavus* by its broader rim and lenticular central area, and from *Parhabdolithus liasicus* by its broader rim, lenticular central area, and thinner, shorter spine.

Occurrence. Brenha, Lower Sinemurian to *jamesoni* Zone; DSDP Site 547, Sinemurian to Lower Pliensbachian; Hock Cliff, *semicostatum* Zone; Mochras, *semicostatum* Zone to *jamesoni* Zone; Timor, mid-Pliensbachian; Trunch, *oxynotum* Zone to *jamesoni* Zone.

Range. *raricostatum* Zone to *ibex* Zone (Prins 1969), *oxynotum* Zone to *ibex* Zone (Crux 1984).

Genus TUBIRHABDUS Prins *ex* Rood, Hay and Barnard, 1973

Type species. *Tubirhabdus patulus* Prins *ex* Rood *et al.*, 1973.

Diagnosis. 'Narrowly elliptical eiffellithalid coccoliths with a broadly oval to circular spinoid central structure in the minor axis of the margin' (Rood *et al.* 1973, p. 373).

Remarks. Goy (1981) observed that the large circular spine is supported by a central cross structure and not simply by a minor axis bar as stated by Rood *et al.* (1973). In the present study the spine has been observed variously supported by a minor axis bar, a cross structure, and a complete basal plate. It thus appears that variation occurs within the genus, which may be due to preservation.

Tubirhabdus patulus Prins *ex* Rood, Hay and Barnard, 1973

Plate 2, figs. 4-6; Plate 12, figs. 11 and 12

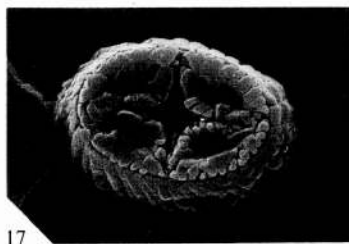
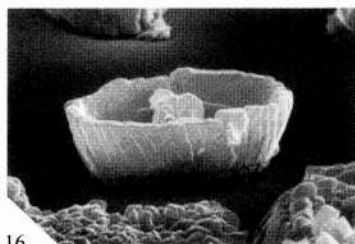
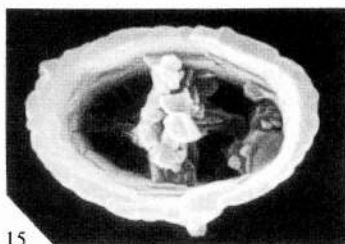
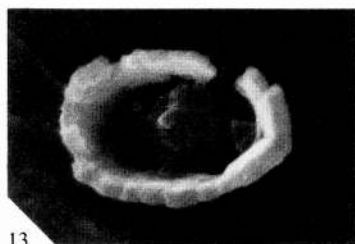
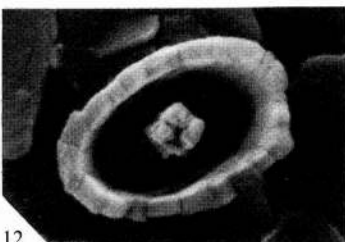
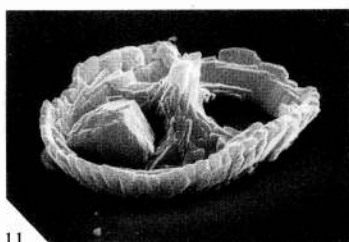
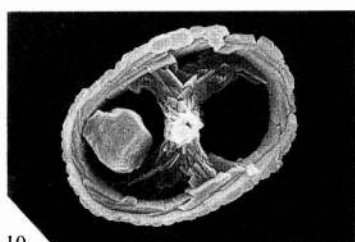
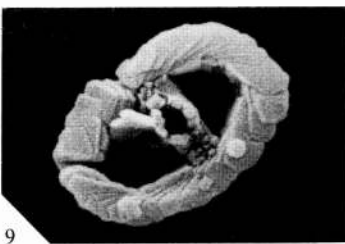
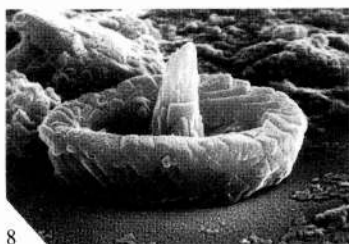
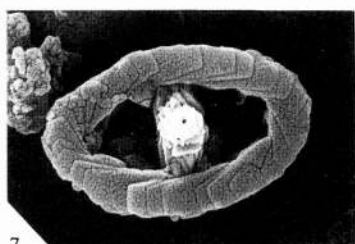
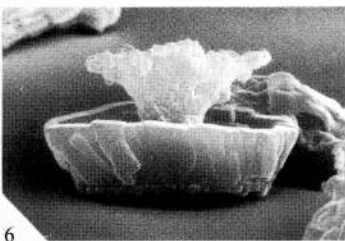
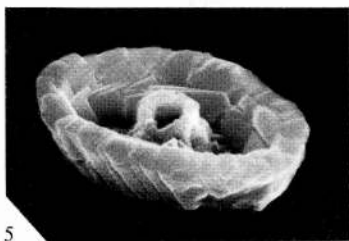
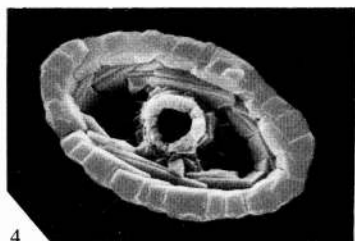
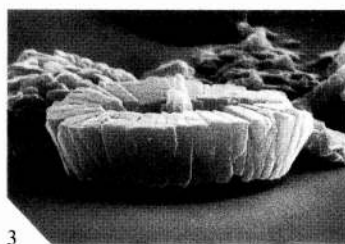
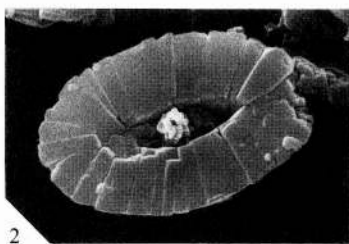
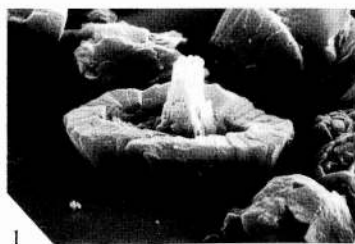
- 1969 *Tubirhabdus patulus* Prins, pl. 1, fig. 10A-C, fig. 9 (*nom. nud.*).
 1973 *Tubirhabdus patulus* Prins *ex* Rood *et al.*, pp. 373-374, pl. 2, fig. 3.
 1974 *Tubirhabdus ?rhombicus* Grün *et al.*, p. 309, pl. 20, figs. 4-6.
 1980 *Parhabdolithus rhombicus* (Grün *et al.*); Grün and Zweili, pl. 14, figs. 2-4.
 1981 *Tubirhabdus patulus* Prins *ex* Rood *et al.*; emend. Goy, pp. 29-30, pl. 7, figs. 2-7; pl. 8, fig. 1; text-fig. 6.
 1987 *Tubirhabdus patulus* Prins *ex* Rood *et al.*; Bown, pl. 1, figs. 3 and 4.

Diagnosis. 'A small species of *Tubirhabdus* with a very broadly open oval to circular central spine' (Rood *et al.* 1973, p. 373).

Description. A narrowly elliptical coccolith possessing a typical loxolith rim structure, composed of a relatively tall and thin distal shield constructed from twenty-six to thirty steeply inclined elements, and a proximal

EXPLANATION OF PLATE 2

- Figs. 1-3. *Crepidolithus plienschachensis* Crux, 1985. 1, oblique view of Plate 1, fig. 18, UCL-2177-28, $\times 4000$. 2, distal view, UCL-2117-11, Timor, mid-Pliensbachian (J237), $\times 6150$. 3, oblique view of fig. 2, UCL-2117-10, $\times 6050$.
 Figs. 4-6. *Tubirhabdus patulus* Prins *ex* Rood *et al.*, 1973. 4, distal view, UCL-2014-4, DSDP Site 547, Lower Pliensbachian (15-1), $\times 8350$. 5, oblique view of fig. 4, UCL-2014-5, $\times 8400$. 6, side view, UCL-2072-20, Timor, mid-Pliensbachian, $\times 6850$.
 Figs. 7-9. *Zeughrabdotos erectus* (Deflandre, 1954) Reinhardt, 1965. 7, distal view, UCL-1888-21, Mochras, *levesquei* Zone (M367), $\times 8350$. 8, oblique view of fig. 7, UCL-1888-20, $\times 8300$. 9, distal view, UCL-2173-26, Brenha, Bajocian (3617), $\times 8500$.
 Figs. 10 and 11. *Bucanthus decussatus* gen. et sp. nov. Timor, mid-Pliensbachian (J237). 10, holotype, distal view, UCL-2117-30, $\times 4650$. 11, oblique view of fig. 10, UCL-2117-33, $\times 5950$.
 Figs. 12-14. *Crucirhabdus minutus* Jafar, 1983. 12, distal view, UCL-2025-23, Weissloferbach, *marshi* Zone (E39), $\times 14\ 450$. 13, distal view, UCL-2040-13, Weissloferbach, *marshi* Zone (13b), $\times 15\ 250$. 14, distal view, UCL-2025-9, Weissloferbach, *marshi* Zone (E39), $\times 16\ 000$.
 Figs. 15-18. *C. primulus* Prins *ex* Rood *et al.*, 1973. 15, distal view, UCL-2189-4, Timor, mid-Pliensbachian (J237), $\times 7500$. 16, oblique view of fig. 15, UCL-2189-6, $\times 6000$. 17, proximal view, UCL-2095-12, Trunch, *jamesoni* Zone (20), $\times 5200$. 18, oblique view of fig. 17, UCL-2095-11, $\times 5100$.



BOWN, early Mesozoic coccoliths

shield with triangular distal extensions which create a tangential inner cycle reaching half-way up the inner surface of the distal shield. The central area is filled by a large circular spine base which has a diameter equal to or just less than the width of the minor axis. This spine may be supported by a minor axis bar, a cross structure, or a complete basal plate. The spine is formed from granular microcrystals and flares distally, above the coccolith rim, to form an elongate, elliptical funnel aligned along the major axis of the ellipse.

Dimensions. L: 4.0–5.6 (4.0) μm , W: 2.6–3.6 (2.5) μm , RH: 1.1–2.1 μm , Spine base diameter: 0.9–1.6 μm , Spine funnel length: 2.7–3.6 μm , Spine funnel width: 0.8–2.1 μm , SH: 2.1–4.1 μm .

Remarks. *T. patulus* is an extremely long-ranging, conservative species which is common and consistent throughout the Lower Jurassic. It is distinguished from species of *Zeugrhabdotus* and *Crepidolithus* by its large, circular spine base and flaring distal funnel.

Occurrence. Badenweiler, *variabilis* Zone to *aalensis* Zone; Ballrechten, *bifrons* Zone to *levesquei* Zone; Brenha, Lower Sinemurian to Middle Jurassic; DSDP Site 547, Sinemurian to Toarcian; Hock Cliff, *bucklandi* Zone to *semicostatum* Zone; Longobucco, Pliensbachian to Lower Toarcian; Mochras, *semicostatum* Zone to *levesquei* Zone; Picun Leufu, Upper Pliensbachian to Toarcian; Timor, mid-Pliensbachian; Trimeusel, *tenicostatum* Zone to *levesquei* Zone; Trunch, *bucklandi* Zone to *jamesoni* Zone; Tunisia, Upper Pliensbachian to Toarcian; Unterstürmig, Lower Toarcian.

Range. Reported from throughout the Lower Jurassic in all the literature concerned. Its earliest occurrence was recorded from the *lasicus* Zone by Barnard and Hay (1974).

Genus ZEUGRHABDOTUS Reinhardt, 1965

Type species. *Zyolithus erectus* Deflandre, 1954.

Diagnosis. 'Two elliptical rings spanned by a single bar with a central process' (Reinhardt 1965, p. 37).

Remarks. *Zeugrhabdotus* is used in preference to *Zygodiscus* due to the differences in both structure and range. *Zygodiscus* has a Palaeocene type-species, *Z. adamas* Bramlette and Sullivan 1961, and while displaying a morphological likeness to the Mesozoic forms, is unlikely to be closely, if at all, related to them. In addition, the tall, thin wall of the Tertiary zygodiscids is distinguishable from the thick, blocky loxolith rims of the Mesozoic forms.

The emendation proposed by Black (1973), including a perforated basal membrane in the generic diagnosis, is rejected due to the dependence of this feature on exceptionally good preservation and its invisibility in the LM. The original *Zyolithus* has had a rather confusing history before becoming a junior synonym for *Neococcolithes*, leaving a number of species in need of transfer to an appropriate genus; a full discussion of its taxonomic history is given in Rood *et al.* (1971) and Medd (1979).

Zeugrhabdotus differs from *Archaeozygodiscus* in having a dextrally imbricating distal shield.

Zeugrhabdotus erectus (Deflandre, 1954) Reinhardt, 1965

Plate 2, figs. 7–9

- 1954 *Zyolithus erectus* Deflandre in Deflandre and Fert, p. 150, pl. 15, figs. 14–17; text-figs. 60–62.
- 1965 *Zeugrhabdotus erectus* (Deflandre); Reinhardt, p. 37.
- 1966 *Zyolithus erectus* Deflandre; Reinhardt, p. 40, pl. 15, fig. 3.
- 1971 *Zeugrhabdotus noeli* Rood *et al.*, pp. 252–253, pl. 1, fig. 4.
- 1973 *Zeugrhabdotus choffati* Rood *et al.*, pp. 369–370, pl. 1, fig. 7.
- 1973 *Zeugrhabdotus noeli* Rood *et al.*; Noël, pp. 99–100, pl. 1, figs. 1–4.
- 1974 *Zeugrhabdotus noeli* Rood *et al.*; Barnard and Hay, pl. 3, fig. 8; pl. 6, fig. 7.
- 1976a *Zeugrhabdotus noeli* Rood *et al.*; Moshkovitz and Ehrlich, pl. 1, figs. 1 and 2.
- 1984 *Zeugrhabdotus erectus* (Deflandre); Crux, fig. 10 (7, 8); fig. 13 (15, 16).

Diagnosis. 'Elliptical, with a relatively thick rim; perforated central area, cross-bar forms a bridge surmounted by a horn' (Deflandre 1954, p. 150).

Description. A small normally elliptical coccolith possessing a loxolith rim composed of a moderately high, vertical distal shield with twenty-five to thirty-five steeply inclined elements and a thin proximal shield constructed from around twenty-five subsquare elements with radial sutures and showing no distal extension. The proximal shield is spanned by a bar aligned along the minor axis of the ellipse, which bears a tall, central, hollow spine or spine base with a diameter equal to that of the bar's width and one-third of the width of the minor axis.

Dimensions. L: 2.5–4.6 (4.9) μm , W: 1.9–2.9 (3.3) μm , RH: \sim 1.0 μm , SH: \sim 2.6 μm .

Remarks. At least three specific names have been applied to Jurassic coccoliths which have a loxolith rim spanned by a spine-bearing bar aligned along the minor axis of the ellipse: *Zeughrabdodus erectus*, *Z. choffati*, and *Z. noeli*. After studying the published illustrations and descriptions, and comparing these with observations made in the present study, it is thought that the variation encountered within these three species is insufficient to warrant such separation and is acceptable as intraspecific variation. In the present work *Z. erectus* showed little morphological variation apart from in size and was identical to the original figures of Deflandre (1954). Further research in the Middle and Upper Jurassic may reveal stratigraphically useful and morphologically significant variation in this genus which has not yet, in my opinion, been successfully established.

The range of *Z. erectus* recorded here is limited to the uppermost Pliensbachian and Toarcian (perhaps earlier at DSDP Site 547), and throughout this range it is rare and inconsistent. This result contrasts with that of Barnard and Hay (1974) and Medd (1982) in which much earlier occurrences are claimed, but is confirmed by Prins (1969) and Crux (1984). Such a large discrepancy in range can only be explained by misidentification (e.g. *Z. erectus* and *P. liasicus* appear similar in the LM) or contamination. *Z. erectus* is distinguished from *Tubirhabdus patulus* by its smaller spine diameter, from *Crepidolithus cavus* by its smaller size, lower rim, and broader bar and spine, and from *A. koessenensis* by its dextral rim imbrication and lack of an inner cycle.

Occurrence. Badenweiler, *thouarsense* Zone to *aalensis* Zone; Ballrechten, *bifrons* Zone to *variabilis* Zone; Brenha, *spinatum* Zone to *levesquei* Zone; DSDP Site 547, Lower Pliensbachian; Mochras, *spinatum* Zone to *levesquei* Zone; Picun Leufu, Toarcian.

Range. Oxfordian (Deflandre 1954), Oxfordian (Noël 1965), *angulata* Zone to Kimmeridgian (Barnard and Hay 1974), *angulata* Zone to Portlandian (Medd 1982), *tenuicostatum* Zone (Crux 1984).

Family PARHABDOLITHACEAE BOWN, 1987

Diagnosis. 'Coccoliths with a protolith rim structure, i.e. a rim typically consisting of a dominant and characteristic distal shield composed of laths arranged vertically and subvertically and tangentially to an ellipse with sutures perpendicular to the coccolith base; and a proximal shield composed of elements with a triangular cross-section which form a flat coccolith base with radiating sutures and also extend upwards to form an inner cycle to the distal shield' (Bown 1987).

LM characteristics. As for the Zygodiscaceae; the imbrication or non-imbrication of the distal shield elements cannot be distinguished.

Remarks. The subfamily Parhabdolithoideae erected by Gartner (1968) was defined to include genera possessing loxolith rim structures, based on the misconception that *Parhabdolithus* typified loxolith construction. The family Apertiaceae erected by Goy (1981) is also unavailable as it is based on a coccolith which is a junior synonym of *Crucirhabdus primulus*. The Crepidolithaceae Black, 1971 is not used, as the genus *Crepidolithus* includes a majority of species which show considerable inclination of their outer wall elements and thus belong to the Zygodiscaceae Hay and Mohler, 1967.

Included genera. *Bucanthus*, *Crucirhabdus*, *Diductius*, *Mitrolithus*, *Parhabdololithus*, *Timorella*.

Range. Upper Triassic to ?Middle Jurassic.

Genus *CRUCIRHABDUS* Prins *ex* Rood, Hay and Barnard, 1973 emend.

Type species. *Crucirhabdus primulus* Prins *ex* Rood *et al.*, 1973.

Original diagnosis. 'Coccoliths with an eiffellithalid rim having a central structure in the form of a symmetrical cross in the major and minor axes of the ellipse, supported by one or more diagonal bars in each quadrant' (Rood *et al.* 1973, p. 367).

Emended diagnosis. Protolith coccoliths with a relatively high, narrow distal shield composed of vertical to subvertical elements and a proximal shield which is a thin basal disc composed of rectangular elements with triangular distal extensions forming a tangential inner cycle to the distal shield. The central area is spanned by a cross, aligned along the principal axes of the ellipse, which may be supported by one or more diagonal bars in each quadrant. The centre of the cross supports a tall, hollow spine.

Remarks. The genus *Crucirhabdus* was first used by Prins (1969) and included two species, *C. primulus* and *C. expansus*, with four additional 'varieties'. The lack of any formal description in the publication rendered these names invalid and in 1973, Rood *et al.* validated the genus and included two species, *C. primulus* and *C. prinsii*. The holotype proposed for the type species, *C. primulus*, is a narrow rimmed coccolith with a central cross and three diagonal bars in each quadrant. The paratype is a side view displaying the high rim composed of vertical to subvertical elements and a tall spine. Despite this the coccolith was described as possessing an eiffellithalid rim in which the outer wall is imbricating. Since 1973, *C. primulus* has been repeatedly used as a biostratigraphic marker and is well described and illustrated from the LM, e.g. Prins (1969), Thierstein (1976) and Jafar (1983). However, the species remained poorly illustrated via the SEM with only four micrographs published as *C. primulus*, two of these being the original holotype and paratype. In the present study *C. primulus* was easily recognizable in the LM but in the SEM, although a large number of specimens were observed, only very few possessed the supposedly diagnostic diagonal bars. These bars were present in three out of the five varieties of *Crucirhabdus* originally illustrated by Prins (1969) and were given generic significance by Rood *et al.* (1973). It is quite possible that the absence of these diagonal bars is due to preservation and/or original morphological variation. Thus an emended diagnosis is proposed which removes the restrictive need for one or more diagonal bars, to reflect the more usual modes of preservation. In addition, it includes more precise information concerning the rim structure.

Crucirhabdus minutus Jafar, 1983

Plate 2, figs. 12–14; Plate 12, figs. 15 and 16

1983 *Crucirhabdus minutus* Jafar, p. 247, fig. 12 (8, 9, 10a, 10b, 18).

1985 *Crucirhabdus minutus* Jafar; Bown, p. 33, pl. 1, figs. 4–7.

Abstracted 'diagnosis'. Tiny, broadly elliptical coccoliths (size range: 1.6–2.4 μm) which show similar morphological features under normal and crossed nicols as *C. primulus* but, unlike *C. primulus*, the two knobs visible along the minor axis of the coccolith are somewhat rounded, and distinct extinction lines demarcate equally large knobs at both ends of the major axis (abstracted from the LM description of Jafar 1983, p. 247, who proposed no formal diagnosis).

Diagnosis. An extremely small species of *Crucirhabdus* possessing high vertically to subvertically orientated distal shield elements and a thin proximal shield with only limited distal extension; the central area is spanned by a broad cross, aligned in the principal axes of the ellipse, and bears a tall, hollow central spine (Bown herein).

Description. The distal shield forms a high vertical to subvertical wall composed of around twenty broad, thin elements, joined along vertical sutures; in some specimens the rounded upper edge of each element gives the top of the wall a zigzag profile. The proximal shield takes the form of a thin basal disc which has little or no distal extension on the inner side of the distal wall. The central area is spanned by a broad cross which bears a tall, hollow spine.

Dimensions. L: 1.9–2.3 (1.6–2.4) μm , W: 1.4–1.6 μm , RH: 0.6–1.0 μm , SH: 1.5 μm .

Remarks. *C. minutus* was first observed in the LM only by Jafar (1983) and photographed in the SEM by Bown (1985), both studies based on material from the Upper Triassic of Alpine southern Germany and Austria. It has not yet been recorded from the Lower Jurassic.

C. minutus differs from *C. primulus* by its smaller size and lack of distal extension in its proximal elements.

Occurrence. Fischerwiese, Rhaetian; Weissloferbach, Rhaetian.

Range. Norian to Rhaetian (Jafar 1983).

Crucirhabdus primulus Prins, 1969 *ex* Rood, Hay and Barnard, 1973 *emend.*

Plate 2, figs. 15–18; Plate 3, figs. 1–3; Plate 12, figs. 17–20; text-fig. 10

- 1969 *Crucirhabdus primulus* var. *primulus* Prins, p. 552, pl. 2, fig. 2A–B; pl. 3, fig. 2A–B (*nom. nud.*).
 1969 *Crucirhabdus primulus* var. *nanus* Prins, p. 551, pl. 2, fig. 1A–B; pl. 3, fig. 1A–B; pl. 1, fig. 1A–B (*nom. nud.*).
 1969 *Crucirhabdus primulus* var. *striatulus* Prins, p. 554, pl. 3, fig. 3A–B (*nom. nud.*).
 1973 *Crucirhabdus primulus* Prins *ex* Rood *et al.*, pp. 367–368, pl. 1, figs. 1 and 2.
 1976 *Crucirhabdus primulus* Prins *ex* Rood *et al.*; Thierstein, pl. 2, figs. 1 and 2.
 1979 *Apertius dorei* Goy *in* Goy *et al.*, p. 40, pl. 2, fig. 6.
 1981 *Apertius dorei* Goy; Goy, pp. 34–35, pl. 9, figs. 9 and ?10; pl. 10, figs. 1–3; text-fig. 8.
 1983 *Crucirhabdus primulus* Prins *ex* Rood *et al.*; Jafar, pp. 244, 246, fig. 12 (14a, b, 15a, b).
 1984 *Apertius magnus* (Medd, 1979); Crux, fig. 8 (3).
 1984 *Stradnerlithus comptus* Black, 1971; Crux, fig. 10 (6).

Original diagnosis. 'A species of *Crucirhabdus* with 3 to 5 diagonal bars in each quadrant' (Rood *et al.* 1973).

Emended diagnosis. A species of *Crucirhabdus* which may possess up to five diagonal bars in each quadrant but which is more often observed possessing none.

Description. A normally elliptical protolith coccolith with a high, narrow, steep rim and a central area spanned by a spine-bearing cross. The distal shield is composed of twenty to thirty broad, thin elements, joined along vertical to subvertical sutures. The proximal shield is a thin basal ring of rectangular elements with triangular distal extensions creating a tangential inner cycle to the distal shield. The central area of the proximal shield is spanned by a cross, aligned along the principal axes of the ellipse, constructed from four curving bars upon which microcrystals have formed. A tall, hollow spine rises from the centre of the cross. A number of diagonal bars are occasionally observed in each quadrant formed by the crossbars.

Dimensions. L: 2.5–6.5 (2.9) μm , W: 1.7–4.5 (1.7) μm , RH: 0.5–2.0 μm , SH: ~4.5 μm .

Remarks. The comments made concerning the generic diagnosis also apply to *C. primulus* itself. The general absence of diagonal bars is thought to be predominantly a preservational feature, although it is also possible that this is due to intraspecific variation or dimorphism. Additional morphological variation includes rim height, rim inclination, element imbrication, and coccolith size. The rim varies in height between 0.5 and 2.0 μm and its inclination ranges from subvertical to 50° from horizontal. The elements within the rim are predominantly vertical, forming a typical protolith rim structure. However, some slight deviation from the vertical has been observed. The presence of size variation is especially clear in the Tethyan sections of Brenha and DSDP Site 547. Many Site 547 specimens also have lower rim heights and well-developed diagonal bars and are

thought to represent a morphological trend towards *Stradnerlithus clatriatus* which is also recorded from the same section.

Goy (1979, 1981) named, described, and illustrated a number of coccoliths which are considered to be synonymous with *C. primulus*. *Apertius dorei* possesses a sloping protolith rim and a central cross very similar to many specimens of *C. primulus* observed here. In addition, another coccolith illustrated by Goy (1979, 1981), *Saeprella vicina*, is almost identical to the *C. primulus* holotype but possesses a number of longitudinal elements linking together the diagonal bars. These illustrations highlight the problems which may arise when studying exceptionally well-preserved material in which delicate structures are retained that are normally lost or obscured. This problem can be eased by using central structure details for species designation only.

C. primulus differs from *P. liasicus* in having a lower rim height, a longitudinal bar, and subsidiary diagonal bars. It differs from members of the genus *Staurorhabdus/Stauroolithes* in possessing vertical rim elements.

Occurrence. Brenha, Lower Sinemurian to *davoei* Zone; DSDP Site 547, Sinemurian to Lower Pliensbachian; Hock Cliff, *bucklandi* Zone to *semicostatum* Zone; Mochras, *bucklandi* Zone to *margaritatus* Zone; Picun Leufu, Upper Pliensbachian; St Audries Slip, *angulata* Zone; Timor, mid-Pliensbachian; Trunch, *angulata* Zone to *jamesoni* Zone; Weissloferbach, *marshi* Zone, Rhaetian.

Range. Rhaetian to *tenuicostatum* Zone (Prins 1969), Lower Sinemurian to *margaritatus* Zone (Hamilton 1979), Lower Toarcian (Goy 1979, 1981), *suessi* Zone to *marshi* Zone (Jafar 1983), *oxynotum* Zone to *spinatum* Zone (Crux 1984).

C. primulus ranges from the Rhaetian to the *tenuicostatum* Zone (Lower Toarcian) but is rare and inconsistent in the upper part of its range and is often not recorded after the *margaritatus* Zone and *spinatum* Zone of the Upper Pliensbachian.

Genus DIDUCTIUS Goy, 1979

Type species. *Diductius constans* Goy, 1979.

Diagnosis. 'Coccoliths with a marginal rim of the Apertiaceae, i.e. Parhabdolitheaceae (2 superimposed series of elements; the distal series made up of vertical to subvertical elements, high and narrow) and a central area closed by a grid' (Goy 1979, p. 40).

Remarks. The type genus of the Apertiaceae, *Apertius*, is thought to be a synonym of *Crucirhabdus* and as the family is typified by an invalid generic name it is rendered invalid. The rim structure

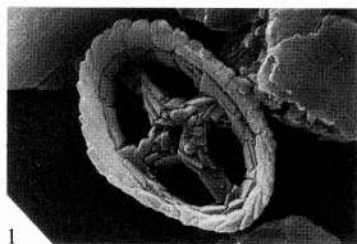
EXPLANATION OF PLATE 3

Figs. 1-3. *Crucirhabdus primulus* Prins ex Rood *et al.*, 1973. 1, distal view, UCL-2095-8, Trunch, *jamesoni* Zone (20), $\times 5000$. 2, oblique view of fig. 1, UCL-2095-9, $\times 5100$. 3, distal view, UCL-2193-8, DSDP Site 547, Sinemurian (18-1), $\times 8800$.

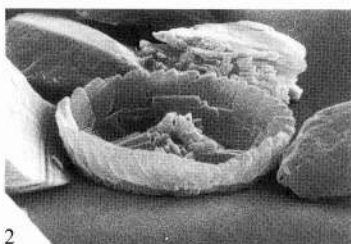
Figs. 4 and 5. *Diductius constans* Goy, 1979. Brenha, Bajocian (3617). 4, distal view, UCL-2173-6, $\times 4500$. 5, distal view, UCL-2198-35, $\times 8250$.

Figs. 6-15. *Mitrolithus elegans* Deflandre, 1954. 6-9, Trunch, *jamesoni* Zone (16). 6, side view, UCL-2097-33, $\times 6300$. 7, side view, UCL-2097-26, $\times 5650$. 8, distal view, spine missing, UCL-2095-25, $\times 5600$. 9, oblique view of fig. 8, UCL-2095-27, $\times 5650$. 10, detached spine, proximal view, UCL-1917-25, Mochras, *jamesoni* Zone (M306), $\times 9350$. 11, oblique view of fig. 10, UCL-1917-26, $\times 9000$. 12, broken, cross-sectioned spine, UCL-2149-1, Timor, mid-Pliensbachian (J237), $\times 4700$. 13, oblique view of fig. 12, UCL-2148-35, $\times 6200$. 14, distal view, UCL-2072-22, Timor, mid-Pliensbachian (J237), $\times 4700$. 15, side view of fig. 14, UCL-2072-23, $\times 4050$.

Figs. 16-18. *M. jansae* (Wiegand, 1984) Bown and Young, 1986. 16, side view, UCL-2046-36, DSDP Site 457, Sinemurian (22-1), $\times 7250$. 17, distal view of fig. 16, UCL-2047-8, $\times 9650$. 18, side view, UCL-2190-1, DSDP Site 547, Sinemurian (20-1), $\times 6550$.



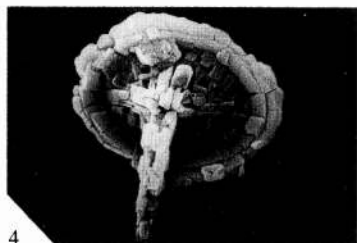
1



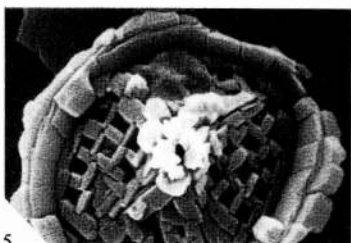
2



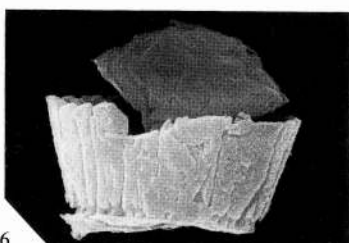
3



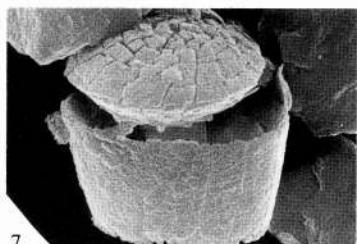
4



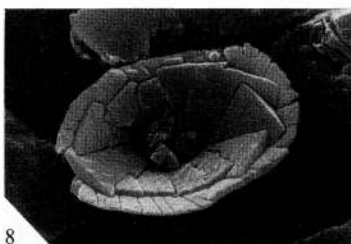
5



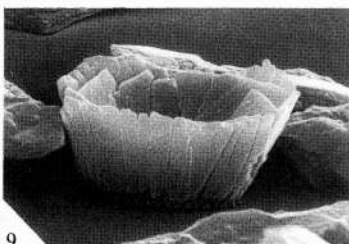
6



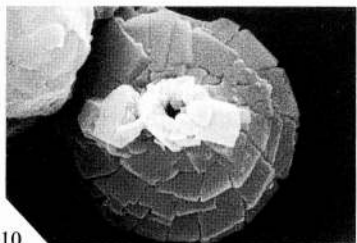
7



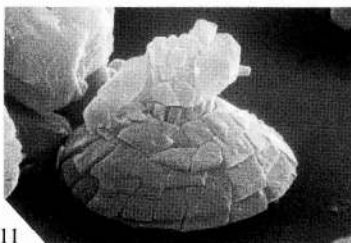
8



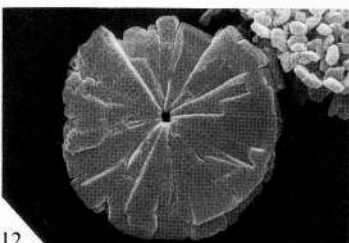
9



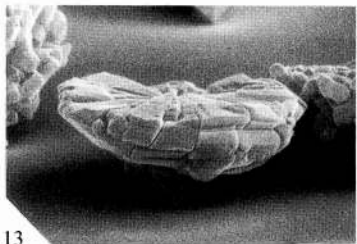
10



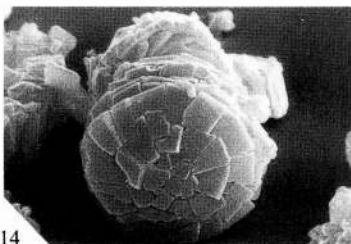
11



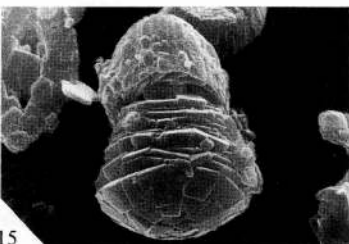
12



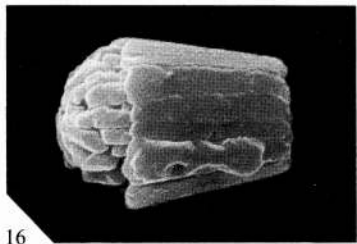
13



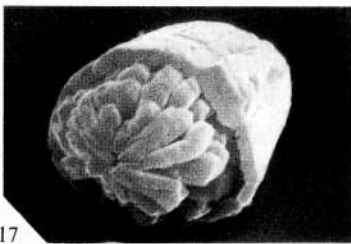
14



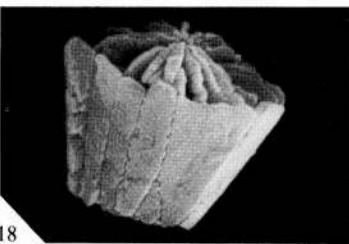
15



16



17



18

BOWN, *Crucirhabdus*, *Diductius*, *Mitrolithus*

described by Goy (1981) and characterizing his Family Apertiaceae is the protolith rim structure described in this paper.

Diductius differs from *Crucirhabdus* in having a lower rim height, shallower rim inclination, and a more complex central grill structure, and from *Stradnerlithus* by its gently sloping rim and well-developed inner cycle.

Diductius constans Goy, 1979

Plate 3, figs. 4 and 5; Plate 12, figs. 21 and 22; text-fig. 10

- 1979 *Cretarhabdus* sp. 1 Hamilton, pl. 2, figs. 6, 7, ?8.
 1979 *Diductius constans* Goy in Goy *et al.*, p. 40, pl. 2, fig. 7.
 1981 *Diductius constans* Goy; Goy, p. 36, pl. 10, figs. 5-8.

Diagnosis. 'A species of *Diductius* with a very marked longitudinal bar. The species is characterised by the presence of a grid with 3 rows of regularly aligned perforations' (Goy 1979, p. 40).

Description. A normally elliptical protolith coccolith with a low, gently sloping rim. The distal shield is constructed from around twenty-four non-imbricating elements. The proximal shield reaches half to three-quarters of the way up the inner surface of the distal shield and is composed of about twenty elements. The central area is filled by a distinctive convex grid structure supporting a central, tall, hollow spine. The grid is composed of a well-developed longitudinal bar aligned along the major axis, a very delicate bar aligned along the minor axis, five diagonal bars in each quadrant (formed by the principal axes crossbars) and three curving longitudinal bars which bisect the diagonal bars forming three regular rows of perforations. The diagonal and curving longitudinal bars are delicate structures formed from small interlocking laths.

Dimensions. L: 4.0-6.0 (3.4) μm , W: 3.0-5.0 (2.7) μm , RH: \sim 0.5 μm , SH: \sim 4.0 μm .

Remarks. *D. constans* is recorded from the Toarcian/Bajocian boundary of Brenha, the Upper Toarcian of Mochras, and from the Lower Toarcian of the Paris Basin by Goy (1979, 1981). The reason for its apparent absence in the other Toarcian sections is unknown but could be due to preservation, provincialism, or rarity after its first appearance in the Lower Toarcian. The specimens observed from Mochras have steeper rims and less well-defined inner cycles than the holotype and Brenha specimens, and they are similar to specimens of *Stradnerlithus*.

Occurrence. Brenha, uppermost Toarcian/Bajocian; Mochras, *falciferum* Zone.

Range. Lower Toarcian (Goy 1979, 1981), Bajocian (Hamilton 1979).

Genus MITROLITHUS Deflandre, 1954 emend. Bown and Young in Young *et al.* 1986

Type species. *Mitrolithus elegans* Deflandre, 1954.

Emended diagnosis. 'Coccoliths with an outer rim of thin, broad calcite laths orientated perpendicular to the base and tangential to the ellipse. The central area is filled by a massive boss or spine consisting of several superimposed cycles of radial calcite elements. The spine sits in the coccolith rim on an inner cycle of elements and is attached via a narrow, hollow spine base' (Bown and Young in Young *et al.* 1986, p. 129).

Mitrolithus elegans Deflandre, 1954

Plate 3, figs. 6-15; Plate 12, figs. 23-28

- 1954 *Mitrolithus elegans* Deflandre in Deflandre and Fert, p. 148, pl. 15, figs. 9-11; text-figs. 66 and 67.
 1965 *Alvearium dorsetense* Black, pp. 133, 136, fig. 5.
 1967 *Alvearium dorsetense* Black, p. 139.
 1987 *Mitrolithus elegans* Deflandre; Bown, pl. 3, figs. 1-3.

Diagnosis. 'Basin which in lateral view is slightly flaring, surmounted by a mace (masse) which is initially narrow before broadening out and rounds off at its top' (Deflandre 1954, p. 148).

Description. A protolith coccolith with a steeply sloping, tall, distal shield constructed from twenty-five to thirty tangentially and vertically arranged rectangular elements; the proximal shield forms a basal disc which completely fills the central area around a central hole. The proximal shield elements also have triangular distal extensions forming an inner cycle to the distal shield. This inner cycle is composed of twelve to thirty elements arranged tangentially on the inner surface of the distal shield, each element overlapping the next in a counter-clockwise direction. The elements slope inwards towards a small central circle of elements which is the hollow spine base (the inner cycle and spine base can only be seen if the spine is missing). The spine rises from the spine base and rapidly flares out, following the contours of the sloping inner cycle 'basin', until a point just above the coccolith rim (where its diameter often exceeds that of the coccolith base) from where it terminates in a domed upper surface. The spine is lenticular in cross-section, circular in plan view, and constructed from five or six superimposed conical rings of differing diameters, each consisting of radiating wedge-shaped elements. The ring with the greatest diameter has sixteen to eighteen elements and up to seventy elements are visible on the upper face of the spine (Pl. 3, figs. 10-14). A number of specimens from the Timor sample displayed further elevation of the spine due to an increased number of superimposed rings of equal diameter forming a broad, parallel-sided column before terminating in the domed top (Pl. 3, fig. 15).

Dimensions. L: 3.6-7.2 (5.5) μm , W: 2.6-5.6 μm , RH: 1.9-3.2 μm , Spine diameter: 3.7-5.8 (4.6) μm , SH: 4.2-6.4 (5.9) μm , Spine base: 0.7-1.2 μm .

Remarks. A highly distinctive coccolith characteristic of very early Jurassic assemblages. The spine and base commonly become separated and this has led to the separate naming of the spine as *Alvearium dorsetense*.

Occurrence. Brenha, Lower Sinemurian to *spinatum* Zone; DSDP Site 547, Sinemurian to Upper Pliensbachian; Hock Cliff, *semicostatum* Zone; Longobucco, Lower Pliensbachian to Lower Toarcian (*tenuicostatum* Zone); Mochras, *semicostatum* Zone to *davoei* Zone; Timor, mid-Pliensbachian; Trunch, *bucklandi* Zone to *jamesoni* Zone; Tunisia, Upper Pliensbachian.

Range. Oxfordian (Deflandre 1954), *bucklandi* Zone to *margaritatus* Zone (Prins 1969), *ibex* Zone (Rood *et al.* 1973), *jamesoni* Zone to *bifrons* Zone (Crux 1984).

The range of *M. elegans* recorded in the present study was Lower Sinemurian to Lower Toarcian. It becomes rare and sporadic in occurrence during the Upper Pliensbachian. Both the spine and base have been recorded in younger sediments, e.g. Deflandre (1954), Medd (1982, Appendix IIc), and this is due to reworking.

Mitrolithus jansae (Wiegand, 1984) Bown and Young in Young *et al.* 1986

Plate 3, figs. 16-18; Plate 4, figs. 1-3; Plate 13, figs. 1-4

1969 *Mitrolithus irregularis* Prins, pl. 1, fig. 12 (*nom. nud.*).

1984a *Calcivascularis jansae* Wiegand, pp. 1151-1152, fig. 1 (A-G).

1984b *Calcivascularis jansae* Wiegand; Wiegand, pp. 665-666, pl. 3, fig. 4.

1986 *Mitrolithus jansae* (Wiegand); Bown and Young in Young *et al.*, pp. 130-131, pl. 1, figs. A, D, G, H.

1987 *Mitrolithus jansae* (Wiegand); Bown, pl. 3, fig. 4.

Diagnosis. 'A basket shaped nannolith filled with a core consisting of many radially arranged elements' (Wiegand 1984, p. 1152).

Description. The description given in Wiegand (1984a) is comprehensive, but there is great variation in the dimensions of the coccolith rim, especially in height. This variation appears to have no stratigraphic significance, with much variance encountered in all the samples studied. It is thus considered intraspecific variation, perhaps related to the position of the coccolith on the coccosphere.

Dimensions. L: 3.0-4.6 (3.5) μm , W: 2.2-3.2 μm , RH: 2.3-5.3 (2.5) μm .

Remarks. *M. jansae* has an almost completely restricted Tethyan distribution, where it dominates Sinemurian to Lower Toarcian nannofossil assemblages and characterizes a Tethyan nannofloral

realm. It has been found very rarely in the Mochras and Trunch sections and is recorded by Prins (1969) suggesting only occasional movement into the Boreal nannofloral realm. The striking similarity and possible evolutionary links between *M. jansae* and the Upper Triassic nannofossil *Conusphaera zlabachensis* are discussed later in the paper.

M. jansae is distinguished from *M. elegans* by its taller morphology and differing spine shape and construction, from *C. zlabachensis* by its differentiated central core and core ultrastructure, and from species of *Calcicalathina* by its regularly structured, radiating spine structure and stratigraphic range.

Occurrence. Brenha, Lower Sinemurian to *spinatum* Zone; DSDP Site 547, Sinemurian to Upper Pliensbachian; Longobucco, Lower Pliensbachian to *tenuicostatum* Zone; Mochras, *jamesoni* Zone to *tenuicostatum* Zone; Trunch, *rariocostatum* Zone to *jamesoni* Zone; Tunisia, Upper Pliensbachian to Lower Toarcian.

Range. *davoei* Zone to *spinatum* Zone (Prins 1969); Upper Sinemurian to Lower Pliensbachian (Wiegand 1984b).

The Tethyan range of *M. jansae* is at least Lower Sinemurian to Lower Toarcian. In the north-west European area the range appears to be similar but *M. jansae* is always extremely rare or absent.

Mitrolithus lenticularis sp. nov.

Plate 4, figs. 4–7; Plate 12, figs. 29 and 30

Diagnosis. A species of *Mitrolithus* with a spine which completely fills the central area and has a domed upper surface which coincides with the rim top; the spine is irregularly structured and oval in plan view.

Description. A coccolith with a protolith rim structure very similar to that of *M. elegans*. The central area is completely filled by a lenticular spine with a domed upper surface which fits flush with the upper edge of the coccolith rim. The upper surface of the spine is made up of eighteen to twenty square and rectangular blocks which are intergrown in a random arrangement.

Dimensions. L: 4.5–5.4 (4.5) μm , W: 2.7–3.7 (2.7) μm , RH: 1.9–3.2 (2.1) μm , SH: 3.3–4.2 (3.7) μm .

Remarks. *M. lenticularis* is distinguished from *M. elegans* by its smaller size, its flush spine, and the less regular spine construction.

Derivation of name. From Latin *lenticularis*, lentil-like, referring to the spine shape.

EXPLANATION OF PLATE 4

Figs. 1–3. *Mitrolithus jansae* (Wiegand, 1984) Bown and Young, 1986. 1, side view, UCL-2046-31, DSDP Site 547, Lower Pliensbachian (15-1), $\times 6850$. 2, distal view, UCL-2190-3, DSDP Site 547, Sinemurian (20-1), $\times 7050$. 3, damaged specimen revealing inner structure, UCL-2190-6, DSDP Site 547, Sinemurian (20-1), $\times 6100$.

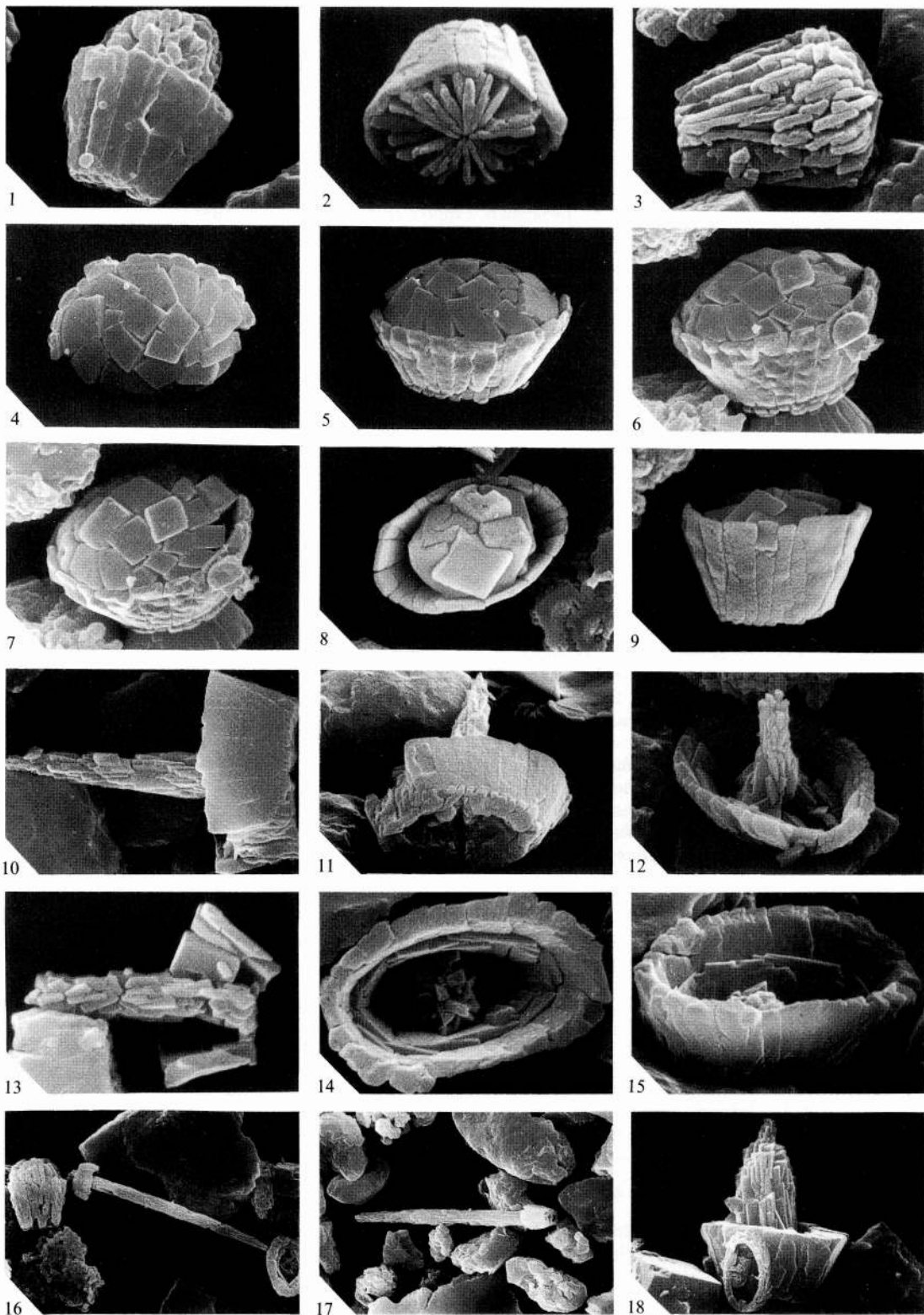
Figs. 4–7. *M. lenticularis* sp. nov. Timor, mid-Pliensbachian (J237). 4, isotype, distal view, UCL-2148-25, $\times 6750$. 5, side view of fig. 4, UCL-2148-26, $\times 6450$. 6, holotype, oblique view, UCL-2074-14, $\times 7300$. 7, distal view of fig. 6, UCL-2074-15, $\times 7300$.

Figs. 8 and 9. *Mitrolithus* sp. DSDP Site 547, Sinemurian (20-1). 8, distal view, UCL-2189-35, $\times 6050$. 9, side view, $\times 6550$, UCL-2189-30, $\times 6550$.

Figs. 10–15. *Parhabdololithus liasicus distinctus* Deflandre, 1952 ssp. nov. 10, side view, UCL-1937-11, Mochras, *rariocostatum* Zone (M292), $\times 6100$. 11, proximal view of fig. 10, UCL-1937-10, $\times 6150$. 12, distal view, UCL-2190-14, DSDP Site 547, Sinemurian (22-2), $\times 6150$. 13, cross-section, UCL-2074-33, Timor, mid-Pliensbachian (J237), $\times 7300$. 14, distal view, UCL-1916-15, Mochras, *ibex* Zone (M339), $\times 8200$. 15, oblique view of fig. 14, UCL-1916-14, $\times 8250$.

Figs. 16 and 17 *P. l. liasicus* Deflandre, 1952 ssp. nov. DSDP Site 547, Lower Pliensbachian (15-1). 16, side view, UCL-2199-23, $\times 2100$. 17, side view, UCL-2028-36, DSDP Site 547, $\times 2150$.

Fig. 18. *P. marthae* Deflandre, 1954. 18, side view, UCL-2268-34, Hock Cliff, *bucklandi* Zone (H3), $\times 4300$.



BOWN, *Mitrolithus*, *Parhabdolithus*

Holotype. UCL-2074-14, UCL-2074-15 (Pl. 4, figs. 6 and 7).

Isotype. UCL-2148-25, UCL-2148-26 (same specimen).

Type level. Mid-Pliensbachian (J237).

Type locality. Timor.

Occurrence. Brenha, *ibex* Zone to *davoei* Zone; DSDP Site 547, Upper Sinemurian to Lower Pliensbachian; Mochras, *jamesoni* Zone; Timor, mid-Pliensbachian; Trunch, *ravicostatum* Zone; Tunisia, Upper Pliensbachian to Lower Toarcian.

Genus PARHABDOLITHUS Deflandre, 1952 emend. Bown, 1987

Type species. *Parhabdolithus liasicus* Deflandre, 1952.

Emended diagnosis. 'Coccoliths with a high protolith rim and a central area bearing a spine which may vary greatly in diameter and height. The spine is borne on a bar or basal plate and has an axial canal' (Bown 1987).

Parhabdolithus liasicus Deflandre, 1952

Remarks. *P. liasicus* is considered to be represented by two subspecies which will be described separately below.

Parhabdolithus liasicus distinctus Deflandre, 1952 ssp. nov.

Plate 4, figs. 10–15; Plate 13, figs. 5–8

- 1952 *Parhabdolithus liasicus* Deflandre, p. 466, text-fig. 362 (J, L, M, non K).
 1954 *Parhabdolithus liasicus* Deflandre; Deflandre in Deflandre and Fert, p. 162, text-figs. 105–108 (non 104; non pl. 15, figs. 28–31).
 1965 *Parhabdolithus liasicus* Deflandre; Noël, p. 92, pl. 3, fig. 7; text-fig. 22d (non pl. 4, figs. 3, 4, 7; text-fig. 22a–c, e).
 1965 *Parhabdolithus marthae* Deflandre 1954; Noël, pl. 4, fig. 6; pl. 3, fig. 6; text-fig. 23b–e.
 1974 *Parhabdolithus liasicus* Deflandre; Barnard and Hay, pl. 4, fig. 9; (non pl. 1, fig. 9).
 1977 *Parhabdolithus liasicus* Deflandre; Hamilton, pl. 4, figs. 7 and 8.
 1979 *Parhabdolithus marthae* Deflandre; Medd, pl. 1, fig. 10.
 1984 *Parhabdolithus liasicus* Deflandre; Crux, fig. 8 (8, 10); fig. 14 (5, 8, 12); (non fig. 8 (9), fig. 14 (13, 15)).

Diagnosis. A subspecies of *P. liasicus* possessing a tall, hollow spine which tapers to a point; the spine diameter varies between one-third and one-fifth of the coccolith length, and spine height varies between two and six times the coccolith rim height.

Description. A normally elliptical protolith coccolith composed of a moderately narrow, steeply sloping and high distal shield formed from approximately thirty vertically arranged, rectangular laths, and a proximal shield with around thirty subsquare elements which extend vertically to form a tangential inner cycle to the distal shield. The proximal shield is spanned, along the minor axis, by a bar which has a median groove along its length and a central hole. On its distal side the bar supports a tall, hollow, tapering spine constructed from elongate, intergrown, and radiating rhombohedral elements. In some specimens the central area is completely infilled with granular calcite and the spine rises from this basal plate. The spine dimensions are highly variable between the limits stated in the species diagnosis.

Dimensions. L: 3.7–6.8 μm , W: 2.4–4.3 μm , RH: 1.2–2.5 μm , SH: 5.0–8.0 μm (holotype dimensions unknown).

Remarks. The original illustrations of *P. liasicus* in Deflandre (1952, 1954) and all subsequent studies recorded great variety in spine morphology, quite apart from the additional species *P. marthae* and *P. robustus*. In the present study the variation encountered was not continuous but fell into two categories. The first category included coccoliths coinciding with the *P. liasicus*

illustrations of Deflandre (1952, fig. 362J, L) possessing a deep, basin-like rim from which a relatively thin spine arose. The second category included coccoliths coinciding with the illustrated holotype of Deflandre (1954, fig. 104) with a proportionally small, deep basin from which an extremely tall spine arose which is broad compared to the basin's width. Both these groups appear to share the same range, with the former category almost always much more abundant than the latter. It seems reasonable to assume that they represent an example of coccosphere dimorphism. The extremely long spines of the second category, *P. l. liasicus*, are quite typical of the specialized coccoliths and scales in many present-day prymnesiophytes, where they are commonly positioned around the flagella bases or at either end of elongated coccospheres, e.g. *Chrysochromulina prinsheimii* Parke and Manton, 1962. Such a coccosphere in the case of *P. liasicus* would explain the coincident stratigraphic range of the two coccolith types and also account for the consistently differing abundances. Thus, it is proposed that the 1954 holotype illustration of *P. liasicus* (Deflandre 1954, fig. 104) becomes the holotype of *P. l. liasicus*, while the 1952 illustration of *P. liasicus* (Deflandre 1952, fig. 362L) becomes the holotype of *P. l. distinctus*. This division was recognized by Prins (1969) but his lack of formal description renders his naming invalid.

P. l. distinctus is an abundant, distinctive, and consistent component of the nannofossil assemblages from the Hettangian to the lowermost Toarcian. Specimens found higher than the upper range limit stated are thought to be reworked, e.g. the Oxfordian assemblage of Deflandre (1952, 1954).

Occurrence. Brenha, Lower Sinemurian to *spinatum* Zone; DSDP Site 547, Sinemurian to Pliensbachian; Hock Cliff, *bucklandi* Zone to *semicostatum* Zone; Mochras, *semicostatum* Zone to *tenuicostatum* Zone; Picun Leufu, Upper Pliensbachian; Timor, mid-Pliensbachian; Trunch, *bucklandi* Zone to *jamesoni* Zone.

Range. Oxfordian (Deflandre 1952, 1954); Sinemurian to Bajocian (Stradner 1963); Pliensbachian to Portlandian (Noël 1965); *bucklandi* Zone to *tenuicostatum* Zone (Prins 1969); *bucklandi* Zone to *margaritatus* Zone (Barnard and Hay 1974); Hettangian to Oxfordian (Medd 1982); *oxynotum* Zone to *bifrons* Zone (Crux 1984).

Parhabdolithus liasicus liasicus Deflandre, 1952 ssp. nov.

Plate 4, figs. 16 and 17; Plate 13, figs. 9 and 10

- 1952 *Parhabdolithus liasicus* Deflandre, text-fig. 362K.
 1954 *Parhabdolithus liasicus* Deflandre; Deflandre in Deflandre and Fert, text-fig. 104; pl. 15, figs. 28-31.
 1965 *Parhabdolithus liasicus* Deflandre; Noël, text-fig. 22c; pl. 4, figs. 3 and 4.
 1969 *Parhabdolithus longispinus* Prins, pl. 2, fig. 5 (*nom. nud.*).
 1974 *Parhabdolithus liasicus* Deflandre; Barnard and Hay, pl. 1, fig. 9.
 1984 *Parhabdolithus liasicus* Deflandre; Crux, fig. 8 (9); fig. 14 (13, 15).

Diagnosis. A subspecies of *P. liasicus* with a much reduced rim from which an extremely tall spine rises, tapering gradually to a point but parallel or subparallel for much of its length. The spine diameter is between one-third and one-half the length of the coccolith rim and has a height at least eight times that of the rim height.

Description. Similarly constructed to *P. l. distinctus*; however, the rim dimensions are reduced while the spine is similar in diameter but much longer and less rapidly tapering.

Dimensions. L: 2.8-3.6 (3.5) μm , W: 1.6-2.0 μm , RH: 1.0-2.0 (2.0) μm , SH: 13.5-17.6 (14.2) μm .

Remarks. See *P. l. distinctus*.

Occurrence. Brenha, Lower Sinemurian to *davoei* Zone; DSDP Site 547, Sinemurian to Pliensbachian; Hock Cliff, *bucklandi* Zone to *semicostatum* Zone; Mochras, *semicostatum* Zone to *margaritatus* Zone; Picun Leufu, Upper Pliensbachian; Timor, mid-Pliensbachian; Trunch, *bucklandi* Zone to *jamesoni* Zone.

Range. *jamesoni* Zone to *davoei* Zone (Prins 1969).

Parhabdolithus marthae Deflandre, 1954

Plate 4, fig. 18; Plate 5, figs. 1 and 2; Plate 13, figs. 11–14

- 1954 *Parhabdolithus marthae* Deflandre in Deflandre and Fert, p. 163, pl. 15, figs. 22 and 23; text-figs. ?101 and ?102 (*non* 103).
 1965 *Parhabdolithus marthae* Deflandre; Noël, pp. 93–94, text-fig. 23a (*non* pl. 3, fig. 6; pl. 4, fig. 6; text-fig. 23b–e).
 1965 *Parhabdolithus robustus* Noël, text-fig. 24.
 1965 *Parhabdolithus liasicus* Deflandre 1952; Noël, text-fig. 22a, b, e.
 1969 *Parhabdolithus marthae* Deflandre; Prins, pl. 2, fig. 6A, B.
 1980 *Parhabdolithus marthae* Deflandre; Grün and Zweili, p. 290, pl. 13, figs. 11 and 12.

Diagnosis. 'Basal basin with a bottom little or not raised, bearing a robust stem, whose initial diameter exceeds one third the length of the basin; short, conical spine or more expanded, but does not exceed much over double the height of the basin, with a very distinct axial canal. Shape of its appearance is rather variable as regards the development of the spine but it is always more robust than *P. liasicus*' (Deflandre 1954, p. 163).

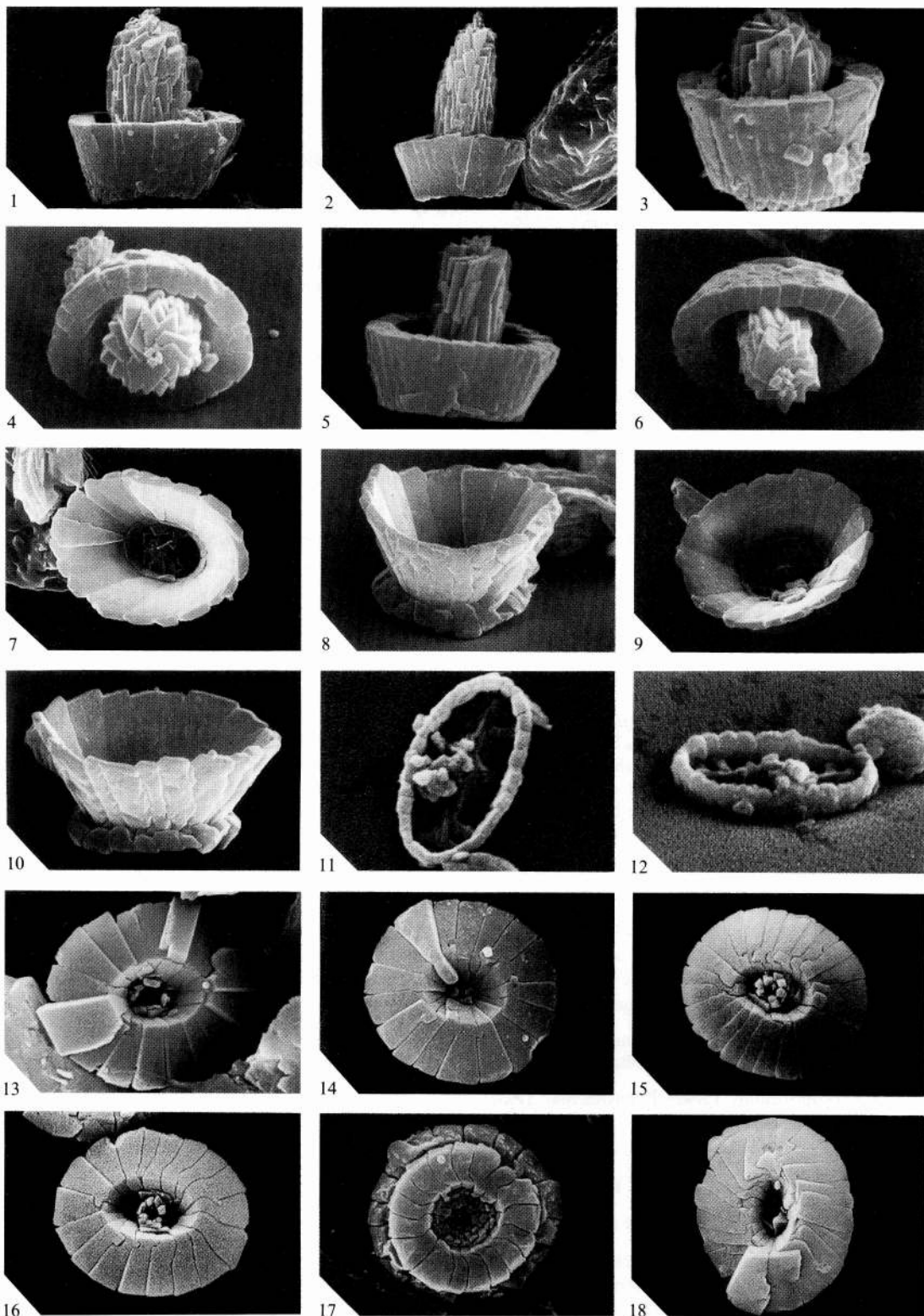
Description. A coccolith possessing a thick, steep protolith rim typical of *Parhabdolithus*. The distal shield is composed of approximately twenty thick, vertical elements. The proximal shield is a thin basal disc with triangular vertical extensions. In distal view the deep central area is completely filled by a very broad spine which may be parallel sided for some of its length before tapering sharply to a point. In proximal view the central area is filled by microcrystals which form a central depression marking the axial canal of the spine. The spine is formed from elongate, intergrown rhombohedra and has a width around one-half the length of the rim. Spine height rarely exceeds three times the rim height.

Dimensions. L: 5.1–5.9 (5.7) μm , W: 4.0–4.5 μm , RH: 2.2–2.7 (3.5) μm , SH: 5.8–8.0 (10.0) μm .

Remarks. *P. marthae* has been repeatedly used as a total range zone fossil, but none the less remains a badly illustrated and poorly defined species. Deflandre (1954) described *marthae* as a *Parhabdolithus* species bearing a bloated conical spine. Noël (1965) used line diagrams to illustrate the variations found in both *P. marthae* and *P. liasicus* and included continuous variation from thin, tall spines (fig. 22c), through short, tapering spines (figs. 23a–e and 24) to bloated spines (fig. 22b, e). Noël (1965) placed those forms with short, tapering spines in *P. marthae* and those with tall thin spines and bloated spines in *P. liasicus*. Two of the latter category (fig. 22b, e) are almost identical to the holotype of *P. marthae* (Deflandre 1954). Prins (1969) illustrates *P. marthae* with

EXPLANATION OF PLATE 5

- Figs. 1 and 2. *Parhabdolithus marthae* Deflandre, 1954. 1, side view, UCL-2082-30, Hock Cliff, *semicostatum* Zone (H13), $\times 5150$. 2, side view, UCL-2268-33, Hock Cliff, *bucklandi* Zone (H3), $\times 3800$.
 Figs. 3–6. *P. robustus* Noël, 1965. 3, side view, UCL-2072-5, Timor, mid-Pliensbachian (J237), $\times 8000$. 4, distal view of fig. 3, UCL-2072-3, $\times 8150$. 5, side view, UCL-2097-3, Trunch, *raricostatum* Zone (TR21), $\times 6400$. 6, distal view of fig. 5, UCL-2097-4, $\times 6800$.
 Figs. 7–10. *Timorella cypella* gen. et sp. nov. Timor, mid-Pliensbachian (J237). 7, holotype, distal view, UCL-2149-6, $\times 4900$. 8, side view of fig. 7, UCL-2149-4, $\times 6300$. 9, isotype, distal view, UCL-2117-16, $\times 6650$. 10, side view of fig. 9, UCL-2117-15, $\times 8350$.
 Figs. 11 and 12. *Stradnerlithus clatriatus* (Prins ex Rood *et al.*, 1973) Goy, 1979. DSDP Site 547, Sinemurian (22-1). 11, distal view, UCL-2049-6, $\times 9400$. 12, oblique view of fig. 11, UCL-2049-7, $\times 10\ 500$.
 Figs. 13–17. *Biscutum novum* (Goy, 1979) Bown, 1987. 13, distal view, UCL-1952-19, Mochras, *ibex* Zone (M341), $\times 8300$. 14, distal view, UCL-2290-26, Ballrechten, *thouarsense* Zone (9), $\times 6000$. 15, distal view displaying some suture cross-cutting, UCL-2178-27, Brenha, Upper Toarcian (3606), $\times 6150$. 16, distal view, UCL-2170-36, Brenha, *ibex* Zone (3531), $\times 7500$. 17, proximal view, UCL-2290-27, Ballrechten, *thouarsense* Zone (9), $\times 6500$.
 Fig. 18. *B. finchii* Crux, 1984. 18, distal view, UCL-2170-23, Brenha, *ibex* Zone (3531), $\times 4900$.



BOWN, *Parhabdolithus*, *Timorella*, *Stradnerlithus*, *Biscutum*

a short, bloated spine and records its range as limited to the Lower Sinemurian, a range which has also been reported in subsequent studies.

P. marthae must be used with care as a zonal fossil as its morphology may be imitated by overgrowth on *P. liasicus*.

Occurrence. Brenha, Lower Sinemurian; Hock Cliff, *bucklandi* Zone to *semicostatum* Zone; Mochras, *semicostatum* Zone; Trunch, *bucklandi* Zone.

Range. Oxfordian (Deflandre 1954); Pliensbachian (Noël 1965); *bucklandi* Zone to *semicostatum* Zone (Prins 1969); *bucklandi* Zone to *semicostatum* Zone (Barnard and Hay 1974); Lower to Upper Sinemurian (Hamilton 1977); *bucklandi* Zone to Kimmeridgian (Medd 1982); Lower Sinemurian (Wiegand 1984b).

As with *P. liasicus*, *P. marthae* is found reworked in rocks far younger than its restricted Lower Jurassic range.

Parhabdolithus robustus Noël, 1965

Plate 5, figs. 3–6; Plate 13, figs. 15 and 16

1965 *Parhabdolithus robustus* Noël, p. 95, pl. 4, figs. 1 and 2 (*non* text-fig. 24).

1969 *Bidiscorhabdus ocellatus* Prins, pl. 2, fig. 7B (*nom. nud.*).

1987 *Parhabdolithus robustus* Noël; Bown, pl. 1, figs. 5 and 6; pl. 2, figs. 8 and 9.

1987 *Parhabdolithus zweilii* Crux, pl. 1, figs. 1–4.

Diagnosis. '*Parhabdolithus* of classic structure: massive calcite pieces inclining very little constitute the wall resting on a floor made up of small blades of calcite which are thick and horizontal, raised from its centre at the start of the spine; the spine is very stocky, broadly truncated at its extremity, composed of calcite rhombohedra arranged in a star shape around a central canal' (Noël 1965, p. 95).

Description. *P. robustus* has a rim structure very similar to that of *P. marthae* with a steeply sloping, high distal shield composed of around twenty-five tall, vertical elements and a proximal shield of subsquare elements with distal extensions forming an inner cycle to the distal shield. The central area is almost entirely filled by a short, broad spine which terminates bluntly without tapering. The spine has a diameter greater than half the width of the coccolith base and terminates at or just above the coccolith rim but usually at a height no greater than twice that of the rim itself. The spine is composed of eight to fifteen intergrown columnar, radial calcite rhombohedra which give it a star-like appearance in plan view. On its flattened top a small ring of tiny elements surrounds a central canal.

Dimensions. L: 3.7–5.0 (3.2) μm , W: 2.0–3.6 (2.0) μm , RH: 1.8–3.1 (1.2) μm , Spine diameter: 1.6–3.0 (1.2) μm , SH: 3.5–4.4 (3.6) μm , SH above rim: 0.2–2.6 (1.6) μm .

Remarks. *P. robustus* is a distinctive coccolith which is rare and sporadic in the lower part of its range (Sinemurian) but fairly abundant in *jamesoni* Zone assemblages. It is very abundant in Timor sample J237. *P. robustus* is distinguished from other species of *Parhabdolithus* by its broad, short and bluntly terminated spine.

Occurrence. Brenha, Lower Sinemurian to *jamesoni* Zone; DSDP Site 547, Sinemurian; Mochras, *turneri* Zone to *ibex* Zone; Timor, mid-Pliensbachian; Trunch, *jamesoni* Zone.

Range. Charmouthian, Lower Pliensbachian (Noël 1965); ?*jamesoni* Zone to *davoei* Zone (Prins 1969).

Genus TIMORELLA gen. nov.

Type species. *Timorella cypella* sp. nov.

Derivation of name. From the type locality, Timor.

Diagnosis. Elliptical, tapering cup-like nannofossil with vertically arranged distal elements and a distinctive proximal ring of elements which form a basal flange on which the distal elements sit. The floor of the deep central area is filled with a granular plate in the type species.

Remarks. The genus *Timorella* has been placed in the Parhabdolithaceae because of its protolith rim structure which is only slightly modified.

Timorella cypella sp. nov.

Plate 5, figs. 7-10; Plate 13, figs. 17 and 18

Diagnosis. A species possessing the distinctive rim structure of the genus and having a central area filled with a granular plate.

Description. A sloping distal shield is formed by sixteen to twenty tall, tapering rectangular elements which are non-imbricating and joined along vertical sutures. The distal elements form an elliptical tapering cup around a small central area. The proximal shield forms a low inner cycle around the central area but also extends outwards, some way beyond the edge of the distal elements to form a sloping outer flange which may be likened to a pedestal on which the cup sits. The proximal shield is formed from around twenty non-imbricating elements. The central area is filled by a plate formed from granular calcite rhombohedra.

Dimensions. L: 4.7-6.6 (6.6) μm , W: 3.7-4.6 (4.6) μm , H: 1.7-2.8 (2.2) μm ; Central area L: (2.2) μm , W: (1.5) μm .

Derivation of name. From Latin *cypellum*, cup.

Holotype. UCL-2149-6, UCL-2149-4 (Pl. 5, figs. 7 and 8).

Isotype. UCL-2117-15, UCL-2117-16 (same specimen).

Type locality. Timor.

Type level. Mid-Pliensbachian (J237).

Occurrence. Found only in the type material.

Genus *BUCANTHUS* gen. nov.

Type species. *Bucanthus decussatus* sp. nov.

Derivation of name. From Latin *bu-*, prefix meaning large, and *canthus*, rim.

Diagnosis. Large, elliptical coccoliths with a low, sloping protolith rim consisting of a distal shield of non-imbricating, vertically arranged elements and a proximal shield with vertical extensions forming an inner cycle to the distal shield; wide central area spanned by crossbars bearing a spine.

Remarks. The genus *Bucanthus* is distinguished from *Chiastozygus* by its vertically arranged rim elements and from other genera with protolith rims by its very large, low rim and its wide central area spanned by an asymmetric cross (in the case of the type species).

Bucanthus decussatus sp. nov.

Plate 2, figs. 10 and 11; Plate 12, figs. 13 and 14

Diagnosis. Large coccolith with a low, sloping protolith rim, a prominent inner cycle, and a wide central area spanned by an asymmetric cross, bearing a central spine. The longitudinal bars are parallel but considerably offset, to the left and right of the major axis; and the transverse bars are slightly offset above and below the minor axis.

Description. The large protolith rim is low, sloping, relatively narrow and composed of around fifty vertical distal shield elements and thirty-five proximal shield elements which form a tangential inner cycle three-quarters of the height of the distal elements. The wide, open central area is spanned by an asymmetric cross structure which bears a central spine. When viewed distally, the upper longitudinal bar is offset to the left and the lower longitudinal bar to the right of the major axis of the ellipse; the left transverse bar is offset above and the right transverse bar offset below the minor axis of the ellipse. The bars are approximately

parallel with the respective principal axes of the ellipse and curve into the centre of the central area to support a central spine. The bars are constructed from numerous, elongate calcite elements.

Dimensions. L: (7.0) μm , W: (5.2) μm , RH (1.1) μm .

Remarks. *B. decussatus* has only been recorded from Timor and it is probable that this species has a restricted distribution in the southern Tethys-Pacific. Such a large, distinctive coccolith would not have escaped notice in north-west European and Mediterranean-Tethys studies.

Derivation of name. From Latin *decussatus*, like the letter X.

Holotype. UCL-2117-30, UCL-2117-33 (Pl. 2, figs. 10 and 11).

Isotype. UCL-2265-18, UCL-2265-19 (same LM specimen).

Type locality. Timor (J237).

Type level. Mid-Pliensbachian.

Family STEPHANOLITHIACEAE Black, 1968

Diagnosis. 'Hollow coccoliths with a cylindrical or polygonal wall consisting of elements which are not markedly imbricate, and within the wall an open framework of rods arranged radially or otherwise' (Black 1973, p. 92).

LM characteristics. The narrow rim, central area bars, and lateral appendages are all of high relief in p-c and very dim in c-p.

Included genera. See Perch-Nielsen 1985, pp. 397-398.

Range. Sinemurian to Upper Cretaceous.

Genus STRADNERLITHUS Black, 1971

Type species. *Stradnerlithus comptus* Black, 1971.

Diagnosis. 'Elongate coccoliths with a marginal wall on the distal side consisting of parallel elements which are not markedly imbricate. The proximal side has a solid bar running along the line of maximum length and lateral branches join this bar to the outer wall. In some species a slender spine arises from the centre of the distal side' (Black 1971, p. 414; see also Noël 1973, p. 103).

Stradnerlithus clatriatus (Rood, Hay and Barnard, 1973) Goy, 1979

Plate 5, figs. 11 and 12; text-fig. 10

1969 *Nodosella clatriata* Prins, pl. 3, fig. 5 (*nom. nud.*).

1973 *Nodosella clatriata* Prins *ex* Rood *et al.*, p. 371, pl. 1, fig. 9.

1979 *Stradnerlithus clatriatus* (Prins *ex* Rood *et al.*); Goy *in* Goy *et al.*, p. 41, pl. 3, fig. 2.

1981 *Stradnerlithus clatriatus* (Prins *ex* Rood *et al.*); Goy, p. 39, pl. 11, figs. 9-11; pl. 12, figs. 1-3; text-fig. 9.

Diagnosis. 'Elliptical coccoliths with a long, narrow central island connected to the margin by 16 to 18 subradial bars' (Rood *et al.* 1973, p. 371).

Description. A small, narrowly elliptical coccolith with twenty-five to thirty subsquare elements forming a low, vertical wall (distal shield); the elements are joined along vertical, radial sutures and the element tops are usually tapered to give a zigzag profile to the upper wall surface. The proximal shield is thin with little vertical extension. The central area is filled by a longitudinal bar, aligned with the major axis of the ellipse, and sixteen evenly spaced lateral bars.

Dimensions. L: 3.4 (2.5) μm , W: 1.8 (1.7) μm .

Remarks. This coccolith has a similar number and arrangement of lateral bars as the specimens of *S. clatriatus* illustrated by Goy (1979, 1981) but differs slightly in possessing a more elongate, narrowly elliptical outline.

S. clatriatus was found in only one of the Lower Jurassic sections studied and the abundance recorded by Goy (1981) is exceptional. Species of *Stradnerlithus* appear to be found abundantly only in restricted facies (D. Noël, pers. comm.).

Occurrence. DSDP Site 547, Sinemurian.

Range. Upper Toarcian (Rood *et al.* 1973); Lower Toarcian (Goy 1981).

Order PODORHABDALES Rood, Hay and Barnard, 1971 emend.

Diagnosis. 'Coccoliths with a marginal area constructed of 2 petaloid cycles of elements which are not at all, or only very slightly imbricate. The marginal area of the members of this order have a characteristic appearance in bright phase contrast illumination, being much darker than the background' (Rood *et al.* 1971, p. 260).

Emended diagnosis. Radiating placolith coccoliths, i.e. two or more shields composed of non-imbricating, radially arranged elements.

Included families. Biscutateae, Calyculaceae, Mazaganellaceae, Podorhabdaceae, Prediscosphaeraceae.

Range. Sinemurian to Palaeocene.

Family MAZAGANELLACEAE fam. nov.

Type genus. *Mazaganella* gen. nov.

Diagnosis. Coccoliths which possess a rim composed of three shields, the elements of each shield displaying very little or no imbrication and joined along radial or near radial sutures; the distal shield may be vertically extended. The central area is wide and may be filled with a variety of crossbars and grills.

LM characteristics. Large dark shields in p-c with constituent elements usually visible. Dark to grey in c-p. The three-shielded structure is occasionally seen in side view.

Remarks. The genus *Mazaganella* has a morphology quite distinct from most other coccoliths of the Lower Jurassic. The two species included in this genus are both large, elliptical coccoliths which possess a fairly narrow rim composed of three shields of non-imbricating, radial elements and a central area spanned by a composite plate or cross bearing a central spine. The type species, *M. pulla*, has adpressed shields and resembles members of the Cretaceous family Arkhangelskiellaceae, which have a similar shape, rim construction, and central area filling. However, the second species of *Mazaganella*, *M. protensa*, which clearly evolved from the first, shows a modification to this rim structure with the distal shield elements being vertically extended. This trend is similar to that seen in the Biscutateae with the evolution of *Calyculus*, although this genus possesses only two shields. The only other coccoliths in the Lower Jurassic with a similar rim morphology to *M. protensa* is a species of *Triscutum* which is found in the late Toarcian of the Picun Leufu and Brenha sections and in the Middle Jurassic in north-west Europe (Dockerill 1987). Both genera have a similar rim construction with the trend towards vertical extension, first seen in *M. protensa*, continued in *Triscutum*. The two genera do differ, however, with species of *Triscutum* in the Middle Jurassic having complex central area grills as opposed to the composite plate and crosses of *Mazaganella*. Thus, any evolutionary development between the two genera would have involved central area modifications but as this is often observed in coccolith lineages it appears quite feasible. The two genera *Mazaganella* and *Triscutum* are thus thought to be closely related and are grouped together in the Mazaganellaceae. The only other three-shielded coccoliths

found in the Lower Jurassic, *Bussonius prinsii* and *B. leufuensis*, are only superficially similar in structure to *Mazaganella* and *Triscutum* and are actually constructed from imbricating and inclined elements and are evolutionary relations of *Lotharingius*.

The Mazaganellaceae is at present placed in the Order Podorhabdales due to the non-imbricating and radial nature of their rim elements. Further work may reveal that their true affinities lie elsewhere as they do not appear typical of this group.

Included genera. *Mazaganella*, *Triscutum*.

Range. Sinemurian to Middle Jurassic.

Genus MAZAGANELLA gen. nov.

Type species. *Mazaganella pulla* sp. nov.

Derivation of name. From the type locality, DSDP Site 547 on the Mazagan Plateau edge, continental shelf north-west Morocco.

Diagnosis. Elliptical coccoliths with a rim consisting of three shields, each possessing elements showing little or no imbrication and joined along radial or near radial sutures; the large, open central area may be filled with a composite plate or cross, usually supporting a central spine.

Remarks. See remarks for the Mazaganellaceae.

Mazaganella pulla sp. nov.

Plate 8, figs. 10–18; Plate 14, figs. 22 and 23; text-fig. 8

Diagnosis. A species of *Mazaganella* possessing three adpressed shields and a central area filled with a composite plate which may show the variable development of four vacant quadrants, thus delineating a broad cross structure aligned along the principal axes of the ellipse. A short, central, hollow spine is usually present.

Description. A large, narrowly elliptical coccolith usually arched about the minor axis of the ellipse. The three shields are adpressed, narrow, and horizontally arranged. The distal shield is made up of fifteen to twenty-five flat, rectangular elements joined along radial elements which may display some kinking; no imbrication has been observed. The intermediate shield is only slightly smaller than the distal shield and is the thinnest of the three shields. It is constructed from a similar number of elements showing little or no imbrication at their outer edges; no further details have been observed. The proximal shield is the same size as the intermediate one and composed of thirty-five to forty-five non-imbricating elements joined along distinctly kinking sutures. These sutures are initially radial but bend in a clockwise direction about halfway along their length; a small hole is often present between the elements at the 'knee' of the suture bend. The central area of the proximal shield is filled by an arched, composite plate formed from granular elements, with a central depression surrounding a hole, marking the position of the distal spine. Variably developed vacant quadrants may be present, thus delineating a broad cross aligned along the principal axes. In specimens with complete central plates, the areas which make up the vacant quadrants are usually formed from larger, granular crystals and the position of the crossbars may be marked by a median groove. In distal view the central plate is made up of larger rhombohedral elements and is usually set at a slightly lower level than the surface of the distal shield (text-fig. 8). An inner wall lining to the central area may be present, probably representing the inner edge of the lower shields. The central spine is hollow and tapers to a point. Occasionally the lower two shields may become fused, probably due to preservational effects, giving the appearance of two shields.

LM description. This large coccolith is very dark in the LM, p-c, and c-p, and is rather ragged in appearance with a broad central cross.

Dimensions. L: 5.1–7.6 (7.0) μm , W: 3.6–4.5 (4.4) μm , RH: 0.8–1.2 (0.8) μm .

Remarks. The discovery of this species has led to a review of the early evolution of coccoliths. *M. pulla* is found in the lowermost Lower Jurassic samples of DSDP Site 547, well below the first

appearance of *Biscutum novum* and thus represents the first placolith-like coccolith structure to appear. The absence of *M. pulla* in north-west Europe must be due to a restricted distribution.

M. pulla is distinguished from *M. protensa* by its adpressed shields and its central plate or poorly delineated cross.

Derivation of name. From Latin *pullus*, dark coloured, and referring to its appearance in the LM.

Holotype. UCL-2193-31 (Pl. 8, fig. 10).

Isotypes. UCL-2189-32, UCL-2189-33, UCL-2190-10, UCL-2193-28, UCL-2049-36, UCL-2046-10.

Type locality. DSDP Site 547-23-2, 25–27 cm, north-west Morocco continental edge.

Type level. Sinemurian. NB. All dating of DSDP Site 547 is based upon calcareous nannofossils, ostracodes, and Foraminifera.

Range. Sinemurian to Pliensbachian (23-2 to 14-2).

Mazaganella protensa sp. nov.

Plate 9, figs. 1–5; Plate 14, figs. 24 and 25; text-fig. 8

Diagnosis. A species of *Mazaganella* possessing a narrow rim with a vertically extended distal shield, a distinct inner wall, and a well-developed central area cross, bearing a hollow spine.

Description. A large normally elliptical coccolith with a narrow three-shielded rim and a well-developed central cross. The distal shield is approximately twice the height of the lower two shields and its elements rise subvertically before flaring out to form a horizontal distal surface. The central area is correspondingly deep and steeply sloping, lined by the extended elements of the distal shield and lower down by an inner cycle of near vertical elements which represents the inner edge of the lower two shields. The distal shield is constructed from around thirty elements, vertically arranged and joined along radial sutures. The intermediate shield is thin and made up of approximately thirty flat, non-imbricating elements. The proximal shield is thin, closely fitted to the intermediate shield, and consists of thirty-five non-imbricating elements joined along kinked sutures which are initially radial but bend in a clockwise direction, halfway along their length. The large central area of the proximal shield is spanned by a prominent cross which is domed and bears a central, hollow spine. In proximal view the cross is formed from granular crystal growth with grooves running along the centre of each bar, leading into a central depression surrounding a central hole. The distal surface of the crossbars are formed by more elongate crystal growth and additional inner cycle elements ('feet') mark the contact of the bars and the inner edge of the central area.

LM description. The coccolith is dark in p-c but displays a bright inner ring to the rim in c-p.

Dimensions. L: 5.4–6.8 (6.5) μm , W: 4.2–5.7 (4.7) μm , RH: 0.9–1.7 (1.1) μm , SH: \sim 3.0 μm

Derivation of name. From Latin *protensus*, extended.

Holotype. UCL-2007-32, UCL-2007-31 (Pl. 9, figs. 1 and 2).

Isotypes. UCL-2007-22, UCL-2148-17.

Type locality. DSDP Site 547-15-1, 2–4 cm, north-west Morocco continental edge.

Type level. Lower Pliensbachian.

Range. Lower Pliensbachian (15-1).

Genus TRISCUTUM Dockerill, 1987

Type species. *Triscutum beaminsterensis* Dockerill, 1987

Diagnosis. 'Elliptical placoliths with three shields in which the distal shield extends vertically to form a high collar, the elements of which diverge distally to form a wide distal margin. The two proximal shields are closely adjacent to one another' (Dockerill 1987, p. 2).

Remarks. *Triscutum* includes a number of very large coccoliths possessing three shields, with the distal one always vertically extended; the central area is spanned by a grill complex. It also encompasses a number of species first placed in *Proculithus* Medd, 1979, which is a junior synonym of *Calyculus*. *Triscutum* is distinguished from *Mazaganella* by its greater vertical extension, broader ellipticity, and complex central grills.

Triscutum sp. 1

Plate 9, figs. 6-9; Plate 14, figs. 26 and 27

Description. An extremely large three-shielded coccolith with a wide, vacant central area. The distal shield is narrow and shows considerable vertical extension. Its constituent elements are radially and vertically arranged. The intermediate shield is smaller than the distal one and composed of elements showing little or no imbrication. The proximal shield is slightly smaller than the intermediate shield and composed of elements showing little or no imbrication and joined along sutures with a distinct kink.

Dimensions. L: 8.0-10.4 μm , W: 6.0-8.0 μm , RH: 1.8-3.0 μm .

Remarks. The lack of any central structure, probably due to dissolution, prevents specific classification.

Occurrence. Brenha, Upper Toarcian/Lower Bajocian; Picun Leufu, Toarcian.

Triscutum sp. 2

Plate 9, fig. 10

Description. A three-shielded coccolith in which the distal shield is extremely extended.

Remarks. Only one specimen has been observed (in the SEM) from the Toarcian of the Picun Leufu section (sample 57).

Family BISCUTACEAE Black, 1971 emend.

Original diagnosis. 'Imperforate coccoliths consisting of 2 shields closely moulded against each other, each shield constructed of radial, petaloid elements without imbrication at their contacts' (Black 1971).

Emended diagnosis. Radiating placolith coccoliths (i.e. composed of non-imbricating, radially arranged rim elements), with broad shields and a small central area which may be imperforate, vacant or spanned by a variety of central structures.

LM characteristics. Radial arrangement of the shield elements causes them to appear dark in p-c and very dim in c-p. They are therefore best viewed in p-c where the dark shields contrast with the bright mounting medium. Constituent rim elements are usually visible.

Remarks. The term imperforate is both misleading and unnecessarily restrictive in the context of a family grouping. The majority of Lower Jurassic members, while obviously belonging to this distinctive group of coccoliths, possess central areas which contain hollow tubes, spines, bars, and crosses, and are therefore not imperforate. The family is thus emended to include perforate coccoliths as well as the imperforate forms that Black first described.

Range. Upper Sinemurian to Palaeogene.

Subfamily BISCUTOIDEAE Hoffman, 1970

Diagnosis. 'Both shields lie immediately above each other. The shield elements of the distal shield are arranged like a fan; those of the proximal shield lie next to each other. As a rule the central area is covered by granulae' (Hoffmann 1970, p. 861).

Genus *BISCUTUM* Black *in* Black and Barnes 1959

Type species. Biscutum testudinarium Black *in* Black and Barnes 1959.

Diagnosis. 'Biscutaceae with broadly elliptical or near circular shields and bilateral symmetry' (Black 1972, p. 26).

Remarks. The above diagnosis automatically includes the emendment stated for the family and thus allows the inclusion of both perforate and imperforate coccoliths.

Black (Black and Barnes 1959) erected the genus *Biscutum* and included good TEM photographs illustrating the distinctive rim construction of this group of coccoliths. Noël (1965, 1973) defined the genus *Palaeopontosphaera* for Jurassic coccoliths which are very similar to those Cretaceous forms included in *Biscutum*. Subsequent use of *Palaeopontosphaera* has generally been confined to Jurassic forms with some central structure, e.g. a tubular spine or cross, however, the genus is considered a junior synonym of *Biscutum*.

Biscutum novum (Goy, 1979) Bown, 1987

Plate 5, figs. 13-17; Plate 13, figs. 19 and 20; text-fig. 11

- 1965 *Palaeopontosphaera dubia* Noël, pp. 76-78, pl. 7, figs. ?2, 3, ?4, ?11, ?12, ?13 (*non* pl. 7, figs. 1, 5-10); text-fig. 8.
 1969 *Palaeopontosphaera veterna* Prins, ?pl. 2, fig. 9 (*nom. nud.*).
 1969 *Striatococcus opacus* Prins, ?pl. 2, fig. 15 (*nom. nud.*).
 1969 *Striatococcus grandiculus* Prins, ?pl. 2, fig. 14 (*nom. nud.*).
 1973 *Palaeopontosphaera dubia* Noël; Rood *et al.*, p. 378, pl. 3, fig. 1.
 1973 *Palaeopontosphaera dubia* Noël; emend. Noël, p. 117, pl. 13, fig. 3 (*non* pl. 13, figs. 1, 2, 4, 5).
 1974 *Palaeopontosphaera dubia* Noël; Barnard and Hay, pl. 2, fig. 2.
 1974 *Biscutum dubium* (Noël); Grün *in* Grün *et al.*, pp. 297-298, pl. 14, figs. 1-3.
 1977 *Biscutum ellipticum* (Górka 1957) Grün 1975; Hamilton, pl. 1, fig. 7; pl. 3, fig. 7.
 1979 *Biscutum ellipticum* (Górka); Hamilton, pl. 1, fig. 15.
 1979 *Palaeopontosphaera nova* Goy *in* Goy *et al.*, p. 42, pl. 4, fig. 5.
 1981 *Palaeopontosphaera nova* Goy; Goy, pp. 52-53, pl. 19, figs. 4-7; pl. 20, figs. 1 and 2; text-fig. 12.
 1984 *Biscutum dubium* (Noël); Crux, p. 168, fig. 9 (5, 6); fig. 13 (6).
 1986 *Biscutum* sp.; Young *et al.*, pl. 1, fig. F.
 1987 *Biscutum novum* (Goy); Bown, pl. 2, figs. 1 and 2.

Diagnosis. 'A species of the genus *Biscutum* with an imperforate central area, the central spine is attached all around the rim margin. The presence of a furrow is characteristic of the proximal face' (Goy 1979, p. 42).

Description. A species possessing a simple radiating placolith structure consisting of two unicyclic shields. The sixteen to eighteen elements of the distal shield are joined along radial sutures, a number of which may show a sharp, zig-zag kink; no imbrication is observed. The distal elements slope gently outwards to form the broad, convex distal shield but their inner edges slope steeply inwards to create the deep central area. The proximal shield is usually narrower than the distal shield and consists of a similar number of non-imbricating elements joined along consistently kinking sutures. The sutures all vee in a counter-clockwise direction. The central area of the proximal shield is filled with granular calcite forming a funnel-like structure which protrudes as the spine/tube on the distal side. Only rarely is the central, hollow tube found as a fully developed spine and this may represent a dimorphic feature or simply be due to preservation.

Dimensions. L: 3.6-4.8 (4.7) μm , W: 2.4-4.4 (4.5) μm .

Remarks. The holotype of *B. dubium* (Noël 1965, pl. 7, Fig. 1) was an Upper Jurassic coccosphere of poorly preserved biscutatean coccoliths approximately 2 μm in length. While some controversy has since arisen over the use of the species name *dubia* it has generally been applied to biscutatean coccoliths with a narrow central area filled with a central tube-like spine base, including the earliest Lower Jurassic forms. These Lower Jurassic specimens are much larger than those from the type level and are composed of two unicyclic shields, as opposed to the bicycle distal shields observed

in the later forms. Goy (1979) erected the species *nova* for these distinct Lower Jurassic Biscutaceae.

B. novum is the first species of *Biscutum* to appear in the early Jurassic and also the first placolith coccolith recorded in north-west Europe. It is thus extremely useful as a biostratigraphic tool and also of great evolutionary significance. *B. novum* is a robust coccolith, resistant to dissolution and occurs abundantly and consistently throughout its range in the Lower Jurassic. Morphological variations are frequent as *B. novum* appears to be a root stock from which many diversifications originated. It follows that a proportion of the *B. novum* population showed intermediate structures between the typical *B. novum* morphology and the fully developed descendant species. Examples of this include trends towards increasing circularity and reduction of the central area as *Discorhabdus* developed, expansion of the central area, and inner cycle formation as *B. intermedium* developed and increasing size and suture kinking as *B. finchii* developed.

Occurrence. Badenwieler, *bifrons* Zone to *aalensis* Zone; Ballrechten, *bifrons* Zone to *levesquei* Zone; Brenha, Upper Sinemurian to Middle Jurassic; DSDP Site 547, Upper Sinemurian to Toarcian; Mochras, *jamesoni* Zone to *levesquei* Zone; Longobucco, Lower Pliensbachian to Lower Toarcian; Picun Leufu, Upper Pliensbachian to Toarcian; Trimeusel, *spinatum* Zone to *levesquei* Zone; Tunisia, Upper Pliensbachian to Lower Toarcian; Unterstürmig, Lower Toarcian.

Range. Most authors record the first occurrence datum of *B. novum* within the *jamesoni* Zone (Lower Pliensbachian) in north-west Europe (Prins 1969; Crux 1984), although Barnard and Hay (1974) recorded it in the Upper Sinemurian. It appears to have an earlier occurrence in the Tethyan area, appearing in the Upper Sinemurian.

Biscutum finchii Crux, 1984 emend. Bown, 1987

Plate 5, fig. 18; Plate 6, figs. 1-3; Plate 13, figs. 21 and 22; text-fig. 11

1984 *Biscutum finchii* Crux, p. 168, fig. 9 (?3, 4).

1987 *Biscutum finchii* Crux; emend. Bown, pl. 2, figs. 3, 4, 10, 11.

Original diagnosis. 'A species of *Biscutum* with a large central area and no spine. The central area is filled with irregular granular calcite' (Crux 1984, p. 168).

Emended diagnosis. A large normally elliptical species of *Biscutum* with a modified radiating placolith structure. The distal shield is composed of non-imbricating elements with a gentle outer slope forming the shield and a steep inner edge producing a deep central area. The sutures are sharply kinked at the point from which the elements slope and they also have a slight anticlockwise precession due to the kinking. The proximal shield is only slightly smaller than the distal shield;

EXPLANATION OF PLATE 6

Figs. 1-3. *Biscutum finchii* Crux, 1984. 1, distal view, UCL-2178-37, Brenha, *ibex* Zone (3531), $\times 4000$. 2, distal view, UCL-2147-24, Mochras, *spinatum* Zone (81), $\times 5150$. 3, proximal view, UCL-2147-13, Mochras, *spinatum* Zone (81), $\times 5050$.

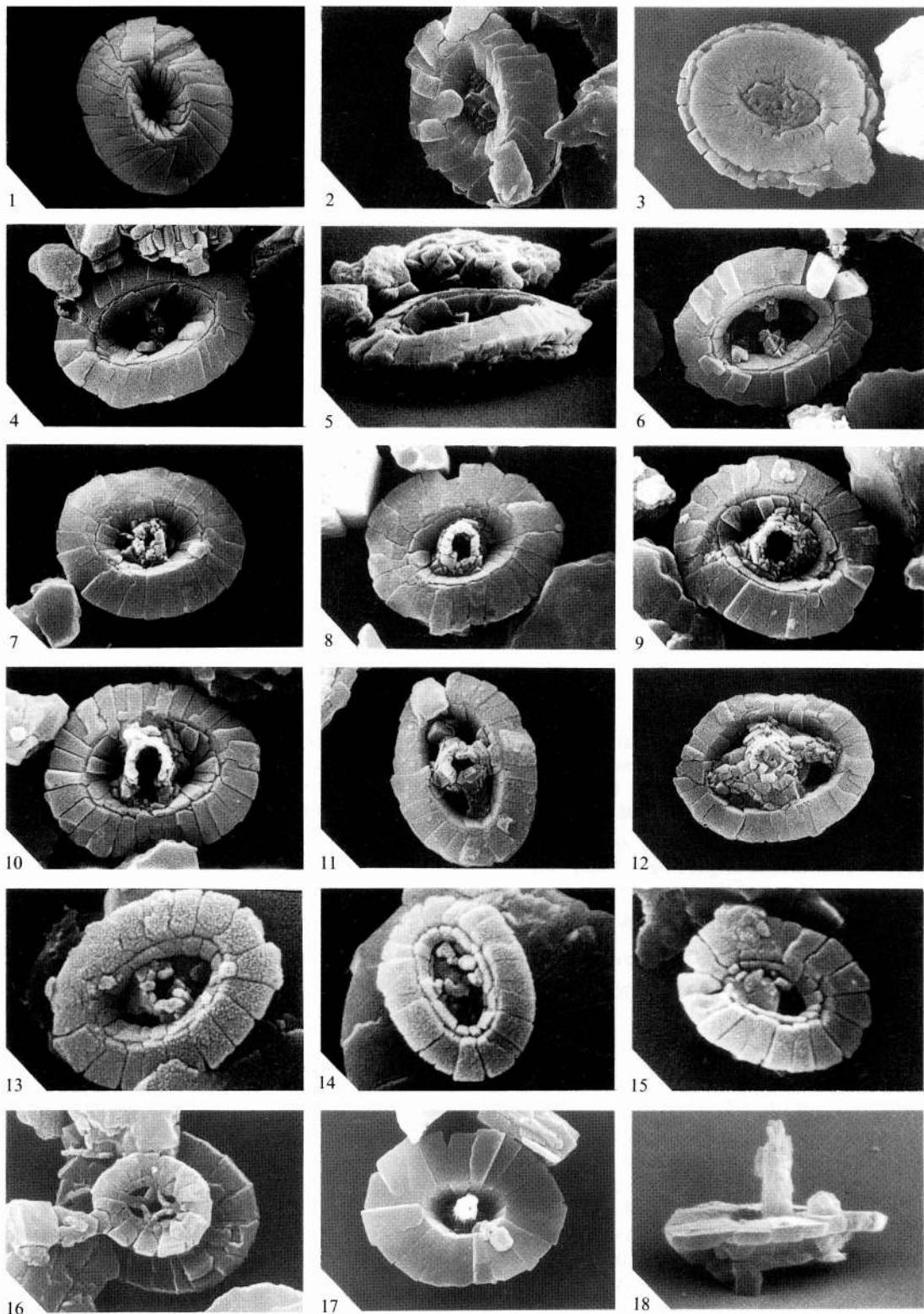
Figs. 4-6. *B. grandis* sp. nov. 4, holotype, distal view, UCL-2170-15, Brenha, *ibex* Zone (3531), $\times 4700$. 5, oblique view of fig. 4, UCL-2170-16, $\times 6100$. 6, isotype, distal view, UCL 2173-32, Brenha, *davoei* Zone (6107), $\times 4800$.

Figs. 7-10. *B. intermedium* sp. nov. 7 and 8, Brenha, Upper Toarcian (3606). 7, distal view, UCL-2178-24, $\times 6050$. 8, distal view, UCL-2199-12, $\times 6200$. 9 and 10, Brenha, Bajocian (3617). 9, holotype, distal view, UCL-2173-20, $\times 5625$. 10, isotype, distal view, UCL-2198-12, $\times 6100$.

Figs. 11 and 12. *B. depravatus* (Grün and Zweili, 1980) comb. nov. Brenha, Bajocian (3617). 11, distal view, UCL-2173-17, $\times 5350$. 12, distal view, UCL-2198-26, $\times 5250$.

Figs. 13-15. *B. dubium* (Noël, 1965) Grün in Grün *et al.* 1974. 13, distal view, UCL-1993-4, Mochras, *falciferum* Zone (M57), $\times 14\ 450$. 14 and 15, Brenha, Upper Toarcian (3606). 14, distal view, UCL-2178-28, $\times 11\ 100$. 15, distal view, UCL-2205-26, $\times 12\ 100$.

Figs. 16-18. *B. planum* sp. nov. Timor, mid-Pliensbachian (J237). 16, holotype, proximal view, UCL-2074-8, $\times 6400$. 17, isotype, distal view, UCL-2148-32, $\times 6100$. 18, isotype, side view, UCL-2072-30, $\times 4200$.



BOWN, *Biscutum*

its elements are non-imbricating with sutures only slightly deviating from the radial pattern. The central area is filled with granular elements.

Description. The diagnosis above is also a fairly comprehensive description. In addition, the distal shield possesses twenty to twenty-five elements, the proximal shield twenty-five to thirty elements. The central area is elliptical, small, with a steeply sloping edge. A number of the distal shield sutures may display double kinking, the first kink near the central depression and the second towards the outer edge of the shield (Pl. 6, fig. 1).

Dimensions. L: 5.8–8.5 (5.6) μm , W: 4.8–7.0 (4.7) μm .

Remarks. A large, resistant, and distinctive coccolith which appears to have a restricted range within the Lower Jurassic. The Argentinian section yielded very large specimens of *B. finchii* (7.0–8.5 μm) while the Mochas and Brenha sections both yielded slightly smaller forms (5.8–7.0 μm).

B. finchii is much larger than most other species of *Biscutum* and its unicyclic distal shield and kinking sutures distinguish it from the similarly sized *B. grandis*.

Occurrence. Badenweiler, Upper Pliensbachian; Brenha, *jamesoni* Zone to *spinatum* Zone; Mochras, *margaritatus* Zone to *falciferum* Zone; Picun Leufu, Upper Pliensbachian to Toarcian; Trimeusel, *tenuicostatum* Zone; Tunisia, Upper Pliensbachian to Lower Toarcian.

Range. *spinatum* Zone to *tenuicostatum* Zone (Crux 1984).

Biscutum grandis sp. nov.

Plate 6, figs. 4–6; Plate 13, figs. 23–25; text-fig. 11

Diagnosis. A large, normal to narrowly elliptical species of *Biscutum* possessing a bicyclic distal shield and a relatively large central area spanned by a thin bar bearing a central spine base.

Description. The distal shield consists of two cycles; the broader outer cycle is constructed from twenty-five to thirty elements sloping gently outwards and joined along radial sutures which are occasionally sharply kinked (and rarely double kinked). The inner edge of these elements is hidden by an inward sloping cycle of elements which line the deep central area; the inner cycle is composed of around twenty tangentially arranged, subsquare elements joined along radial sutures. The central area is relatively open and spanned by a thin bar of microcrystals, aligned along the minor axis of the ellipse; the bar supports a small, central spine base. The bar is frequently broken or missing, and the central area can be vacant or filled with granular calcite.

LM description. The broad outer distal cycle and proximal shield appear as dark cycles, but the distal inner cycle is a distinctive bright ring outlining the central area. The minor axis bar is usually seen as two bright lobes at either end of the minor axis.

Dimensions. L: 6.2–7.0 (6.8) μm , W: 4.6–5.2 (5.0) μm .

Derivation of name. From Latin *grandis*, great.

Holotype. UCL-2170-15, UCL-2170-16 (Pl. 6, figs. 4 and 5).

Isotype. UCL-2173-32.

Type locality. Brenha, Portugal.

Type level. *davoei* Zone.

Remarks. A large, resistant, and distinctive coccolith with a restricted range within the Lower Jurassic. It is similar in size to *B. finchii* and appears to represent an evolutionary progression from the latter, with the development of an inner cycle of elements.

Although both *B. finchii* and *B. grandis* have been recorded from the Upper Pliensbachian and Lower Toarcian of the Mochras borehole section it is significant that they have not been recorded in the north-west European studies of Noël (1965, 1973), Barnard and Hay (1974), Grün *et al.* (1974), and Goy (1981), or from the German sections in the present study (excepting one sample each from Trimeusel and Ballrechten in which *B. finchii* was observed). It is possible that *B. finchii*

and *B. grandis* have escaped notice in previous studies, but this appears unlikely due to their large and distinctive appearance. It is more likely that they display a restricted distribution occurring abundantly in the Tethyan province and to the west of Britain, but only rarely or not at all in the French and German basins.

Occurrence. Brenha, *jamesoni* Zone to *spinatum* Zone; Mochras, *spinatum* Zone to *falciferum* Zone; Longobucco, *spinatum* Zone; Picun Leufu, Upper Pliensbachian to Toarcian; Tunisia, Upper Pliensbachian to Lower Toarcian.

Range. Prins (1969) illustrated a coccolith, *Palaeopontosphaera binodosa* (*nom. nud.*), very similar to the species described here and with a range of *margaritatus* Zone to *spinatum* Zone.

Biscutum dubium (Noël, 1965) Grün in Grün *et al.* 1974

Plate 6, figs. 13–15; Plate 14, figs. 3 and 4; text-fig. 13

- 1965 *Palaeopontosphaera dubia* Noël, pp. 76, 78, pl. 7, figs. 1, 5–10 (?pl. 7, figs. 2, 4, 11–13; *non* pl. 7, fig. 3).
 1973 *Palaeopontosphaera dubia* Noël; emend. Noël, p. 117, pl. 13, figs. 1, 2, 4, 5 (*non* fig. 3)
 1980 *Biscutum dubium* (Noël); emend. Grün and Zweili, p. 245, pl. 1, figs 1 and 2; text-fig. 4.
non 1973 *Palaeopontosphaera dubia* Noël; Rood *et al.*, p. 378, pl. 3, fig. 1.
non 1974 *Palaeopontosphaera dubia* Noël; Barnard and Hay, pl. 2, fig. 2.
non 1974 *Biscutum dubium* (Noël); Grün in Grün *et al.*, pp.297–298, pl. 14, figs. 1–3.
non 1979 *Palaeopontosphaera dubia* Noël; emend. Goy in Goy *et al.*, p. 42, pl. 4, fig. 4.
non 1981 *Palaeopontosphaera dubia* Noël; Goy, pp. 50–51, pl. 18,
non 1984 *Biscutum dubium* (Noël); Crux, p. 168, fig. 9 (5, 6,); fig. 13 (6).

Diagnosis. 'Elliptical coccoliths formed of 2 closely fitted shields; the principal shield (slightly broader than the proximal shield) is indented in its centre to permit the passage of a central spine with an axial canal' (Noël 1973, p. 117).

Description. The distal shield, outer cycle is composed of eighteen to twenty-two rectangular and wedge-shaped elements showing no imbrication and joined along radial sutures. The elements slope outwards at a low angle and their inner edges are hidden by the inwardly sloping inner cycle, which consists of fifteen to twenty small, subsquare elements joined along radiating sutures. The relatively open and shallow central area is usually filled with granular microcrystals and a central, circular, hollow spine base.

Dimensions. L: 2.6 (1.9) μm , W: 1.9–2.0 (1.6) μm .

Remarks. *B. dubium* has previously been used to encompass the larger Lower Jurassic biscutatean species, *B. novum*, which possesses a unicyclic distal shield and a central hollow spine base. In this study *B. dubium* is considered to include only those biscutatean coccoliths of small size with bicyclic distal shields and a central hollow spine base. It also differs from *B. novum* by its shallower shield slopes, more open central area, and distal inner cycle of elements. The species of *Biscutum* with a central cross name *Palaeopontosphaera dubia* by Goy (1979, 1981) is considered a separate form not found during this research.

Occurrence. Ballrechten, *bifrons* Zone to *thoursense* zone; Brenha, *davoei* Zone to Middle Jurassic; Mochras, *falciferum* Zone; Trimeusel, *falciferum* Zone to *variabilis* Zone.

Range. Oxfordian–Portlandian (Noël 1965); Oxfordian (Rood *et al.* 1971); Kimmeridgian (Noël 1973); Oxfordian (Medd 1979); Oxfordian (Grün and Zweili 1980).

Biscutum planum sp. nov.

Plate 6, figs. 16–18; Plate 14, figs. 5 and 6.

Diagnosis. A species of *Biscutum* composed of two planar, unicyclic shields, the proximal shield being considerably smaller than the distal shield, and possessing a small central area spanned by four curving bars which form a cross, supporting a tall, hollow spine.

Description. The distal shield is broadly elliptical and constructed from sixteen to nineteen thin, non-imbriating elements which are arranged horizontally and joined along straight radial sutures. The inner edges of these elements terminate abruptly to form a vertically sided central area through which a tall spine protrudes. The proximal shield is similarly constructed to the distal shield but is two to three times smaller. The two shields are well separated at their outer edges. The central area of the proximal shield is spanned by four curving bars which form a cross, aligned along the principal axes, supporting a central, thin, tall, hollow spine.

LM description. The two shields appear dark but translucent and both can be seen as concentric ellipses.

Dimensions. Distal shield L: 3.8–5.4 (5.0) μm , W: 2.9–4.0 (4.0) μm ; Proximal shield L: 2.8–(2.9) μm , W: 2.4–(2.5) μm , RH: 0.8–1.6 μm , SH: 2.7–6.0 μm .

Remarks. *B. planum* is distinguished from other species of *Biscutum* by its planar shield arrangements, lack of a sloping central depression, and the considerably differing shield sizes. In the latter respect it is similar to *B. boletum* Wind and Wise 1976 from the Maastrichtian.

Derivation of name. From Latin *planus*, flat.

Holotype. UCL-2074-8 (Pl. 6, fig. 16).

Isotypes. UCL-2148-32, UCL-2072-30.

Type locality. Timor (J237).

Type level. Mid-Pliensbachian.

Occurrence. At present only recorded from the type material. It thus appears likely that this species has a distribution limited to the Pacific province.

Biscutum depravatus (Grün and Zweili, 1980) comb. nov.

Plate 6, figs. 11 and 12; Plate 14, figs. 1 and 2; text-fig. 14

1980 *Axopodorhabdus depravatus* Grün and Zweili, p. 266, pl. 5, fig. 12; pl. 6, figs. 1–4; text-fig. 22.

Description. A relatively open *Biscutum* rim with a central area spanned by an asymmetric cross structure. The distal shield is composed of twenty-five to thirty-six rectangular and wedge-shaped elements showing no imbrication and joined along radial sutures. These sutures may have distinct kinks, especially at or near the crest from which the elements slope outwards, to form the convex shield, and abruptly inwards, to form the steeply sided central area. The central area slope may possess no inner cycle elements or an inner cycle in varying stages of development. The proximal shield is closely fitted to the distal shield but no further details have been observed. The central area is spanned by a cross structure formed from granular crystals and bearing a large, hollow spine base. The four crossbars are approximately parallel to the principal axes of the ellipse but offset: the upper longitudinal bar to the left, the lower longitudinal bar to the right, the left transverse bar upwards, and the right transverse bar downwards (when viewed distally).

Dimensions. L: 4.5–6.2 (5.5) μm , W: 3.7–4.7 (4.2) μm .

Remarks. The specimens of *B. depravatus* observed in the present study, from the Picun Leufu and Brenha sections, appear slightly different from those illustrated by Grün and Zweili (1980). The original forms have slightly narrower rims and wider central areas and these features may justify inclusion in *Axopodorhabdus*. Here the specimens show a range of morphologies, from those with typically *Biscutum* rims, bearing the distinctive asymmetric cross, to specimens approaching the appearance of the holotype. It seems probable that these late Toarcian forms, which are closely related to *B. novum* and retain the distinctive rim structure of *Biscutum*, gave rise to the Callovian specimens of Grün and Zweili (1980) which have undergone some morphological modification. It is thus considered that these coccoliths are best classified as *Biscutum* due to their morphological and evolutionary closeness to other species of *Biscutum*, rather than *Axopodorhabdus*, in the late Toarcian. The asymmetry of the central cross is also thought atypical of *Axopodorhabdus*. Thus with parallel patterns of evolution producing similar morphological developments, within the

biscutatean group particularly, classification is most effective within the context of an evolutionary scheme.

Occurrence. Brenha, Upper Toarcian/Bajocian; Picun Leufu, Toarcian.

Range. Callovian to Middle Oxfordian (Grün and Zweili 1980).

Biscutum intermedium sp. nov.

Plate 6, figs. 7-10; Plate 13, figs. 26-28; text-fig. 14

Diagnosis. A broadly elliptical species of *Biscutum* which possesses a deep central area, lined with an inner distal cycle of elements, and spanned by a broad bar which is aligned at about 20°, clockwise, to the minor axis of the ellipse; the bar is perforated by a large central, circular or elliptical hole or spine base.

Description. The distal shield is composed of two cycles; the outer cycle consists of twenty-two to twenty-nine rectangular and wedge-shaped, non-imbricating elements joined along radial sutures which may display a variable amount of kinking. The outer slope of these elements forms the convex shield and their inner edge is hidden by the inner cycle of twenty-two to twenty-nine small, rectangular elements which line the central depression. This inner cycle is occasionally observed only partially developed. The proximal shield is closely fitted to the underside of the distal shield but further details have not been observed. The small, steep-sided central area is spanned and almost filled by a broad bar, constructed from small, granular microcrystals, and is pierced by a large, circular or elliptical pore which may be a spine base. The pore is usually equal in diameter to the width of the central area but the bar continues up the sides of the central depression and is thus strictly wider than the central area hole. The bar is aligned at an angle of about 20°, clockwise, to the minor axis of the ellipse. The two vacant windows in the north-east and south-west of the central area are often extremely reduced.

Dimensions. L: 4.5-5.9 (5.8) μm , W: 4.0-5.3 (4.8) μm .

Remarks. A continuous variation of morphologies is observed between *B. intermedium* and *B. novum* (see Pl. 6, figs. 7-10). *B. intermedium* is distinguished from *B. novum* by its distal inner cycle and central area windows; from *B. grandis* by its more broadly elliptical shape, smaller central area, and large central tube structure; from *B. dubium* by its larger size, steeply sloping shield surface, and broad central bar; and from species of *Podorhabdus* and *Tetrapodorhabdus* by its small central area and broad *Biscutum* rim structure.

Derivation of name. From Latin *intermedius*, intermediate.

Holotype. UCL-2173-20 (Pl. 6, fig. 9).

Isotype. UCL-2198-12.

Type locality. Brenha, Portugal.

Type level. Bajocian.

Occurrence. Badenweiler, *levesquei* Zone to *aalensis* Zone; Brenha, Upper Toarcian to Bajocian; Mochras, *levesquei* Zone; Picun Leufu, Toarcian; Trimeusel, *levesquei* Zone.

GENUS DISCORHABDUS Noël, 1965

Type species. *Discorhabdus patulus* (Deflandre, 1954) Noël, 1965.

Diagnosis. Circular base composed of 2 superimposed simple shields, joined firmly, perforated in the centre to allow the passage of a variably developed spine. The distal shield is constructed from a single series of calcite lamellae which are radially disposed, joined all along their length giving the disc a continuous surface, without festoons. The proximal disc, generally smaller than or equal to the distal disc, is formed from the same number of calcite plates, flat, often thinner, similarly joined and radially disposed. This proximal disc, slightly convex, forms a solid base pierced only at its centre by the root of the spine. The axial spine with a variable diameter and of variable

length and morphology, is made up of crystals of calcite, almost cubic, or elongate rhombohedra, arranged about a central canal. The outer edge of the spine is closely coupled to the inner edge of the perforations of the distal and proximal disc' (Noël 1965, p. 138).

Remarks. The distinction between circular and elliptical coccolith outlines has been stressed by Kamptner (1958, in Black 1972, p. 64) who insisted on their taxonomic separation, also arguing that circular forms are the more primitive of the two shapes. This taxonomic concept has generally been accepted and the genus *Discorhabdus*, erected to include circular placolith coccoliths with radial, non-imbricate elements and large variable spines is a consequence of it. The hypothesis of circular forms being the more primitive of the two coccolith shapes is not, however, substantiated in the present work. The first circular coccoliths to appear in the Lower Jurassic, *D. ignotus*, clearly evolved from the earlier elliptical coccolith, *B. novum*. This pattern is also repeated in the Watznaueriaceae, with the elliptical genus *Lotharingius* appearing well before the circular genus *Cyclagelosphaera*.

The taxonomic separation of *Discorhabdus* from *Biscutum* is clearly warranted as both groups form distinct lineages after their separation in the Lower Jurassic. The discorhabdids went on to evolve large, tall, flaring spines in the Middle Jurassic, quite distinct from the coccoliths of *Biscutum*. A number of problems are encountered in the Lower Jurassic. The first is the continuous variation initially observed between the elliptical and subcircular *B. novum* coccoliths and the truly circular *D. ignotus* coccoliths; the second is the fact that the large spines, so characteristic of the Middle Jurassic discorhabdids and important for their specific and generic diagnosis, are either poorly developed or completely absent in the Lower Jurassic species. The first problem is resolved by placing only those coccoliths with truly circular outlines in *Discorhabdus*. The second problem could be avoided by using the Cretaceous generic name, *Bidiscus*, which was erected to include circular coccoliths of the Biscutaceae which lack spines. It is most likely that these early circular Biscutaceae gave rise to the discorhabdids of the Middle Jurassic, and thus while not possessing large spines (which perhaps should not be given generic importance) are closely related to the *Discorhabdus* group, rather than the Cretaceous *Bidiscus*. The lack of large spines in the earliest *Discorhabdus* species reflects their evolution from *B. novum*, which only possesses a small central tube which may be a spine base. It was only after the establishment of the *Discorhabdus* genus that the large spines began to appear.

The development of circular *Discorhabdus* from elliptical *Biscutum* and the continuing similarity of their radial and non-imbricate shields, justify their inclusion in the Biscutaceae, with coccolith outline considered significant only to the generic level.

Discorhabdus ignotus (Górka, 1957) Perch-Nielsen, 1968

Plate 7, figs. 1–5; Plate 14, figs. 7 and 8; text-fig. 11

1957 *Tremalithus ignotus* Górka, pp. 248, 272, fig. 9.

1968 *Discorhabdus ignotus* (Górka); Perch-Nielsen, p. 81, text-fig. 41; pl. 28, fig. 6.

1969 *Striatococcus nebulosus* Prins, pl. 2, fig. 16 (*nom. nud.*).

1975 *Bidiscus ignotus* (Górka) Hoffman, 1970; Grün and Allemann, p. 157, text-fig. 4; pl. 1, figs. 8–10.

1984 *Discorhabdus superbus* (Deflandre, 1954); Crux, fig. 9 (7, 8).

1986 *Discorhabdus* sp.; Young *et al.*, pl. 1, fig. E.

1987 *Discorhabdus superbus* (Deflandre); Crux, pl. 1, figs. 8–10.

Description. A circular coccolith very similar in general structure to *B. novum*. The unicyclic distal shield is constructed from fourteen to twenty-one wedge-shaped elements displaying no imbrication and joined along radiating sutures. One or more of the suture lines often displays one or two kinks and intergrowth may occasionally create element fragmentation. The elements slope outwards to form a distinctly convex shield surface and their inner edges slope steeply inwards to form a small, conical, central depression. This depression may have at its centre a tiny hollow spine base or two to four intergrown rhombs of calcite. The depression is occasionally sub-central, giving the coccolith a distinctly asymmetrical appearance. The proximal shield is slightly smaller than the distal shield and closely fitted to its underside. It is constructed from around eighteen

non-imbricating elements joined along distinctly kinked sutures veering in a counter-clockwise direction. The central area is circular and small and filled with granular microcrystals. A number of specimens with detached proximal shields have been observed, leaving only the inner edges of the proximal elements (see Hamilton 1977, pl. 2, fig. 8; Crux 1987, pl. 1, fig. 10; Medd 1979, pl. 7, fig. 7).

LM description. Circular in outline, the two shields are visible and dark in both p-c and c-p; the individual shield elements are discernible.

Dimensions. Diameter: 3.5–6.4 μm .

Remarks. As stated above, *D. ignotus* is similar in structure to *B. novum* and an evolutionary continuum between the two species is observed. *D. ignotus* is distinguished from *B. novum* by its circularity and reduced central area; from *D. criotus* by its unicyclic distal shield; from Middle Jurassic discorhabdids by its lack of a well-developed spine; and from the proximal shield of *Carinolithus superbis* by its larger size, strong convexity, and steeply sloping central depression.

Variations in the morphology of *D. ignotus* include the degree of sutural kinking, infilling of the central depression, position of the central depression, and convexity of the distal shield surface. The sutural kinking is similar to that seen in *B. novum* and may have led to the development of the inner cycle in *D. criotus*. The small central area may be occupied by a tiny spine base or a number of intergrown rhombs; this latter feature may be a product of overgrowth but has been observed in numerous specimens. Specimens with off-centre central areas are occasionally observed and may be due to either malformation or the position of the coccolith on the coccosphere.

Occurrence. Badenweiler, *variabilis* Zone to *aalensis* Zone; Ballrechten, *variabilis* Zone to *levesquei* Zone; Brenha, *ibex* Zone to Middle Jurassic; Longobucco, *margaritatus* Zone to *tenuicostatum* Zone; Mochras, *falciferum* Zone to *levesquei* Zone; Picun Leufu, Toarcian; Trimeusel, *bifrons* Zone to *levesquei* Zone.

Range. *falciferum* Zone (Prins 1969), Upper Sinemurian to Middle Jurassic (Hamilton 1977), Toarcian to Maastrichtian (Perch-Nielsen 1985).

Discorhabdus criotus sp. nov.

Plate 6, figs. 6–9; Plate 14, figs. 9 and 10; text-fig. 11

1969 *Palaeopontosphaera repleta* Prins, pl. 2, fig. 11 (*nom. nud.*).

1977 *Discorhabdus ignotus* (Górka, 1957) Perch-Nielsen, 1968; Hamilton, pl. 2, fig. 2.

Diagnosis. A species of *Discorhabdus* with a small, distal inner cycle set deep in the central depression, and radiating sutures which bend in a counter-clockwise direction near the outer edge of the shield; no spine is present and the central area is a small circular pore.

Description. The distal shield, outer cycle is composed of eleven to thirteen wedge-shaped elements which have radial sutures for most of their length but display a distinctive counter-clockwise bend near their outer edge. The elements slope gently outwards to form the broad convex shield and sharply inwards to form the steeply sided central depression which is lined in its lower half by the small inner cycle. The inner cycle consists of eleven to thirteen tiny triangular elements with radial sutures surrounding a small central pore. The proximal shield is narrower than the distal shield and formed from sixteen elements joined along radial sutures with a kink near the inner edge. The central area is a circular depression filled by a ring of seven to thirteen triangular elements surrounded by granular microcrystals. These elements appear to represent the proximal faces of the distal inner ring, the elements having a pyramid-like habit.

LM description. The outer cycle appears dark and featureless in c-p and the inner cycle is a bright ring crossed by four straight isogyres. In p-c the individual shield elements can be seen.

Dimensions. Diameter: 3.6–5.6 (5.4) μm .

Remarks. Some variation in coccolith outline is observed, with a number of subcircular specimens photographed. This leaves open the possibility that *D. criotus* may have evolved separately from *B. novum* as well as the more obvious evolutionary progression from *D. ignotus*. The deeply set

inner cycle, which apparently reaches through to the proximal surface, is slightly different from the inner cycles developed in *Biscutum* but is probably produced by a similar process of complex element intergrowth. The counter-clockwise kinking at the outer edges of the distal shield sutures is an unusual feature and perhaps a product of the double-kink intergrowth often observed in biscutatean coccoliths.

Derivation of name. From Greek *kriotus*, made of rings.

Holotype. UCL-2074-23 (Pl. 7, fig. 6).

Isotypes. UCL-2178-3, UCL-2170-5.

Type locality. Ballrechten, south Germany.

Type level. *thouarsense* zone, Upper Toarcian.

Occurrence. Badenweiler, *thouarsense* Zone to *aalensis* Zone; Ballrechten, *variabilis* Zone to *levesquei* Zone; Brenha, *variabilis* Zone to *levesquei* Zone; Mochras, *levesquei* Zone; Trimeusel, *levesquei* Zone.

Subfamily SOLLASITEOIDEAE Rood, Hay and Barnard, 1971 emend.

Original diagnosis. 'Elliptical coccoliths with a podorhabdid rim, a transverse bar and 3 or more longitudinal or sublongitudinal bars. No central stem is present' (Rood *et al.* 1971, p. 263).

Emended diagnosis. Elliptical coccoliths with a slightly modified biscutatean rim, having a wider central area which is spanned by a bar along the minor axis of the ellipse and several longitudinal bars which may or may not bear a central spine or boss. Additional lateral bars and plates may also occur in the central area.

Remarks. The *Sollasites* rim is basically the same as *Biscutum*, but the central area is slightly more open; it is not as narrow as the related podorhabdid rim. Central stems have been recorded from three species of *Sollasites* in the Lower Jurassic and the presence of a spine is considered taxonomically insignificant and unnecessarily restrictive in diagnosis.

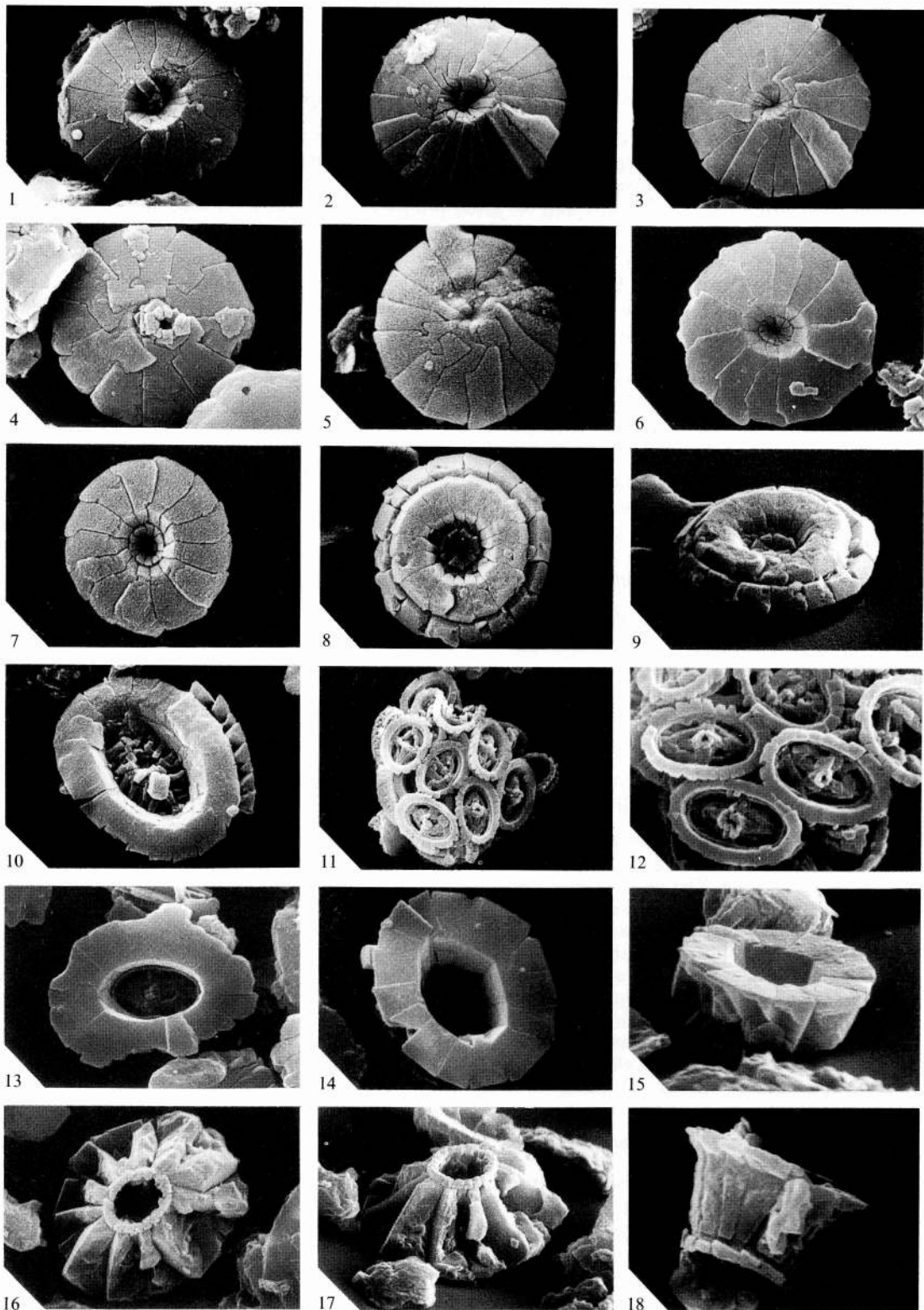
Range. Pliensbachian to Palaeogene.

Genus SOLLASITES Black, 1967

Type species. *Sollasites barringtonensis* Black, 1967.

EXPLANATION OF PLATE 7

- Figs. 1-3. *Discorhabdus ignotus* (Görka, 1957) Perch-Nielsen, 1968. 1, distal view, UCL-2177-15, Brenha, Upper Toarcian (3558), $\times 6000$. 2, distal view, UCL-2173-36, Brenha, *davoei* Zone (6107), $\times 4700$. 3, distal view, UCL-2205-24, Brenha, Upper Toarcian (3606), $\times 4600$.
- Figs. 4 and 5. *D. cf. ignotus* (Görka, 1957) Perch-Nielsen. 4, distal view, UCL-1916-25, Mochras, *variabilis* Zone (M25), $\times 7400$. 5, distal view, UCL-2199-9, Brenha, Upper Toarcian (3606), $\times 8050$.
- Figs. 6-9. *D. criotus* sp. nov. 6, holotype, distal view, UCL-2074-23, Ballrechten, *thouarsense* Zone (9), $\times 5550$. 7, isotype, distal view, UCL-2178-3, Brenha, Upper Toarcian (3594), $\times 7800$. 8, isotype, proximal view, UCL-2170-5, Brenha, Upper Toarcian (3594), $\times 5750$. 9, oblique view of fig. 8, UCL-2170-7, $\times 6850$.
- Fig. 10. *Sollasites arctus* (Noël, 1973) comb. nov. Unterstürmig, Lower Toarcian (6), distal view, UCL-2034-24, $\times 6800$.
- Figs. 11 and 12. *Calyculus depressus* sp. nov. Unterstürmig, Lower Toarcian (6). 11, holotype, coccosphere, UCL-2034-24, $\times 3400$. 12, enlargement of fig. 11, UCL-2034-22, $\times 6200$.
- Fig. 13. *C. cribrum* Noël, 1973. Timor, mid-Pliensbachian (J237), distal view, UCL-2074-9, $\times 5950$.
- Figs. 14-18. *Calyculus* sp. indet. 14, distal view, UCL-2034-23, Unterstürmig, Lower Toarcian (6), $\times 6150$. 15, oblique view of fig. 14, UCL-2034-22, $\times 6450$. 16, proximal view, UCL-2034-7, Unterstürmig, Lower Toarcian (6), $\times 4300$. 17, oblique view of fig. 16, UCL-2034-8, $\times 4450$. 18, side view, UCL-2205-16, Picun Leufu, Toarcian (57), $\times 6100$.



BOWN, *Discorhabdus*, *Sollasites*, *Calyculus*

Diagnosis. 'Elliptical coccoliths consisting of 2 petaloid shields in which the component rays lie side by side without imbrication, enclosing a large central opening spanned by one cross bar along the shorter diameter and several bars along the length of the opening' (Black 1973, p. 63).

Remarks. Grün *et al.* (1974) erected a new genus, *Noellithina*, with *N. arcta* (= *Polypodorhabdus arctus* Noël, 1973) as its type species and also including *N. prinsii* (= *Staurorhabdus prinsii* Noël, 1973). The two species are clearly unrelated as *N. prinsii* possesses distinctly imbricating distal elements and three separate shields and *N. arcta* possesses two shields of non-imbricating, radial elements. Goy (1979) placed *N. prinsii* in a new genus, *Bussonius*, and *N. arcta* back into *Polypodorhabdus*. The rim of *N. arcta*, however, is not like that of the polypodorhabdids but very similar to the rims possessed by the Lower Jurassic species *Sollasites prinstinus* and *S. lowei*. Further detailed analysis of the central area of *N. arcta* reveals that it also has features similar to the two *Sollasites* species, with a minor axis bar and a longitudinal bridge which bifurcates towards the middle of the central area forming a lozenge-shaped island. It differs from the two species of *Sollasites* in that this central lozenge is infilled to form a solid island. A number of published specimens of *N. arcta* display the presence of two oblique slots (see Grün *et al.* 1974, pl. 19, fig. 3 and Goy 1981, pl. 15, figs. 1, 4, 5) which delineate the separate longitudinal components of the central lozenge, and reveals the morphological structures which characterize the genus *Sollasites*. Therefore, *Noellithina* is a junior synonym of *Sollasites* and its two original species have been assigned to *Sollasites* and *Bussonius*.

Sollasites arctus (Noël, 1973) comb. nov.

Plate 7, fig. 10; Plate 14, figs. 11 and 12

1973 *Polypodorhabdus arctus* Noël, pp. 110–111, pl. 8, figs. 1–6; text-fig. 7.

1974 *Noellithina arcta* (Noël); Grün and Zweili in Grün *et al.*, pp. 300–301, pl. 19, figs. 1–4; text-fig. 4.

1979 *Polypodorhabdus arctus* Noël; Goy in Goy *et al.*, pl. 3, fig. 7.

1981 *Polypodorhabdus arctus* Noël; Goy, p. 45, pl. 15, figs. 1–9.

Diagnosis. '*Polypodorhabdus* with a relatively large, deep marginal rim with a small central area, flat, with large buttresses; small central button' (Noël 1973, p. 110).

Description. A *Biscutum*-like rim structure with a slightly more open central area filled with a complex structure. The distal shield is moderately broad and composed of twenty to thirty radial elements which show little or no imbrication. The elements slope gently outwards to form the convex shield and sharply inwards at their inner edge to create the steep-sided central area. This central depression is also lined by a low inner cycle or wall which may be a discrete, second distal cycle or the inner edge of the proximal shield. The proximal shield is slightly smaller than the distal shield and composed of twenty to thirty elements which are joined along kinked sutures with a clockwise precession. The proximal shield central area is spanned by a prominent longitudinal bridge, aligned along the major axis of the ellipse, which broadens out towards the centre, to form a lozenge-shaped island supporting a central spine. The bridge is actually formed from two curving bars, which bifurcate from either end of the central area, and the space between them is usually completely filled with additional elements. In well-preserved material two oblique slots clearly delineate the separate components. The central lozenge is additionally supported by twenty equally spaced lateral bars which merge in the minor axis to form a transverse bar.

Dimensions. L: 4.0–4.9 (4.0) μm , W: 2.9–3.2 (3.1) μm .

Remarks. *S. arctus* is distinguished from other members of *Sollasites* by its solid central lozenge structure and lateral bars; from members of *Biscutum* by its wider central area and complex central structures; from species of *Lotharingius* by its radial and non-imbricating rim elements; and from species of *Polypodorhabdus* by its biscutatean rim (non-retacapsoid) and deep central depression. *S. arctus* has an identical central structure to *Calyculus noelae* but possesses a biscutatean rim rather than the vertically extended *Calyculus*-rim (text-fig. 15).

Some morphological variation is observed within the species, with a number of specimens displaying very narrow central areas and a more narrowly formed central complex.

Occurrence. Unterstürmig, Lower Toarcian.

Range. Lower Toarcian (Noël 1973); Lower Toarcian (Grün *et al.* 1974); Lower Toarcian (Goy 1979, 1981).

Sollasites lowei (Bukry, 1969) Rood, Hay and Barnard, 1971

Text-fig. 13

- 1969 *Costacentrum lowei* Bukry, p. 44, pl. 22, figs. 5 and 6.
 1971 *Sollasites lowei* (Bukry); Rood *et al.*, p. 264, pl. 4, fig. 1.
 1974 *Sollasites lowei* (Bukry); Grün *et al.*, p. 299, pl. 18, figs. 1-3; text-fig. 3.
 1981 *Sollasites lowei* (Bukry); Goy, p. 48, pl. 17, figs. 2-6.

Diagnosis. 'An elliptical coccolith composed of a proximal and distal rim and a large, open central area spanned by a distinctive cross structure. The central structure is a cross coinciding with the long and short axes of the ellipse. In addition another cross bar forms a complete ring just inside the central area margin. Little or no imbrication is observed in the rim elements which show radial sutures on the distal shield and slight clockwise inclination on the proximal shield' (Bukry 1969, p. 44).

Description. A well-described coccolith, see especially Grün *et al.* (1974) and Goy (1981).

Dimensions. L: 4.0-4.4 (4.9) μm W: 3.0-3.1 (3.8) μm .

Remarks. *S. lowei* has been found only rarely in the present work. In a number of the Toarcian sections *Sollasites*-like rims are observed which lack central structures (*Sollasites* sp. indet.). It appears that the central structures of the *Sollasites* species are only retained in well-preserved material and this is confirmed by their recorded abundance in the paper shales of the Paris Basin and south Germany (Grün *et al.* 1974; Goy 1981).

Occurrence. Brenha, *ibex* Zone; Trimeusel, *falciferum* Zone.

Range. Upper Toarcian (Rood *et al.* 1973); Lower Toarcian (Grün *et al.* 1974); Lower Toarcian (Goy 1979, 1981); Toarcian (Medd 1982); Lower Pliensbachian to Lower Toarcian (Crux 1984); Toarcian to Upper Cretaceous (Perch-Nielsen 1985).

Family CALYCVLACEAE Noël, 1973

Diagnosis. 'Elliptical to subcircular coccoliths, in the form of a cup with a deep, conical central opening, with constituent subvertical elements which widen and flatten out in their distal portion; central area, closed by a grill' (Noël 1973, p. 115).

LM characteristics. In plan view the distal shield appears dark but translucent in p-c, and grey in c-p (although varies depending on rim thickness); individual elements are well defined. In side view the reduced proximal shield and flaring distal shield are highly distinctive.

Remarks. Members of the Calyculaceae display an extreme modification of the radiating placolith rim structure, but the radial, non-imbricating rim element arrangement is still retained and their close evolutionary relationship to members of the Sollasitoideae has been clearly demonstrated (text-fig. 15). It is thus considered appropriate that this group of coccoliths is given the rank of family within the Podorhabdalaes.

The inclusion of *Calyculus* and *Carinolithus* in the Goniolithaceae Deflandre, 1957 by Grün *et al.* (1974) and Tappan (1980) appears wholly inappropriate as the two groups differ greatly in both morphology and range.

Included genera. *Carinolithus*, *Calyculus*.

Range. Pliensbachian to Middle Jurassic (Bajocian).

Genus CALYCVLUS Noël, 1973

Type species. *Calyculus cribrum* (Noël, 1973) Goy, 1981.

Diagnosis. 'Elliptical to subcircular coccoliths made up of subvertical elements placed side by side, enlarged and flattened in their distal region; the central area is slightly conical, deep and closed by a grill' (Noël 1973, p. 115).

Remarks. Goy (1979) erected three genera each possessing a rim structure typical of *Calyculus* but divided on the fine detail of their central area grill structures (which are normally not preserved). The fine detail of the central area is considered to be a feature of specific significance but inappropriate for generic discrimination. *Incerniculum*, *Vikosphaera*, and *Catillus* are thus considered synonyms of *Calyculus* (see also Crux 1987).

Calyculus sp. indet.

Plate 7, figs. 14–18; Plate 14, figs. 13 and 14

Description. The typical construction of *Calyculus* consists of a large, broadly elliptical, vertically extended distal shield and a reduced proximal shield. The distal shield is composed of ten to fifteen large elements which form a deep, vertically sided central area before flaring out and flattening to form a broad, horizontal, planar distal surface. In side view the elements are usually shaped like a 'Y', flaring to the left in the distal region. They are generally joined along vertical sutures and display radial sutures on the distal surface. The proximal shield marks the base of the flaring distal shield and consists of around fifteen small, subsquare elements which form a thin, narrow ring.

Dimensions. Distal shield L: 5.5–8.5 μm , W: 4.5–6.5 μm ; Proximal shield L: 2.5–5.5 μm , W: 1.5–4.5 μm , RH: 1.0–5.0 μm .

Remarks. The highly individual structure of the *Calyculus* rim allows its immediate recognition in both LM and SEM. In the present work, the majority of the *Calyculus* coccoliths observed had lost their central area structures and thus classification at species level was rendered impossible. This contrasts markedly with the results published by Goy (1981) where he illustrates abundant assemblages of many species of *Calyculus*, all with well-preserved central grills.

Morphological variation is very common and the genus appears to be an evolutionary dynamic group in the Upper Pliensbachian and Lower Toarcian. Although no central structures were observed, variation was noted in the height and width of the distal shield. The evolutionary lineage from *Biscutum* through *Sollasites* and *Calyculus* to *Carinolithus* (text-figs. 9 and 15) explains the presence of this variation, with *Carinolithus magharensis* representing the end member displaying extreme extension of the distal elements and reduction of the proximal shield.

Occurrence. Badenweiler, *bifrons* Zone to *aalensis* Zone; Ballrechten, *bifrons* Zone to *levesquei* Zone; Brenha, *davoiei* Zone to Middle Jurassic; DSDP Site 547, Pliensbachian; Mochras, *ibex* Zone to *levesquei* Zone; Picun Leufu, Upper Pliensbachian to Toarcian; Timor, mid-Pliensbachian; Trimeusel, *tenuicostatum* Zone to *levesquei* Zone; Unterstürmig, Lower Toarcian.

Range. Lower Toarcian (Prins 1969); Lower Toarcian (Noël 1973); Lower Toarcian (Grün *et al.* 1974); Lower Sinemurian to Lower Toarcian (Hamilton 1977); Lower Toarcian (Goy 1979, 1981); *margaritatus* Zone to *aalensis* Zone (Crux 1984).

Calyculus cribrum Noël, 1973 emend. Goy, 1979

Plate 7, fig. 13; text-fig. 15

- 1973 *Calyculus cribrum* Noël, p. 116, pl. 12, fig. 1 (*non* 2–5).
 1974 *Calyculus pugnatum* Grün and Zweili in Grün *et al.*, pp. 311–313, pl. 19, fig. 5.
 1979 *Calyculus cribrum* Noël; emend. Goy in Goy *et al.*, p. 43, pl. 5, fig. 3.
 1981 *Calyculus cribrum* Noël; Goy, pp. 60–61, pl. 25, figs. 1–6; pl. 26, figs. 1–3; text-fig. 15.
non 1974 *Calyculus cribrum* Noël; Grün *et al.*, p. 311, pl. 15, figs. 4–6; text-fig. 11.

Diagnosis. 'A species of *Calyculus* with not very pronounced bars in the axes of the ellipse, determined with 2 curved longitudinal bars, 8 perforations: 4 central and 4 peripheral' (Goy 1979, p. 43).

Description. The rim structure has already been described for *Calyculus* sp. indet. The central area is filled with a small cross, aligned along the principal axes, and two curving longitudinal bars which run concentrically around the inner edge of the central area. This structure is identical to that seen in *S. lowei*.

Dimensions. Distal shield L: 5.8 (6.4) μm , W: 5.2 (5.7) μm ; Central area L: 2.3 (3.6) μm , W: 1.4 (2.8) μm , RH: 1.0 μm .

Remarks. The holotype of *C. cribrum* (Noël 1973, pl. 12, fig. 1) possessed no clear central structure but was accompanied by a number of illustrations with complex central grills. These additional specimens represented a separate species from the holotype. Grün *et al.* (1974) recognized this and assigned the *C. cribrum* name to another coccolith with a wide central grill but this also differed from the holotype. In the same paper they illustrated a new species *C. pugnatum* which corresponded with the holotype of *C. cribrum* and was thus a junior synonym. Goy (1979) correctly described *C. cribrum* and illustrated its diagnostic *lowei*-like grill.

Occurrence. Timor, mid-Pliensbachian (J237).

Range. Lower Toarcian (Noël 1973); Lower Toarcian (Grün *et al.* 1974); Lower Toarcian (Goy 1979, 1981); *spinatum* Zone to *bifrons* Zone (Crux 1984).

Calyculus depressus sp. nov.

Plate 7, figs. 11 and 12; text-fig. 15

Diagnosis. A small species of *Calyculus* with a narrow rim, only slightly extended vertically, and possessing a central area spanned by a cross and two curving longitudinal bars; the coccosphere is monomorphic.

Description. The thin, relatively high distal shield is formed from twenty-three elements; in distal view the elements are joined along radial sutures and in side view the sutures are initially vertical but bend to the left at their distal end, a feature typical of the *Calyculus* rim. The proximal shield is a thin, basal ring of around twenty elements, spanned by a cross, bearing a central, hollow spine base, and two curving longitudinal bars. A collapsed coccosphere was observed bearing only one morphotype and comprising around twenty-five to thirty coccoliths.

Dimensions. L: (3.5) μm , W: (2.1) μm .

Remarks. A coccolith sharing the distinctive central complex of *S. lowei* and *C. cribrum* but which possesses a different rim structure possibly intermediate between the two. The evolutionary development from *S. lowei* to *C. cribrum* has been described by Crux (1987) and would involve a narrowing of the *Sollasites* rim followed by a vertical extension and distal flaring of the constituent rim elements. *C. depressus* represents a transitional rim type, which has considerably narrowed but only begun to extend vertically and shows very little distal flaring. *C. depressus* is similar to *C. hommerilii* (*Catillus hommerilii* Goy 1979) but lacks the additional lateral bars in the central area.

Derivation of name. From Latin *depressus*, low.

Holotype. UCL-2034-24 (Pl. 7, fig. 11).

Type locality. Unterstürmig.

Type level. Lower Toarcian.

Occurrence. Trimeusel, *falciferum* Zone; Unterstürmig, Lower Toarcian.

Genus *CARINOLITHUS* Prins in Grün *et al.* 1974 emend.

Type species. *Carinolithus superbus* (Deflandre, 1954) Prins in Grün *et al.* 1974.

Diagnosis. 'The distal rim, which is built extremely high, widens considerably at the distal end. The proximal disc consists of more than one circle of elements. The central area is closed or shows a very narrow uncovered opening' (Prins in Grün *et al.* 1974, p. 313).

Emended diagnosis. Coccoliths with a small, unicyclic, circular to subcircular proximal shield constructed from wedge-shaped, non-imbricating elements radiating from a central opening, and a spine-like distal shield made up of extremely extended vertical elements forming an elongate, hollow stem which flares distally to create a flat distal surface.

Remarks. The illustrations of *C. superbus* in Grün *et al.* (1974) are thought to be proximal views of a discorhabdid. The shields are far too large to be from *C. superbus* and are also multicyclic.

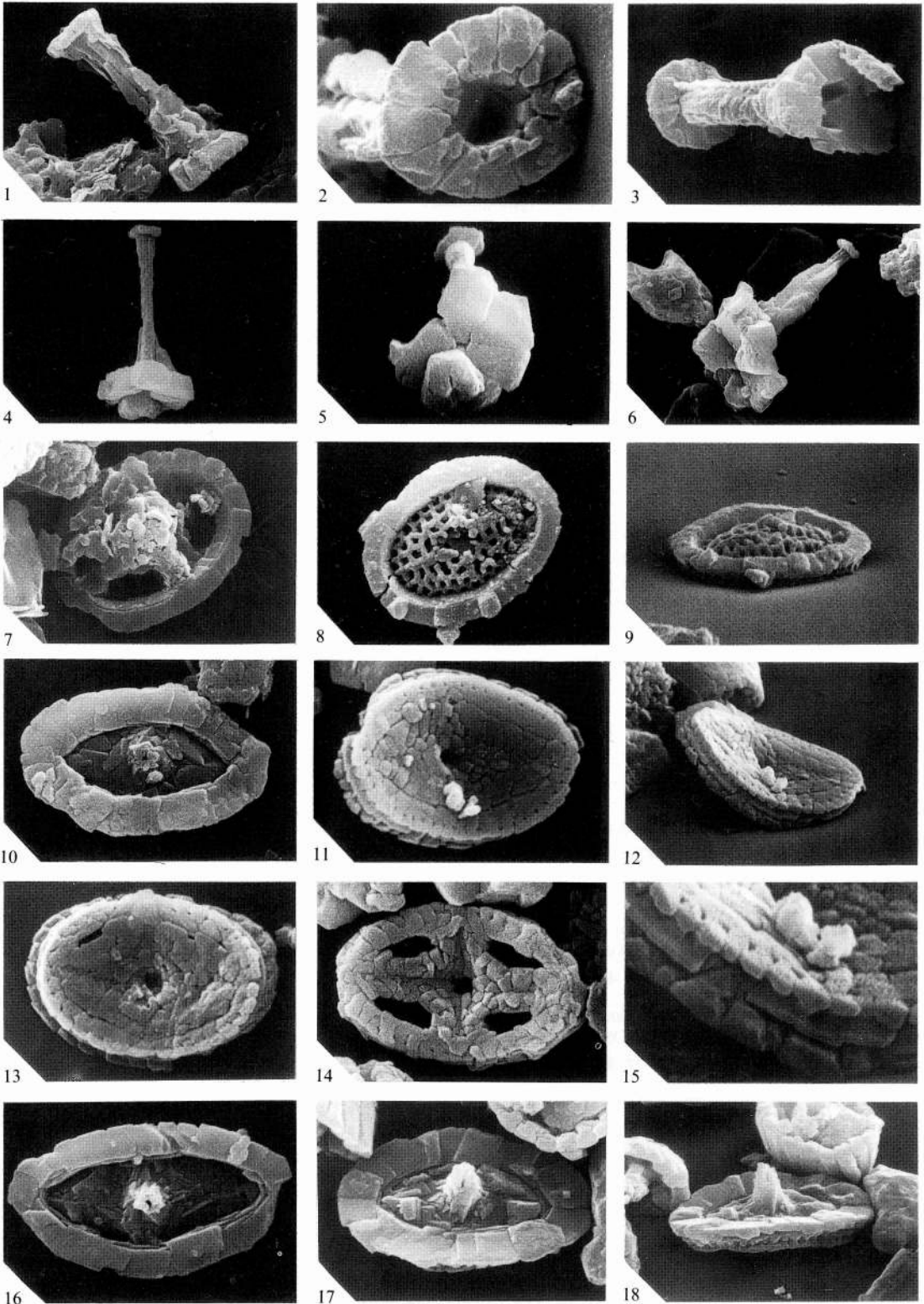
Carinolithus superbus (Deflandre, 1954) Prins in Grün *et al.* 1974

Plate 8, figs. 1-3; Plate 14, figs 15 and 16.

- 1954 *Rhabdolithus superbus* Deflandre in Deflandre and Fert, p. 160, pl. 15, figs. 24 and 25; text-fig. 93.
 1954 *Rhabdolithus sceptrum* Deflandre in Deflandre and Fert, p. 159, pl. 15, figs. 34 and 35; text-fig. 94.
 1954 *Rhabdolithus clavatus* Deflandre in Deflandre and Fert, p. 160, pl. 15, figs. 36-39.
 1969 *Carinolithus superbus* (Deflandre); Prins, p. 549, pl. 1, fig. 7 (*nom. nud.*).
 1977 *Carinolithus superbus* (Deflandre); Hamilton, pl. 4, figs. 2 and 3.
 1977 *Discorhabdus ignotus* (Górka, 1957) Perch-Nielsen 1968; Hamilton, pl. 2, fig. 11.
 1979 *Carinolithus suberbus* (Deflandre); Medd, pp. 58-59, pl. 2, fig. 1.
 1979 *Carinolithus sceptrum* (Deflandre); Medd, pp. 58-59, pl. 2, fig. 2.
 1979 *Carinolithus clavatus* (Deflandre); Medd, pp. 58-59, pl. 1, figs. 11 and 12.
 1984 *Discorhabdus superbus* (Deflandre); Crux, p. 168, fig. 9 (9); fig. 11 (9, 10); fig. 13 (19, 20); (*non* fig. 9 (7, 8)).
 1985 *Discorhabdus ignotus* (Górka); Perch-Nielsen, fig. 20 (10).
 1987 *Discorhabdus superbus* (Deflandre); Crux, pl. 1, figs. 11, 12, 17 (*non* figs. 8-10).
 1987 *Carinolithus superbus* (Deflandre); Bown, pl. 3, figs. 7 and 8.
non 1974 *Carinolithus superbus* (Deflandre); Prins in Grün *et al.*, p. 313, pl. 15, figs. 1-3; text-fig. 13.

EXPLANATION OF PLATE 8

- Figs. 1-3. *Carinolithus superbus* (Deflandre, 1954) Prins in Grün *et al.* 1974. 1, side view, UCL-1993-23, Mochras, *bifrons* Zone (M45), $\times 4050$. 2, proximal disc of fig. 1, UCL-1993-25, $\times 12\ 950$. 3, distal oblique view, UCL-2049-26, Trimeusel, *bifrons* Zone (6), $\times 6100$.
 Figs. 4-6. *C. magharensis* (Moshkovitz and Ehrlich, 1976) comb. nov. Brenha, Bajocian (3617). 4, side view, UCL-2173-16, $\times 3350$. 5, proximal view of fig. 4, UCL-2177-15, $\times 5000$. 6, proximal oblique view, UCL-2198-14, $\times 3000$.
 Fig. 7. *Axopodorhabdus atavus* (Grün *et al.*) comb. nov. Mochras, *levesquei* Zone (M367), distal view, UCL-2150-10, $\times 5250$.
 Figs. 8 and 9. *Ethmorhabdus gallicus* Noël, 1965. Trimeusel, *bifrons* Zone (6). 8, distal view, UCL-2049-18, $\times 6150$. 9, oblique view of fig. 8, UCL-2049-19, $\times 6500$.
 Figs. 10-18. *Mazaganella pulla* gen. nov. sp. nov. 10, holotype, distal view, UCL-2193-31, Site 547, Sinemurian (23-2), $\times 5400$. 11, isotype, proximal view, UCL-2189-32, DSDP Site 547, Sinemurian (20-1), $\times 6250$. 12, oblique view of fig. 11, UCL-2189-33, $\times 4850$. 13, isotype, proximal view, UCL-2190-10, DSDP Site 547, Sinemurian (20-1), $\times 7500$. 14, isotype, proximal view, UCL-2193-28, DSDP Site 547, Sinemurian (23-2), $\times 6650$. 15, enlargement of fig. 12, UCL-2189-34, $\times 14\ 200$. 16, isotype, distal view, UCL-2049-36, DSDP Site 547, Sinemurian (22-2), $\times 6050$. 17, distal view, UCL-2046-9, DSDP Site 547, Sinemurian (22-2), $\times 6000$. 18, oblique view of fig. 17, UCL-2046-10, $\times 4700$.



BOWN, *Carinolithus*, *Axopodorhabdus*, *Ethmorhabdus*, *Mazaganella*

Diagnosis. 'A small, smooth and thick base, passing on to a stem which is narrow at first and then opens out to take the general form of a trumpet (height, 10.3 μm ; width of base, 2.7 μm and width at apex, 4.3 μm). Morphologically similar to the rhabdoliths of *Discosphaera tubifer* of present-day seas, *R. superbus* is differentiated by its greater height' (Deflandre 1954, p. 160).

Description. A subcircular to circular proximal shield, around 2.5 μm in diameter, made up of twelve wedge-shaped, non-imbricating elements with radial sutures. From the centre of this shield the distal elements extend to form a flaring, trumpet-like shield with a flattened distal surface, usually wider than the proximal disc, on which ten elements are revealed, with radial sutures surrounding a central canal.

Dimensions. Proximal shield diameter: 2.3–2.8 (2.7) μm ; Distal surface L: 2.7–3.2 (4.3) μm , W: 2.2–2.6 μm , H: 7.5–8.5 (10.3) μm .

Remarks. As noted above, the SEM photographs and text illustrations given by Prins (*in Grün et al.* 1974) I consider to be proximal views of *Discorhabdus* sp. They differ from the proximal views of *C. superbus*, photographed here in detail, by being much larger, truly circular, multicyclic (with up to three cycles), and consisting of more elements (twenty-eight as opposed to twelve). Similarly, only one of Crux's (1984) proximal illustrations is of *C. superbus*, the remaining specimens are *discorhabdids*.

The hypothesis that the genus *Discorhabdus* was descended from *C. superbus* (Crux 1984, 1987) is rejected here (see below).

Crux (1987) clearly demonstrates the evolutionary lineage from *Calyculus* to *Carinolithus*, with a series of LM photographs which show the gradual extension of the distal elements, reduction of the proximal shield, and the closing of the central area to a narrow, axial canal. Thus, morphological variation is encountered but only the forms with the *C. superbus* structure *sensu stricto*, i.e. a long flaring distal stem, narrow axial canal, small basal disc, are named as such, and all other transitional forms are included in *Calyculus*. The transition occurs during the *tenuicostatum* Zone.

The only other species of *Carinolithus*, *C. sceptrum* and *C. clavatus*, are not used in the present taxonomy. Specimens like those of *C. clavatus* have been observed throughout the range of *C. superbus* and it is probable that they represent damaged specimens of the latter which have lost the flared distal surface. Alternatively, they may represent a dimorph or intraspecific variation. The holotype of *C. sceptrum* is also thought to be within the range of reasonable intraspecific variation.

Deflandre (1954) first pointed out the similarity in morphologies of *C. superbus* and *Discosphaera tubifer* (Murray and Blackman) Ostenfeld and it is interesting to speculate on the form of the original *C. superbus* coccosphere. As in the present-day *D. tubifer*, the distally extended coccoliths would presumably create an almost continuous exathecae much greater in diameter than the cell body and separated from it by a relatively thick boundary layer, equal in width to the stem height. The lack of any other distinctive coccolith appearing unaccountably in the *falciferum* Zone, with the same range as *C. superbus*, appears to preclude any dimorphism within the species.

Occurrence. Badenweiler, *bifrons* Zone to *aalensis* Zone; Ballrechten, *bifrons* Zone to *levesquei* Zone; Brenha, *bifrons* Zone to *levesquei* Zone; DSDP Site 547, Toarcian; Mochras, *falciferum* Zone to *levesquei* Zone; Trimeusel, *falciferum* Zone to *levesquei* Zone; Tunisia, Toarcian.

Range. Crux (1984) confirms the first appearance datum as the *falciferum* Zone, as is observed in this study. After its appearance *C. superbus* is a common, consistent, and resistant component of the Toarcian assemblages.

Carinolithus magharensis (Moshkovitz and Ehrlich, 1976) comb. nov.

Plate 8, figs. 4–6; Plate 14, figs. 17–20

1976a *Hexalithus magharensis* Moshkovitz and Ehrlich, p. 16, pl. 8, figs. 12–15.

1984b *Hexalithus* sp. cf. *H. magharensis* Moshkovitz and Ehrlich; Wiegand, p. 666, pl. 1, figs. 1–4.

Original diagnosis. 'Hexalith more or less hexagonal in shape, composed of 6 distinct triangular elements. Towards the margins the corners of these triangles are obliquely truncated. This form which was observed in LM only, shows in polarised light that each of the elements has its own optical orientation' (Moshkovitz and Ehrlich 1976a, p. 16).

Emended diagnosis. A species of *Carinolithus* possessing a very reduced, subcircular to circular proximal shield from which the distal shield extends as a long, thin stem which flares sharply at its distal extremity to form a broad hexalith composed of six wedge-shaped elements.

Description. *C. magharensis* has an extremely reduced proximal shield consisting of around ten wedge-shaped elements, with radial sutures. The six distal elements initially extend from the centre of the proximal shield and form a long, thin tube, parallel-sided or gently tapering, which flares out and flattens sharply to form a broad distal surface in the shape of a hexalith. Each of the distal surface elements is wedge-shaped and supported by a thin strut from which they flare. The hexalith has radial sutures and a very small or no central opening.

Dimensions. Proximal shield diameter: 1.0–1.6 μm ; Distal hexalith diameter: 4.5–5.9 μm , RH: 7.7–8.5 μm .

Remarks. The tiny proximal disc, thin distal tube, and seemingly top-heavy hexalith render this coccolith prone to breakage, dissolution, and overgrowth, and this has led to the separate naming of isolated components. In the present study *C. magharensis* has been observed in varying states of preservation including isolated hexaliths, hexalith and stem with no proximal disc, and isolated proximal discs. Moshkovitz and Ehrlich (1976a) observed only the distal hexalith and placed it in the genus *Hexalithus*. Wiegand (1984b, pl. 1, figs. 1–4) illustrated the isolated hexalith (LM), and the distal hexalith and stem (SEM), interpreting the hexalith as the proximal coccolith base and the stem as a distal spine.

C. magharensis has so far been recorded from Tethyan and Pacific areas only.

C. magharensis differs from *C. superbis* in possessing a smaller proximal shield, thinner distal stem, and a more sharply flaring distal disc in the form of a hexalith with only six elements.

Occurrence. Brenha, Upper Toarcian/Bajocian; Picun Leufu, Toarcian.

Range. Middle to Upper Bajocian (Sinai) (Moshkovitz and Ehrlich 1976a); Upper Lias (Israel) (Maync in Moshkovitz and Ehrlich 1976a); ?Middle Jurassic (north-west Morocco continental edge) (Wiegand 1984b).

Family PODORHABDACEAE Noël, 1965

Diagnosis. 'Elliptical coccoliths composed of a relatively narrow marginal rim, formed from 2 superimposed series of calcite elements, surrounding a large central area built of microcrystals and in the centre we often find a large or delicate spine supported by a variable number of pillars or a vaulted grill' (Noël 1965, p. 100).

LM characteristics. Narrow rims with wide central areas, dark in p-c with radial suture striations distinctive. Very dim in c-p.

Remarks. A useful taxonomic unit in which to group all those coccoliths with distinct podorhabdid rims, i.e. a narrow, placolith structure composed of non-imbricating elements joined along radial sutures and a wide central area variously filled or bridged.

Range. Upper Pliensbachien to Upper Cretaceous.

Subfamily PODORHABDOIDEAE Reinhardt, 1967

Remarks. Members of the Podorhabdoideae possess typical podorhabdid rims generally consisting of two narrow shields of radial, non-imbricating elements and a wide central area covered by a variety of bars and grills supporting a central hollow spine or spine base. They differ from members of the Retacapoideae (aceae) in lacking the narrow distal shield outer cycle which characterizes

the retacapsoid rim. In addition, the latter group generally has cruciform central structures and a solid central spine or boss.

Included genera. See Perch-Nielsen 1985, p. 380.

GENUS AXOPODORHABDUS Wind and Wise *in* Wise and Wind 1976

Type species. *Podorhabdus cylindratus* Noël, 1965.

Diagnosis. 'Forms with a podorhabdid rim and hollow spine supported by wide bars aligned parallel to the major and minor axes of the coccolith' (Wind and Wise *in* Wise and Wind 1976, p. 297).

Remarks. Noël (1965) erected the genus *Podorhabdus* to include coccoliths which possessed a spine supported by four large bars. Further examination of the holotype of the type species (Noël 1965, pl. 9, figs. 1 and 2) by Wind and Wise (*in* Wise and Wind 1976) led them to the conclusion that *P. grassei* only possesses two bars, and thus the designated type species and generic diagnosis of *Podorhabdus* were in fact different. Wind and Wise (Wise and Wind 1976) redefined the genus *Podorhabdus* to include coccoliths with two large bars with *P. grassei* as the type species, and erected the genus *Axopodorhabdus* for coccoliths with four large bars aligned with the principal axes of the ellipse.

Axopodorhabdus atavus (Grün, Prins and Zweili, 1974) comb. nov.

Plate 8, fig. 7; Plate 14, fig. 21; text-fig. 14

- 1969 *Podorhabdus cylindratus* Noël, 1965; Prins, pl. 3, fig. 7A, B.
 1974 *Staurorhabdus? atavus* Grün *et al.*, p. 308, pl. 21, figs. 4–6.
 1979 *Podorhabdus atavus* (Grün *et al.*); Goy *in* Goy *et al.*, p. 41, pl. 3, fig. 6.
 1981 *Podorhabdus atavus* (Grün *et al.*); Goy, pp. 43–44, pl. 14, figs. 5–10; text-fig. 10.
 1984 *Staurorhabdus quadriarcullus* Noël, 1965; Crux, p. 177, fig. 12 (1).

Diagnosis. 'A species of the genus *Axopodorhabdus* with 4 large perforations roughly triangular determined by the bars aligned along the axes of the ellipse. The support of the prominent spine is important on the proximal face. The margin is marked on the same face by a characteristic median furrow' (Goy 1979, p. 41).

Description. This species is well described and illustrated in Goy (1981, pp. 43–44, pl. 14, figs. 5–10; text-fig. 10).

Dimensions. L: 4.7–6.5 (6.6) μm , W: 3.4–5.0 (4.5) μm .

Remarks. *A. atavus* is generally rare and sporadic in its Lower Jurassic occurrence. However, it has a distinctive LM appearance and has been used as a biostratigraphic marker in a number of published zonation schemes, e.g. Barnard and Hay (1974), Thierstein (1976), Hamilton (1977, 1979, 1982). In the majority of these studies the name *P. cylindratus* has been applied to Lower Jurassic podorhabdid coccoliths with a cross in the central area. More recent SEM work by Grün *et al.* (1974) and Goy (1979, 1981) has revealed that these Lower Jurassic podorhabdids differ considerably from the species *cylindratus* which was originally described and illustrated from the Upper Jurassic (Noël 1965, pl. 9, figs. 3 and 7). *A. cylindratus* possesses a marginal rim which slopes gently into the central area where four circular perforations are delineated by the crossbars. *A. atavus*, however, has a rim with a steep inner edge and a central area with four triangular perforations delineated by the crossbars. While it is possible that *A. atavus* represents the ancestor of the Middle Jurassic *A. cylindratus* it is clear that the end members are distinct species.

Occurrence. Badenweiler, *bifrons* Zone to *aalensis* Zone; Ballrechten, *bifrons* Zone to *levesquei* Zone; Brenha, *variabilis* Zone to Middle Jurassic; Mochras, *spinatum* Zone to *levesquei* Zone; Trimeusel, *falciferum* Zone to *levesquei* Zone; Unterstürmig, Lower Toarcian.

Range. *davoei* Zone to *tenuicostatum* Zone (Prins 1969); *davoei* Zone to Kimmeridgian (Barnard and Hay 1974); Upper Pliensbachian to Oxfordian (Thierstein 1976); *ibex* Zone to Middle Jurassic (Hamilton 1977); Lower Toarcian (Goy 1979, 1981); *spinatum* Zone (Crux 1984).

Genus ETHMORHABDUS Noël, 1965

Type species. *Ethmorhabdus gallicus* Noël, 1965.

Diagnosis. 'Elliptical coccoliths with a base in the form of a narrow border, made up of a double series of calcite elements, surrounding a very large central area, which is made up of microcrystals arranged to give a slightly arched grill and supporting in its centre a cylindrical and hollow stem, frequently damaged or broken' (Noël 1965, p. 110).

Ethmorhabdus gallicus Noël, 1965

Plate 8, figs. 8 and 9

1965 *Ethmorhabdus gallicus* Noël, pp. 110-112, pl. 10, figs. 1, 2, 5; text-figs. 33 and 34.

1979 *Ethmorhabdus gallicus* Noël; Medd, pp. 66-67, pl. 6, figs. 7 and 8.

Diagnosis. *Ethmorhabdus* complying with the definition of the genus with a central area of a hexagonal mesh' (Noël 1965, p. 110).

Description. A coccolith possessing a typical podorhabdid rim consisting of a narrow, distal shield with two cycles. The broader outer cycle slopes gently outwards and is formed from around thirty radial, non-imbricating elements. The extremely narrow inner cycle slopes in towards the central area and is composed of around thirty radial elements. The large central area is spanned by a convex grill with seventy to eighty hexagonally shaped holes in four to five concentric rings. The centre of the grill bears a spine base. The narrow proximal shield is closely fitted to the underside of the distal shield and is composed of around thirty elements displaying some kinking of the sutures.

Dimensions. L: 5.5 (4.4) μm , W: 4.1 (3.6) μm .

Remarks. This species has never previously been recorded from the Lower Jurassic and is usually recorded appearing in the Bajocian. The species *E. crucifer* has been described from the Lower Toarcian (Noël 1973; Goy 1981) and the appearance of *E. gallicus* later in the Toarcian is therefore not improbable. It is recorded rarely and sporadically from the Trimeusel section.

Occurrence. Trimeusel, *bifrons* Zone to *levesquei* Zone.

Range. Oxfordian (Noël 1965); Callovian and Oxfordian (Rood *et al.* 1971); Bajocian to Kimmeridgian (Barnard and Hay 1974); Bathonian to Kimmeridgian (Thierstein 1976); Bajocian to Kimmeridgian (Medd 1982).

Order WATZNAUERIALES *ordo nov.*

Diagnosis. Imbricating placolith coccoliths with two or more shields, the distal shield composed of imbricating elements joined along inclined sutures.

Included families. Watznaueriaceae.

Family WATZNAUERIACEAE Rood, Hay and Barnard, 1971 emend.

Diagnosis. 'Elliptical or circular coccoliths having a coccolithid rim with crystallites orientated so that both shields produce an interference figure between crossed polarizers' (Rood, Hay and Barnard 1971, p. 268).

Emended diagnosis. Imbricating placolith coccoliths, i.e. composed of imbricating, inclined shield elements, typically possessing a bicyclic distal shield and a unicyclic proximal shield

joined by a connecting inner wall. The central area differs in size and may be vacant or variously bridged/filled.

LM characteristics. Broad shields, silvery in p-c, white to yellow in c-p and crossed by four isogyres. Element sutures and inner distal cycle are usually visible.

Remarks. The genus *Ellipsagelosphaera* is thought to be a junior synonym of *Watznaueria* and thus the Ellipsagelosphaeraceae is invalid.

Included genera. See Perch-Nielsen 1985, p. 369.

Range. Pliensbachian to Palaeogene.

GENUS *LOTHARINGIUS* Noël, 1973 emend. Goy, 1979

Type species. *Lotharingius barozii* Noël, 1973.

Diagnosis. 'Elliptical or subcircular coccoliths with a marginal rim composed of 2 shields closely coupled and both imbricating. The distal shield is slightly larger than the proximal shield and composed of 2 superimposed cycles the upper cycle (inner) is generally more prominent in relation to the lower cycle. The elements of the distal shield are overlapping in the dextral direction, those of the proximal shield are overlapping in the sinistral direction. The central area is occupied by 2 bars situated in the axes of the ellipse. The radiating bars complete the central apparatus. At the centre is erected a hollow spine' (Goy 1979, p. 43).

Remarks. Noël (1965) first recognized coccoliths with *Watznaueria*-like rim structures from Lower Jurassic samples and included them in *E. frequens*. In 1969, Prins found similar coccoliths and named them *Colvillea crucicentralis*, *Lucidiella crucifer*, *L. perforata*, and *L. intermedia*, the latter species proposed as an intermediate between the ancestral *Crucirhabdus primulus* var. *striatulus* and the true *Colvillea* forms (= *Watznaueria*). Medd (1971) observed a species similar to that drawn by Prins (1969) and named it *E. crucicentralis*, thus validating the species of Prins (1969). Noël (1973) observed a species of the Watznaueriaceae from the Toarcian but misinterpreted its slightly raised distal inner cycle, typical of the aforementioned family, thinking it to be an unusual reduced distal shield, resting on a larger proximal shield. The larger proximal shield was in fact the outer cycle of the distal shield, the true proximal shield, smaller and adpressed, was hidden beneath. Based on these observations, Noël (1973) erected a new genus, *Lotharingius*, and a new family, Lotharingiaceae. The type species was given as *L. barozii* which possessed a typical watznaueriacean rim with a slightly raised distal inner cycle and a central area spanned by a cross supported by lateral bars. Grün *et al.* (1974) described and illustrated four species of *Lotharingius*, including *L. barozii*, correctly interpreting their structure and placing them in the Watznaueriaceae. However, they offered no comment on the original designation of Noël (1973) and no explanation as to the criteria governing the genus, leaving the original, misleading diagnosis as the only formal description. Also during this period, in papers by Rood *et al.* (1973), Barnard and Hay (1974), and Hamilton (1977, 1979), these same coccoliths were named as *Palaeopontosphaera veterana* and *Striatomarginis primitivus*. The former genus contained coccoliths with non-imbricating, radial rim elements and thus these watznaueriaceans were wrongly assigned. The latter genus, *Striatomarginis*, was junior to *Lotharingius* by seven months. It was not until 1979 that Goy proposed a corrected and precise definition of the genus *Lotharingius*, reaffirming its relationship within the Watznaueriaceae but also stating its independence as a discrete genus.

Lotharingius is a useful taxonomic division for the grouping of those earliest forms of the Watznaueriaceae which appear in the Pliensbachian and all possess a distinctive central area cross and usually additional lateral bars. It is thus a group which is coherent in both morphological characteristics and temporal distribution and warrants its status as a separate genus within the Watznaueriaceae.

Lotharingius primigenius sp. nov.

Plate 9, figs. 11 and 12; Plate 14, figs. 28 and 29; text-figs. 13 and 16

Diagnosis. A broadly elliptical placolith coccolith with a unicyclic distal shield displaying kinked and inclined sutures typical of the Watznaueriaceae but lacking any inner cycle; the central area is small and no central structures have been observed. The coccosphere is spherical and includes around twenty-five coccoliths.

Description. The distal shield is formed from fourteen to eighteen elements joined along counter-clockwise inclined sutures with a distinct V-shaped kink towards their inner edge. The elements are blocky in side view and appear to be non-imbricating. The intergrowth of these elements along kinked and inclined sutures causes pinching out towards their inner edges and a number of the elements may be entirely isolated from the edge of the central area. The central area is a small pore, bounded by the vertical inner edges of the distal elements. The proximal shield has been observed in side view only but appears to be similarly constructed. Separation between the two shields is not great but interlocking of the coccoliths on the coccosphere is observed.

Dimensions. L: 3.3–3.8 (3.4) μm , W: 2.7–3.0 (2.9) μm ; Central area L: 0.8–1.6 (0.9) μm , W: 0.4–0.9 (0.4) μm ; Coccosphere diameter: 8.1 μm .

Remarks. *L. primigenius* possesses a simple Watznaueriaceae structure with a distal cycle displaying the kinked and inclined sutures typical of the family but lacking the distal inner cycle. While this is a diagnostic generic character it is considered unnecessary to place this form in a new genus or to emend *Lotharingius* due to its apparent transitional nature. The lack of an inner cycle reveals the structure of the distal shield usually hidden by the inner cycle and it is seen to exhibit the potential for the structural fragmentation displayed in more typical members of *Lotharingius*. It is similar in both shape and size to the earliest *Lotharingius* to appear, *L. hauffii*, and may have been the ancestral form. It is conceded that these coccoliths may represent *L. hauffii* coccoliths which have undergone a freak diagenetic process which has left the coccoliths and coccospheres intact but removed all trace of the distal inner cycle. However, many specimens have been photographed all revealing identical structures and none displaying any relic inner cycle, such as a sunken ledge or dissolution pores (cf. *Calolithus*). In addition, in the same samples another species of *L. imprimus* has been recognized which displays a structural development intermediate between *L. primigenius* and typical *Lotharingius*.

Derivation of Name. From Latin *primigenius*, first of its kind.

Holotype. UCL-2190-15 (Pl. 9, fig. 11).

Isotype. UCL-2190-21.

Type locality. DSDP Site 547-10-4, 75–77 cm, north-west Moroccan continental edge.

Type level. Lower Toarcian.

Occurrence. DSDP Site 547, Upper Pliensbachian to Lower Toarcian (11-4 to 10-1).

Lotharingius imprimus sp. nov.

Plate 9, figs. 13–15; Plate 14, fig. 30; Plate 15, fig. 1; text-fig. 16

Diagnosis. A normally elliptical coccolith with a large central area, recognizable as a watznaueriacean but possessing only a partially developed distal inner cycle.

Description. In distal view three concentric cycles are visible. At either end of the major axis of the coccolith the inner cycle is incomplete and the inner wall is undifferentiated from the outer cycle elements. The distal shield outer cycle is formed from twenty-two to twenty-eight elements showing strong counter-clockwise inclination but no observable imbrication. The outer cycle displays an inner lowered ledge or shelf on which the inner cycle of small rectangular elements lies. A number of these elements are still closely associated with

the outer cycle elements and joined to them at their corners. At either end of the major axis of the coccolith the inner cycle is undeveloped and the outer cycle elements extend through to the central area forming the vertical inner edge. These elements display sharp sutural kinking and pinching out of the inner portions. The remaining edges of the central area also appear to be formed from the vertical inner edges of the outer cycle elements but the points of contact are hidden by the inner cycle. The central area is large and empty.

Dimensions. L: 4.8–5.6 (5.0) μm , W: 3.6–4.3 (3.6) μm ; Central area L: 2.5–2.8 (2.8) μm , W: 1.3–1.8 (1.6) μm .

Remarks. *L. imprimus* appears to represent an evolutionary stage between the completely undifferentiated, unicyclic shield of *L. primigenius* and the fully developed bicyclic shield of typical species of *Lotharingius*. The partially developed nature of the shield reveals the processes by which rim differentiation takes place and this is discussed below. In *L. imprimus* both the distal inner cycle and inner wall are created by structural fragmentation of the distal shield elements, brought about by complex crystal intergrowth which leads to element isolation.

As for *L. primigenius*, it is conceivable that *L. imprimus* represents a preservational freak. However, numerous specimens have been observed all displaying identical features and showing the partially developed inner cycle in exactly the same way.

Derivation of Name. From Latin *imprimus*, among the first.

Holotype. UCL-2190-23 (Pl. 9, fig. 13).

Isotype. UCL-2190-27.

Type locality. DSDP Site 547-10-4, 75–77cm, north-west Moroccan continental edge.

Type level. Lower Toarcian.

Occurrence. Lower Toarcian (10-4 to 10-1).

Lotharingius sigillatus (Stradner, 1961) Prins in Grün *et al.* 1974

Plate 9, figs. 17 and 18; Plate 10, figs. 1–6; Plate 15, figs. 6 and 7; text-fig. 16

1961 *Discolithus sigillatus* Stradner, p. 79, figs. 14 and 15.

1969 *Colvillea crucicentralis* var. *parva* Prins, pl. 3, fig. 12 (*nom. nud.*).

1969 *Colvillea crucicentralis* Prins, pl. 3, fig. 13 (*nom. nud.*).

1973 *Striatomarginis primitivus* Prins, 1969 *ex Rood et al.*, p. 379, pl. 3, fig. 4.

1973 *Palaeopontosphaera veterna* Prins, 1969 *ex Rood et al.*, p. 378, pl. 3, figs. 2 and 3.

EXPLANATION OF PLATE 9

Figs. 1–5. *Mazaganella protensa* gen. et sp. nov. 1–4, Site 547, Lower Pliensbachian (15-1). 1, holotype, distal view, UCL-2007-32, $\times 4900$. 2, oblique view of fig. 1, UCL-2007-31, $\times 6150$. 3, isotype, proximal view, UCL-2007-22, $\times 4850$. 4, oblique view of fig. 3, UCL-2007-23, $\times 6150$. 5, isotype, distal view, UCL-2148-17, Timor, mid-Pliensbachian (J237), $\times 5750$.

Figs. 6–9. *Triscutum* sp. 1. Picun Leufu, Toarcian (57). 6, distal view, UCL-2065-13, $\times 4050$. 7, oblique view of fig. 6, UCL-2065-12, $\times 4450$. 8, proximal view, UCL-2065-18, $\times 4000$. 9, oblique view of fig. 8, UCL-2065-17, $\times 4100$.

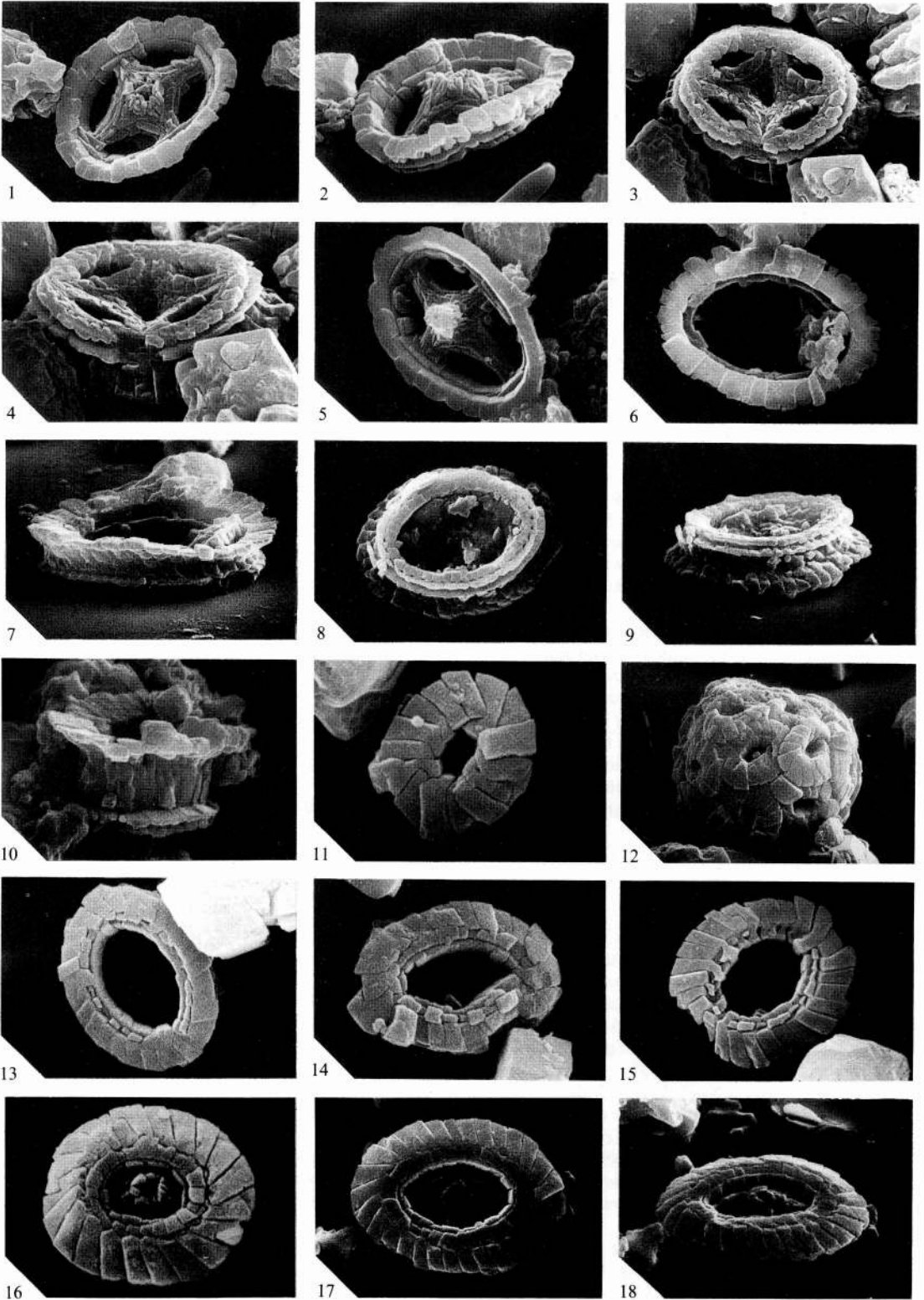
Fig. 10. *Triscutum* sp. 2. Picun Leufu, Toarcian (57), side view, UCL-2064-19, $\times 6050$.

Figs. 11 and 12. *Lotharingius primigenius* sp. nov. Site 547, Toarcian (10-4). 11, holotype, distal view, UCL-2190-15, $\times 7800$. 12, isotype, coccosphere, UCL-2190-21, $\times 3750$.

Figs. 13–15. *L. imprimus* sp. nov. 13 and 14, Site 547, Toarcian (10-4). 13, holotype, distal view, UCL-2190-23, $\times 6100$. 14, isotype, distal view, $\times 6550$, UCL-2190-27, $\times 6550$. 15, distal view, UCL-2205-5, Site 547, Toarcian (10-3), $\times 5900$.

Fig. 16. *L. hauffii* Grün and Zweili in Grün *et al.* 1974. Distal view, UCL-2177-35, Brenha, Upper Toarcian (3594), $\times 8150$.

Figs. 17 and 18. *L. sigillatus* (Stradner, 1961) Prins in Grün *et al.* 1974. Mochras, *levesquei* Zone (3). 17, distal view, UCL-2007-15, $\times 6300$. 18, oblique view of fig. 17, UCL-2006-16, $\times 6300$.



BOWN, *Mazaganella*, *Triscutum*, *Lotharingius*

- 1974 *Striatomarginis primitivus* Prins ex Rood *et al.*; Barnard and Hay, pl. 2, fig. 3.
 1974 *Palaeopontosphaera veterna* Prins ex Rood *et al.*; Barnard and Hay, pl. 2, fig. 4.
 1974 *Lotharingius sigillatus* (Stradner); Prins in Grün *et al.*, p. 304, pl. 17, figs. 3 and 4; text-fig. 8.
 1976 *Watznaueria crucicentralis* (Medd, 1971); Thierstein, p. 351, pl. 2, figs. 8 and 9.
 1976 *Striatomarginis veterna* (Prins ex Rood *et al.*); Wind and Wise in Wise and Wind, p. 306.
 1979 *Striatomarginis veterna* (Prins ex Rood *et al.*); Hamilton, pl. 1, fig. 18.
 1979 *Striatomarginis primitivus* Prins ex Rood *et al.*; Hamilton, pl. 1, fig. 17.
 1981 *Lotharingius sigillatus* (Stradner); emend. Goy, pp. 66–67, pl. 30, figs. 5 and 6.
 1984 *Lotharingius crucicentralis* (Medd); Crux, p. 176, fig. 12 (6, 7); fig. 13 (11, 12).
 1987 *Lotharingius sigillatus* (Stradner); Bown, pl. 2, figs. 5, 6, 7.

Diagnosis. 'A species of the genus *Lotharingius* with a broad, marginal rim. The central area is occupied by weakly developed buttresses in the axes of the ellipse and a system of radial bars' (Goy 1981, p. 66).

Description. Large, broadly elliptical coccoliths with a rim composed of a bicyclic distal shield, a monocyclic proximal shield with a connecting vertical inner wall.

The distal shield outer cycle is the broader of the two distal cycles and composed of twenty-three to twenty-eight rectangular elements which are imbricating dextrally and displaying sutures with strong counter-clockwise inclination; this cycle slopes gently outwards giving the shield its convex upper surface. In many of the specimens observed there is little or no imbrication of the distal elements, which may be due to preservation or a feature of early watznauerians.

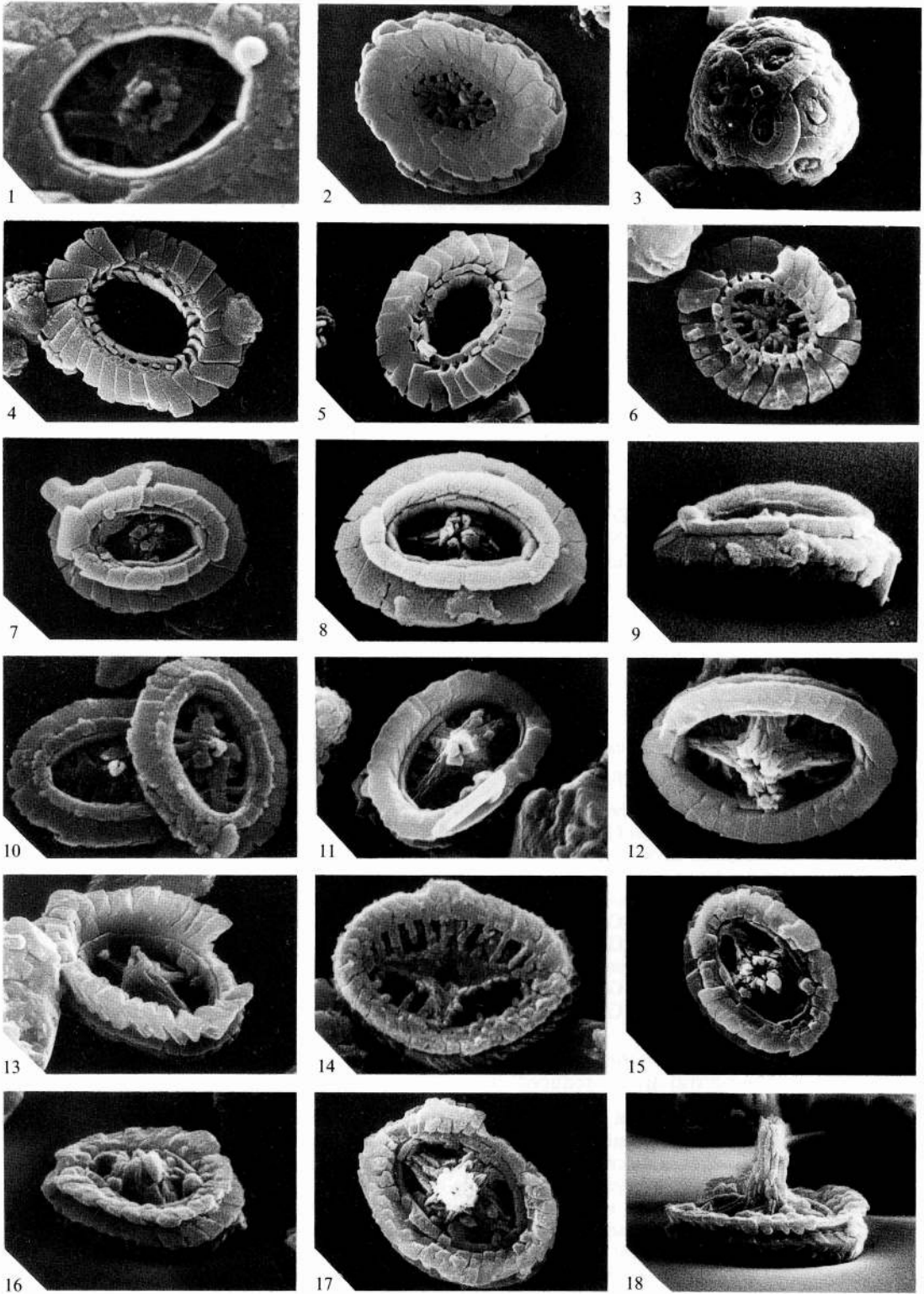
The distal shield inner cycle lies on a narrow ledge on the inner edge of the outer cycle. The outer cycle is against its outer edge and the inner wall around its inner edge. The cycle is composed of twenty-three to twenty-eight subsquare elements which may imbricate dextrally but display near radial sutures with some tendency towards clockwise inclination. The upper surface of the inner cycle is horizontal or slightly inward sloping.

The third and innermost cycle, visible in distal view, is the inner wall composed of twenty-three to twenty-eight subsquare elements joined along radial and vertical sutures. The inner wall is not observed in proximal view but its position coincides with a sharp kink in the proximal shield sutures. The proximal elements are thus crystallographically continuous with the inner wall elements. In addition, the observation of damaged specimens in which the distal inner cycle elements have been lost reveals crystallographic continuity between the outer distal cycle elements and the inner wall (Pl. 10, figs. 4–6). Therefore, the distal shield and proximal shield elements are in fact crystallographically continuous, and joined along the vertical inner wall (this is also clearly displayed in *L. imprimus*).

The proximal shield is slightly smaller than the distal shield and slopes gently inwards. It is constructed

EXPLANATION OF PLATE 10

- Figs. 1–6. *Lotharingius sigillatus* (Stradner, 1961) Prins in Grün *et al.*, 1974. 1, detail of central area structure, UCL-2057-21, Trimeusel, *levesquei* Zone (4), $\times 14\ 050$. 2, proximal view, UCL-2007-17, Mochras, *levesquei* Zone (3), $\times 6300$. 3, coccosphere, UCL-2178-12, Brenha, Upper Toarcian (3606), $\times 2900$. 4, etched specimen, distal view, UCL-1994-21, Mochras, *levesquei* Zone (3), $\times 6600$. 5, etched specimen, distal view, UCL-2178-20, Brenha, Upper Toarcian (3606), $\times 4650$. 6, damaged specimen, proximal view, UCL-2205-17, Picun Leufu, Toarcian (57), $\times 5450$.
- Figs. 7–10. *L. barozii* Noël, 1973. 7, distal view, UCL-2170-31, Brenha, *ibex* Zone (3531), $\times 7150$. 8, distal view, UCL-2170-17, Brenha, *ibex* Zone (3531), $\times 9090$. 9, oblique view of fig. 8, UCL-2170-19, $\times 9150$. 10, distal view, UCL-2049-22, Trimeusel, *bifrons* Zone (6), $\times 9300$.
- Figs. 11–14. *Bussonius prinsii* (Noël, 1973) Goy, 1979. 11, distal view, UCL-2054-6, Trimeusel, *falciferum* Zone (12), $\times 6700$. 12, distal view, UCL-2047-17, Trimeusel, *bifrons* Zone (6), $\times 6250$. 13, oblique view, UCL-2036-19, Unterstürmig, Lower Toarcian (6), $\times 6550$. 14, proximal view, UCL-2034-15, Unterstürmig, Lower Toarcian (6), $\times 7900$.
- Figs. 15–18. *B. leufuensis* sp. nov. Picun Leufu, Toarcian (57). 15, holotype, distal view, UCL-2054-14, $\times 4950$. 16, oblique view of fig. 15, UCL-2054-13, $\times 6150$. 17, isotype, distal view, UCL-2065-8, $\times 5250$. 18, oblique view of fig. 17, UCL-2065-11, $\times 4800$.



BOWN, *Lotharingius*, *Bussonius*

from twenty-three to twenty-eight elements which show little or no sinistral imbrication and counter-clockwise inclining sutures (when viewed proximally). A very sharp kink is displayed by all the proximal suture lines near their inner edge, the sutures veering in a clockwise direction.

The central area of the coccolith varies in size but is always filled with a complex of elements and bars which stem from the inner edge of the proximal shield. The major axis of the ellipse is spanned by a bar, which is very broad at its centre and tapers towards each end. A bar in the minor axis is more weakly developed and tapers sharply from the broad centre of the longitudinal bar. Both these crossbars are formed from microcrystals which are overlain by larger flat elements on the distal surface. The centre of the cross bears a hollow spine base. The four quadrants formed by the crossbars are usually filled with up to three lateral bars, completing the central complex.

Dimensions. L: 4.6–6.0 μm , W: 3.7–4.7 μm ; Central area L: 1.9–2.9 μm , W: 1.1–1.9 μm (holotype dimensions unknown).

Remarks. Prins (in Grün *et al.* 1974) uses the species name *sigillatus*, first used by Stradner (1961) for a *Discolithus* coccolith from the Upper Toarcian of South Germany. The holotype is a simple line drawing showing an *Watznaueria*-like rim with a prominent longitudinal bar in the central area. *L. sigillatus* is an extremely abundant and resistant coccolith in the assemblages of the late early Jurassic. Considerable variation is encountered in rim size, width, and central area width in these forms. It is distinguished from other species of *Lotharingius* by its large, broad shield and prominent, platy longitudinal bar in the central area.

Occurrence. Badenweiler, *bifrons* Zone to *aalensis* Zone; Ballrechten, *bifrons* Zone to *levesquei* Zone; Brenha, *ibex* Zone to Middle Jurassic; Mochras, *tenuicostatum* Zone to *levesquei* Zone; Picun Leufu, Upper Pliensbachian to Toarcian; Trimeşel, *tenuicostatum* Zone to *levesquei* Zone; Tunisia, Upper Pliensbachian to Lower Toarcian; Unterstürmig, Lower Toarcian.

Range. *variabilis* Zone (Stradner 1961); *margaritatus* Zone to *tenuicostatum* Zone (Prins 1969); Lower Toarcian (Prins in Grün *et al.* 1974); *levesquei* Zone to Middle Jurassic (Barnard and Hay 1974); *ibex* Zone to Middle Jurassic (Hamilton 1977, 1979); Lower Toarcian (Goy 1979, 1981); Upper Toarcian to Middle Jurassic (Hamilton 1982); *margaritatus* Zone to Middle Jurassic (Crux 1984).

Lotharingius hauffii Grün and Zweili in Grün *et al.* 1974

Plate 9, fig. 16; Plate 15, figs. 2 and 3; text-figs. 5 and 13

1965 *Ellipsagelosphaera frequens* Noël, pl. 16, figs. 8, 10, 11.

1974 *Lotharingius hauffii* Grün and Zweili in Grün *et al.*, p. 306, pl. 16, figs. 1–6; text-fig. 10.

1974 *Bennocyclus decussatus* Zweili and Grün in Grün *et al.*, pp. 302–303, pl. 14, figs. 4–6; text-fig. 6.

1977 *Ellipsagelosphaera communis* Reinhardt, 1964; Nicosia and Pallini, pl. 2, fig. 2.

1979 *Lotharingius hauffii* Grün and Zweili; emend. Goy in Goy *et al.*, p. 43, pl. 5, fig. 6.

1981 *Lotharingius hauffii* Grün and Zweili; Goy, pp. 65–66, pl. 29, figs. 5–7; pl. 30, figs. 1–3.

1981 *Bennocyclus decussatus* Zweili and Grün; Goy, p. 66, pl. 30, fig. 4.

1984 *Lotharingius hauffii* Grün and Zweili; Crux, p. 176, fig. 12 (3, 4); fig. 13 (7).

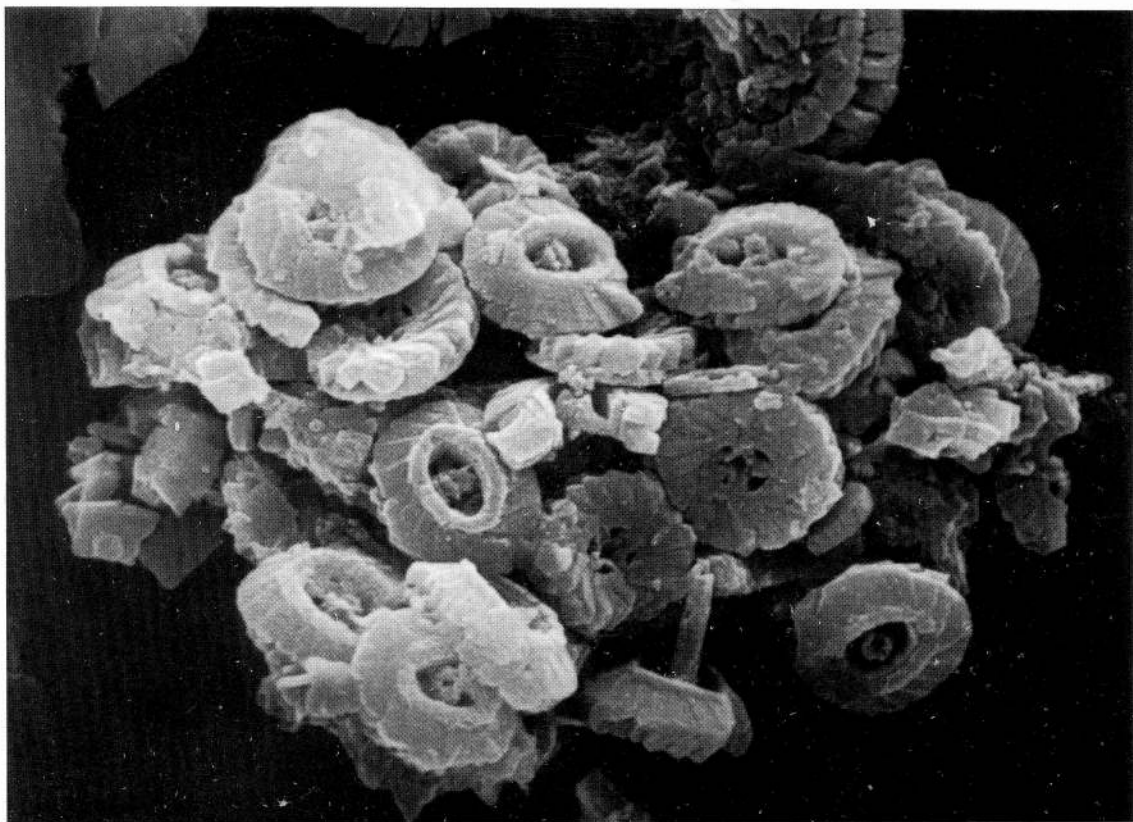
1986 *Lotharingius hauffii* Grün and Zweili; Young *et al.*, p. 125, pl. 1, figs. b and c.

Diagnosis. 'A species of *Lotharingius*, of broad elliptical to subcircular shape, with bars in the axes of the ellipse. The central area is reduced' (Goy 1979, p. 43).

Description. For details of the rim structure see the description given for *L. sigillatus*. *L. hauffii* is a small, broadly elliptical coccolith possessing the typical rim features of the watznaueriaceans and a reduced central area spanned by a spine-bearing cross. The distal shield outer cycle is constructed from eighteen to twenty elements; the distal shield inner cycle may be slightly raised above the height of the outer cycle surface and inner wall and consists of sixteen to twenty elements. The inner wall consists of around twenty subsquare, vertical elements. The proximal shield is only slightly smaller than the distal shield and is formed from around twenty elements. The small central area has a cross, aligned along the principal axes of the ellipse, which is made up of four curving bars and supports a central, tall, hollow spine.

Dimensions. L: 2.8–3.6 (3.7) μm , W: 2.5–3.3 (3.3) μm .

Remarks. Grün and Zweili in Grün *et al.* (1974) included SEM photographs of the proximal views of *L. hauffii* and interpreted them as a new circular species of a new genus, *Bennocyclus decussatus*. All the views are proximal (despite the figure captions) and the coccoliths are not circular as their text-figure suggests. Detailed SEM observation in the present study included the tilting of suitably orientated specimens of *L. hauffii* and revealed *B. decussatus*-like faces on the proximal side (text-fig. 5). Goy (1981) illustrates a specimen of *B. decussatus* but only discussed it within *L. hauffii*, claiming that it imbricates in the opposite direction to *L. hauffii*. This does not appear to be the case.



TEXT-FIG. 5. *Lotharingius hauffii* Grün and Zweili in Grün *et al.* 1974. Collapsed coccosphere including distal, proximal, and side views together with a broken, cross-sectioned specimen and a rarely observed spine bearing specimen. UCL-2034-10, Unterstürmig, Lower Toarcian, $\times 8150$.

L. hauffii is an abundant, consistent, and resistant component of the Upper Pliensbachian and Toarcian assemblages and is the first fully developed *Lotharingius* species to appear. It is distinguished from other species of *Lotharingius* by its small size, broadly elliptical shape, and reduced central area.

Occurrence. Badenweiler, Upper Pliensbachian to *aalensis* Zone; Ballrechten, *bifrons* Zone to *levesquei* Zone; Brenha, *ibex* Zone to Middle Jurassic; Mochras, *margaritatus* Zone to *levesquei* Zone; Longobucco, Upper Pliensbachian; Picun Leufu, Toarcian; Trimeusel, *spinatum* Zone to *levesquei* Zone; Tunisia, Upper Pliensbachian to Toarcian; Unterstürmig, Lower Toarcian.

Range. Toarcian (Noël 1965); Lower Toarcian (Grün *et al.* 1974); Lower Toarcian (Nicosia and Pallini 1977); Lower Toarcian (Goy 1979, 1981); *tenuicostatum* Zone to *levesquei* Zone (Crux 1984); Upper Pliensbachian to Lower Toarcian (Young *et al.* 1986).

Lotharingius barozii Noël, 1973

Plate 10, figs. 7–10; Plate 15, figs. 4 and 5; text-fig. 17

- 1969 *Lucidiella intermedia* Prins, pl. 3, fig. 9 (*nom. nud.*).
 1973 *Lotharingius barozii* Noël, pp. 114–115, pl. 11, figs. 1–7; text-fig. 9.
 1974 *Lotharingius barozii* Noël; Grün *et al.*, pp. 303–304, pl. 17, figs. 1 and 2; text-fig. 7.
 1979 *Lotharingius barozii* Noël; emend. Goy in Goy *et al.*, p. 43, pl. 5, fig. 5.
 1981 *Lotharingius barozii* Noël; Goy, pp. 64–65, pl. 28, figs. 1–9; pl. 29, figs. 1–4.
 1984 *Lotharingius crucicentralis* (Medd. 1971); Crux, p. 176, fig. 12 (5).

Diagnosis. 'A species of *Lotharingius* with massive buttresses in the axes of the ellipse and a system of asymmetric radial bars. The coccosphere is slightly ovoid possessing about 20 coccoliths' (Goy 1979, p. 43).

Description. The specimens observed in the present study are all fairly small, narrowly elliptical coccoliths with a narrow rim. The distal inner cycle is raised above the height of the outer cycle and the central area is narrow. The transverse crossbar usually displays some clockwise deviation from the minor axis and the lateral bars are often asymmetrically arranged, e.g. Goy 1981, pl. 28, fig. 2.

Dimensions. L: 3.5–4.3 (3.1) μm , W: 2.5–3.3 (2.4) μm .

Remarks. Only rarely found in the present study, which may be due to difficulty in distinguishing it from *L. sigillatus* in the LM. *L. barozii* is distinguished from other species of *Lotharingius* by its narrowly elliptical shape, prominent distal shield inner cycle, and asymmetric central area complex.

Occurrence. Brenha, *ibex* Zone; Trimeusel, *bifrons* Zone.

Range. *davoei* Zone to *tenuicostatum* Zone (Prins 1969); Lower Toarcian (Noël 1973); Lower Toarcian (Grün *et al.* 1974); Lower Toarcian (Goy 1979, 1981).

Genus BUSSONIUS Goy, 1979

Type species. *Bussonius prinsii* (Noël, 1973) Goy, 1979.

Diagnosis. 'Elliptical coccoliths where the marginal rim is composed of a superposition of 3 series of elements, the distal series possesses elements which are distinctly inclined. The central area is occupied by a system of buttresses in the axes of the ellipse, with a spine base at the centre. The apparatus is completed with radial bars' (Goy 1979, p. 40).

Remarks. The species *B. prinsii* was first placed in *Staurorhabdus* by Noël (1973), into *Noellithina* by Grün and Zweili in Grün *et al.* (1974), and most recently into *Bussonius* by Goy (1979). The placolith rim structure of *B. prinsii* prevents its inclusion in the loxolith genus, *Staurorhabdus*, and the additional features of three distinct shields and imbricating elements also excludes it from *Noellithina* (= *Sollasites*). Thus, Goy (1981) erected *Bussonius* to include this species allowing for its unique morphology. Goy's proposal of a separate family Bussoniaceae is considered unnecessary as *B. prinsii* is closely related to *L. barozii*, both species possessing analogous and in some cases identical structural components (text-fig. 17). *B. prinsii* is considered an evolutionary descendant of *L. barozii* and its modified watznaueriacean rim can be accommodated in the Watznaueriaceae.

Bussonius prinsii (Noël, 1973) Goy, 1979

Plate 10, figs. 11–14; Plate 15, figs. 8–10; text-fig. 17

- 1973 *Staurorhabdus prinsii* Noël, pp. 100–101, pl. 2, fig. 9; text-fig. 1.
 1974 *Noellithina prinsii* (Noël); Grün and Zweili in Grün *et al.*, pp. 301–302, pl. 18, figs. 4–6; text-fig. 5.

- 1979 *Bussonius prinsii* (Noël); Goy in Goy *et al.*, p. 40, pl. 2, fig. 5.
 1981 *Bussonius prinsii* (Noël); Goy, pp. 32–33, pl. 8, figs. 10 and 11; pl. 9, figs. 1–8; text-fig. 7.
 1984 *Noellithina prinsii* (Noël); Crux, pp. 176–177, fig. 12 (8, 9, 10); fig. 13 (9, 10, 11).

Diagnosis. 'As for the genus' (Goy 1979, p. 40).

Description. *B. prinsii* is a narrowly elliptical coccolith with a thin rim consisting of three superimposed monocyclic shields. The distal shield is the thickest of the three and composed of twenty-five to thirty tall elements, dextrally imbricating. The sutures on this shield vary between approximately radial and distinctly clockwise in inclination. The intermediate and proximal shields are both thin, and linked by an inner wall which appears as a vertical lining to the central area, below the level of the distal shield. The two lower shields are occasionally fused together and appear as one shield. The proximal shield is formed from around thirty elements which show some imbrication in the opposite direction to that seen in the distal shield. The proximal elements are joined along sutures which are markedly clockwise in inclination, with a distinct V-shaped kink near their inner edge. The central area of the proximal shield is spanned by a cross structure supporting a tall central, hollow spine. Four additional radial bars are situated in each of the quadrants created by the cross. The minor axis bar is not always aligned with the minor axis of the ellipse, usually making an angle of 65 to 75° with the longitudinal bar.

Dimensions. L: 3.7–5.6 (5.4) μm , W: 2.5–4.5 (3.1) μm , RH: 0.8–1.1 μm , SH: \sim 2.6 μm .

Remarks. It has become clear from detailed morphological observation and stratigraphic considerations that *B. prinsii* and *L. barozii* are closely related, with *B. prinsii* developing from the latter in the Pliensbachian (text-fig. 17). The proximal shields and central structures of the two species are identical and only modification of the two distal shield cycles of *B. prinsii* separates it from *L. barozii*. The development from *L. barozii* is described later in the paper.

The appearance of only two shields in some specimens appears to be a product of overgrowth, fusing the two, thin and adpressed lower shields.

Occurrence. Badenweiler, *variabilis* Zone to *aalensis* Zone; Ballrechten, *bifrons* Zone to *levesquei* Zone; Brenha, *ibex* Zone to *levesquei* Zone; Mochras, *spinatum* Zone to *levesquei* Zone; Picun Leufu, Toarcian; Timor, mid-Pliensbachian; Trimeusel, *bifrons* Zone to *levesquei* Zone; Unterstürmig, Lower Toarcian.

Range. Lower Toarcian (Noël 1973); Lower Toarcian (Grün *et al.* 1974); Lower Toarcian (Goy 1979, 1981); *spinatum* Zone to *levesquei* Zone (Crux 1984).

Bussonius leufuensis sp. nov. Bown and Kielbowicz

Plate 10, figs. 15–18; Plate 15, figs. 11 and 12

Diagnosis. A normally elliptical species of *Bussonius* possessing three broad shields of similar thickness and a central cross bearing a tall spine.

Description. The distal shield is composed of around thirty flat, rectangular elements, joined along clockwise inclined sutures and displaying dextral imbrication. The distal shield is usually the same size as the lower two shields but may be smaller, revealing the outer portion of the underlying, intermediate shield. The intermediate shield is composed of around thirty, flat elements imbricating dextrally and joined along counter-clockwise inclined sutures. It appears to be joined to the proximal shield via a vertical inner wall, which lines the central area below the level of the distal shield. The distal shield is horizontal or slopes slightly inwards and the intermediate shield slopes outwards. The proximal shield has been observed in side view only and consists of around thirty elements with sinistral imbrication. The central area is spanned by a cross, aligned along the principal axes of the ellipse, supporting a hollow, central spine.

Dimensions. L: 6.1–6.6 (6.4) μm , W: 4.7–4.9 (4.7) μm , RH: 1.2–1.5 μm , SH: 4.5–4.8 μm .

Remarks. *B. leufuensis* is distinguished from *B. prinsii* by its greater size and thinner, flatter distal shield (unlike the almost loxolithic development seen in *B. prinsii*). The lack of any radial bars in the central area may be an original feature or the result of diagenetic loss.

As with *B. prinsii*, it is constructed from three rim components which are analogous to those found in *Lotharingius*. *B. leufuensis* retains the horizontal or inward sloping distal shield cycle

(distal shield inner cycle of *Lotharingius*) and the convex intermediate shield (distal shield outer cycle) typical of the watznaueriacean rim and resembles *L. sigillatus* rather than *L. barozii*.

Derivation of Name. From the type locality, Picun Leufu, Argentina.

Holotype. UCL-2054-14 (Pl. 10, fig. 15).

Isotype. UCL-2065-8, UCL-2065-11 (same specimen).

Type locality. Picun Leufu.

Type level. Toarcian.

Occurrence. Found in type material only.

INCERTAE SEDIS

Genus CONUSPHAERA Trejo, 1969

Type species. *Conusphaera mexicana* Trejo, 1969.

Remarks. The type species, *C. mexicana*, has its first occurrence in the Upper Jurassic (Tithonian) and is thus separated by a large time gap from the Triassic *C. zlambachensis* of similar structure. While it is at present uncertain whether these two nannofossils are related *C. zlambachensis* will be retained in *Conusphaera* until its affinities can be more clearly established.

Conusphaera zlambachensis Moshkovitz, 1982

Plate 11, figs. 1-3; Plate 15, figs. 13 and 14

1982 *Conusphaera zlambachensis* Moshkovitz, p. 612, 613, pl. 1, figs. 1-10.

1983 *Eoconusphaera tollmanniae* Jafar, p. 228, 229, fig. 6 (1, 2, 3).

Description. A nannofossil shaped like a truncated cone and subcircular in plan view. The core of the cone is formed from around forty thin lamellae which radiate from a fine central canal and are twisted in a clockwise direction. The core is surrounded by an outer layer of ten to fifteen plates, joined along vertical sutures. The internal lamellae protrude distally from the outer plates to give a domed distal surface.

Dimensions. H: 4.0-6.0 (8.0) μm ; Distal diameter: 3.0-5.0 (5.0) μm ; Proximal diameter: 1.5-2.5 (3.5) μm .

EXPLANATION OF PLATE 11

Figs. 1-3. *Conusphaera zlambachensis* Moshkovitz, 1982. Weissloferbach, *marshi* Zone (13b). 1, distal view, UCL-2036-36, $\times 6750$. 2, proximal view, UCL-2036-35, $\times 6600$. 3, damaged specimen showing cross-section, UCL-2041-1, $\times 6950$.

Fig. 4. *Orthogonoides hamiltoniae* Wiegand, 1984. DSDP Site 547, Lower Pliensbachian (15-1), UCL-2028-22, $\times 5250$.

Figs. 5 and 6. *Prinsiosphaera triassica* Jafar, 1983. 5, UCL-2014-23, Fischerwiese, *marshi* Zone (F2), $\times 4350$. 6, UCL-2036-29, Weissloferbach, *marshi* Zone (13b), $\times 4000$.

Figs. 7-9. *Schizosphaerella punctulata* Deflandre and Dangeard, 1938. 7, UCL-2052-12, Trimeusel, *levesquei* Zone (4), $\times 2650$. 8, internal view of isolated valve, UCL-1917-14, Mochras, *raricostatum* Zone (M285), $\times 4150$. 9, detail of fig. 8, UCL-1917-15, $\times 8300$.

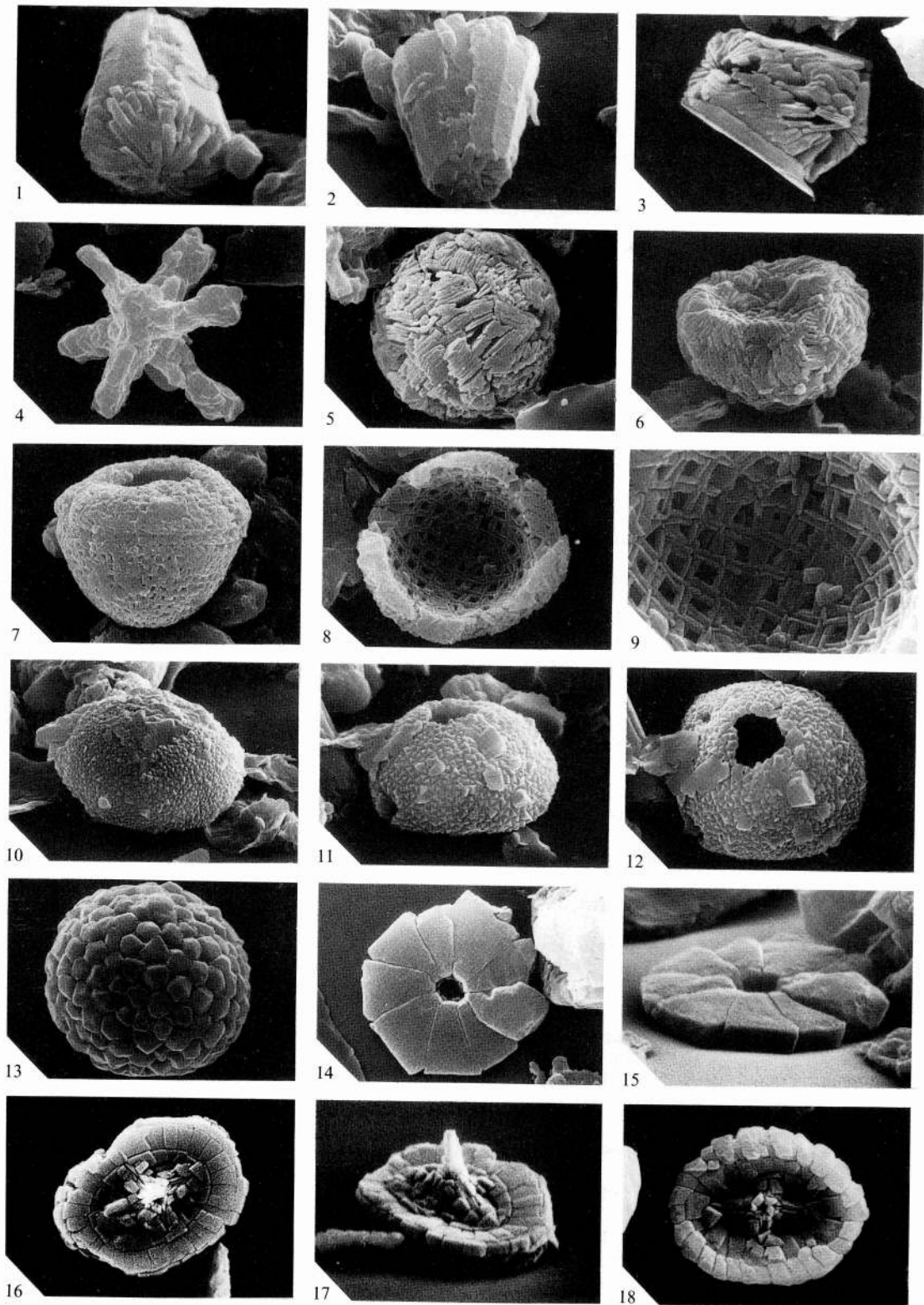
Figs. 10-12. *Thoracosphaera geometrica* (Jafar, 1983) comb. nov. Weissloferbach, *marshi* Zone (13b). 10, UCL-2041-2, $\times 3050$. 11, UCL-2040-27, $\times 4400$. 12, as fig. 11, UCL-2040-28, $\times 4450$.

Fig. 13. Pyrite frambooid. Mochras, *semicostatum* Zone (M169), UCL-1888-31, $\times 3600$.

Figs. 14 and 15. Undetermined unicyclic disc. Brenha, Upper Toarcian (3606). 14, UCL-2193-36, $\times 6000$.

15, oblique view of fig. 14, UCL-2193-35, $\times 7000$.

Figs. 16-18. *Retacapsa* sp. Brenha, Bajocian (3617). 16, distal view, UCL-2173-1, $\times 5750$. 17, oblique view of fig. 16, UCL-2173-2, $\times 6600$. 18, distal view, UCL-2173-22, $\times 5900$.



BOWN, early Mesozoic nannofossils

Remarks. Both Moshkovitz (1982) and Jafar (1983) comment on the similarity between this nannofossil and the Upper Jurassic *C. mexicana*. The former places it within *Conusphaera* and the latter erected a new genus, *Eoconusphaera*.

C. zlabachensis is also extremely similar, particularly in external appearance, to the Lower Jurassic nannofossil *Mitrolithus jansae*, and the possible relationship between these two forms is discussed later.

Occurrence. Fischerwiese, Rhaetian; Weissloferbach, *suessi* Zone to *marshi* Zone.

Range. *marshi* Zone (Moshkovitz 1982); *suessi* Zone to *marshi* Zone (Jafar 1983); Rhaetian (Posch and Stradner 1987).

Genus ORTHOGONOIDES Wiegand, 1984

Type species. *Orthogonoides hamiltoniae* Wiegand, 1984a.

Diagnosis. 'Nannolith with 6 orthogonal rays' (Wiegand 1984a, p. 1152).

Orthogonoides hamiltoniae Wiegand, 1984

Plate 11, fig. 4; Plate 15, figs. 15 and 16

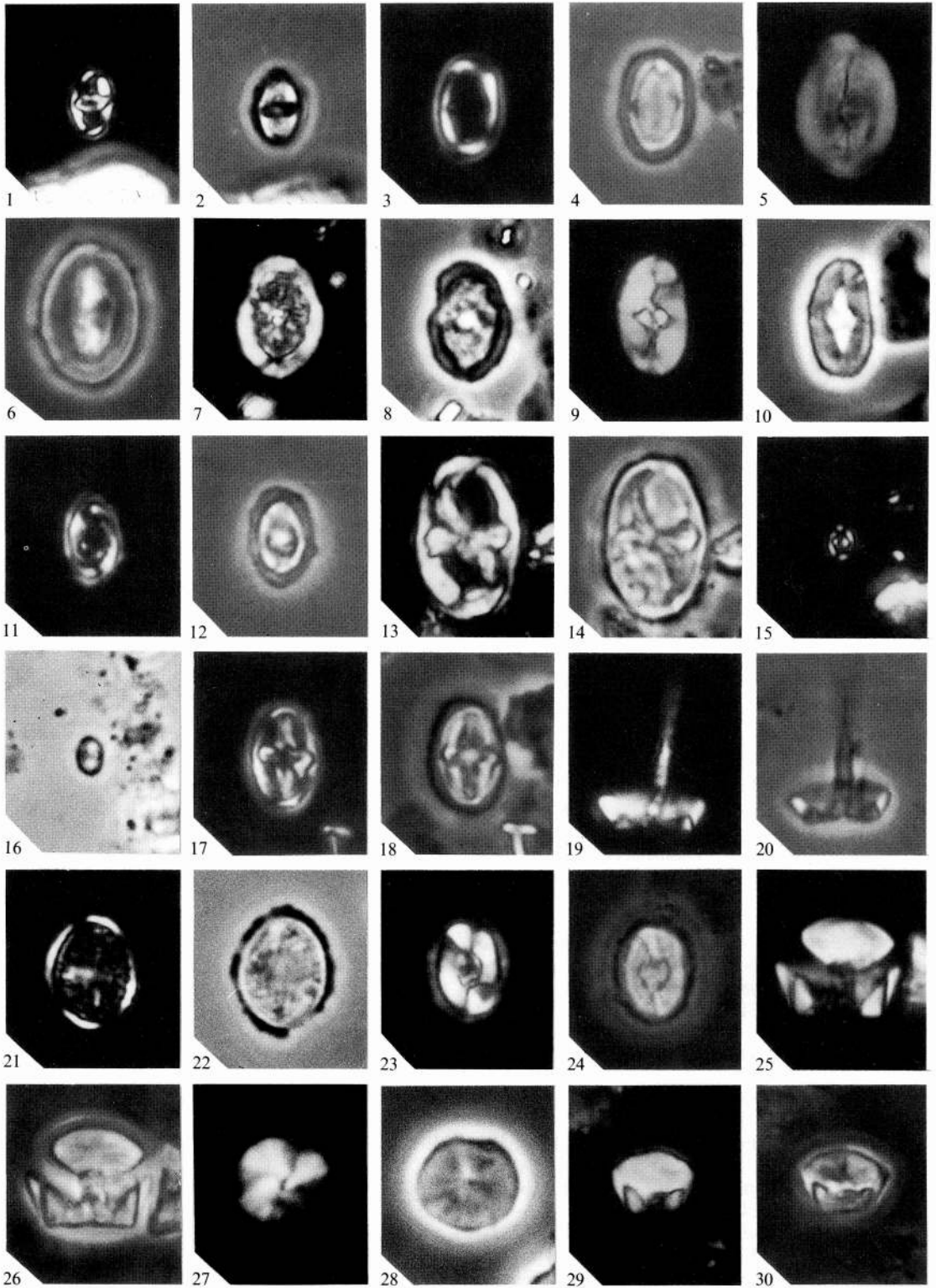
1984a *Orthogonoides hamiltoniae* Wiegand, p. 1155, pl. 2, figs. A-E.

1984b *Orthogonoides hamiltoniae* Wiegand; Wiegand, p. 666, pl. 3, fig. 5.

EXPLANATION OF PLATE 12

All light micrographs, approximately $\times 2700$.

- Figs. 1 and 2. *Archaeozygodiscus koessenensis* Bown, 1985. 1, c-p, UCL-2274-13, Fischerwiese, *marshi* Zone (F1). 2, as fig. 1, p-c, UCL-2274-11.
- Figs. 3 and 4. *Crepidolithus cavus* Prins ex Rood *et al.*, 1973. 3, c-p, UCL-2452-8, Unterstürmig, Lower Toarcian (6). 4, as fig. 3, p-c, UCL-2452-9.
- Figs. 5 and 6. *C. crassus* (Deflandre, 1954) Noël, 1965. 5, c-p, UCL-2260-30, Trimeusel, *bifrons* Zone (6). 6, as fig. 5, p-c, UCL-2260-31.
- Figs. 7 and 8. *C. granulatus* sp. nov. 7, c-p, UCL-2289-17, Brenha, *davoei* Zone (6107). 8, as fig. 7, p-c, UCL-2290-18.
- Figs. 9 and 10. *C. plienschachensis* Crux, 1985. 9, c-p, UCL-2289-5, DSDP Site 547, Sinemurian (18-1). 10, as fig. 9, p-c, UCL-2289-6.
- Figs. 11 and 12. *Tubirhabdus patulus* Prins ex Rood *et al.*, 1973. 11, c-p, UCL-2455-24, Picun Leufu, Toarcian (57). 12, as fig. 11, p-c, UCL-2455-25.
- Figs. 13 and 14. *Bucanthus decussatus* gen. et sp. nov. 13, c-p, UCL-2265-19, Timor, mid-Plienschachian. 14, as fig. 13, p-c, UCL-2265-18.
- Figs. 15 and 16. *Crucirhabdus minutus* Jafar, 1983. 15, c-p, UCL-2274-9, Weissloferbach, *marshi* Zone (13b). 16, as fig. 15, p-c, UCL-2274-10.
- Figs. 17-20. *C. primulus* Prins ex Rood *et al.*, 1973. 17, c-p, UCL-2093-30, Mochras, *ravicostatum* Zone (289). 18, as fig. 17, p-c, UCL-2093-31. 19, c-p, UCL-2455-14, Hock Cliff, *bucklandi* Zone (11). 20, as fig. 19, p-c, UCL-2455-16.
- Figs. 21 and 22. *Diductius constans* Goy, 1979. 21, c-p, UCL-2201-34, Brenha, Bajocian (3617). 22, as fig. 21, p-c, UCL-2201-33.
- Figs. 23-28. *Mitrolithus elegans* Deflandre, 1954. 23, distal view without spine, c-p, UCL-2452-20, Trunch, *jamesoni* Zone (10). 24, as fig. 23, p-c, UCL-2452-22. 25, side view, c-p, UCL-2455-5, Trunch, *jamesoni* Zone (10). 26, as fig. 25, p-c, UCL-2455-7. 27, isolated spine, c-p, UCL-2311-14, Mochras, *jamesoni* Zone (M303). 28, as fig. 27, p-c, UCL-2311-15.
- Figs. 29 and 30. *M. lenticularis* sp. nov. 29, c-p, UCL-2265-26, Timor, mid-Plienschachian. 30, as fig. 29, p-c, UCL-2265-27.



BOWN, early Mesozoic coccoliths

Diagnosis. 'A species of *Orthogonoides* with 6 straight orthogonally joined rays. Bifurcation appears at the end of the rays' (Wiegand 1984a, p. 1155).

Description. See Wiegand (1984a).

Dimensions. Maximum dimension: 6.8–11.5 (9.7) μm .

Occurrence. Badenweiler, Upper Pliensbachian; Brenha, Lower Sinemurian to *jamesoni* Zone; DSDP Site 547, Sinemurian to Pliensbachian; Mochras, *oxynotum* Zone to *falciferum* Zone; Picun Leufu, Upper Pliensbachian; Trimeusel, *falciferum* Zone; Trunch, *raricostatum* Zone to *jamesoni* Zone; Tunisia, Toarcian; Unterstürmig, Lower Toarcian.

Range. Sinemurian to Lower Pliensbachian (Wiegand 1984b).

Division PYRROPHYTA Pascher, 1914

Class DINOPHYCEAE Fritsch, 1929

Order, THORACOSPHAERALES Tangen *et al.*, 1982

Family SCHIZOSPHAERELLACEAE Deflandre, 1959

Genus SCHIZOSPHAERELLA Deflandre and Dangeard, 1938

Diagnosis. *Schizosphaerella* is characterized by a roughly globular test (10–30 μm in diameter) composed of two interlocking sub-hemispherical valves with a complex wall structure based on the intergrowth of one fundamental structural element, a tiny parallelogram shaped calcite lamella (abstracted from Kälin and Bernoulli 1984, pp. 412–413).

Schizosphaerella punctulata Deflandre and Dangeard, 1938

Plate 11, figs. 7–9; Plate 15, figs. 25 and 26

1938 *Schizosphaerella punctulata* Deflandre and Dangeard, p. 115, figs. 1–6.

1961 *Nannopatina grandaeva* Stradner, p. 78, figs. 1–10.

EXPLANATION OF PLATE 13

All light micrographs, approximately $\times 2700$.

Figs. 1–4. *Mitrolithus jansae* (Wiegand, 1984) Bown and Young, 1986. 1, side view, c-p, UCL-2289-1, DSDP Site 547, Sinemurian (20-1). 2, as fig. 1, p-c, UCL-2289-2. 3, side and distal views, c-p, UCL-2289-9, DSDP Site 547, Lower Pliensbachian (15-1). 4, as fig. 3, p-c, UCL-2289-10.

Figs. 5–8. *Parhabdolithus liasicus distinctus* Deflandre, 1952 ssp. nov. 5, c-p, UCL-2311-12, Mochras, *jamesoni* Zone (M303). 6, as fig. 5, p-c, UCL-2311-13. 7, c-p, UCL-2311-17, DSDP Site 547, Lower Pliensbachian (15-2). 8, as fig. 7, p-c, UCL-2311-18.

Figs. 9 and 10. *P. l. liasicus* Deflandre, 1952 ssp. nov. 9, c-p, UCL-2289-7, DSDP Site 547, Sinemurian (18-1). 10, as fig. 9, p-c, UCL-2289-8.

Figs. 11–14. *P. marthae* Deflandre, 1954. 11, c-p, UCL-2455-12, Hock Cliff, *semicostatum* Zone (11). 12, as fig. 11, p-c, UCL-2455-13. 13, c-p, UCL-2270-29, Hock Cliff, *bucklandi* Zone (1). 14, as fig. 13, p-c, UCL-2270-30.

Figs. 15 and 16. *P. robustus* Noël, 1965. 15, c-p, UCL-2093-9, Trunch, *jamesoni* Zone (14). 16, as fig. 15, p-c, UCL-2093-10.

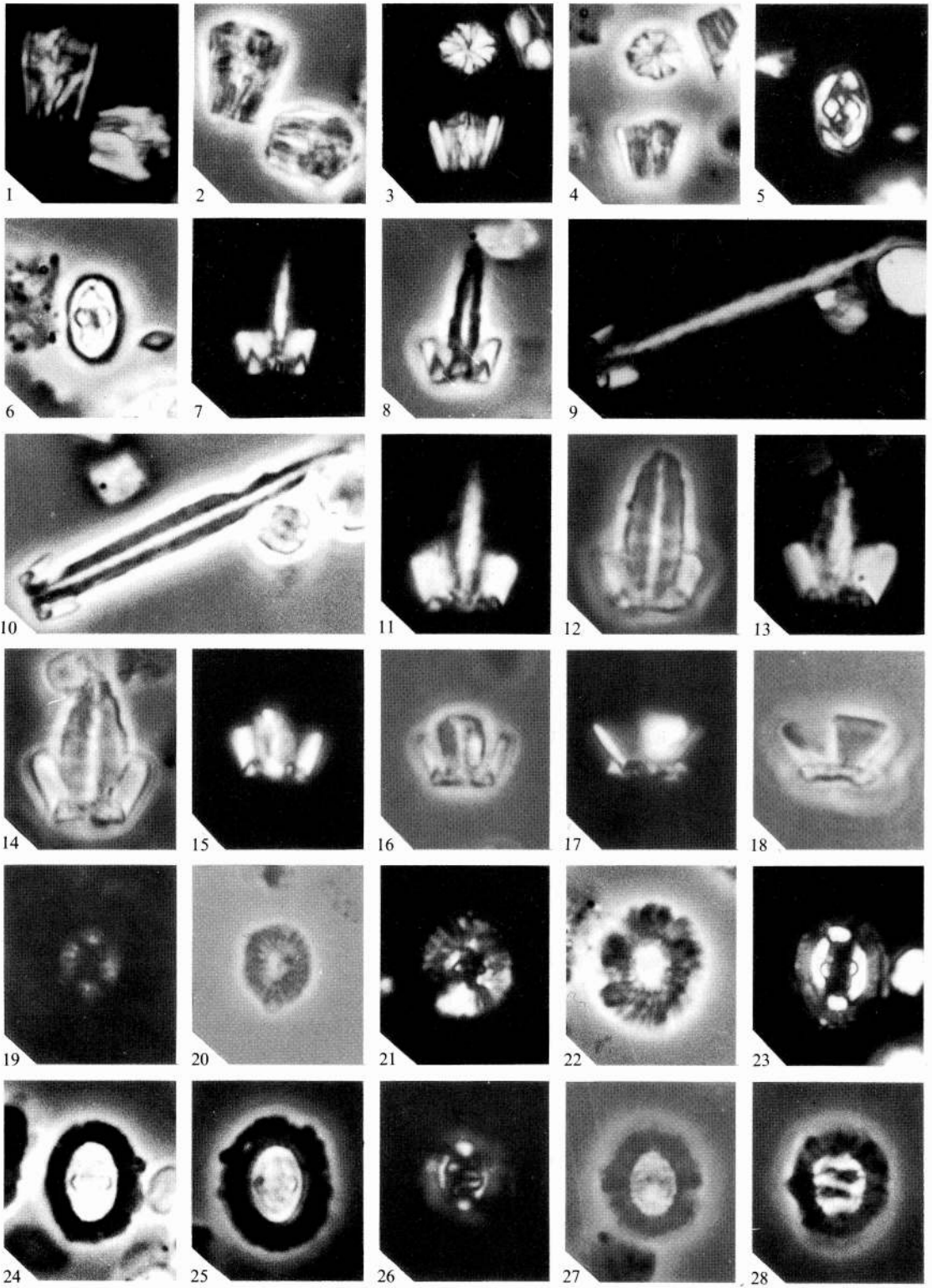
Figs. 17 and 18. *Timorella cypella* gen. et sp. nov. 17, c-p, $\times 4352$, UCL-2093-18, Timor, mid-Pliensbachian. 18, as fig. 17, p-c, UCL-2093-19.

Figs. 19 and 20. *Biscutum novum* (Goy, 1979) Bown, 1987. 19, c-p, UCL-2452-6, Unterstürmig, Lower Toarcian (6). 20, as fig. 19, p-c, UCL-2452-7.

Figs. 21 and 22. *B. finchii* Crux, 1984. 21, c-p, UCL-2311-20, Picun Leufu, Upper Pliensbachian (46). 22, as fig. 21, p-c, UCL-2311-19.

Figs. 23–25. *B. grandis* sp. nov. 23, c-p, UCL-2311-1, Brenha, *davoei* Zone (6107). 24, as fig. 23, p-c, UCL-2311-3. 25, p-c, UCL-2203-26, Brenha, *ibex* Zone (3531).

Figs. 26–28. *B. intermedium* sp. nov. 26, c-p, UCL-2452-30, Brenha, Bajocian (3617). 27, as fig. 26, p-c, UCL-2452-31. 28, p-c, UCL-2201-30, Brenha, Bajocian (3617).



BOWN, *Mitrolithus*, *Parhabdolithus*, *Timorella*, *Biscutum*

- 1979 *Schizosphaerella punctulata* Deflandre and Dangeard; Moshkovitz, p. 458, pl. 1, figs. 1-10.
 1980 *Schizosphaerella punctulata* Deflandre and Dangeard; Kälın, pp. 983-1008, figs. 4-6, 14.

Diagnosis. *S. punctulata* shows a striking variability in test shape and typically has a refined system of hingement with the valves interlocking along a ring-shaped groove developed at the periphery of the hypovalve; the wall ultrastructure is based on a rectangular (tetragonal) mutual disposition of oblique parallelogram-shaped elementary crystallites (abstracted from Kälın and Bernoulli 1984, p. 412).

Description. *S. punctulata* has been described and illustrated in great detail by Aubry and Depeche (1974), Moshkovitz (1979), Kälın (1980), and Kälın and Bernoulli (1984).

Dimensions. Diameter of test: 8.0-12.0 μm .

Remarks. Moshkovitz (1979) described a new species of *Schizosphaerella*, *S. astrea*, which differs from *S. punctulata* in possessing a simplified hingement and a more random crystallite arrangement, with groups of four to six radiating in a star-like pattern from the same point. This species was not recognized in the present study.

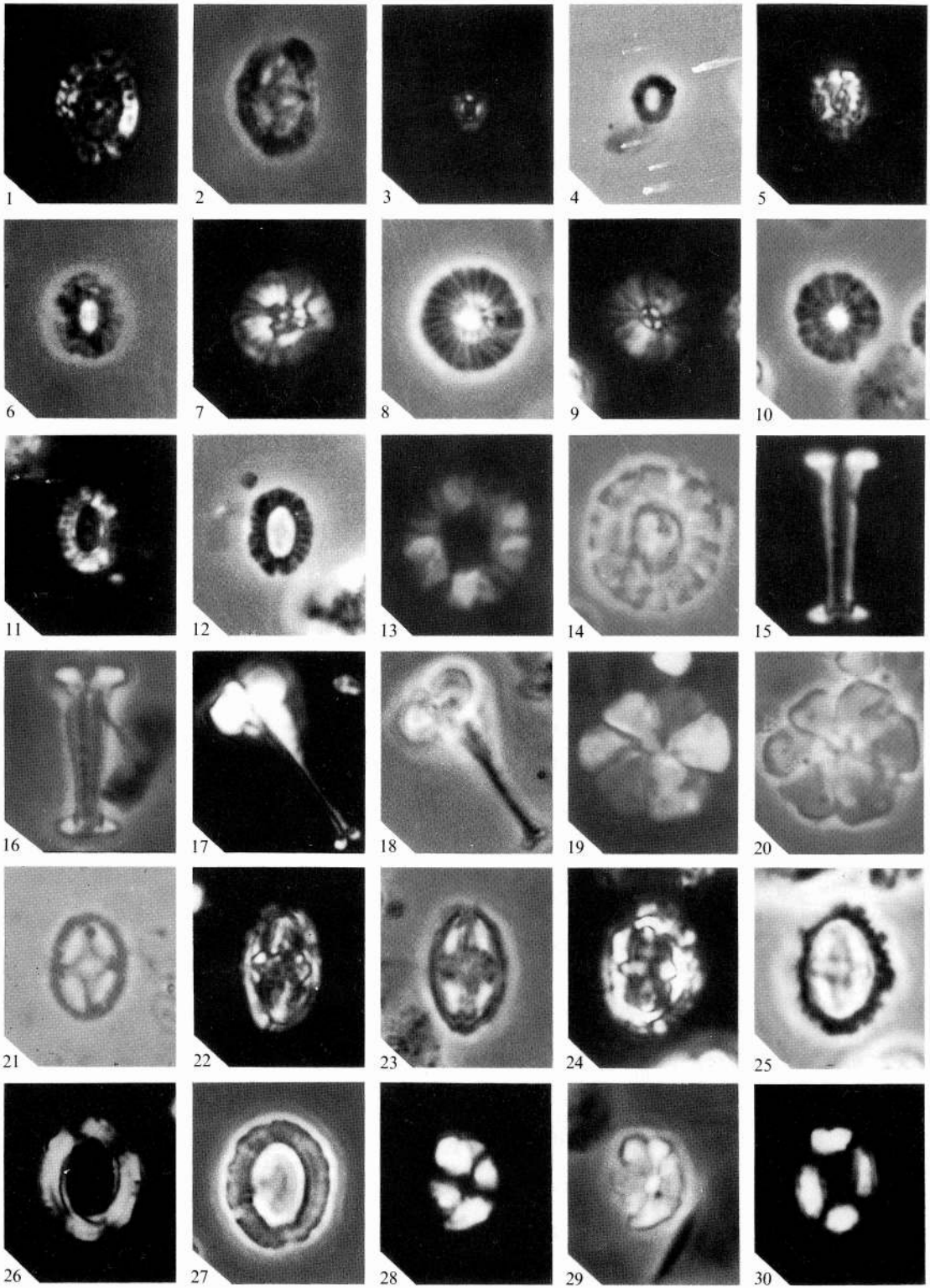
S. punctulata is found as broken pieces or more rarely as complete valves throughout the Lower Jurassic. It is especially common in the Hettangian and Sinemurian where it often forms abundant monospecific assemblages. Its rock forming and diagenetic attributes are discussed in the papers already listed.

The biological affinities of *S. punctulata* are discussed at length in Kälın and Bernoulli (1984)

EXPLANATION OF PLATE 14

All light micrographs, approximately $\times 2700$.

- Figs. 1 and 2. *Biscutum depravatus* (Grün and Zweili, 1980) comb. nov. 1, c-p, UCL-2201-22, Brenha, Bajocian (3617). 2, as fig. 1, p-c, UCL-2201-21.
 Figs. 3 and 4. *B. dubium* (Noël, 1965) Grün in Grün *et al.* 1974. 3, c-p, UCL-2311-5, Brenha, Bajocian (3617). 4, as fig. 3, p-c, UCL-2311-6.
 Figs. 5 and 6. *B. planum* sp. nov. 5, c-p, UCL-2265-17, Timor, mid-Pliensbachian. 6, as fig. 5, c-p, UCL-2265-16.
 Figs. 7 and 8. *Discorhabdus ignotus* (Górka, 1957) Perch-Nielsen, 1968. 7, c-p, UCL-2265-9, Badenweiler, *thouarsense* Zone (5). 8, as fig. 7, p-c, UCL-2265-8.
 Figs. 9 and 10. *D. criotus* sp. nov. 9, c-p, UCL-2265-6, Badenweiler, *thouarsense* Zone (5). 10, as fig. 9, p-c, UCL-2265-7.
 Figs. 11 and 12. *Sollasites arctus* (Noël, 1973) comb. nov. 11, c-p, UCL-2311-11, Unterstürmig, Lower Toarcian (6). 12, as fig. 11, p-c, UCL-2311-10.
 Figs. 13 and 14. *Calyculus* sp. indet. 13, c-p, UCL-2452-10, Unterstürmig, Lower Toarcian (6). 14, as fig. 13, p-c, UCL-2452-11.
 Figs. 15 and 16. *Carinolithus superbus* (Deflandre, 1954) Prins in Grün *et al.* 1974. 15, c-p, UCL-2056-9, Trimeusel, *levesquei* Zone (4). 16, as fig. 15, p-c, UCL-2056-10.
 Figs. 17-20. *C. magharensis* (Moshkovitz and Ehrlich, 1976) comb. nov. 17, c-p, UCL-2270-9, Brenha, Bajocian (3617). 18, as fig. 17, p-c, UCL-2270-10. 19, isolated distal hexalith, c-p, UCL-2452-34, Brenha, Bajocian (3617). 20, as fig. 19, p-c, UCL-2452-35.
 Fig. 21. *Axopodorhabdus atavus* (Grün *et al.* 1974) comb. nov. p-c, UCL-2311-8, Mochras, *levesquei* Zone (367).
 Figs. 22 and 23. *Mazaganella pulla* gen. et sp. nov. 22, c-p, UCL-2270-24, Site 547, Lower Pliensbachian (15-1). 23, as fig. 22, p-c, UCL-2270-23.
 Figs. 24 and 25. *M. protensa* gen. et sp. nov. 24, c-p, UCL-2201-4, Site 547, Lower Pliensbachian (15-1). 25, as fig. 24, p-c, UCL-2201-2.
 Figs. 26 and 27. *Triscutum* sp. 1. 26, c-p, UCL-2203-10, Brenha, Bajocian (3617). 27, as fig. 26, p-c, UCL-2203-9.
 Figs. 28 and 29. *Lotharingius primigenius* sp. nov. 28, c-p, UCL-2201-10, Site 547, Toarcian (10-4). 29, as fig. 28, p-c, UCL-2201-9.
 Fig. 30. *L. imprimus* sp. nov. c-p, UCL-2201-16, Site 547, Toarcian (10-4).



BOWN, early Mesozoic coccoliths

who point out significant differences from all groups of similar morphology, i.e., diatoms, Calcisphaerulidae, *Pithonella*, and thoracospheres. They propose, however, that *S. punctulata* should be included in a separate family within the dinoflagellate order Thoracosphaerales, which was intended to embrace all predominantly coccooid, marine planktonic dinophytes having a calcified cell wall in their vegetative phase.

It is generally stated that *S. punctulata* was an organism which favoured extensive shelf areas and this would account for their early and successful colonization of the north-west European epicontinental sea during the Hettangian and Sinemurian. However, its presence in the Picun Leufu and Timor samples clearly demonstrates its worldwide distribution at this time.

Occurrence. Badenweiler, *variabilis* Zone to *aalensis* Zone; Ballrechten, *variabilis* Zone to *levesquei* Zone; Brenha, Lower Sinemurian to Middle Jurassic; DSDP Site 547, Sinemurian to Pliensbachian; Hock Cliff, *bucklandi* Zone to *semicostatum* Zone; Longobucco, Lower Pliensbachian to Lower Toarcian; Mochras, *planorbis* Zone to *levesquei* Zone; Picun Leufu, Upper Pliensbachian to Toarcian; St Audries slip, *liasicus* Zone to *angulata* Zone; Trimeusel, *falciferum* Zone to *levesquei* Zone; Trunch, *angulata* Zone to *jamesoni* Zone; Tunisia, Upper Pliensbachian to Toarcian; Unterstürmig, Lower Toarcian.

Range. *S. punctulata* has been recorded from the Rhaetian Cotham Beds by Hamilton (1982), whereas the present work does not show *S. punctulata* prior to the *planorbis* Zone, Hettangian. The last occurrence of *S. punctulata* is generally given as early Kimmeridgian, but reworking may be responsible for extending its range to this level.

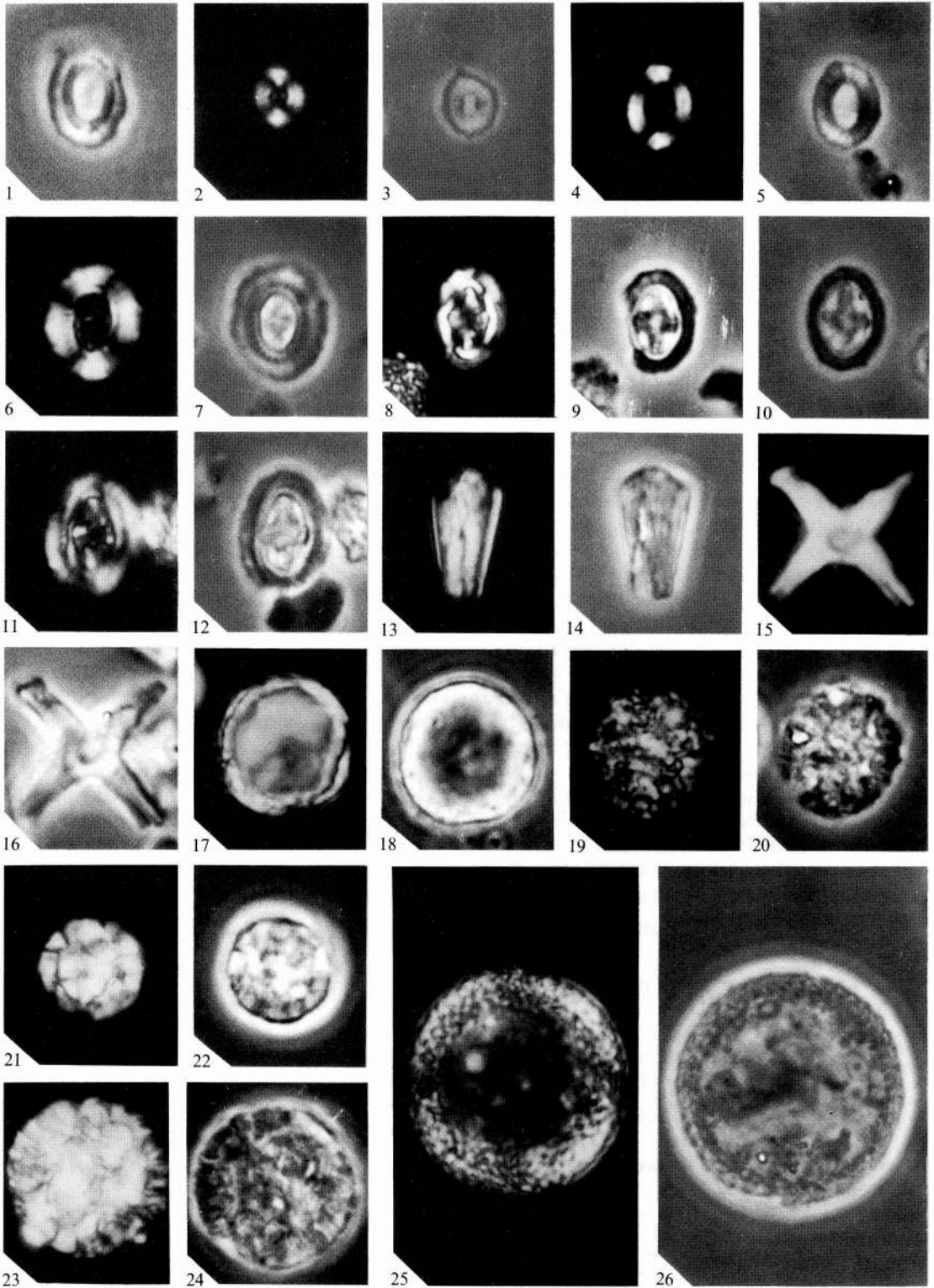
Genus PRINSIOSPHAERA Jafar, 1983

Type species. *Prinsiosphaera triassica* Jafar, 1983.

Diagnosis. 'Spherical to hemispherical solid nannofossils often containing a depression at one end and consisting of parallelly stacked groups of calcite plates orientated in a random fashion' (Jafar 1983, p. 232).

EXPLANATION OF PLATE 15

- Fig. 1. *Lotharingius imprimus* sp. nov. As Plate 14, fig. 30, p-c, UCL-2201-15.
 Figs. 2 and 3. *L. hauffii* Grün and Zweili in Grün *et al.* 1974. 2, c-p, UCL-2056-13, Trimeusel, *variabilis* Zone (5). 3, as fig. 2, p-c, UCL-2056-14.
 Figs. 4 and 5. *L. barozii* Noël, 1973. 4, c-p, UCL-2203-35, Brenha, *ibex* Zone (3531). 5, as fig. 4, p-c, UCL-2203-34.
 Figs. 6 and 7. *L. sigillatus* (Stradner, 1961) Prins in Grün *et al.* 1974. 6, c-p, UCL-2260-27, Trimeusel, *bifrons* Zone (6). 7, as fig. 6, p-c, UCL-2260-28.
 Figs. 8-10. *Bussonium prinsii* (Noël, 1973) Goy, 1979. 8, c-p, UCL-2311-25, Trimeusel, *bifrons* Zone (6). 9, as fig. 8, p-c, UCL-2311-24. 10, p-c, UCL-2260-20, Trimeusel, *bifrons* Zone (6).
 Figs. 11 and 12. *B. leufuensis* sp. nov. 11, c-p, UCL-2270-15, Picun Leufu, Toarcian (57). 12, as fig. 11, p-c, UCL-2270-16.
 Figs. 13 and 14. *Conusphaera zlabachensis* Moshkovitz, 1982. 13, c-p, UCL-2274-27, Weissloferbach, *marshi* Zone (13b). 14, as fig. 13, p-c, UCL-2274-28.
 Figs. 15 and 16. *Orthogonoides hamiltoniae* Wiegand, 1984. 15, c-p, UCL-2289-11, DSDP Site 547, Lower Pliensbachian (15-2). 16, as fig. 15, p-c, UCL-2289-12.
 Figs. 17 and 18. *Prinsiosphaera triassica hyalina* Jafar, 1983. 17, c-p, UCL-2274-14, Weissloferbach, *marshi* Zone (13b). 18, as fig. 17, p-c, UCL-2274-15.
 Figs. 19 and 20. *P. t. ?punctata* Jafar, 1983. 19, c-p, UCL-2274-26, Weissloferbach, *marshi* Zone (13b). 20, as fig. 19, p-c, UCL-2274-27.
 Figs. 21 and 22. *P. t. ?perforata* Jafar, 1983. 21, c-p, UCL-2311-26, Weissloferbach, *marshi* Zone (13b). 22, as fig. 21, p-c, UCL-2311-27.
 Figs. 23 and 24. *P. triassica* Jafar, 1983. 23, c-p, UCL-2311-28, Weissloferbach, *marshi* Zone (13b). 24, as fig. 23, p-c, UCL-2311-29.
 Figs. 25 and 26. *Schizosphaerella punctulata* Deflandre and Dangeard, 1938. 25, c-p, UCL-2260-35, Trimeusel, *levesquei* Zone (4). 26, as fig. 25, UCL-2260-34.



BOWN, early Mesozoic nannofossils

Prinsiosphaera triassica Jafar, 1983

Plate 11, figs. 5 and 6; Plate 15, figs. 17-24

- 1967 Problematic nannofossils; Fischer *et al.*, figs. 79-82.
 1979 *Thoracosphaera* spp. 6 and 7; Jafar, pl. 3, figs. 7a, b and 8a, b.
 1982 Undetermined globular calcite body; Moshkovitz, p. 614, pl. 2, figs. 3 and 4.
 1983 *Prinsiosphaera triassica* Jafar, p. 232, fig. 7 (1-4); fig. 8 (1-3, 6, 7).

Diagnosis. Thick hemispherical to disc-like objects of circular to elliptical outline; one side is often occupied by a depression and the margins may be smooth or serrated. The nannofossil is composed of thin, tabular calcite rhombohedra arranged in parallel groups and several of these randomly arranged groups make up a nannofossil (taken from Jafar 1983, p. 232).

Description. Large, roughly circular spheres, hemispheres, and discs which display a great variety of appearances in the LM but appear less variable in the SEM. The surface of the nannofossil is most commonly made up of square and rectangular units of thin, parallel lamellae. The orientation of these units appears to be random, giving the nannofossil a patchwork appearance. The nannofossils may be hollow or solid and overgrowth is common. The surface is occasionally observed to be completely smooth or covered in blocky crystal growth.

Dimensions. Diameter: 4.8-9.2 (9.0) μm .

Remarks. *P. triassica* occurs abundantly in Upper Triassic rocks of the Alpine area and forms an enigmatic group of nannofossils. As noted in the description, it displays a variety of differing morphologies in the LM which are not observed in the SEM. Jafar erected five subspecies for these LM distinctions and four of these are recognized in the present study and are illustrated in Plate 15, figs. 17-24. It is unclear whether this LM diversity is due to differing patterns of overgrowth or distinctive ultrastructure which is obscured by overgrowth or an outer layer, and thus not visible in the SEM. The organic nature of these nannofossils is assumed, due to their abundance, stratigraphic distribution, structural regularity, and occurrence throughout the Alpine area, but their biological affinities are unknown. Their large, coarsely constructed morphology is thought to be in no way related to coccoliths, as is suggested by Jafar (1983, pp. 234, 255), and their ultrastructure is unlike that of *Thoracosphaera*. The nannofossil they most closely resemble is *S. punctulata*, which also has a similarly sized sub-spherical morphology constructed from numerous individual crystallites. *S. punctulata* differs in possessing a hollow, bivalved test which displays a complex and strictly ordered structure. It is possible that *P. triassica* represents a primitive forerunner of *S. punctulata*, both species occurring abundantly in the Tethyan shelf area and separated only by the late Rhaetian period. Only further work in the Tethyan Rhaetian and Hettangian will reveal the relationship between *S. punctulata* and *P. triassica*.

Occurrence. Fischerwiese, Rhaetian; Kendelbachgraben, Rhaetian; Weissloferbach, *suessi* Zone to *marshi* Zone.

Range. Rhaetian (Moshkovitz 1982); Carnian to Rhaetian (Jafar 1983); Norian to Rhaetian (Posch and Stradner 1987).

Family THORACOSPHAERACEAE Schiller, 1930

Genus THORACOSPHAERA Kamptner, 1927

Type species. *Thoracosphaera heimi* (Lohmann) Kamptner, 1927.

Thoracosphaera geometrica (Jafar, 1983) comb. nov.

Plate 11, figs. 10-12

- 1979 Calcisphaeride (?); Wiedmann *et al.*, pl. 5.
 1982 *Thoracosphaera* sp. 2; Moshkovitz, p. 613, pl. 2, fig. 2.
 1983 *Prinsiosphaera geometrica* Jafar, p. 233, fig. 10 (5, 6); fig. 11 (6).
 1987 *Prinsiosphaera geometrica* Jafar; Posch and Stradner, p. 233, pl. 2, fig. ?9 (*non* figs. 8 and 10).

Remarks. Jafar (1983) illustrated three specimens of this species displaying overgrowth which he interpreted as a base typical of the genus *Prinsiosphaera*. Observation in the present study has shown that *T. geometrica*, when not overgrown, has a test wall quite different to that of the genus *Prinsiosphaera* but very similar to that of *T. tuberosa*. Like *T. tuberosa*, *T. geometrica* has a test constructed from regular three-sided pyramids, but it is far smaller in size being 7–8 μm across compared to the 22–32 μm of *T. tuberosa*. *T. geometrica* is included in the genus *Thoracosphaera* but is by far the oldest representative.

Dimensions. 7.0–8.0 (10.2) μm .

Occurrence. Weissloferbach, Rhaetian.

Range. Rhaetian (Weidmann *et al.* 1979); Rhaetian (Moshkovitz 1982); Norian to Rhaetian (Jafar 1983); Rhaetian (Posch and Stradner 1987).

EARLY EVOLUTIONARY HISTORY OF CALCAREOUS NANNOFOSSILS

Introduction

Evolution may be defined as the modification through time of genes and gene frequencies. In palaeontology it is seen as the modification through time of morphology, assuming that morphology is the phenotypic expression of the genotype. The extent to which coccoliths reflect biological relationships has already been discussed with reference to taxonomy and it is assumed here that coccoliths are an expression of genetic make-up.

Coccolith rim structure groups

Several well-defined groups of coccoliths were present in the late Triassic–early Jurassic time interval which are not well reflected in the existing taxonomy. Each of these groups is characterized by a common, fundamental pattern of rim construction which transcends generic and family boundaries and delineates discrete long-ranging lineages in which most early Mesozoic coccoliths can be placed. Evolution within the lineages is seen as modification of the basic rim structure and variation of the central area structures. By Pliensbachian times five rim structure groups were established, from which all later Jurassic diversification can be traced. The central area structures display no such long-term consistency and represent a lower level of evolutionary and taxonomic significance. Many central area features occur repeatedly throughout the history of coccolithophorids, often occurring contemporaneously in completely unrelated genera and families. It appears that while changes in the rim represent fundamental, long-term evolutionary features, the central area structures reflect evolution at a lower and short-term level of significance. Five major structural groups are recognized.

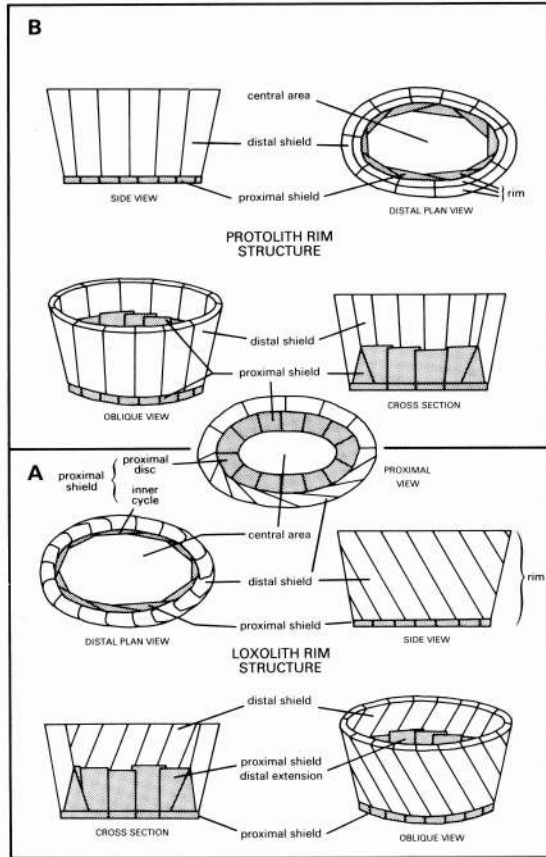
Discoliths

i. Loxolith rim structure group. A loxolith rim is a compound structure comprising a dominant distal shield and a proximal shield with a vertical (distal) extension (text-fig. 6A).

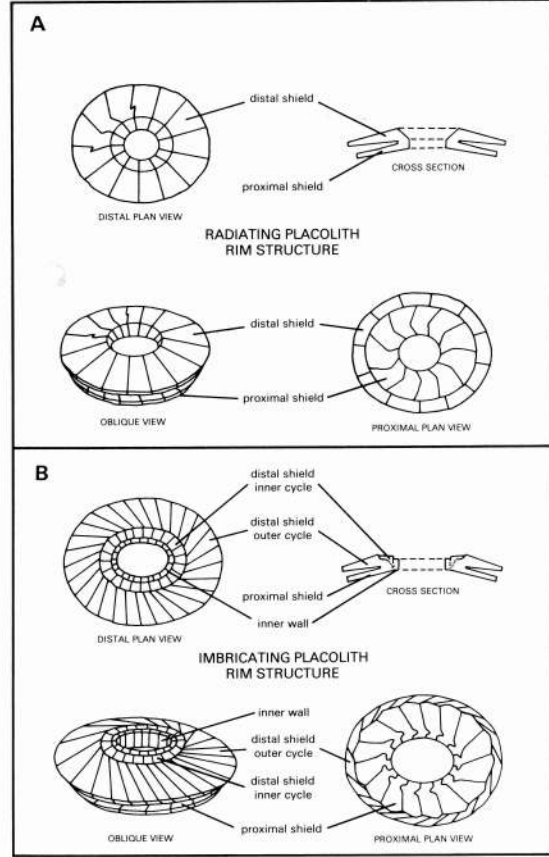
a. distal shield—composed of tall, narrow, steeply inclined, i.e. imbricating, laths.

b. proximal shield—composed of elements with a triangular cross-section which form a flat base to the coccolith, with radiating sutures, which also extend upwards to form an inner cycle to the distal shield appearing as tangential laths joined along vertical sutures on the inner surface of the distal cycle.

The loxolith rim is possessed by the genera *Chiastozygus*, *Crepidolithus*, *Tubirhabdus*, *Staurorhabdus*, *Zeugrhabdotus*, and *Archaeozygodiscus*.



TEXT-FIG. 6. Morphology of the loxolith (A) and protolith (B) rim structure groups.



TEXT-FIG. 7. Morphology of the radiating placolith (A) and imbricating placolith (B) rim structure groups.

ii. *Protolith rim structure group*. A protolith rim is a compound structure comprising a dominant distal shield and a proximal shield with a vertical (distal) extension (text-fig. 6B).

a, distal shield—composed of rectangular elements arranged tangentially to the ellipse and joined along sutures which are perpendicular to the coccolith base without imbrication.

b, proximal shield—identical to that of the loxolith group.

The protolith rim structure is possessed by the genera *Bucanthus* gen. nov., *Crucirhabdus*, *Diductius*, *Mitrolithus*, *Rectilius*, *Stephanolithion*, *Stradnerlithus*, *Parhabdolithus*, and *Timorella* gen. nov.

Placoliths

Placoliths are first observed in the Sinemurian and mark a profound change in coccolith construction with the elements forming broad and thin shields in the horizontal plane as opposed to the earlier tall upright rims which were vertically orientated. It is also interesting to note that the development of the placolith structure, with its clearly separated shields, allowed the first possibility of physical locking together of individual coccoliths on the cell surface to form preservable coccospheres. The earlier loxolith and protolith coccoliths were held on the cell wall by an organic layer to form a coccosphere and dispersed when the organic material decayed after death.

i. Radiating placolith rim structure group. A simple placolith construction comprising a proximal and distal shield. In the earliest examples of this group both the shields are unicyclic (text-fig. 7A).

- a,* distal shield—composed of blade-like laths lying side by side, their broad distal faces level, and the suture lines between each element orientated radially to the centre of the coccolith. Kinking of one or more of the suture lines is common and this gives the impression of suture precession. The elements slope gently outwards to form the convex shield, with their inner edges sloping sharply inwards to form a deep central area.
- b,* proximal shield—similar in structure to the distal shield but without a central depression, and the sutures are all consistently kinked, veeing in a counter-clockwise direction.

The rim structure described above belongs to *Biscutum novum*, the simplest coccolith of this group and first to appear. Later radiating placoliths undergo further structural modifications but retain the basic non-imbricating, radial structure. The genera which display this structure include *Axopodorhabdus*, *Biscutum*, *Discorhabdus*, *Eithmorhabdus*, *Podorhabdus*, and *Sollasites*, and in a modified form *Calyculus* and *Carinolithus*.

ii. Imbricating placolith rim structure group. A compound placolith rim which consists of a bicyclic distal shield, a unicyclic proximal shield, and a connecting inner wall (text-fig. 7B).

- a,* distal shield, outer cycle—composed of blade-like laths which are imbricating and joined along sutures with pronounced anti-clockwise inclination.
- b,* distal shield, inner cycle—this cycle is subordinate to the broad, sloping, outer cycle, and is made up of small, almost square elements usually showing little or no imbrication and suture inclination.
- c,* proximal shield—composed of elements showing little or no imbrication but joined along consistently kinking suture lines, veeing in a clockwise direction.
- d,* inner wall—composed of small, almost square elements joined along vertical sutures and lining the central area. The inner wall is delineated by the distal inner cycle on the distal surface but not observed as a discrete cycle on the proximal surface. The outer distal shield elements and the proximal shield elements are actually crystallographically continuous and joined by the inner wall. On the distal surface, the additional inner cycle of elements conceals the fact that the outer cycle and inner wall are continuous elements.

The imbricating placolith rim structure is possessed by *Lotharingius*, *Watznaueria*, *Cyclagelosphaera*, *Anulospaera*, and, in a modified form, *Bussonius*.

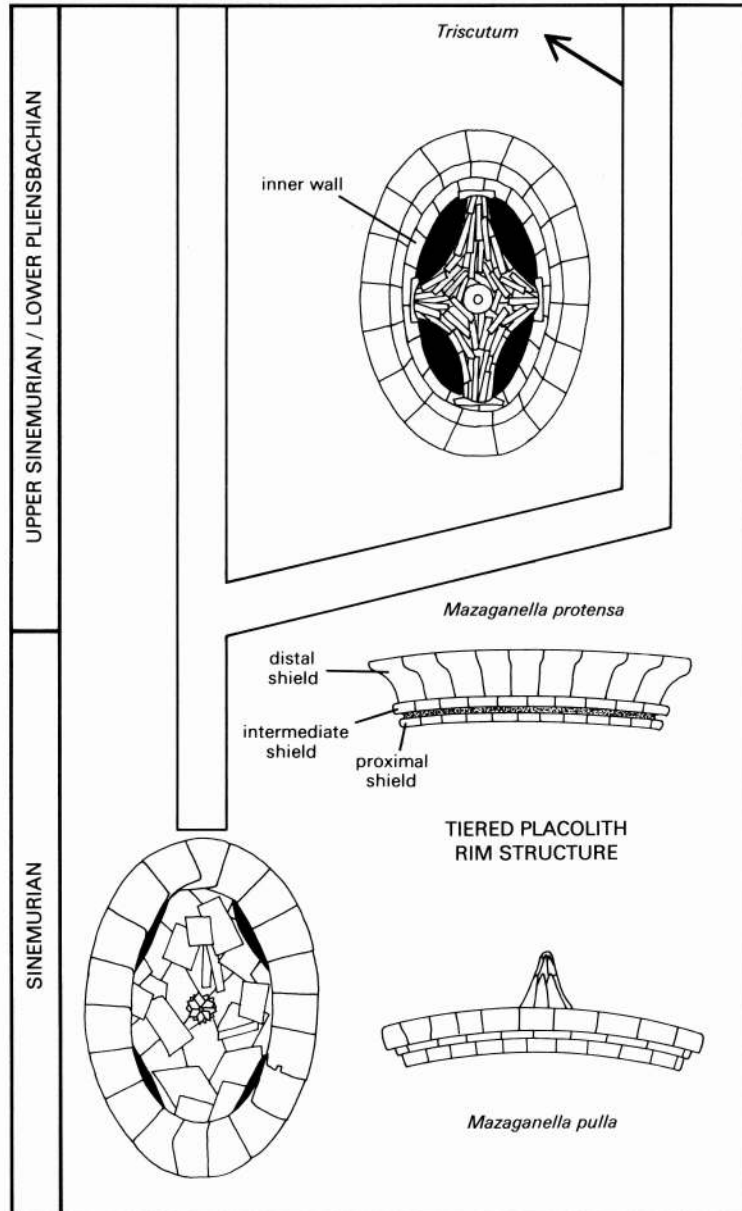
iii. Tiered placolith rim structure group. A placolith rim structure composed of three narrow, superimposed shields (text-fig. 8).

- a,* distal shield—composed of one cycle of elements joined along radial sutures and showing little or no imbrication. The distal shield may be vertically extended.
- b,* intermediate shield—a thin cycle of non-imbricating elements.
- c,* proximal shield—a thin cycle of non-imbricating elements joined along distinctly kinked sutures, veeing in a clockwise direction. The lower two shields are closely appressed and a connecting inner wall may be seen lining the central area.

This rim structure is possessed by *Mazaganella* gen. nov. and *Triscutum* Dockerill (1987).

The rim structure groups in stratigraphic context

The loxolith and protolith rim structure groups are both represented in the late Triassic nannofossil assemblages which have yielded the earliest known true coccoliths. These two groups comprised the only pattern of coccolith construction through the late Triassic and earliest Jurassic until the appearance of the tiered placolith group (*Mazaganella*) in the Sinemurian of the south Tethyan area (DSDP Site 547). This was followed in Tethys by the appearance of the radiating placolith and imbricating placolith groups in the late Sinemurian and early Pliensbachian, respectively. In north-west Europe the tiered placolith group is not found during the early Jurassic and consequently the radiating placolith group is the first placolith to occur (early Pliensbachian) followed by



TEXT-FIG. 8. Morphology and evolutionary relationships within the tiered placolith rim structure group (Family Mazaganellaceae).

imbricating placoliths (late Pliensbachian). The loxolith and protolith groups continue after the appearance of the other groups but become less important components of the assemblages, particularly after the rapid diversification of the radiating placolith group and numerical expansion of the imbricating placolith group; a trend maintained for the rest of the Jurassic. The evolutionary scheme for early Mesozoic calcareous nannofossils is given in text-fig. 9.

Taxonomic significance of the rim structure groups

The coccolith rim structure groups and their various modifications transcend all taxonomic boundaries up to and including families, e.g. the protolith rim structure group, first represented by the Parhabdolothaceae, gave rise to the slightly modified Stephanolithiaceae; similarly the radiating placolith rim structure group, first represented by the Biscutaceae, gave rise to the subfamily Sollasitoideae and the Calyculaceae and Podorhabdaceae. It thus appears that the rim structure groups may reflect ordinal level relationships. In the case of the loxolith and protolith rim structure groups, both possess analogous component rim parts, with the imbrication or non-imbrication of the distal shield being the only feature that divides them. While this warrants a separate structural grouping, it is considered most appropriate to include them in the same order. The orders and families can be organized as follows:

1, loxolith and protolith rim structure groups = Eiffellithales, including, in the Lower Jurassic, the Zygodiscaceae and Parhabdolothaceae.

2, radiating placolith rim structure group = Podorhabdales, including, in the Lower Jurassic, the Biscutaceae (Biscutoideae, Sollasitoideae), Calyculaceae, and Podorhabdaceae.

3, imbricating placolith rim structure group = Watznaueriales, including, in the Lower Jurassic, the Watznaueriaceae.

4, tiered placolith rim structure group = ?Podorhabdales, including the Lower Jurassic, Maza-ganellaceae.

Recognition of the coccolith rim structure groups delineating discrete evolutionary lineages also greatly aids taxonomy by placing the morphologically based classification in an evolutionary context.

The loxolith rim structure group/Zygodiscaceae lineage

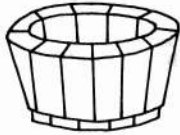
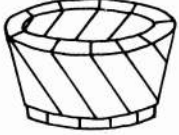
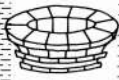
Archaeozygodiscus koessenensis is the oldest known loxolith rim form and occurs in the Tethyan Upper Triassic. It is much smaller than most Jurassic members of the loxolith lineage and also possesses a distal cycle in which the elements display sinistral imbrication as opposed to the dextral imbrication observed in all other Jurassic loxolith coccoliths. The significance of this difference is unclear but at present *A. koessenensis* is considered to be the ancestral species of the loxolith lineage. Lack of information from the Hettangian of the Tethyan area renders the relationship between *A. koessenensis* and the first Jurassic loxolith coccolith (in north-west Europe), *Tubirhabdus patulus*, uncertain. It is feasible that *T. patulus* developed from *A. koessenensis*, a transition which involved an increase in size, a reversal of imbrication direction, and an expansion of the minor axis bar and spine base/pore to produce a wide, flaring-circular spine. Further developments in the loxolith lineage occurred in the Sinemurian when the blocky *Crepidolithus* rim developed, firstly with a spine in *C. plienschachensis*, followed by the vacant central area of *C. crassus*, and the central granular plate of *C. granulatus*. Research in the Tethyan Hettangian is needed to reveal the origins of the genus *Crepidolithus*, however, it may have developed from *T. patulus*.

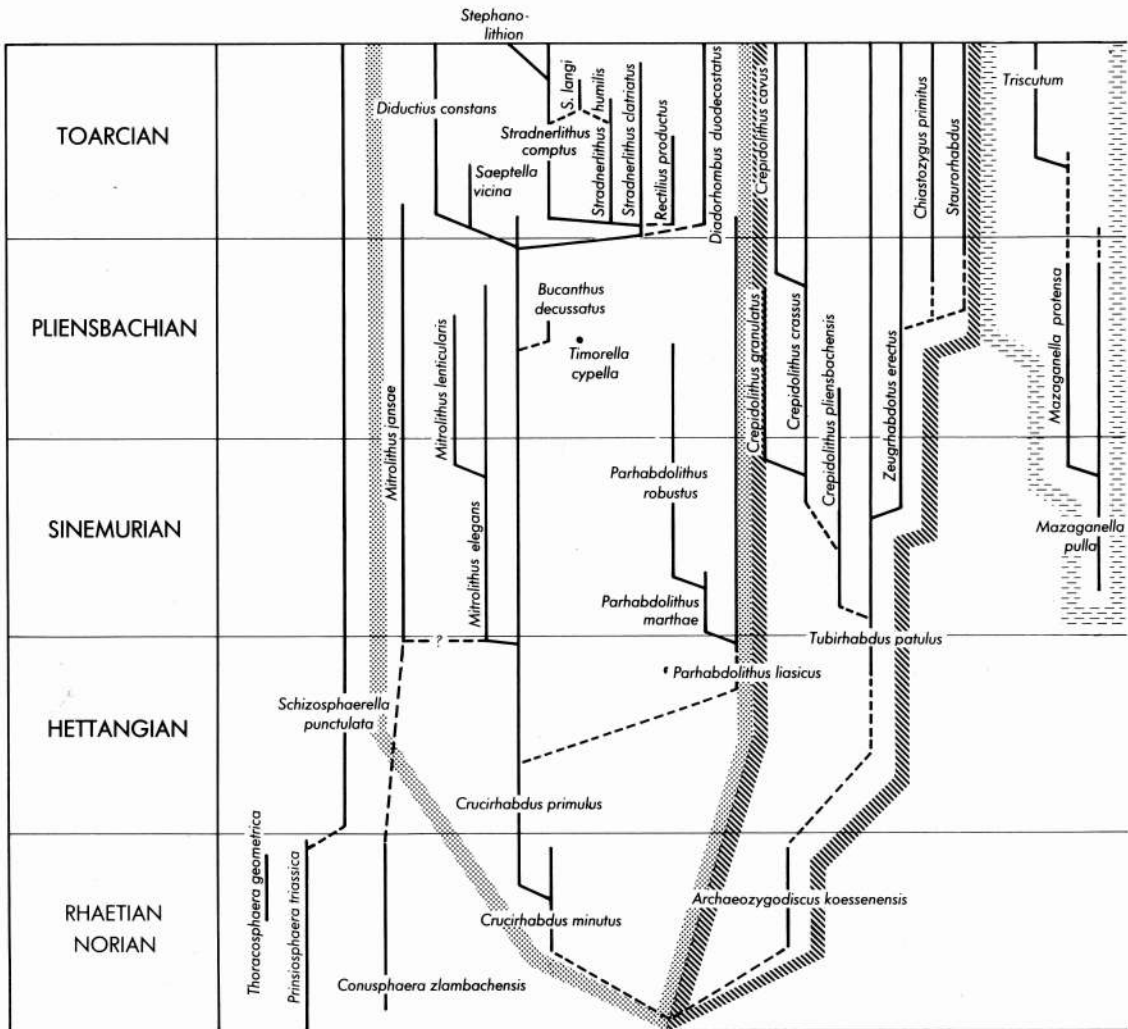
Three further genera with loxolith rims appeared in the early Jurassic: *Zeugrhabdotus* (with minor axis bar), *Staurolithites/Staurorhabdus* (with principal axes cross), and *Chiastozygus* (with X-like cross).

The protolith rim structure group/Parhabdolothaceae lineage

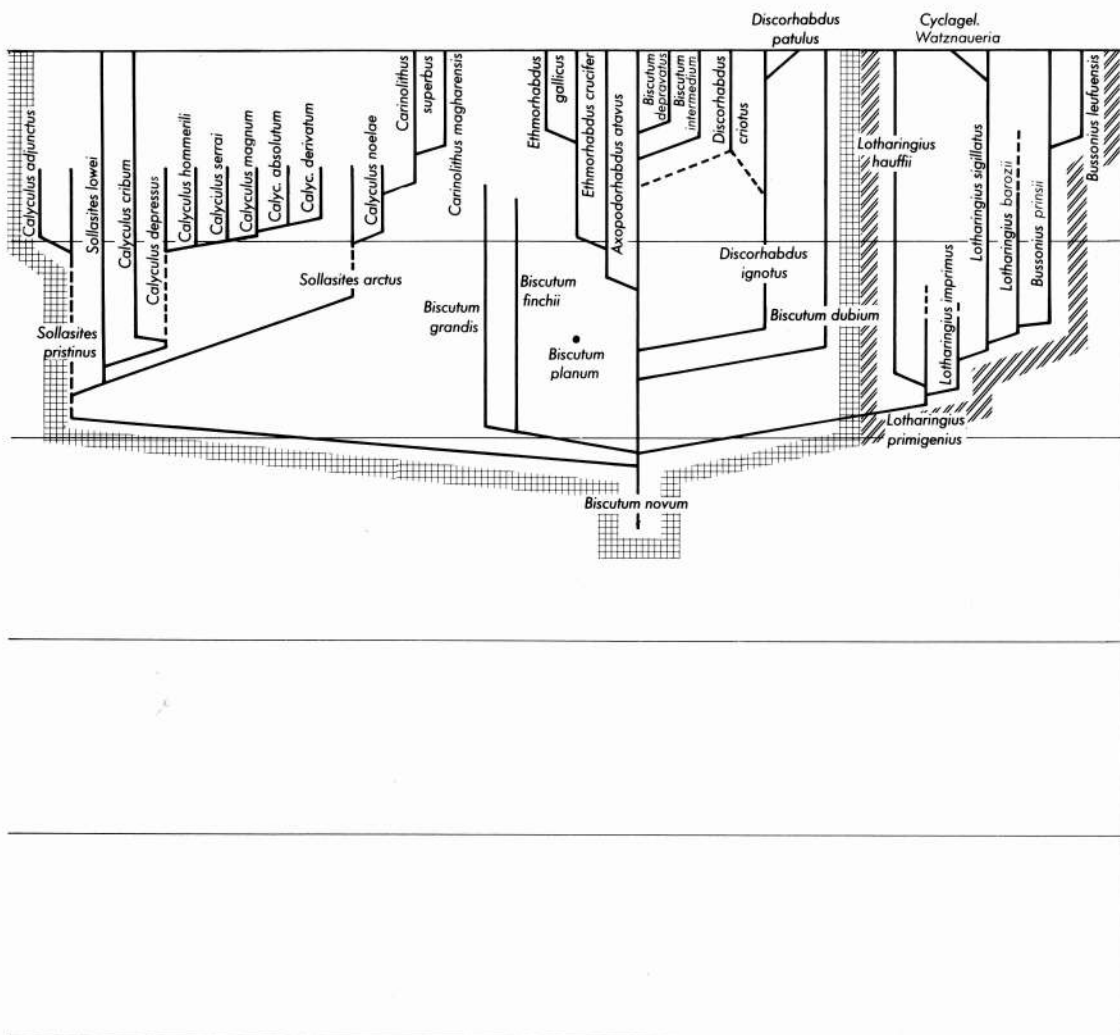
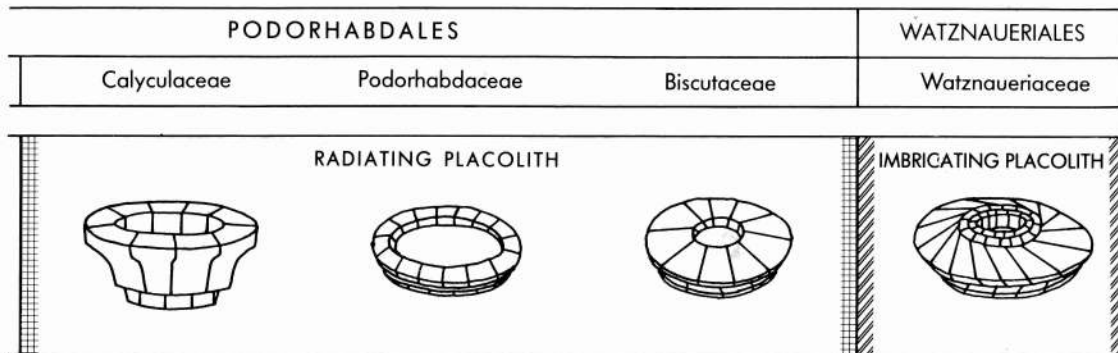
Crucirhabdus, *Parhabdolithus*, and *Mitrolithus*. The protolith rim lineage also had its first representative, *C. minutus*, in the late Triassic. In the Rhaetian *C. minutus* gave rise to *C. primulus*, an evolutionary development which involved an increase in size and vertical extension of the proximal elements. In Hettangian times *C. primulus* appears to have given rise to *P. liasicus*, a transition requiring only an increase in rim height and the loss of the longitudinal bar. In turn *P. liasicus* gave rise to *P. marthae* and *P. robustus* which each differed in the dimensions and shape of the spine.

The development of *Mitrolithus* is less easy to envisage and is hindered by lack of information

ORDER	EIFFELLITHALES		
FAMILY	Stephanolithiaceae Parhabdolithaceae	Zygodiscaceae	Mazaganellaceae
RIM STRUCTURE GROUPS	 <p>PROTOLITH</p>	 <p>LOXOLITH</p>	 <p>3-TIERED PLACOLITH</p>



TEXT-FIG. 9. Evolutionary chart for Upper Triassic and Lower Jurassic calcareous nannofossils.



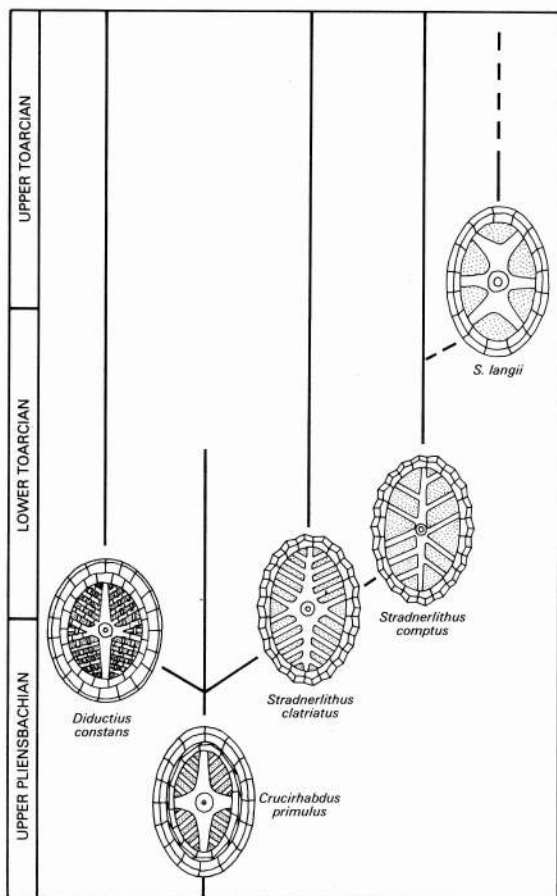
from the Tethyan Hettangian. A number of alternatives are possible: *M. elegans* may have developed from *C. primulus* or *P. liasicus*, involving a closure of the central area by an increase in size of the proximal shield vertical extensions, and a change in morphology of the spine to form the large flaring boss of *M. elegans*. The thinner spines of *C. primulus* and *P. liasicus* are both constructed from radiating calcite elements as are those of *M. elegans*. Thus, the transformation is possible and a matter of long axis orientation of the individual component elements of the spine. This development is supported by the observation on early specimens of *M. elegans* from Hock Cliff which initially display more elongated spines than later forms. It is, therefore, likely that *M. elegans* was descended from either *C. primulus* or *P. liasicus* and may itself have given rise to *M. jansae*, a transformation involving a vertical extension of all component parts. Another possibility is the initial development of *M. jansae* from the Upper Triassic *Conusphaera zlambachensis*, which occurs abundantly in the same assemblages as *Crucirhabdus minutus* and *A. koessenensis*. Both *M. jansae* and *Conusphaera zlambachensis* display strikingly similar morphologies, consisting of a gently tapering outer casing/rim of ten to fifteen thin, vertical plates and an internal core which protrudes distally and is composed of radial elements. In addition, both are extremely abundant in their respective Tethyan assemblages and show considerable variation in their dimensions, particularly height. However, the internal organization of the central core (best seen in the LM) differs in the two forms: *C. zlambachensis* has a longitudinally continuous core of forty sinistrally twisting, radiating elements. *M. jansae* has a core divided longitudinally into two separate units, a lower unit consisting of a cycle of elements surrounding a prominent central canal, and an upper unit which is a spine-like complex of superimposed cycles of radiating elements. The spine resembles that of *M. elegans* hence the generic grouping. Only further work in the Tethyan Hettangian will reveal the true relationships between *M. elegans*, *M. jansae*, *C. zlambachensis*, *Crucirhabdus primulus*, and *P. liasicus*.

The earliest Jurassic saw the protolith rim lineage well established with the genera *Mitrolithus*, *Crucirhabdus*, and *Parhabdololithus* all common. During the late Pliensbachian and early Toarcian, however, all three of these genera became extinct and only two protolith genera, which diversified from the latter forms in the late Pliensbachian, remained to survive into the Middle Jurassic.

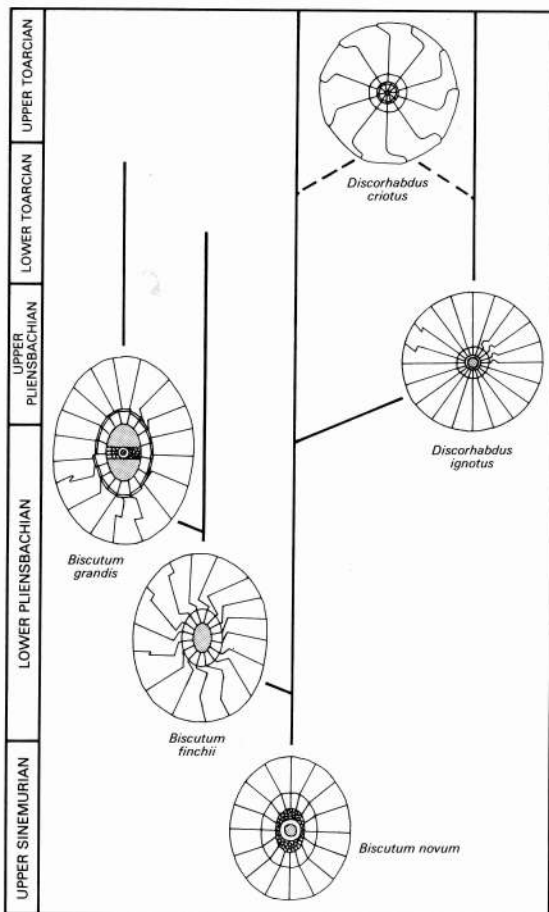
Stradnerlithus. The genus *Stradnerlithus* appeared in the late Pliensbachian with only slight modifications to the protolith rim. The proximal shield vertical extensions were reduced, the rim was slightly lower and vertically orientated, and a tapering of the distal wall elements gave the upper surface a zigzag profile. The DSDP Site 547 yielded a few Sinemurian specimens of *S. clatriatus* and it is likely that the initial speciation event occurred earlier in the Tethyan area. In the Site 547 section *S. clatriatus* appears to have developed from small specimens of *C. primulus* in which the above rim modifications took place, together with reduction in prominence of the crossbars to give equidimensional bars typical of *Stradnerlithus*. Both *C. primulus* and *S. clatriatus* possess the same number and arrangement of bars and thus structural change between the two was small. It is thus no longer logical to think of evolution within *Stradnerlithus* in terms of progressive increase in central bar numbers (cf. Rood and Barnard 1972, fig. 2) but rather the reverse. Thus *S. clatriatus*, with a *C. primulus* derived central area of around twenty bars, was first to appear followed by fewer bars in the Lower Toarcian, e.g. *S. humilis* and *S. comptus* with twelve bars, and further reductions in the upper Toarcian and Bajocian, e.g. *S. langii* with six bars and *S. asymmetricus* with eight bars (text-fig. 10). *Chiasozygus primitus*, postulated by Perch-Nielsen (1985, p. 404) as the ancestor of *Stradnerlithus*, possesses an imbricating distal shield and thus belongs in the loxolith lineage.

Goy (1981) has reported extraordinarily rich and diverse *Stradnerlithus* assemblages from the Lower Toarcian 'Schiste Carton' of the Paris Basin but this is exceptional and only a few specimens were observed here. Goy (1979, 1981) also records *Diadorhombus* (= *Rhombolithion*) and *Rectilius* both of which have *Stradnerlithus*-like rims, but *Diadorhombus* has a rhomboidal rim outline and *Rectilius* has a central area which is filled with a perforated grill.

The modified protolith rim of *Stradnerlithus* gave rise to *Stephanolithion* in the Bajocian. The



TEXT-FIG. 10. Evolution of *Stradnerlithus* and *Diductius* from *Crucirhabdus*.



TEXT-FIG. 11. Evolutionary relationships within the Biscutaceae.

only difference between the two genera is the development of lateral appendages from a varying number of rim elements in *Stephanolithion*. The central area structures of both genera are very similar with a trend towards reduction in a number of bars also seen initially in *Stephanolithion*.

Diductius. *Diductius* represents a similar development to *Stradnerlithus*, occurring contemporaneously (north-west Europe) and sharing a common ancestor, but the *Diductius* rim is not modified in the same way as *Stradnerlithus*, and the central structure also differs slightly. *D. constans* possesses a protolith rim, which is low, shallow sloping and includes a well-developed vertical extension of the proximal shield. The central area is spanned by a grill formed from principal axis crossbars, lateral diagonal bars, and curving longitudinal bars. It is thus possible that *D. constans* developed from *Crucirhabdus primulus*, as both the rim and central area structures would require only minor modifications (text-fig. 10). The addition of longitudinal bars to the central area of *C. primulus* is displayed in a new species illustrated by Goy (1979, 1981: *Saeptella vicina*). The development of *D. constans* probably took place during the late Pliensbachian.

Thus, *C. primulus* is thought to have given rise to *Diductius* and *Stradnerlithus* before its extinction in the early Toarcian and it was through these genera that the protolith rim structure

was continued into the Middle Jurassic. *Diductius* appears to have remained a monospecific genus while *Stradnerlithus* diversified and continued into the late Cretaceous.

Tiered placolith rim structure group/Mazaganellaceae lineage

The tiered placolith group, which includes two species of *Mazaganella* gen. nov. has not previously been recorded due to its absence in north-west Europe. *Mazaganella* has been found in DSDP Site 547 and Timor and appears to have a distribution restricted to the southern edge of Tethys. Previous work on Lower Jurassic nannofossils, based almost exclusively on material from north-west Europe, has always recorded *Biscutum novum* as the first placolith coccolith to appear during the late Sinemurian/early Pliensbachian (excluding the dubious claim in Jafar (1983) of a Triassic specimen of *Palaeopontosphaera* sp.). Numerous Sinemurian samples from Site 547 have yielded the three-tiered placolith *M. pulla*, before the first appearance of *B. novum* in the section. A second species, *M. protensa*, appears higher in the section and has a vertically extended distal shield and prominent central cross. It is clearly descended from *M. pulla*, which possessed closely appressed shields and a poorly delineated central cross or plate (text-fig. 8).

M. pulla appears to be the earliest placolith coccolith but is problematic because its morphology is quite unlike most other Lower Jurassic coccoliths. Three-tiered rims are possessed by two other Lower Jurassic genera, *Bussonius* and *Triscutum*. The former evolved from the three component *Lotharingius* rim during the Pliensbachian (see below). The latter possesses complex central grills unlike those of *Mazaganella* and first occurs in Tethyan sections in the Toarcian (Picun Leufu, Argentina). Despite the difference in central area structure, *Mazaganella* and *Triscutum* are of similar size and rim morphology. The younger species of *Mazaganella*, *M. protensa*, also shows a tendency towards vertical extension of the distal shield which characterizes *Triscutum*. It is thus probable that *Triscutum* is a descendant of *Mazaganella*, the transition taking place in Tethys, where they are both first found, before *Triscutum* moved into north-west Europe during the Bajocian.

Mazaganella may be related to *Biscutum*, as both genera display radial suture patterns with non-imbricating elements in a placolith type rim. However, the third shield, large size and open central area of *Mazaganella* appears to preclude any close relationship and in fact the proximal shield of *Mazaganella* is morphologically closer to *Lotharingius* with its kinked sutures veeing in a clockwise direction. *Mazaganella* is thus regarded as a separate Lower Jurassic lineage with unknown ancestry but giving rise to *Triscutum*. *M. pulla* is morphologically reminiscent of the Cretaceous Arkhangelskiellaceae coccoliths, but *M. protensa* displays a vertically extended morphology, as do the coccoliths of *Triscutum*, and it is unlikely that these coccoliths are related to the Cretaceous group.

Radiating placolith rim group/Podorhabdales lineage

The first representative is *B. novum*, appearing in the late Sinemurian and early Pliensbachian in the Tethyan and north-west European areas respectively. *B. novum* has a very simple placolith construction consisting of two unicyclic shields of non-imbricating, radially arranged elements. It represents a successful long-ranging species which formed a root stock from which many diversifications occurred. During the Pliensbachian and Toarcian the lineage underwent repeated diversification and was by far the most dynamic of the Lower Jurassic coccolith groups. At least ten individual diversifications can be recognized.

Biscutum finchii, *B. grandis*, and *B. dubium*. *B. finchii* first appeared three to four ammonite zones after the initial occurrence of *B. novum*. The morphological changes leading towards its development are first apparent in increasing size and initiation of sutural kinking within the *B. novum* population. The transition from *B. novum* to *B. finchii* involved an increase in size, an increase in the number of rim elements, a dramatic increase in sutural kinking, and loss of the central spine base (text-fig. 11). Specimens have been observed displaying intermediate features between these two species.

Detailed SEM observation revealed sutural kinking to be of major evolutionary significance in *B. finchii* and throughout the radiating placolith lineage. Suture lines represent the visible portion of the surface along which the individual rim elements are joined. Most specimens of *B. novum* possess sutures displaying a regular radial disposition. However, it is normal to find a small number of these sutures with a distinctive kink occurring in a position just outside the central depression. These kinks comprise a sharp bend in a counter-clockwise direction, before rapidly veering back to a radial or near radial direction (when following the suture from the centre to the shield edge). The amount of kinking observed in *B. novum* is highly variable and appears to be related to many of the evolutionary developments which the *B. novum* lineage undergoes. In *B. finchii* every suture line in the distal shield displays a distinct V-shaped kink, positioned just outside or at the crest of the central depression (a less consistently developed second kink may also occur near the outer edge of the distal shield). Such consistent kinking gives an impression of slight clockwise suture precession. The kinking, which reflects a more complex intergrowth of the individual rim elements, may be linked with the accommodation of a greater number of rim elements into the structure. Additional elements may be more efficiently accommodated by complex intergrowth, or such intergrowth may be dictated by the geometry of the elliptical form. Whatever the reason for, or cause of the sutural kinking it is a process which led to an important evolutionary development allowing a greater diversity in coccolith morphology in all subsequent placolith lineages. The lack of any similar process in the loxolith and protolith structures explains the relatively conservative and limited rim morphologies observed in those groups.

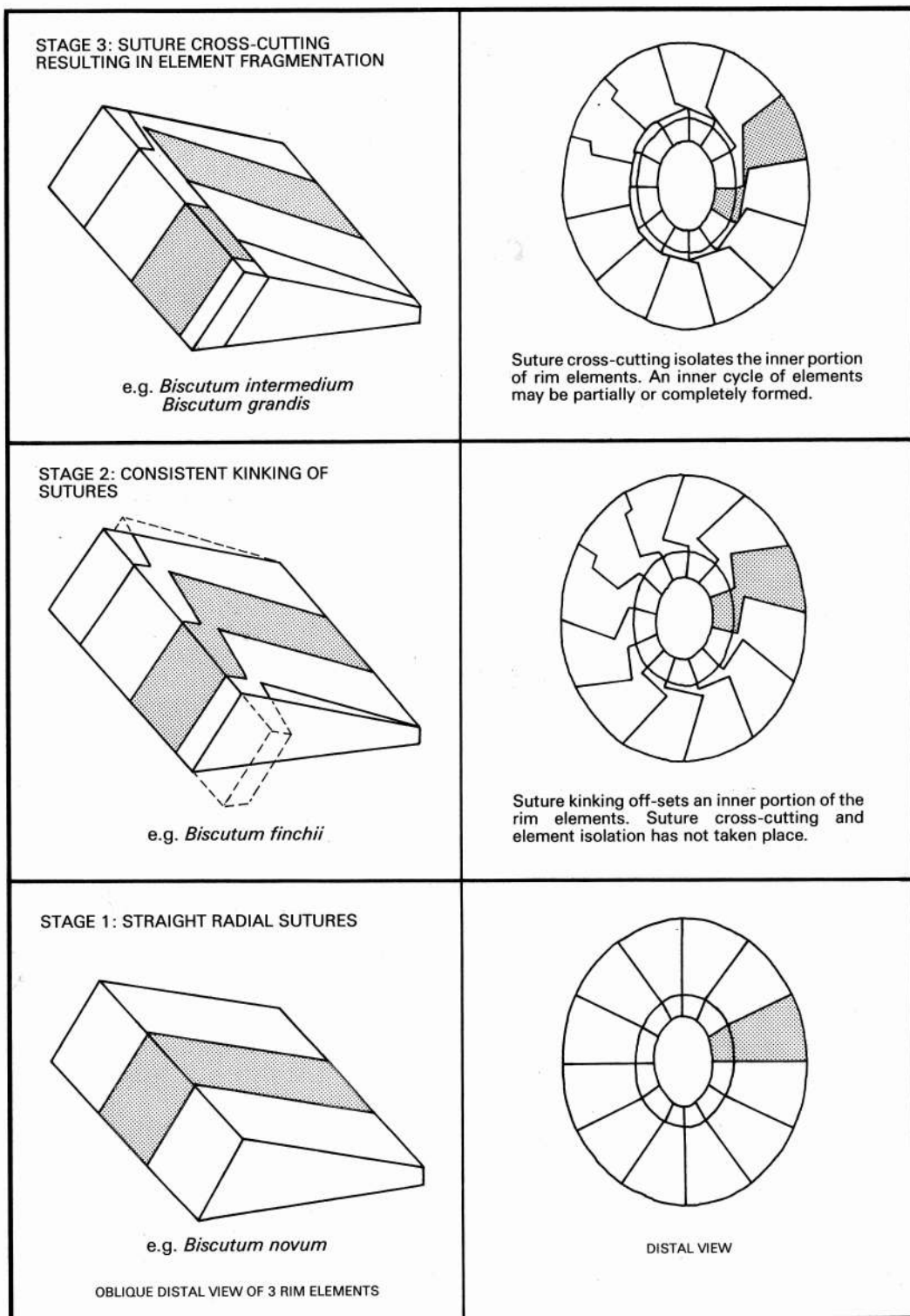
Sutural kinking in *B. finchii* includes some interference of adjacent sutures causing limited fragmentation of the rim elements (text-fig. 12). This suture cross-cutting occurs at the apex of the suture kink near the edge of the central depression and divides the elements into two discrete parts. *B. finchii* clearly displays the potential for development of a complete inner cycle.

B. grandis appeared soon after *B. finchii* and represents the next evolutionary stage possessing a complete, discrete inner cycle of elements lining the central area. In addition, it has no suture kinking, a narrower elliptical outline, and a more open central area. After the process of sutural kinking and cross-cutting has formed a complete inner cycle the radial pattern of straight suture lines is re-established. The sutures belong to two separate elements and therefore the kinking is no longer present. The element intergrowth is such that discrete elements are produced, and the inner and outer elements are no longer crystallographically continuous. The fragmentation usually forms large outer elements and rather thin, superficial inner elements which line the central depression. The process of rim fragmentation is illustrated in text-fig. 12. It appears that the *B. novum* lineage underwent a similar evolutionary development in the early Pliensbachian, to produce *B. dubium*. This species is very similar to *B. novum* but is smaller and possesses an inner distal cycle (text-fig. 13).

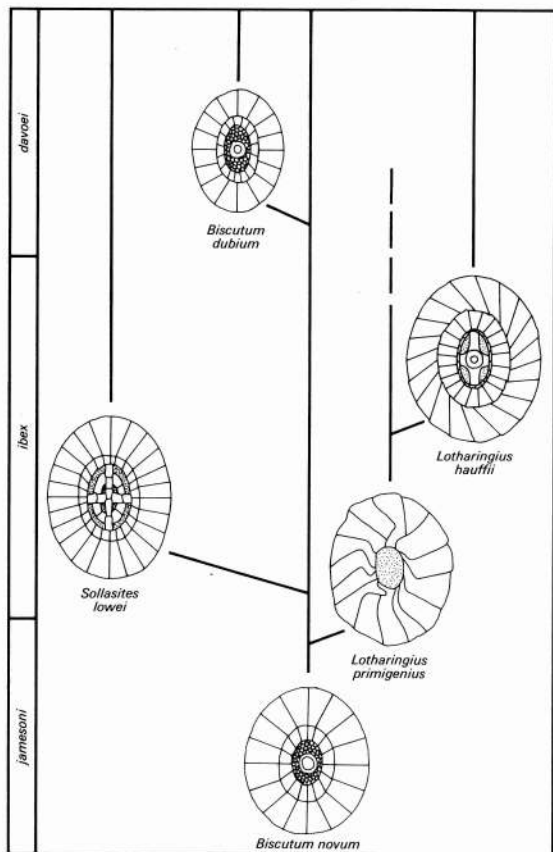
It should be noted that throughout the Biscutaceae lineage kinking of the sutures often reoccurred in the distal outer cycle soon after the completion of an inner cycle or was already present as a second kink near the outer edge of the shield.

Axopodorhabdus atavus. The first occurrence datum of *A. atavus* is variously recorded in the literature but it appears to be within three to four ammonite zones of the first appearance of *B. novum* (i.e. late Pliensbachian). The development of the podorhabdid-rim included the following modifications to the basic radiating placolith rim of *B. novum*: a narrowing of the rim width, the formation of a narrow distal inner cycle, and the opening of a large central area. In the case of *A. atavus* this central area is spanned by a cross structure, aligned along the principal axes of the ellipse (text-fig. 14). The cross is formed from granular microcrystals identical to the microcrystals observed in the central areas of *B. novum*. No transitional forms have yet been recognized. In addition, *Axopodorhabdus* is thought to have given rise to *Ethmorhabdus* during the late Pliensbachian/early Toarcian interval (text-fig. 14).

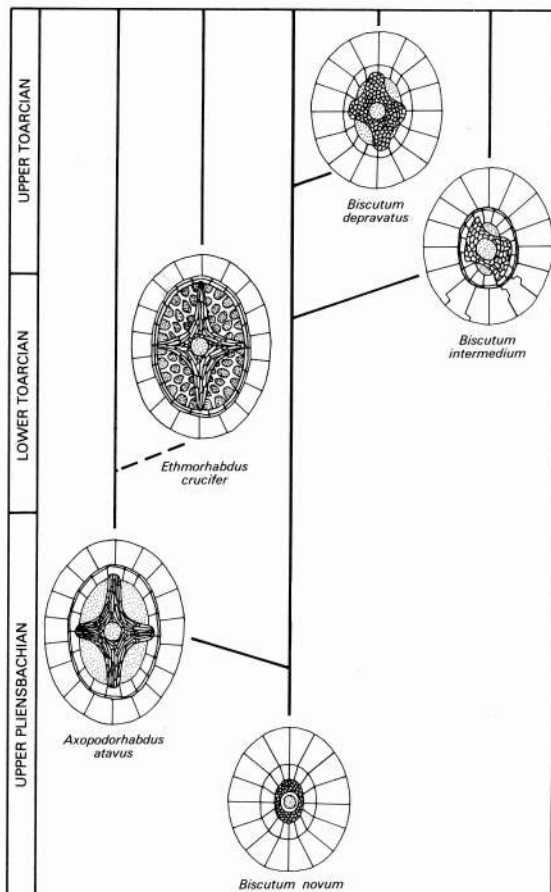
Discorhabdus. During the late Pliensbachian, specimens of *B. novum* began to display greater circularity of coccolith outline. In Toarcian times a continuous variation is observed, between the



TEXT-FIG. 12. The process of additional rim cycle formation.



TEXT-FIG. 13. The evolution of *Sollasites*, *Lotharingius*, and *Biscutum dubium*.



TEXT-FIG. 14. The evolution of *Biscutum intermedium*, *B. depravatus*, *Axopodorhabdus*, and *Ethmorhabdus*.

typically broadly elliptical outline of *B. novum* to slightly larger, subcircular and truly circular coccoliths. These circular coccoliths also possess a reduced central depression with a small (or absent) spine base and are classified here as *D. ignotus*. Later in the Toarcian, a second circular placolith appeared, *D. criotus* sp. nov., which has characteristically hooked sutures near the distal shield edge and a distal inner cycle set deep in the central depression which is also visible on the proximal side. Some variation in outline is also observed within this species, with circular and subcircular forms recorded. It is thus possible that *D. criotus* was a descendant of either *B. novum* or *D. ignotus* (text-fig. 11). No transitional forms have been observed but the sutural kinking observed in both *B. novum* and *D. ignotus* displays the potential for development of an inner cycle as possessed by *D. criotus*.

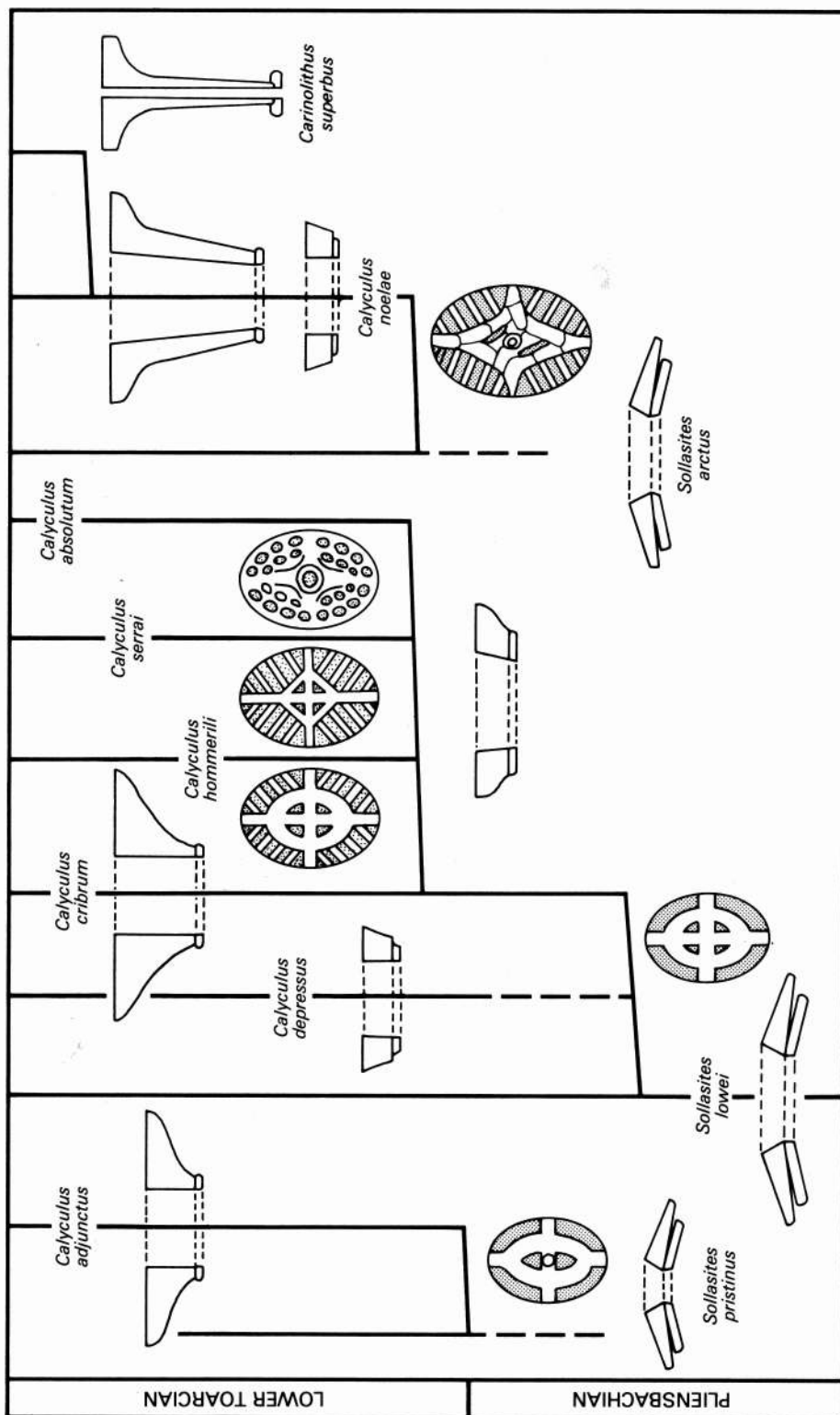
Sollasites. Although only rarely observed in the present study, the three species of *Sollasites* (*S. arctus* comb. nov., *S. lowei*, *S. pristinus*) are all extremely well illustrated in the papers of Noël (1973), Grün *et al.* (1974), Goy *et al.* (1979), and Goy (1981). Their stratigraphic ranges are less well established, with Crux (1984, 1987) recording *S. lowei* in the Lower Pliensbachian while the other two species are recorded only from the Lower Toarcian. The three species all share a common rim structure which is a slight modification of the *Biscutum*-rim structure. The modification includes

a slight widening of the central area, without reduction of the rim width, the development of a low inner cycle in the central depression (which may be the inner edge of the proximal shield and not a discrete distal cycle), and the inclusion of a variety of complex central area grids (text-figs. 13 and 15). Very little sutural kinking is observed and the suture arrangement is generally perfectly radial. The central area grid in all three species has a longitudinal bridge which bifurcates soon after leaving the central area edge, to form a central oval or lozenge-shaped feature which is bisected by a transverse bar along the minor axis of the ellipse. In *S. lowei* the two curving longitudinal bars are supplemented by a third, straight, major axis bar and in *S. arctus* the spaces between these three bars are usually completely filled in; only occasionally are oblique slits visible, delineating the three component parts. *S. arctus* also has radial bars supporting the central lozenge-shaped central structure.

The *Sollasites*-rim appears to have developed from *B. novum* during the early Pliensbachian but the order in which the three species appear is unknown. Goy (1981, pl. 18, fig. 6) illustrated a coccolith named *S. cf. pristinus* displaying intermediate features between *B. novum* and *S. pristinus* with a closed *Biscutum*-like rim and a small *pristinus*-like central grid. It is feasible that *S. pristinus* developed first from *B. novum* and then gave rise to the increasingly complex *S. lowei* and *S. arctus*. It is also possible that the three species arose separately from *B. novum* although the similarity of their central areas suggests their development from one another. Post Lower Jurassic specimens of *S. lowei* (e.g. Rood *et al.* 1971, pl. 4, fig. 1) display well-developed distal inner cycles and thus *S. lowei* parallels the evolutionary development of other members of the Biscutaceae.

Calyculus. A typical *Calyculus* rim is composed of radially arranged elements with an extended vertical portion which flares distally to create a broad horizontal distal face. The proximal shield is very reduced and usually forms a small proximal ring. Variation in height and width of the rim is quite considerable. The morphological trend towards the *Calyculus* rim is first seen in specimens of *S. lowei* which display a reduction of the proximal shield and a thickening of the distal shield elements (see Crux 1984, fig. 9.2). The trend is continued in *C. depressus* sp. nov., as the distal shield becomes narrow and more vertically extended (text-fig. 15). In *C. cribrum*, the vertical extension also flares horizontally to form the characteristically broad distal surface. Thus the morphological changes observed in the rims of *S. lowei* and *C. depressus* are good evidence for the evolution of *Calyculus* from *Sollasites*. However, an additional and striking line of evidence for this development also exists in the central areas of the two genera involved. Of the eight species of Calyculaceae that Goy (1981) illustrated, three possessed central area grills identical to those found in the three species of *Sollasites* and three possessed grills with only slight modifications to the *Sollasites* grills (text-fig. 15). The grill of *S. lowei* corresponded exactly to that of *C. cribrum*, *S. pristinus* to that of *C. adjunctus*, and *S. arctus* to that of *C. noelae* (= *Vickosphaera*). *C. hommerilii* (= *Catillus*) and *C. serrai* (= *Catillus*) both possess *lowei*-like central grills with additional radial bars and Goy's genus *Incerniculum* (= *Calyculus*) includes three species which possess central areas filled with a perforated grill structure. Thus, the evolutionary development from *Sollasites* to *Calyculus* initially affected the rim structure only, with identical central grids illustrating the close relationship between the two genera. The high degree of similarity of these corresponding central areas confirms the *Sollasites-Calyculus* relationship, as the repetition of such complex and perfectly matched structures is very unlikely.

The fact that three species of one genus, *Sollasites*, gave rise to three species of another genus, *Calyculus*, over the same time interval raises a number of problems. One possible explanation is that the three species are actually three different phases in the life cycle of a single biological species. Goy (1981) illustrates coccospheres of all three species and so trimorphism can be discounted. This evolutionary phenomenon can best be explained with reference to the genetic make-up of the three species involved. The morphological similarities and subsequent inclusion of the three species into the genus *Sollasites* is assumed to reflect a biological relationship which fundamentally involves a certain degree of shared genetic material. Thus, the genetic similarity of the three *Sollasites* species must have been such that they carried an equal potential for evolution



TEXT-FIG. 15. The polyphyletic evolution of *Calyculus*.

in a certain direction. Their striking parallel evolution justifies their inclusion in the same genus. A similar phenomenon is also seen in other parts of the radiating placolith lineage. For example, separate branches within the lineage undergo the same development of a distal inner cycle and a wider central area (cf. *B. intermedium* and *B. grandis*). Again these parallel developments may be attributed to the shared genetic material which gives an equal evolutionary potential for certain trends. However, there is also a degree of genetic uniqueness which produces differing morphologies allowing division of the lineage into species and genera. If the three *Sollasites* species do represent the starting points of three lineages which develop into *Calyculus* rims we would expect at least slight differences between the lineages and this is what is observed. For example, the *S. arctus* to *C. noelae* transition also includes the development of dimorphism and very high distal rims not observed in other *Calyculus* species, and both the *S. lowei* and *S. pristinus* developments include extremely wide distal surfaces (i.e. *C. cribrum* and *C. adjunctus*). *Calyculus* is thus considered a polyphyletic genus with the three *Sollasites*-derived species first to appear. It is probable that the additional five species of *Calyculus* were later developments from the first three (text-fig. 15).

Carinolithus. The evolutionary trend towards distal shield extension, first observed in the development of *Calyculus*, was carried still further in the evolution of *Carinolithus*. The distal elements of *Carinolithus* form a long, thin tube which flares to form a horizontal distal surface, the proximal shield is reduced to a small subcircular to circular disc and the central area is merely an axial canal. The lack of any central structure prevents a direct link being made with any of the *Calyculus* species, however, the trend from *Calyculus* to *Carinolithus* is convincing and has been illustrated in the LM by Crux (1987) and SEM by Goy (1981, pl. 23, figs. 5 and 6). The most extended species of *Calyculus* appears to be *C. noelae* (Goy 1981, pl. 21, figs. 5 and 6) and it is possible that *Carinolithus* was descended from this species during the *tenuicostatum* Zone (Lower Toarcian) (text-fig. 15).

Later in the Toarcian, *Carinolithus superbus* gave rise to a second species, *C. magharensis* comb. nov., in which the distal stem is further narrowed and formed from only six elements which flare sharply at their distal end to form a hexalith-like plate, the proximal shield is also reduced to a tiny basal disc.

The evolution of *Discorhabdus* from *Carinolithus* as proposed by Crux (1987) is not followed here for the following reasons:

- i, a clear development from *B. novum* to *D. ignotus* has been observed here.
- ii, the structure of *Carinolithus* is distinct from that of *Discorhabdus*, with the stem of the former constructed from the distal shield elements, and the large spines of the latter formed from central area microcrystals.
- iii, the proximal discs of *Carinolithus* are very much smaller in size than the shields of contemporaneous *Discorhabdus*.

Biscutum intermedium sp. nov. The transition from *B. novum* to *B. intermedium* is best observed in the Upper Toarcian of the Brenha Road section. The development involved an increase in size, the formation of an inner distal cycle, widening of the central area, increase in diameter of the hollow spine base, and a breakdown of the granular central area filling to produce a thick, oblique bar delineated by two, lenticular windows (text-fig. 14). The transition is gradual with all intermediate stages observed in the Brenha section (Pl. 6, figs. 7-10). This evolutionary development appears to be towards a podorhabdid-type coccolith and it is possible that *B. intermedium* is an ancestor of one or all of the Middle Jurassic genera *Podorhabdus*, *Tetrapodorhabdus*, and *Hemipodorhabdus*. *B. intermedium* is another example of the way in which similar evolutionary developments arise quite independently within the radiating placolith lineage; it appears that the Podorhabdaceae, like the Calyculaceae, was derived from more than one ancestral species and thus forms a polyphyletic family.

Biscutum depravatus comb. nov. *B. depravatus* occurs soon after *B. intermedium* in the Brenha section, but from the lack of an inner distal cycle in the rim of *B. depravatus* it appears that it

evolved from *B. novum* and not *B. intermedium*. The evolution of *B. depravatus* was in a similar direction to that of *B. intermedium* described above, but the two species arose independently from the *B. novum* lineage. The development from *B. novum* involved a slight increase in coccolith size, a gradual opening of the central area, and a breakdown of the granular central area filling to produce an asymmetric cross structure (text-fig. 14). The rotation of the crossbars from the principal axes of the ellipse is in a clockwise direction, as seen in *B. intermedium*, and the central area size is also comparable. The development of *B. depravatus* did not include fragmentation of the distal shield and thus its development from *B. intermedium* is unlikely, as such a transition would necessarily involve the loss of a rim cycle, a development which has not been observed.

Sutural kinking displays the potential for inner cycle development and, like *B. intermedium*, *B. depravatus* is another species which may have given rise to podorhabdid coccoliths in the Middle Jurassic.

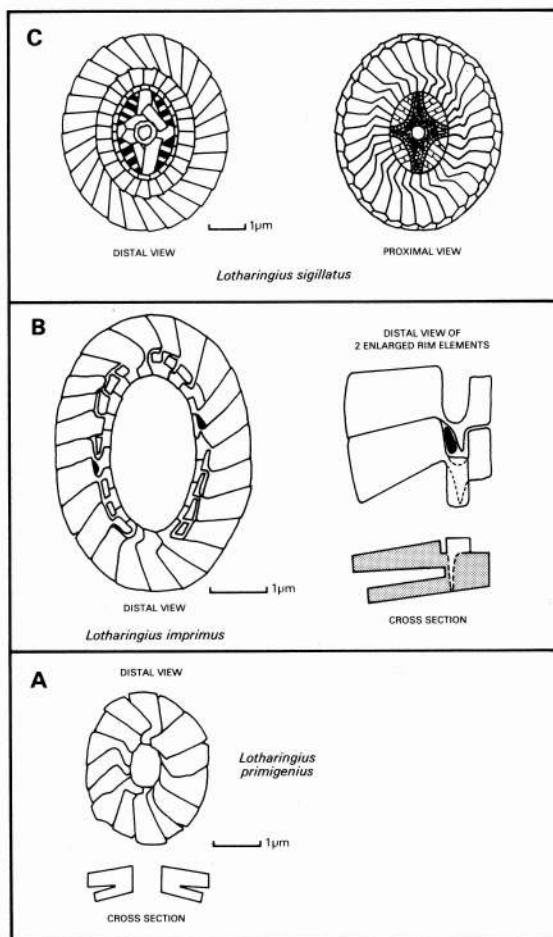
Imbricating placolith rim structure group/Watznaueriaceae lineage

The three principal species of *Lotharingius* in the Lower Jurassic (*L. hauffii*, *L. sigillatus*, and *L. barozii*) all appeared during the Pliensbachian with fully developed complex, compound rims and intricate central structures. The discovery of two new species from DSDP Site 547, which may represent ancestral forms of these *Lotharingius* species, has provided a clear insight into the evolutionary processes which gave rise to the tricyclic, placolith rim so characteristic of the Watznaueriaceae.

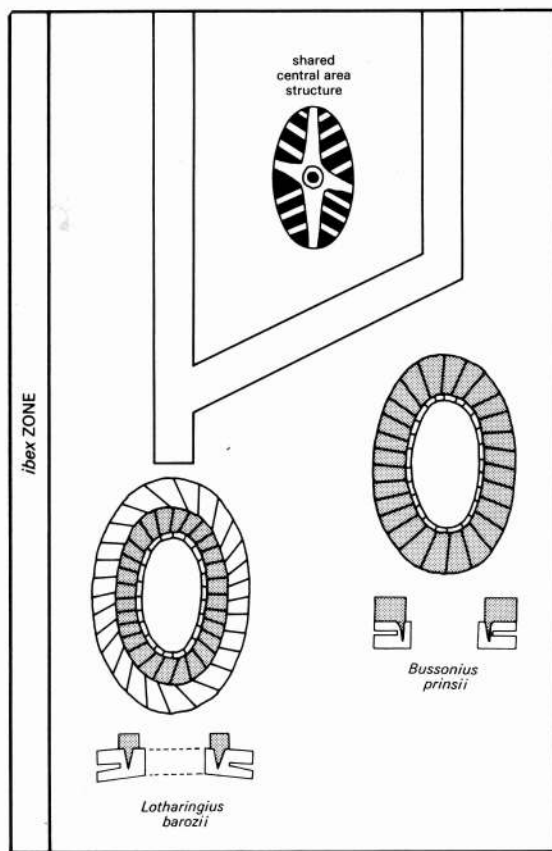
Lotharingius primigenius and *L. imprimus*. The earliest of these two species is *L. primigenius*, possessing a simple, unicyclic placolith structure similar in shape and size to *L. hauffii*. The elements of the distal shield are joined along distinctly kinked sutures with a pronounced anticlockwise inclination, identical to that seen in the later three species of *Lotharingius*, although the kinked part of the suture is usually hidden by the distal inner cycle. The suture kinking is near the inner edge of the elements, as seen in the Biscutaceae, but the direction of kinking is opposite to that observed in the latter group, the sutures veeing in a clockwise direction. Although no element fragmentation has been seen in *L. primigenius*, the suture kinking is such that 'pinching-out' of the elements has taken place and the potential for structural differentiation is clearly evident (text-figs. 13 and 16A).

A second species, *L. imprimus*, appears soon after *L. primigenius* and represents an intermediate evolutionary stage between *L. primigenius* and the fully developed *Lotharingius* (e.g. *L. sigillatus*). *L. imprimus* is a larger coccolith than *L. primigenius* with many more rim elements, a wider central area, and a partially developed distal inner cycle and inner wall. The partially formed rim of *L. imprimus* reveals the way in which the initially unicyclic shield has broken down into three components (text-fig. 16B). The first process is similar to that described for members of the Biscutaceae and involves progressively associated suture kinking near the central area producing a pinching-out of the elements which almost completely isolates an offset inner portion. These semi-isolated portions are the inner wall cycle which appear as discrete cycles in fully developed coccoliths of the Watznaueriaceae (where the distal inner cycle covers the kinked linking portion, which joins the inner, semi-isolated portion to the outer part of the element). Broken specimens of *L. sigillatus* have revealed that the link between the inner and outer parts of the elements is still retained in the fully developed *Lotharingius* rims, although the potential for a completely independent inner wall is evident. In addition, the outer distal shield elements and proximal shield elements are crystallographically continuous and joined at the inner wall. Similar suture kinking and pinching-out delineates the inner wall on the proximal surface (text-fig. 16C).

The second process of rim differentiation concerns the formation of the distal inner cycle which in the fully developed *Lotharingius* structure appears as a relatively superficial ring of flat elements lying on the outer cycle elements with the inner wall at its inner edge. In *L. imprimus* the inner distal cycle is only partially developed. The process leading to its formation appears to be a more



TEXT-FIG. 16. A, *Lotharingius primigenius*, B, *L. imprimus*, and C, *L. sigillatus*.



TEXT-FIG. 17. The evolution of *Bussonius prinsii* from *Lotharingius barozii*.

complex method of element intergrowth than that already described from the Biscutaceae, causing fragmentation of the distal element in both the horizontal and vertical planes. The product of this process is a rectangular element which lies on the elements from which it has been isolated but which also has a deeply penetrating root (text-fig. 16B). This root passes between the outer cycle elements at a bend in the sutures and it is these root holes which appear as a ring of perforations in specimens of *Calolithus* Noël, 1965. *Calolithus* coccoliths are considered to be damaged and etched specimens of Watznaueriaceae which have lost the distal inner cycle.

L. primigenius and *L. imprimus* thus appear to illustrate the various stages of element intergrowth which lead to the formation of a complex compound rim. These two species are at present only known from the DSDP Site 547 section where the stratigraphic control is uncertain and further work is required to confirm the validity of these forms as precursors of the fully developed *Lotharingius* coccoliths. *L. hauffii*, *L. barozii*, and *L. sigillatus* are recorded from the Pliensbachian, *L. hauffii* appearing first followed closely by the larger and more open rimmed *L. sigillatus* and *L. barozii*. *L. sigillatus* appears to show an increase in size in the late Toarcian and additionally includes more circular specimens. These trends clearly preceded the development of the larger *Watznaueria* coccoliths and circular *Cyclagelosphaera*.

Bussonius prinsii. *B. prinsii* possesses a central area structure identical to that seen in *L. barozii*. Further observation revealed specimens of *L. barozii* with expanded distal inner cycles, protruding well above the level of the distal outer cycle and proportionally wider than in other species of *Lotharingius*. It is apparent that *B. prinsii*, with its unusual three-shield structure, is an evolutionary descendant of *L. barozii*, in which the distal inner cycle became expanded to form a discrete distal shield. The former distal outer cycle narrowed and was left as the intermediate shield, while the proximal shield retained its position and central structure. The lower two shields remained joined along the inner wall, which was left below the level of the 'new' distal shield. This observation is confirmed by the identical imbrication and inclination directions displayed by the three analogous rim components involved (text-fig. 17). Thus, the enlarged inner cycle of *L. barozii* is not a product of overgrowth (Perch-Nielsen 1985, p. 371) but an evolutionary development which produces a rim with three shields during the Pliensbachian. A second species of *Bussonius*, *B. leufuensis*, has been found in the Argentinian Toarcian. This species is larger, more broadly elliptical, and lower in distal shield height than *B. prinsii* and it is possible that *B. leufuensis* was a parallel development from *L. sigillatus* rather than *L. barozii*. Alternatively it may simply be a modification of the earlier *B. prinsii*.

Interlineage relationships

The earliest calcareous nannofossils to appear in the Triassic were the abundant spheres and discs of *Prinsiosphaera*. These coarsely constructed objects were likely to have been the product of some planktonic organism (perhaps a calcareous dinoflagellate), but they bear no resemblance to true coccolithophorids which appeared soon after. The *Prinsiosphaera* ultrastructure of one fundamental crystallite bears some resemblance to the construction of *Schizosphaerella*, which appeared slightly later around the Upper Triassic/Lower Jurassic boundary. It is not impossible that these two nannofossils are related, but *Schizosphaerella* displays a far more symmetrical and ordered bivalved test. Both these relatively large, spherical nannofossils dominated Tethyan assemblages, *Prinsiosphaera* during the late Triassic and *Schizosphaerella* in the early Jurassic, and they may have occupied a similar environmental niche.

Next to appear in the late Triassic was *Conusphaera zlabachensis*, a nannofossil which may be related to the Upper Jurassic *C. mexicana*, the Lower Jurassic *Mitrolithus jansae*, or to neither. *Thoracosphaera geometrica* also occurs in these assemblages but its relationship to later members of the genus is uncertain. The long gap between its occurrence in the Triassic and the next appearance of a species of *Thoracosphaera* could be explained either by restricted distribution in the southern hemisphere or a capability to revert to a non-calcified cell cover.

True coccoliths are first recorded in the *suessi* Zone of the Upper Triassic and representatives of both the loxolith and protolith rim groups are present. It is possible that *Archaeozygodiscus koessenensis* (loxolith) and *Crucirhabdus minutus* (protolith) shared a common ancestor in the Triassic or that one of the two gave rise to the other. The relatively sudden appearance of nannofossils in the late Triassic could be a calcification event in which the ancestral but previously naked group of algae developed the ability to calcify their organic cell wall, thus allowing their preservation as fossils.

The next lineage to appear was the tiered placolith group represented by *Mazaganella* and recorded from the Sinemurian and Pliensbachian of southern Tethys areas only. Nothing is known of its ancestry although it is thought to have given rise to the genus *Triscutum* in the Toarcian. An *incertae sedis* nannofossil, *Orthogonoides hamiltoniae*, also appears in the early Sinemurian and ranges through to the early Toarcian with no apparent ancestry or descendants.

The fourth coccolith lineage, the radiating placolith rim group, appeared in the late Sinemurian represented by *B. novum*. This simple placolith coccolith could have conceivably developed from either the loxolith or protolith structures. Both these earlier coccolith types possess two rim components and central structures which stem from the inner edge of the proximally situated rim elements. No coccoliths with intermediate structures have yet been observed. It is also possible that *B. novum* was descended from *Mazaganella*, however, the morphologies are only vaguely

similar and no intermediates have been observed in the DSDP Site 547 section. Both *Mazaganella* and *Biscutum* could also represent calcification of a previously naked lineage. The placolith morphological development appears to have been an adaptive innovation which led to an episode of rapid evolution. The two placolith orders increased greatly in both diversity and abundance, while the Eiffellithales was dramatically reduced in what appears to have been an ecological replacement of an older group by a new.

The final lineage to appear in the early Jurassic was the imbricating placolith group during the Pliensbachian. The development of this group from the radiating placoliths would have involved the least radical structural reorganization, and with the discovery of what are considered to be intermediate forms (*L. primigenius* and *L. imprimus*) this now appears to be the case. *L. primigenius* is a simple, unicyclic placolith which could easily have developed from *B. novum*, a transition which would involve only the introduction of sutural kinking with pronounced inclination in a direction opposite to any observed in the radiating placolith lineage. This transition is thought to be confirmed by the similarity of evolutionary developments which both lineages underwent at this time. Each lineage showed increasingly complex element intergrowth creating additional rim cycles. Within the radiating placolith lineage inner distal cycles repeatedly evolved, while in the imbricating placolith group a similar inner cycle developed before the lineage became more conservative.

Causes, direction, and location of Lower Jurassic coccolithophorid diversification

The knowledge of present-day coccolithophorids is still limited and the processes of speciation and other evolutionary mechanisms are relatively unknown. It is possible that some morphological variation is the product of random genetic drift which has persisted without necessarily being favoured by the processes of natural selection. This appears to be justifiable as many of the morphological variations observed in coccoliths are difficult to reconcile with any additional functional advantage. However, until the true function of coccoliths is successfully established, any proposals including functional advantages have no real basis. It must be assumed that the development of calcified coccoliths and their subsequent diversification brought a functional advantage to the cell, the evolutionary modifications of which were directed by natural selection. The extent to which the aquatic environment exerts selective pressure on coccolithophorids is uncertain but like all phytoplankton they are controlled by ecological factors, such as temperature, nutrients, and salinity, together with predation. In addition, it is generally agreed that most speciation is a result of the isolation of populations and their subsequent development into reproductively isolated gene pools. The processes by which populations of coccolithophorids could become isolated are uncertain. Romein (1979) suggested that coccolithophorids, while able to reproduce sexually, may reproduce asexually for many generations leading to the formation of large clones (rather than interbreeding populations) which after a period of time become sexually isolated from other groups. However, he favoured a second mechanism in which ecological factors, such as temperature, light intensity, salinity, and nutrients, form barriers (cf. water mass fronts) which vertically and laterally isolate populations. Speciation may then occur within these vertically zoned populations and this would explain the co-occurrence of ancestral and descended species in nannofossil assemblages (Romein 1979, p. 19). Gartner and Keany (1979) have also suggested geographical isolation but by land barriers, although it seems unlikely that repeated geographic isolation is the cause for the majority of coccolithophorid speciation.

The initial location of coccolithophorid populations appears, from presently available information, to have been in the Tethys Ocean. It is probable that the subtropical and tropical position of much of Tethys constituted the optimum environment for coccolithophorids as is the case today. Thus, their early development occurred in Tethys before moving into the cooler, more stressful north-west European shelf sea (perhaps in response to competition in the environmentally favourable Tethys). It is possible that the appearance of coccolithophorids in the Triassic represented the evolution of a new phytoplanktonic organism which was moving into and exploiting the oceanic environment which had been largely emptied by the mass extinctions of the Permian. Such extinctions are known to have effected every level of the ecosystem and thus extinction of the

Palaeozoic plankton cannot be ruled out. Equally likely is the hypothesis that prymnesiophytes or very similar algae inhabited the same or similar habitats during the Palaeozoic but remained naked or covered only with organic scales and are thus unrepresented in the fossil record. In present-day coccolithophorids the calcified portion of the coccolith is formed on a large, organic base plate which appears first and is essential to the formation of the coccolith. It is possible that prymnesiophytes bore only these organic plates in their early history and that their retention, after successful calcification, is a recapitulation of their early evolution (Outka and Williams 1971, p. 288). This can be compared with the history of dinoflagellates which, while first appearing in the early Mesozoic, are thought to have had their precursors, i.e. acritarchs in the Palaeozoic.

Throughout the Lower Jurassic evolutionary diversification appears to have taken place in Tethys, followed by a delay, before movement into the north-west European shelf area. The reason for such a delay may have been an absence of ocean currents or a need for acclimatization before colonizing the more stressful northern environment.

Processes of Lower Jurassic nannofossil evolution

Macroevolution. Detailed SEM observation confirmed the conclusion of most workers that the coccolith rim is the morphological feature of greatest evolutionary significance. The rim construction transcends the species boundaries and represents the macroevolution of the group. In the early Jurassic the rim developments within the orders are mostly easily understood, good examples being the development of the discorhabdid, *Sollasites*, *Calyculus*, and podorhabdid rim types from the simple *Biscutum* rim, and the *Stradnerlithus* and *Stephanolithion* rim types from the protolith *Crucirhabdus* rim type. The relationships between the higher taxa, with the exception of the Podorhabdales and Watznaueriales, are less well understood due to the lack of intermediate forms, e.g. the relationships between the Eiffellithales and Podorhabdales, and Biscutaceae and Mazaganellaceae are unknown. It is anticipated that data from the Tethys area will clarify these problems.

Although the rim is of major evolutionary significance it is clear that usually only the distal component displays radical evolutionary change, while the proximal shield is a conservative feature across family and even order boundaries. For example, the proximal shields of the Mazaganellaceae, Biscutaceae, and Watznaueriaceae are all very similar, differing only in the direction of inclination/suture kinking.

Microevolution. Detailed variation in the central area structure is used to define species, and while not strictly at the level of microevolution (usually reserved for intra-population/intra-specific evolutionary change) it is used here as a convenient expression of lower level morphological significance. The central structures almost always extend from the inner edge of the proximal shield and in some genera, e.g. *Watznaueria*, they are actually a continuation of the proximal shield elements. Thus, perhaps the central structures should be thought of as an extension of the proximal shield which, while remaining a conservative feature in its outer area, reflects species-level evolutionary change in its central area. The central area structures thus show fairly short range evolutionary changes which occur within the more stable and evolutionary significant rim structures. Many homeomorphic central structures are observed occurring within unrelated rim groups. In the case of the evolutionary developments between *Sollasites* and *Calyculus*, and *Lotharingius* and *Bussonius*, the central structures remained stable and unaltered while the rims underwent significant evolutionary change.

Rim fragmentation. The vertically orientated discolith structure of the Eiffellithales, consisting of a single distal and proximal cycle of elements, continued through the entire Lower Jurassic relatively unchanged, apart from the height, width, and thickness of the elements and the general outline of the rim. For example:

- i. *Parhabdolithus*—steep, high rim (Hettangian–Lower Toarcian).
- ii. *Diductius*—low, sloping rim (Lower Toarcian–?Bajocian).

- iii. *Stradnerlithus*—low, vertical rim with jagged upper surface (Lower Toarcian–Maastrichtian).
- iv. *Diadorhombus*, *Rhombolithion*—geometric rim outline (Lower Toarcian–Albian).
- v. *Stephanolithion*—low, vertical rim with lateral appendages (Bajocian–Tithonian).

In contrast, soon after the first appearance of placolith coccoliths, the placolith structure displayed a number of significant modifications including the development of additional rim cycles. In the Lower Jurassic this development is seen in both the Biscutaceae (Podorhabdadales) and the Watznaueriaceae (Watznaueriales) and allowed greater diversification of the placolith morphology. In each case, the basic mechanism of rim fragmentation was the same, and consisted of progressive intergrowth of distal rim elements leading to cross-cutting of sutures, and the effective isolation of new, discrete elements (text-fig. 12). The complex rim element intergrowth may result from the increasing number and size of rim elements being incorporated into the restrictive elliptical ring geometry. In the Watznaueriaceae, rim fragmentation followed by further organization of the three rim components led to the development of a three-shield coccolith, *Bussonius*.

Homeomorphy/parallel evolution. Homeomorphy, defined as similar morphological characters in unrelated taxa, is commonly observed in calcareous nannofossils. In the Lower Jurassic it appears that the lineages present had only diverged within the previous 30 million years. Thus the term parallel evolution is perhaps more appropriate for the repetition of morphologies observed. Certainly within the major lineages themselves parallelism is often striking. The *Sollasites* to *Calyculus* transition, for example, saw three separate species of *Sollasites* undergoing independent but identical morphological modifications to form species of *Calyculus*. Such closely parallel patterns must reflect a large proportion of shared genetic material resulting in an equal potential for evolution in the same direction at the same time. A slightly different pattern is seen in the Biscutaceae lineage where the root stock, *Biscutum novum*, repeatedly gave rise to new species all displaying similar rim modifications involving the formation of inner distal cycles and wider central areas. A number of these species appear to be precursors of the podorhabdid-rim forms and it is probable that, like *Calyculus*, the Podorhabdadaeae is a polyphyletic group. The pattern seen in the Biscutaceae can loosely be termed iterative evolution, but there is generally no replacement of the successively evolving species. Examples of 'homeomorphy' in less closely related taxa in the Lower Jurassic include *Triscutum* and *Calyculus*, both possessing vertically extended distal shields and *Triscutum* and *Bussonius*, both possessing three tiered rims.

Phyletic gradualism and punctuated equilibria. From the evidence presently available it appears that both phyletic gradualism and punctuated equilibria occur as methods of evolutionary change in Lower Jurassic coccoliths. Many of the species to species transformations described here are gradualistic in nature with a continuum observed between end members. Populations are observed with increasing variability towards two end members which in time become distinct species. Examples include *Biscutum novum* to *Discorhabdus ignotus*, *B. novum* to *B. intermedium*, and *L. barozii* to *Bussonius prinsii*. A number of genus to genus developments are also interpreted in this way, e.g. *Calyculus* to *Carinolithus*, *Sollasites* to *Calyculus*, *Crucirhabdus* to *Stradnerlithus*, and *Biscutum* to *Lotharingius*. It is also true that many genera and species have cryptogenic appearances e.g. *Biscutum* and *Mazaganella*. This may be a true representation of the evolutionary processes by which coccolithophorids diversify or it may be a distorted view resulting from biased and restricted data. None the less the general pattern of evolution is one of stable, conservative root stocks giving rise to successive new species but not being replaced by them (text-fig. 9). In every case, both the ancestor and descendants continue to be found together. If isolation is indeed the cause of coccolithophorid evolution then a refined model is needed which allows for the continued presence of both ancestral and descendant populations. In addition, Lower Jurassic coccolithophorid evolution commonly includes a high degree of parallelism within the major lineages and a number of polyphyletic genera and families occur.

Size: small to large. On a number of occasions an evolutionary appearance is preceded by very small coccoliths with a similar morphology. This is well illustrated by *C. minutus* and *C. primulus*.

It is also clear that a number of evolutionary developments include a considerable increase in size, e.g. *L. primigenius*/*L. hauffii* gave rise to *L. sigillatus* which itself increases in size before giving rise to *Watznaueria*; *B. novum* to *B. finchii*, etc. Thus, in the late Triassic and early Jurassic an increase in size is a general pattern, with the possible occurrence of evolutionary innovation in smaller size ranges before the development of larger coccoliths. This observation may explain certain cryptogenic appearances, with small ancestral forms being difficult to observe and easy to overlook. Missing links, however, can also be explained by the occurrence of naked intermediaries, perhaps recapitulating the early history of the group, or simply by insufficient information resulting from geographical bias of published accounts, and diagenetic and facies problems.

Central area extension. Many of the earliest representatives of the placolith lineages possess small or closed central areas, e.g. *L. primigenius*/*L. hauffii*, *B. novum*. Developments from these early forms almost always include a widening of the central area and associated development of central bridging structures, e.g. *L. sigillatus*, *Axopodorhabdus atavus*, *Sollasites lowei*. This development may be linked to a functional role for coccoliths as mediating structures at the boundary between the cell and environment. A wider central area filled with a complex grill perhaps fulfils the role more successfully. Closed central area forms, however, continue to be successful throughout the Mesozoic, e.g. *Biscutum*, *Discorhabdus*, *Watznaueria*.

Vertical extension. Distal extension of the coccolith may take place by formation of a spine extending from the central area or by extension of the distal shield elements to produce funnel-like and spine-like morphologies. Spine-bearing morphologies are present in the earliest coccoliths, e.g. *C. minutus*, *C. primulus*, *P. liasicus*, the latter species perhaps having dimorphic coccoliths with extremely extended spines. Such spines may be anti-grazing features or perhaps help control or orientate the cell in the water column. While most Lower Jurassic placoliths possess spines they are generally broken and it is not until the Middle Jurassic that strong, extended and often flaring spines are seen in the podorhabdid and discorhabdid groups. Two of the Lower Jurassic placolith families, Calyculaceae and Mazaganellaceae, display vertical extensions via expansion of their distal shields. In the Calyculaceae the development is extreme with the genus *Carinolithus* possessing a distal shield which forms a tall, narrow spine-like tube which flares distally. The morphology of both families appears to suggest a function related to the creation of an extra-cellular buffer zone which in some way benefits the organism, perhaps in its interaction with the surrounding medium. Such a function is supported by Sykes and Wilbur (1982) who concluded from their experiments with *Emiliania huxleyi* (Lohmann) Hay and Mohler, that by enclosing a volume of water within its coccosphere but outside the cell membrane, the cell gained greater control of the immediate external environment.

BIOSTRATIGRAPHY

Five calcareous nannofossil biostratigraphic zonation schemes have been proposed for the Lower Jurassic interval (Stradner 1963; Prins 1969; Barnard and Hay 1974; Hamilton 1977, 1982). A number of emended versions of these schemes have also been published, e.g. Reinhardt (1965), Amezieux (1972), Van Hinte (1976), and Thierstein (1976). Stradner (1963) presented an overall Mesozoic scheme with only a simplified twofold division for the Lower Jurassic. Prins (1969) produced a refined scheme for the Rhaetian to Lower Toarcian period and apart from the confusion that followed from his lack of formal taxonomic descriptions the paper remains one of the best for the period. Barnard and Hay (1974) proposed a Jurassic zonation scheme but were restricted in the Lower Jurassic by the nature of the Dorset study section in which most of the Upper Pliensbachian and Toarcian time interval is represented by a very condensed limestone sequence (the Junction Bed). Since its appearance this scheme has been repeatedly cited as the standard

Definition and description of the Lower Jurassic nannofossil zones

JL1. *Schizosphaerella punctulata* Zone

Author. First defined here but comparable with the *Crucirhabdus* Zone of Prins (1969).

Definition. First occurrence of *S. punctulata* to the first occurrence of *P. liasicus*.

Range. Upper Rhaetian to *bucklandi* Zone (Lower Sinemurian).

Reference section. St Audries Slip, south-west England.

Remarks. The exact stratigraphic position of the base is uncertain, possibly in the late Rhaetian (Hamilton 1982) but recorded from the *planorbis* ammonite Zone of the basal Hettangian in the present study. Samples from the Rhaetian and Hettangian were predominantly barren. *S. punctulata* is occasionally found abundantly, particularly in the *angulata* Zone. *C. primulus* first occurs in the *angulata* Zone, usually after the first appearance of *S. punctulata*, but is always rare.

JL2. *Parhabdolithus liasicus* Zone

Author. Name first used for a subzone by Prins (1969) and for a zone by Barnard and Hay (1974). The zone as used here is comparable with Hamilton (1982).

Definition. First occurrence of *P. liasicus* to the first occurrence of *Crepidolithus crassus*.

Range. *bucklandi* Zone (Lower Sinemurian) to *oxynotum* Zone (Upper Sinemurian).

JL2a. *Parhabdolithus marthae* Subzone

Author. Prins (1969).

Definition. First occurrence of *P. liasicus* to the last occurrence of *P. marthae*.

Range. *bucklandi* Zone to *semicostatum* Zone (Lower Sinemurian).

Reference section. Hock Cliff, south-west England.

Remarks. *P. liasicus* is usually accompanied by abundant *P. marthae*. *Mitrolithus elegans* may be present throughout the zone or from the mid-*semicostatum* Zone only. *C. plienschachensis* is first recorded in the *semicostatum* Zone. The assemblages may be abundant but are often poor and inconsistent during this time interval.

JL2b. *Mitrolithus elegans* Subzone

Author. Defined here.

Definition. Last occurrence of *P. marthae* to the first occurrence of *C. crassus*.

Range. *semicostatum* Zone to *oxynotum* Zone.

Reference section. Mochras borehole (1519–1341 m).

Remarks. The assemblages may be abundant, or rare and inconsistent. *P. robustus* is rare in the lowest part of its range and only found consistently in the *jamesoni* Zone (JL3/4a).

JL3. *Crepidolithus crassus* Zone

Author. First used as a subzone by Prins (1969) and as a zone by Barnard and Hay (1974). Emended here.

Definition. First occurrence of *C. crassus* to the first occurrence of *B. novum*.

Range. Mid *oxynotum* Zone (Upper Sinemurian) to mid *jamesoni* Zone (Lower Pliensbachian).

Reference section. Mochras borehole (1341–1157 m).

Remarks. Although small *C. crassus*-like coccoliths have been observed in the *semicostatum* Zone, true large *C. crassus* has not been observed until the base of this zone as defined here.

JL4. *Biscutum novum* Zone

Author. Defined here.

Definition. First occurrence of *B. novum* to the first occurrence of *L. hauffii*.

Range. *jamesoni* Zone (Lower Pliensbachian) to *margaritatus* Zone (Upper Pliensbachian).

JL4a. *Crepidolithus plienschachensis* Subzone

Author. Defined here.

Definition. First occurrence of *B. novum* to the last occurrence of *P. robustus*.

Range. *jamesoni* Zone to *ibex* Zone (Lower Pliensbachian).

Reference section. Mochras borehole (1157–1064 m).

Remarks. *B. novum* is a distinctive coccolith and clearly marks the base of this subzone. *P. robustus* has its most consistent and abundant distribution (in north-west Europe) during this zone, and *M. jansae* also occurs. *S. punctulata*, *P. liasicus*, *M. elegans*, and *C. crassus* continue to dominate the assemblages along with *B. novum*.

JL4b. *Crepidolithus granulatus* Subzone

Author. Defined here.

Definition. Last occurrence of *P. robustus* to the first occurrence of *L. hauffii*.

Range. *ibex* Zone to *margaritatus* Zone.

Reference section. Mochras borehole (1064–981 m).

Remarks. *Calyculus* sp. was recorded rarely and sporadically.

JL5. *Lotharingius hauffii* Zone

Author. Defined here.

Definition. First occurrence of *L. hauffii* to the first occurrence of *C. superbus*.

Range. *margaritatus* Zone (Upper Pliensbachian) to top *tenuicostatum* Zone (Lower Toarcian).

Remarks. The zone is additionally characterized by the near total range of *B. finchii*.

JL5a. *Biscutum finchii* Subzone

Author. Defined here.

Definition. First occurrence of *L. hauffii* to the first occurrence of *C. cavus*.

Range. *margaritatus* Zone to lowest *spinatum* Zone.

Reference section. Mochras borehole (981–866 m).

Remarks. The first occurrence of *B. finchii* is also recorded in the *margaritatus* Zone but appears to be slightly earlier than that of *L. hauffii*. Both species represent distinctive coccoliths appearing in the *margaritatus* Zone. The first specimens of *Lotharingius* to appear are often small *Lotharingius* rings and these have been included in *L. hauffii*. *B. finchii* has been recorded from the Mochras borehole and while only rarely found in the German Toarcian sections in the present study, its presence in the German Basin is confirmed in the work of Crux (1984). *C. primulus*, *M. elegans*, and *P. liasicus* become rare and inconsistent in this zone, prior to their extinction in the next zone.

JL5b. *Crepidolithus cavus* Subzone

Author. First used as a subzone by Prins (1969). Emended here.

Definition. First occurrence of *C. cavus* to the first occurrence of *C. superbus*.

Range. *spinatum* Zone to top *tenuicostatum* Zone.

Reference section. Mochras borehole (866–824 m).

Remarks. The species given in text-fig. 18 may be supplemented by the numerous new taxa recorded by Goy (1981). The species include *Chiasozygus primitus*, *Diadorhombus duodecostatus*, *Diductius constans*, *Ethmorhabdus crucifer*, *Lotharingius barozii*, *Saeptella conspicua*, *S. vicina*, *Sollasites lowei*, *S. pristinus*, *Staurorhabdus magnus*, *S. quadriarcellus*, *Stradnerlithus humilis*, *S. clatriatus*, and *S. comptus*.

M. jansae is recorded relatively consistently in this zone before its disappearance in the *tenuicostatum* Zone. *Crucirhabdus primulus* is absent or extremely rare, and *M. elegans* and *Crepidolithus granulatus* are not found. *C. cavus* appears to be the most consistent marker for this zone as *A. cylindratus*, *Bussonius prinsii*, *Calyculus* sp., and *Zeugrhabdotus erectus* may be rare and inconsistent in their distribution, and *Biscutum grandis* has not been recorded from the Paris or German Basins. This zone represents the final turnover of the typically early Lower Jurassic components to the typically late Lower Jurassic assemblages.

JL6. *Carinolithus superbus* Zone

Author. Defined here.

Definition. First occurrence of *Carinolithus superbus* to the first occurrence of *Discorhabdus ignotus*.
Range. *falciferum* Zone.

Reference section. Mochras borehole (824–777 m).

Remarks. *B. finchii*, *Crucirhabdus primulus*, and *M. jansae* are not recorded in this nannofossil zone and *B. grandis* and *Orthogonoides hamiltoniae* disappear near the top of the zone. *Carinolithus superbus* is a distinctive and relatively common component of the assemblages and its gradual evolution from *Calyculus* is observed in the previous zone. One or two specimens of *P. liasicus* and *M. elegans* have been occasionally observed and this is considered to be reworking.

JL7. *Discorhabdus ignotus* Zone

Author. Defined here.

Definition. First occurrence of *D. ignotus* to the first occurrence *B. intermedium*.

Range. Upper *falciferum* Zone to *levesquei* Zone.

Reference section. Mochras borehole (777–626 m).

Remarks. Some care must be taken with the use of *D. ignotus* as a marker because continuous variation of morphologies is observed between *D. ignotus* and *B. novum*. Only truly circular forms with a reduced central area should be classified as *D. ignotus*.

JL8. *Biscutum intermedium* Zone

Author. Defined here.

Definition. First occurrence of *B. intermedium* marks base of zone.

Range. *levesquei* Zone to Aalenian.

Reference section. Mochras borehole (626–601 m).

Remarks. This zone is a tentative proposal as *B. intermedium* is rather rare and only further work on sections crossing the Toarcian/Aalenian boundary will confirm its usefulness or reveal other more suitable taxa for the division of this time interval. The late Toarcian was a time of comparative stasis after the rapid diversification which occurred around the late Pliensbachian/early Toarcian boundary.

Mediterranean–Tethys biostratigraphy

The presence of distinct nannofossil assemblages and earlier first occurrences in the Mediterranean–Tethys area demonstrates the need for a separate zonation scheme. Only one of the Lower Jurassic Tethyan sections studied was dated by ammonites and thus a formal biozonation would be premature. The following section presents those events which appear to form useful biostratigraphic horizons within the Mediterranean–Tethys Realm. The study of additional ammonite dated sections is necessary to confirm the levels of the biohorizons discussed.

1. Earliest occurrence of calcareous nannofossils—although Jafar (1983) reported a number of nannofossils from the Carnian Stage of the Upper Triassic, it is not until the *suessi* Zone of the Upper Norian (? = Rhaetian) that abundant nannofossils including coccoliths were first observed in the present study. The *suessi* Zone and *marshi* Zone of the Austrian and German Alps are both characterized by abundant nannofossil assemblages dominated by *Prinsiosphaera triassica* and *Conusphaera zlabachensis*, together with the rare and diminutive coccoliths, *Crucirhabdus minutus* and *Archaeozygodiscus koessenensis*. *C. primulus* was also recorded from the *suessi* Zone by Jafar (1983) but not found until the *marshi* Zone in the present study.

2. First diversification of coccoliths. The earliest Tethyan Jurassic rocks studied were early Sinemurian and thus an information gap exists between the Rhaetian and Sinemurian. The Lower Sinemurian assemblages from the Brenha section are all abundant, diverse, and dominated by *M. jansae*, together with *Crepidolithus crassus*, *C. plienschachensis*, *Crucirhabdus primulus*, *M. elegans*, *Parhabdololithus liasicus*, *P. marthae*, *Schizosphaerella punctulata*, and *Tubirhabdus patulus*. At

present it is not known whether this diversity of coccoliths was achieved rapidly at some time in the Hettangian, or by a more gradual introduction of species throughout the stage. The earliest nannofossil assemblages in the DSDP Site 547 section, also thought to be of Sinemurian age, contain a very similar group of species but additionally include *Mazaganella pulla* which is not found in any other Mediterranean or north-west European section.

3. Appearance of *Biscutum novum*. The first occurrence of *B. novum* in the Brenha section is recorded in the first Upper Sinemurian sample and it occurs abundantly in the remaining Lower Jurassic. *P. marthae* is not observed after the Lower Sinemurian, and *Crepidolithus granulatus* and *P. robustus* have first occurrences in the Upper Sinemurian.

4. Appearance of *B. finchii* and *B. grandis*. Both these large and distinctive coccoliths appear simultaneously in the Brenha section during the *jamesoni* Zone (Lower Pliensbachian). They have been recorded from all the Mediterranean sections apart from DSDP Site 547. The *jamesoni* Zone also sees the last occurrences of *C. pliensbachensis* and *P. robustus*.

5. Appearance of *Lotharingius hauffii*. Small specimens of *Lotharingius* are first observed in the late *jamesoni* Zone followed by true *L. hauffii*, *L. barozii*, and *L. sigillatus* in the *ibex* Zone.

6. Disappearance of the early Lower Jurassic species. In the Brenha section the *davoei* Zone sees the last occurrence of *Crucirhabdus primulus* and *Crepidolithus granulatus*, the *margaritatus* Zone, the last occurrence of *Mitrolithus elegans* and *P. liasicus*, and the *spinatum* Zone the last occurrence of *B. finchii*, *B. grandis*, and *M. jansae*. The latter three species have all been recorded from the Lower Toarcian of the Longobucco and Tunisian sections and it appears likely that a gap exists in the Brenha section or sample material.

7. Establishment of the late Lower Jurassic assemblage. The appearance of typical late Lower Jurassic coccoliths in the Brenha section occurs in the *bifrons* and *variabilis* Zones. The relatively late record of this event is thought to be a product of the section. The assemblage typically consists of *Axopodorhabdus atavus*, *Bussonius prinsii*, *Calyculus* sp., *Carinolithus superbus*, *Crepidolithus cavus*, *Discorhabdus criotus*, *D. ignotus*, *Sollasites lowei*, and *Z. erectus*.

8. Toarcian/Bajocian boundary appearances. The Upper Toarcian to Upper Toarcian/Lower Bajocian boundary interval in the Brenha section sees the appearance of *Biscutum intermedium*, *B. depravatus*, *Triscutum* sp., *Diductius constans*, *Watznaueria britannica*, *Carinolithus magharensis*, and *Discorhabdus patulus*. The earliest record of the *Retacapsa* genus has also been recorded at this level (see Pl. 11, figs. 16–18).

Similar bioevents to those used in the north-west European biostratigraphic scheme are also recognized in the Mediterranean–Tethys area. The stratigraphic level of these horizons is usually a number of ammonite zones earlier in the Brenha section and presumably elsewhere in the Tethyan area than in north-west Europe. It should be the aim of subsequent research to confirm the findings of the Brenha section, to refine the stratigraphic level of the biohorizons, and to test their application and correlation over a wider area. The DSDP Site 547 section is difficult to compare with the Brenha section due to the lack of any independent dating other than ostracodes and foraminifers, but the presence of *Mazaganella pulla* and *M. protensa* in the former section tends to indicate further provincialism within this area.

Pacific–Tethys biostratigraphy

With information from only two undated sites in Timor and Argentina it is evident that much work is still required in the southern hemisphere before a biozonation can be attempted. The nannofossils observed in the two sections appear to be sufficiently different from the Mediterranean and north-west European assemblages to suggest that a separate scheme will be required for this region.

PROVINCIALISM

Our understanding of nannofossil distribution patterns has been limited by the geographical bias of published data, with only five studies from extra north-west European sites: Israel—Moshkovitz

and Ehrlich (1976b), Apennines, Italy—Nicosia and Pallini (1977), Portugal—Hamilton (1977, 1979), offshore Morocco—Wiegand (1984a, b), and Calabria, southern Italy—Young *et al.* (1986). The seven Tethyan sites included here supplemented the previous work, and the existence of distinct nannofloral provincialism during the early Jurassic was successfully established. The Mediterranean–Tethys sections all yielded similar assemblages with features quite distinct from those of north-west Europe. The TETHYAN REALM is characterized by the following assemblage features:

a. The abundance and dominance of *Mitrolithus jansae* from at least the Lower Sinemurian to the Lower Toarcian. *M. jansae* is usually absent from contemporaneous north-west European assemblages (found rarely and sporadically in the Mochras and Trunch sections), and in addition, was not seen in either of the two southern hemisphere (Pacific–Tethys) sections. *M. jansae* is thus restricted to a equatorial/sub-equatorial zone and its abundant presence reveals the Tethyan affinities of a nannofossil assemblage immediately.

b. The presence of endemic or partially restricted assemblage components. Forms such as *M. lenticularis*, *Triscutum* sp. 1, *C. magharensis*, *B. depravatus*, and *B. grandis* are common in the Mediterranean–Tethys assemblages but are rare or absent in north-west Europe.

c. The considerable difference in ranges observed from one realm to the other. This is especially evident in the earlier occurrence of many biostratigraphically important forms in the Brenha section by as much as four ammonite zones, e.g. *B. novum*, *Crucirhabdus primulus*, *Crepidolithus crassus*, *L. hauffii*, and *B. finchii*.

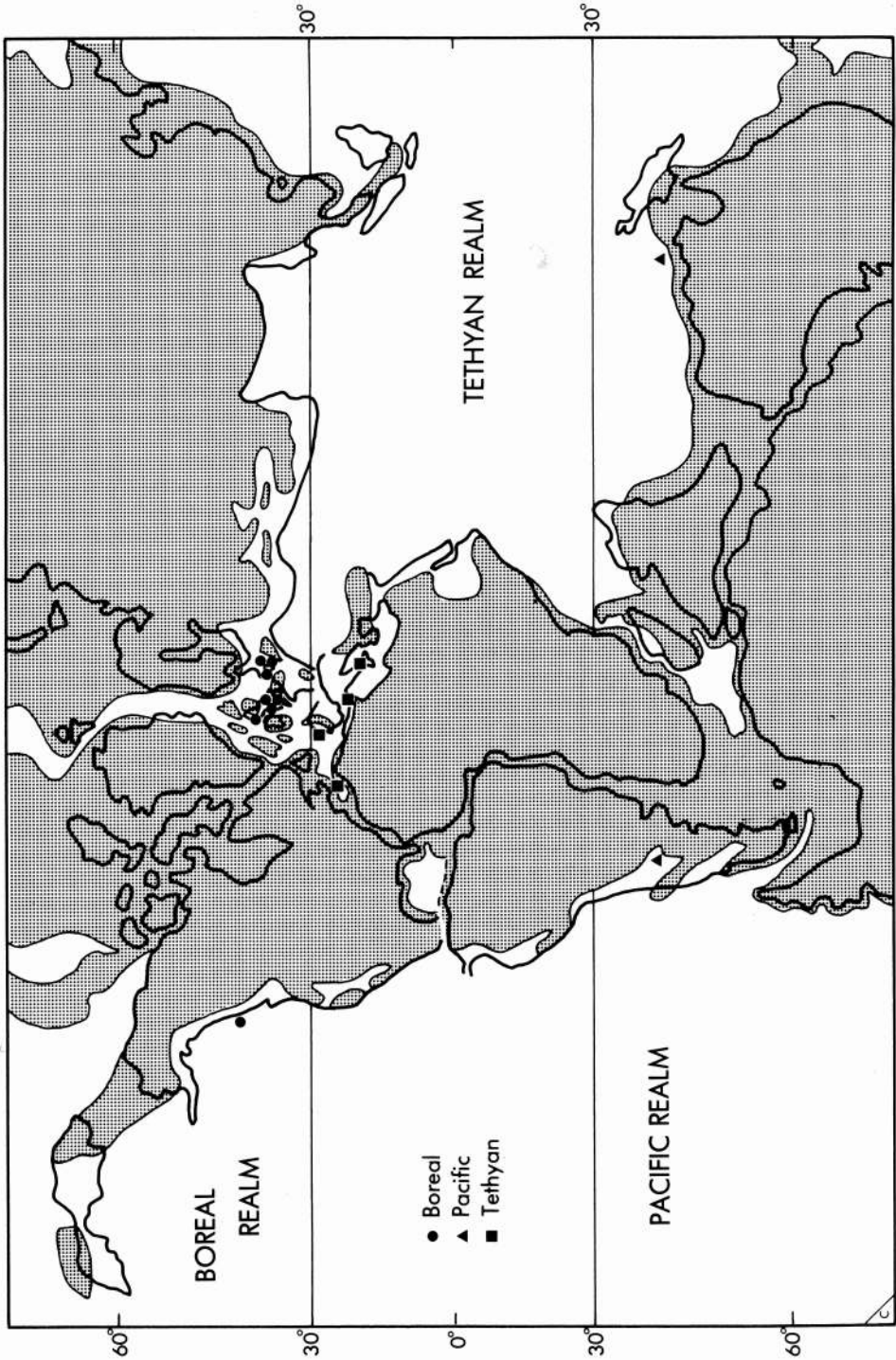
d. The presence of flourishing nannofloras in the late Triassic, including *Prinsiosphaera triassica*, *Conusphaera zlambachensis*, *Crucirhabdus minutus*, *C. primulus*, and *Archaeozygodiscus koessenensis*. Of the five species only *C. primulus* is later observed in north-west Europe.

e. The presence of smaller coccoliths, around 3 μm , which usually consist of smaller forms of known species, e.g. *C. primulus*, *Parhabdolithus liasicus*, and *Tubirhabdus patulus*.

These features allow the recognition of a discrete Tethyan Realm, with its northern boundary passing to the north of Portugal and along the northern edge of the Tethys ocean in the Mediterranean area; its southern boundary is unknown. Major distinctions present in the Timor and Argentinian assemblages, including endemic genera and species, infer a separate PACIFIC–TETHYS REALM, perhaps mirroring the northern Boreal Realm (text-fig. 19). The BOREAL REALM is recognized in north-west Europe and defined by the lack of Tethyan species and the later arrival of Tethyan forms. It is probable that the provincialism displayed by the early Jurassic nannofloras reflects a latitudinal temperature zonation, as do modern coccolithophorid assemblages. The Tethyan Realm probably represented the optimum environment for the early calcareous nannofossils and contained endemic stenothermic species, e.g. *M. jansae*. Eurythermic taxa moved north into the shallow shelf sea, often after a delay, to form the Boreal assemblages. The delay was perhaps due to the environmental changes or an absence of prevailing sea currents.

Assemblage distinctions thus clearly define discrete palaeobiogeographic regions, but many of the commonest Lower Jurassic nannofossils have a cosmopolitan distribution and were apparently successful throughout the marine environment. In addition to the provinces outlined above a number of anomalies exist which are at present difficult to explain.

1. Goy *et al.* (1979) and Goy (1981) illustrated a remarkably abundant and diverse nannofossil assemblage from the 'Schistes Carton' (Lower Toarcian) of the Paris Basin. The study included forty-two species of which twenty-one were previously undescribed. The diversity and superb preservation contrasts with records from adjacent basins. Many of the species present are not usually recorded until later in the Toarcian or the Middle Jurassic, e.g. *Diductius constans*, *Stradnerlithus comptus*, and *Diadorhombus* sp. While it is possible that the basin represented an isolated locus of evolutionary activity, there appears to be no conceivable mechanism for isolating the area so completely from, for example, the British and German Basins. More likely is the explanation that the assemblages represent the product of an exceptional preservation which is rare or unknown in most Lower Jurassic rocks due to their diagenetic history. The combined action of ideal (restricted) environmental, sedimentological, and diagenetic conditions has resulted



TEXT-FIG. 19. Nannofloral provincialism in the early Jurassic (palaeogeography after Barron *et al.* 1981).

in preservation of perhaps the entire nannoflora, including rare and delicate forms, which are normally much less well represented or lost.

2. *Mazaganella pulla* and *M. protensa* are recorded only from Site 547 and Timor and appear to have a distribution limited to the southern edge of the Tethys ocean and with a northerly limit found in Site 547.

3. *Mitrolithus jansae*, *B. finchii*, and *B. grandis* are all recorded abundantly in Mediterranean-Tethys sections but are found rarely in north-west European sections or only in the British area, e.g. *M. jansae* and *B. grandis* were not found in the German sections and are not recorded by Goy (1981) or Grün *et al.* (1974). It is possible that these essentially Tethyan species were sporadically moved into the British area *via* warm sea currents which bypassed the German and Paris Basins. Such an ocean current may also have accounted for the better circulation recorded in the Cardigan Bay Basin at this time (i.e. late Pliensbachian/early Toarcian) compared with the Yorkshire, Paris, and German Basins which contain a contemporaneous bituminous facies.

CONCLUSIONS

The recognition of coccolith rim structure groups defining long ranging lineages leads to an improved evolutionary and taxonomic understanding of early Mesozoic calcareous nannofossils. This is particularly clear for this early period of coccolithophorid history where diversity is low and the taxa possess simple but progressively developing structures. The diverging lineages in the Lower Jurassic formed five major structural groups by the Pliensbachian and these embrace the majority of Mesozoic coccoliths. A full understanding of the structure, evolution, and classification of Lower Jurassic coccoliths is fundamental for the interpretation of all subsequent developments in the group.

The two oldest lineages, the loxolith and protolith groups (possessing discolith morphologies), continued until at least the late Cretaceous (possibly through to the present day) but were never dominant again, as they were in the Hettangian and Sinemurian. The loxolith group (= Zygodiscaceae) is represented by *Tubirhabdus* and *Crepidolithus* which have last occurrences in the Middle Jurassic and more importantly the genera *Zeughrabdotos*, *Chiastozygus*, *Staurolithites* (= *Staurorhabdus/Vekshinella/Vagallapilla*). Further Mesozoic developments include the appearance of *Rhagodiscus* and *Eiffellithus* (*Staurolithites* is thought to have given rise to *Eiffellithus* in the early Cretaceous (Perch-Nielsen 1985, p. 367)). The continuance of this lineage after the Cretaceous/Tertiary boundary extinctions appears to be quite probable as similar rim structures continued in the Palaeocene and through to the present day, e.g. Zygodiscaceae (Upper Triassic to Oligocene) and Pontosphaeraceae (Upper Cretaceous to present). The protolith group was represented after the early Jurassic by members of the Stephanolithiaceae, a morphologically diverse family which is often numerically common and continued into the late Cretaceous. Important genera include *Stradnerlithus*, *Stephanolithion*, and *Rotelapillus*. Analogous protolith rim structures are observed in the Tertiary and present day, e.g. Syracosphaeraceae (Oligocene to present), but the relationship between these and the Mesozoic forms is at present uncertain.

The tiered placolith lineage (= Mazaganellaceae) which was rare and restricted in distribution during the early Jurassic (*Mazaganella*) continued into the Middle Jurassic with *Triscutum* but remained uncommon. No post-Middle Jurassic descendants are known although a similar morphological group, the Arkhangelskiellaceae, appeared in the early Cretaceous (Aptian).

The radiating placolith lineage persisted as an evolutionarily dynamic group particularly within the Podorhabdaceae. The diverse family Retacapsaceae, which includes coccoliths with a new post-Lower Jurassic rim structure (retacapsoid), e.g. *Retacapsa*, *Polypodorhabdus*, *Cretarhabdus*, and *Cruciellipsis*, is also thought to be related to the Podorhabdaceae (Perch-Nielsen 1985, p. 383). In contrast, the genera *Discorhabdus*, *Biscutum*, and *Sollasites* continued through the Middle and Upper Jurassic and Cretaceous with little or no change. Following the terminal Cretaceous extinctions, however, *Biscutum* is generally considered to have formed an extremely important

lineage including *Prinsius-Toweius-Reticulofenestra* leading to the abundant and widespread Quaternary and Recent genera *Gephyrocapsa* and *Emiliania* (Romein 1979; Perch-Nielsen 1985, p. 501, fig. 55). *Sollasites*, similarly, is thought to have given rise to the *Cruciplacolithus-Chiasmolithus-Ericsonia* lineage in the Cenozoic (Perch-Nielsen 1985, p. 460). *Calyculus* and *Carinolithus* which possessed extreme morphological modifications of the radiating placolith structure both had last occurrences in the Middle Jurassic (Bajocian). Further developments within the radiating placolith lineage include the appearance of the important genus *Prediscosphaera* in the early Cretaceous.

The final Lower Jurassic lineage, the imbricating placolith group (= Watznaueriaceae), became numerically dominant in the early Jurassic (Pliensbachian) via *Lotharingius*. It continued to dominate assemblages throughout the remaining Mesozoic with *W. britannica* and *W. fossacincta* in the Middle Jurassic and the ubiquitous *W. barnesae* in the Cretaceous. The lineage remained relatively conservative. The genera *Cyclagelosphaera* and *Markalius* survived the Cretaceous extinctions and may have formed important Tertiary lineages including *Sphenolithus* and *Fasiculithus-Heliolithus-Discoaster* (Perch-Nielsen 1985, p. 434, fig. 5).

While most coccoliths can be integrated into an evolutionary framework there still remain many non-coccolith nannoliths which appear as isolated, often long-ranging, lineages, e.g. *Schizosphaerella punctulata* and *Orthogonoides hamiltoniae* in the Jurassic, and *Lapideacassus/Scampanella* in the Cretaceous and Palaeogene. The reoccurrence of similar nannolith morphologies is seen throughout the history of calcareous nannofossils often separated by large stratigraphic gaps, e.g. *Conusphaera zlbachensis* (Upper Triassic) and *C. mexicana* (Upper Jurassic), and *O. hamiltoniae* (Lower Jurassic) and *Imperiaster obscurus* (Eocene). The biological nature and affinities of most of these groups is at present uncertain.

Acknowledgements. I am indebted to Dr A. R. Lord (University College London) for supervision of the research and assistance in the production of this paper. Samples were kindly provided by individuals and institutions: Dr M. Urlichs (Staatliches Museum für Naturkunde, Stuttgart), Dr W. Ohmert (Geologisches Landesamt, Baden-Württemberg), Dr A. Kielbowicz (Yacimiento Petrolíferos Fiscales, Argentina), Mr B. E. B. Cameron (Geological Survey of Canada), Deep Sea Drilling Project, University College of Wales, Aberystwyth (Professor J. R. Haynes and Dr R. C. Whatley), Nederlandse Aardolie Maatschappij (Dr W. Sissingh), and the British Geological Survey (Dr B. Owens). Assistance in the field was given by Martin Pearson, Richard Thompson, and Kevin Page. Thanks to Jeremy Young, Liam Gallagher, Jackie Burnett, and Kevin Cooper for many valuable discussions, to Martin Gay for technical work, and to Janet Baker and Colin Stuart for cartographic assistance. Dr D. Noël and Dr K. Perch-Nielsen are thanked for their comments on the manuscript. The financial support of the NERC is gratefully acknowledged. Finally, I should like to thank friends, and particularly Janis and both our families, who have continually given support and encouragement.

REFERENCES

- AMEZIEUX, J. 1972. Association de nannofossiles calcaires du Jurassique d'Aquitaine et du Bassin Parisien (France). *Mém. Bur. Rech. géol. Minier.* **77**, 143-151.
- AUBRY, M. P. and DEPECHE, F. 1974. Recherches sur les Schizosphères I—Les Schizosphères de Villers-sur-Mer. *Cah. Micropaléont.* **1**, 1-15.
- BARNARD, T. and HAY, W. W. 1974. On Jurassic coccoliths: a tentative zonation of the Jurassic of southern England and north France. *Eclog. geol. Helv.* **67**, 563-585.
- BARRON, E. J., HARRISON, C. G. A., SLOAN II, J. L. and HAY, W. W. 1981. Palaeogeography, 180 million years ago to the present. *Ibid.* **74**, 443-470.
- BLACK, M. 1965. Coccoliths. *Endeavour*, **24**, 131-137.
- 1967. New names for some coccolith taxa. *Proc. geol. Soc. Lond.* **1640**, 139-145.
- 1968. Taxonomic problems in the study of coccoliths. *Palaeontology*, **11**, 793-813.
- 1971. Coccoliths of the Speeton Clay and Sutterby Marl. *Proc. York. geol. Soc.* **38**, 381-424.
- 1972, 1973, 1975. British Lower Cretaceous coccoliths 1. Gault Clay. *Palaeontogr. Soc. [Monogr.]*, **126**, 1-48 (Pt. 1); **127**, 49-112 (Pt. 2); **129**, 113-142 (Pt. 3).
- and BARNES, B. 1959. The structure of coccoliths from the English Chalk. *Geol. Mag.* **96**, 321-328.

- BOWN, P. R. 1985. *Archaeozygodiscus*—a new Triassic coccolith genus. *INA. Newsl.* **7**, 32–35.
- 1987. The structural development of Early Mesozoic coccoliths and its evolutionary and taxonomic significance. *Abh. geol. Bundesanst.* **39**, 33–49.
- BUKRY, D. 1969. Upper Cretaceous coccoliths from Texas and Europe. *Paleont. Contr. Univ. Kans.* Article **51** (Protista 2), 79 pp.
- CRUX, J. A. 1984. Biostratigraphy of early Jurassic calcareous nannofossils from southwest Germany. *Neues Jb. Geol. Paläont. Abh.* **169** (2), 160–186.
- 1985. *Crepidolithus pliensbachensis nomen novum pro Crepidolithus ocellatus* Crux 1984 non (Bramlette and Sullivan) Noel 1965. *INA Newsl.* **7**, 31.
- 1987. Concerning the dimorphism in early Jurassic coccoliths and the origins of the genus *Discorhabdus* Noel, 1965. *Abh. geol. Bundesanst.* **39**, 51–55.
- DEFLANDRE, G. 1952. Classe de coccolithophoridés. In GRASSÉ, P. P. (ed.). *Traité de Zoologie*, **1**, 439–470.
- 1954. In DEFLANDRE, G. and FERT, C. 1954. Observations sur les coccolithophoridés actuels et fossiles en microscopie ordinaire et électronique. *Annl. Paléont.* **40**, 115–176.
- and DANGEARD, L. 1938. *Schizosphaerella*, un nouveau microfossile méconnu du Jurassique moyen et supérieur. *C. r. Hebd. Séanc. Acad. Sci. Paris*, **207**, 1115–1117.
- DOCKERILL, H. J. 1987. *Triscutum*. A distinctive new coccolith genus from the Jurassic. *Bull. Centres Rech. Explor.-Prod. Elf-Aquitaine*, **11**, 127–131.
- FISCHER, A. G., HONJO, S. and GARRISON, R. E. 1967. *Electron micrographs of limestones and their nannofossils*, 141 pp. Princeton University Press, Princeton.
- GARTNER, S. 1968. Coccoliths and related calcareous nannofossils from Upper Cretaceous deposits of Texas and Arkansas. *Paleont. Contr. Univ. Kans.* **48**, 56 pp.
- 1977. Nannofossils and biostratigraphy: an overview. *Earth Sci. Rev.* **13**, 227–250.
- and KEANY, J. 1979. The coccolith successionism across the Cretaceous/Tertiary boundary in the subsurface of the North Sea (Ekofisk). In CHRISTENSEN, W. K. (ed.). *Cretaceous-Tertiary boundary events symposium*, 103. Copenhagen University Press, Copenhagen.
- GÓRKA, H. 1957. Les coccolithophoridés du Maestrichtien supérieur de Pologne. *Acta Palaeont. pol.* **2**, 235–284.
- GOY, G. 1979. In GOY, G., NOËL, D. and BUSSON, G. Les conditions de sédimentation des schistes-carton (Toarcien inf.) du bassin de Paris déduites de l'étude des nannofossiles calcaires et des diagraphies. *Docums Lab. Géol. Fac. Sci. Lyon*, **75**, 33–57.
- 1981. Nannofossiles calcaires des schistes carton (Toarcien inférieur) du bassin de Paris. *Docums de la RCP*, 459, éditions BRGM, 1–86.
- GRÜN, W. and ALLEMAN, F. 1975. The Lower Cretaceous of Caravaca (Spain): Berriasian calcareous nannoplankton of the Miravetes section (Subbetic Zone, Prov. of Murcia). *Eclog. geol. Helv.* **68**, 147–211.
- PRINS, B. and ZWEILI, F. 1974. Coccolithophoriden aus dem Lias epsilon von Holzmaden (Deutschland). *Neues Jb. Geol. Paläont. Abh.* **147**, 294–328.
- and ZWEILI, F. 1980. Das kalkige Nannoplankton der Dogger-Malm-Grenz im Berner Jura bei Liesberg (Schweiz). *Jb. geol. Bundesanst. Wien*, **123**, 231–341.
- HAMILTON, G. B. 1977. Early Jurassic calcareous nannofossils from Portugal and their biostratigraphic use. *Eclog. geol. Helv.* **70**, 575–597.
- 1979. Lower and Middle Jurassic calcareous nannofossils from Portugal. *Ibid.* **72**, 1–17.
- 1982. Triassic and Jurassic calcareous nannofossils. In LORD, A. R. (ed.). *A stratigraphic index of calcareous nannofossils*, 136–137. British Micropalaeontological Society, Ellis Horwood, Chichester.
- HAQ, B. U. 1983. Nannofossil biostratigraphy. *Benchmark papers in Geology*, **78**, 386 pp. Hutchinson and Ross, Pennsylvania.
- HAY, W. W. 1977. Calcareous nannofossils. In RAMSAY, A. T. S. (ed.). *Oceanic micropalaeontology*, **2**, 1055–1200. Academic Press, London.
- and MOHLER, H. P. 1967. Calcareous nannoplankton from early Tertiary rocks at Pont Labau, France, and Paleocene-early Eocene correlations. *J. Paleont.* **41**, 1505–1541.
- and WADE, M. E. 1966. Calcareous nannofossils from Nal'chic (northwest Caucasus). *Eclog. geol. Helv.* **59**, 379–399.
- HIBBERD, D. J. 1976. The ultrastructure and taxonomy of the Chrysophyceae and Prymnesiophyceae (Haptophyceae): a survey with some new observations on the ultrastructure of the Chrysophyceae. *Bot. J. Linn. Soc.* **72**, 55–80.
- 1980. Prymnesiophytes (= Haptophytes). In COX, E. R. (ed.). *Phytoflagellates. Developments in Marine Biology*, **2**, 273–313.

- HOFFMAN, N. 1970. Coccolithineen aus der weissen Schreikreide (Unter Maastricht) von Jasmund auf Rugen. *Geologie*, **19**, 846-879.
- JAFAR, S. A. 1979. Taxonomy, stratigraphy and affinities of calcareous nannoplankton genus *Thoracosphaera* Kamptner. *4th Int. Palynol. Conf., Lucknow*, **2**, 1-21.
- 1983. Significance of the Late Triassic calcareous nannoplankton from Austria and southern Germany. *Neues Jb. Geol. Paläont. Abh.* **166**, 218-259.
- KÄLIN, O. 1980. *Schizosphaerella punctulata* Deflandre and Dangeard: wall ultrastructure and preservation in deep-water carbonate sediments of the Tethyan Jurassic. *Eclog. geol. Helv.* **73**, 983-1008.
- and BERNOULLI, D. 1984. *Schizosphaerella* Deflandre and Dangeard in Jurassic deep water carbonate sediments, Mazagan continental margin (Hole 547B) and Mesozoic Tethys. *Init. Repts. Deep Sea Drilling Project*, **79**, 411-435.
- KAMPTNER, E. 1927. Beitrag zur Kenntnis adriatischer Coccolithophoriden. *Arch. Protistenk.* **58**, 173-184.
- LORD, A. R. 1982. *A stratigraphic index of calcareous nannofossils*, 192 pp. British Micropalaeontological Society, Ellis and Horewood, Chichester.
- MEDD, A. W. 1971. Some Middle and Upper Jurassic Coccolithophoridae from England and France. *Proc. II Planktonic Conf., Roma 1970*, **2**, 821-844.
- 1979. The Upper Jurassic coccoliths from the Haddenham and Gamlingay boreholes (Cambridgeshire, England). *Eclog. geol. Helv.* **72**, 19-109.
- 1982. Nannofossil zonation of the English Middle and Upper Jurassic. *Mar. Micropalaeont.* **7**, 73-95.
- MOSHKOVITZ, S. 1979. On the distribution of *Schizosphaerella punctulata* Deflandre and Dangeard and *Schizosphaerella astraea* n. sp. in the Liassic section of Stowell Park Borehole (Gloucestershire) and in some other Jurassic localities in England. *Eclog. geol. Helv.* **72**, 455-465.
- 1982. On the findings of a new calcareous nannofossil (*Conusphaera zambachensis*) and other calcareous organisms in the Upper Triassic sediments of Austria. *Ibid.* **75**, 611-619.
- and EHRLICH, A. 1976a. Distribution of Middle and Upper Jurassic calcareous nannofossils in the northeastern Negev, Israel and in Gebel Maghara, northern Sinai. *Bull. geol. Surv. Israel*, **69**, 1-47.
- 1976b. *Schizosphaerella punctulata* Deflandre and Dangeard and *Crepidolithus crassus* (Deflandre) Noel, Upper Liassic calcareous nannofossils from Israel and Northern Sinai. *Israel J. Earth Sci.* **25**, 51-57.
- NICOSIA, U. and PALLINI, G. 1977. Ammonites and calcareous nannoplankton of the Toarcian 'Rosso Ammonitico' in the exposures of the M. la Pelosa (Terni central Appennines, Italy). *Geologica romana*, **16**, 263-283.
- NOËL, D. 1965. *Sur les coccolithes du Jurassique européen et d'Afrique du Nord. Essai de classification des coccolithes fossiles*, 209 pp. Editions du CNRS, Paris.
- 1973. Nannofossiles calcaire de sédiments jurassiques finement laminés. *Bull. Mus. natn. Hist. nat. Paris, sér 3*, **75** (*Sciences de la Terre 14*), 95-156.
- OUTKA, D. E. and WILLIAMS, D. C. 1971. Sequential coccolith morphogenesis in *Hymenomonas carterae*. *J. Protozool.* **18**, 285-297.
- PERCH-NIELSEN, K. 1968. Der Feinbau und die Klassifikation der Coccolithen aus dem Maastrichtien von Dänemark. *K. danske Vidensk. Selsk. Biol. Skr.* **16**, 1-96.
- 1985. Mesozoic Calcareous Nannofossils. In BOLLI, H. M., SAUNDERS, J. B. and PERCH-NIELSEN, K. (eds.). *Plankton Stratigraphy*, 1031 pp. Cambridge University Press, Cambridge.
- POSCH, F. and STRADNER, H. 1987. Report on Triassic nannoliths from Austria. *Abh. geol. Bundesanst.* **39**, 231-237.
- PRINS, B. 1969. Evolution and stratigraphy of coccolithinids from the Lower and Middle Lias. *Proc. I Int. Conf. Planktonic Microfossils, Geneva*, **2**, 547-558.
- REINHARDT, P. 1965. Neue Familien für fossile Kalkflagellaten (Coccolithophoriden, Coccolithineen). *Mber. dt. Akad. Wiss. Berl.* **7**, 30-40.
- 1966. Zur Taxonomie und Biostratographie des fossilen Nannoplanktons aus dem Malm, der Kreide und dem Altetäer Mitteleuropas. *Freiburger Forschungshefte, C196, Paläont.* 5-109. Leipzig.
- ROMEIN, A. J. T. 1979. Evolutionary lineages in early Paleogene calcareous nannoplankton. *Utrecht Micropaleont. Bull.* **22**, 1-231.
- ROOD, A. P. and BARNARD, T. 1972. On Jurassic coccoliths: *Stephanolithion*, *Diadozygus* and related genera. *Eclog. geol. Helv.* **65**, 327-342.
- HAY, W. W. and BARNARD, T. 1971. Electron microscope studies of Oxford Clay coccoliths. *Ibid.* **64**, 245-272.

- ROOD, A. P., HAY, W. W. and BARNARD, T. 1973. Electron microscope studies of Lower and Middle Jurassic coccoliths. *Ibid.* **66**, 365–382.
- STRADNER, H. 1961. Vorkommen von Nannofossilien im Mesozoikum und Alttertiar. *Erdöl-Z. Bohr- u. Fördertech.* **77**, 77–88.
- 1963. New contributions to Mesozoic stratigraphy by means of nannofossils. *Proc. 6th World Petrol. Congr., Section 1, Paper 4 (preprint)*, 167–184.
- SYKES, C. S. and WILBUR, K. M. 1982. Function of coccoliths. *Limnol. Oceanogr.* **27** (1), 18–26.
- TAPPAN, H. 1980. *The paleobiology of plant protists*, xxi + 1028 pp. W. H. Freeman, San Francisco.
- THIERSTEIN, H. R. 1976. Mesozoic calcareous nannoplankton biostratigraphy of marine sediments. *Mar. Micropaleont.* **1**, 325–362.
- TREJO, M. 1969. *Conusphaera mexicana*, un nuevo coccolitoforido del Jurassico Superior de Mexico. *Revista Inst. Mexicana Petrol.* **1**, 5–15.
- VAN HINTE, J. E. 1976. A Jurassic time scale. *Bull. Am. Ass. Petrol. Geol.* **60**, 489–497.
- VERBEEK, J. W. 1977. Calcareous nannoplankton biostratigraphy of Middle and Upper Cretaceous deposits in Tunisia, southern Spain and France. *Utrecht Micropaleont. Bull.* **16**, 1–157.
- WIEDMANN, J., FABRICIUS, F., KRYSZYN, L., REITNER, J. and URLICHS, M. 1979. Über und Umfang Stellung des Rhaet. *Newsl. Stratig.* **8**, 133–152.
- WIEGAND, G. E. 1984a. Two genera of calcareous nannofossils from the Lower Jurassic. *J. Paleont.* **58** (4), 1151–1155.
- 1984b. Jurassic nannofossils from the northwest African margin, DSDP Leg 79. *Init. Reps. Deep Sea Drilling Project*, **79**, 657–670.
- WISE, S. W. and WIND, F. H. 1976. Mesozoic and Cenozoic calcareous nannofossils recovered by DSDP Leg 36 drilling on the Falkland Plateau, Southwest Atlantic sector of the Southern Ocean. *Ibid.* **36**, 269–492.
- YOUNG, J. R., TEALE, C. T. and BOWN, P. R. 1986. Revision of the stratigraphy of the Longobucco Group (Liassic, southern Italy); based on new data from nannofossils and ammonites. *Eclog. geol. Helv.* **79**, 117–135.

PAUL R. BOWN

Postgraduate Unit of Micropalaeontology
Department of Geological Sciences
University College London
Gower Street
London WC1E 6BT

Typescript received 1 April 1987

Revised typescript received 15 June 1987

APPENDIX: CLASSIFICATION AND SPECIES INDEX

- Division PRYMNESIOPHYTA Hibberd, 1976
 Class PRYMNESIOPHYCEAE Hibberd, 1976
 Order EIFFELLITHALES Rood, Hay and Barnard, 1971
 Family ZYGODISACEAE Hay and Mohler, 1967
 Genus *Archaeozygodiscus* Bown, 1985
A. koessenensis Bown, 1985 13
 Genus *Crepidolithus* Noël, 1965
C. cavus Rood, Hay and Barnard, 1973 13
C. crassus (Deflandre 1954) Noël, 1965 16
C. granulatus sp. nov. 17
C. plienschachensis Crux, 1985 emend. 17
 Genus *Tubirhabdus* Prins ex Rood et al., 1973
T. patulus Prins ex Rood, Hay and Barnard, 1973 18
 Genus *Zeughrabdus* Reinhardt, 1965
Z. erectus (Deflandre, 1954) Reinhardt, 1965 20
- Family PARHABDOLITHACEAE BOWN, 1987
 Genus *Bucanthus* gen. nov.
B. decussatus sp. nov. 35
 Genus *Crucirhabdus* Prins ex Rood et al., 1973 emend.
C. minutus Jafar, 1983 22
C. primulus Prins ex Rood et al., 1973 emend. 23
 Genus *Diductius* Goy, 1979
D. constans Goy, 1979 26
 Genus *Mitrolithus* (Deflandre 1954) Bown and Young, 1986
M. elegans Deflandre, 1954 26
M. jansae (Wiegand, 1984) Bown and Young, 1986 27
M. lenticularis sp. nov. 28
 Genus *Parhabdolithus* Deflandre, 1952
P. liasicus Deflandre, 1952 30
P. l. distinctus ssp. nov. 30
P. l. liasicus ssp. nov. 31
P. marthae Deflandre, 1954 32
P. robustus Noël, 1965 34
 Genus *Timorella* gen. nov.
T. cypella sp. nov. 35
- Family STEPHANOLITHACEAE Black, 1968
 Genus *Stradnerlithus* Black, 1971
S. clatriatus (Rood et al., 1973) Goy, 1979 36
- Order PODORHABDALES Rood, Hay and Barnard, 1971
 Family BISCUTACEAE Black, 1971 emend.
 Subfamily BISCUTOIDEAE Hoffman, 1970
 Genus *Biscutum* Black in Black and Barnes 1959
B. depravatus (Grün and Zweili, 1980) comb. nov. 46
B. dubium (Noël 1965) Grün in Grün et al., 1974 45
B. finchii Crux, 1984 42
B. grandis sp. nov. 44
B. intermedium sp. nov. 47
B. novum (Goy, 1979) Bown, 1987 41
B. planum sp. nov. 45
 Genus *Discorhabdus* Noël, 1965
D. criotus sp. nov. 49
D. ignotus (Górka, 1957) Perch-Nielsen, 1968 48
 Subfamily SOLLASITEOIDEAE Rood et al., 1971 emend.
 Genus *Sollasites* Black, 1967
S. arctus (Noël, 1973) comb. nov. 52
S. lowei (Bukry, 1969) Rood et al., 1971 53
- Family CALYCVLACEAE Noël, 1973
 Genus *Calyculus* Noël, 1973
Calyculus sp. indet. 54
C. cribrum Noël, 1973 emend. Goy, 1979 54
C. depressus sp. nov. 55
 Genus *Carinolithus* Prins in Grün et al. 1974 emend.
C. magharensis (Moshkovitz and Ehrlich, 1976) comb. nov. 58
C. superbus (Deflandre, 1954) Prins in Grün et al. 1974 56
- Family PODORHABDACEAE Noël, 1965
 Subfamily PODORHABDOIDEAE Reinhardt, 1967
 Genus *Axopodorhabdus* Wind and Wise in Wise and Wind 1976
A. atavus (Grün, Prins and Zweili, 1974) comb. nov. 60
 Genus *Ethmorhabdus* Noël, 1965
E. gallicus Noël, 1965 61
- Family MAZAGANELLACEAE fam. nov.
 Genus *Mazaganella* gen. nov.
M. protensa sp. nov. 39
M. pulla sp. nov. 38
 Genus *Triscutum* Dockerill, 1987
Triscutum sp. 1 40
Triscutum sp. 2 40
- Order WATZNAUERIALES ordo nov.
 Family WATZNAUERiaceae Rood et al., 1971 emend.
 Genus *Bussonius* Goy, 1979
B. leufuensis sp. nov. 71
B. prinsii (Noël 1973) Goy, 1979 70
 Genus *Lotharingius* Noël, 1973 emend. Goy, 1979
L. barozii Noël, 1973 70
L. hauffii Grün and Zweili in Grün et al. 1974 68
L. imprimus sp. nov. 63
L. primigenius sp. nov. 63
L. sigillatus (Stradner, 1961) Prins in Grün et al. 1974 64
- INCERTAE SEDIS
 Genus *Conusphaera* Trejo, 1969
C. zlabachensis Moshkovitz, 1982 72
 Genus *Orthogonoides* Wiegand, 1984
O. hamiltoniae Wiegand, 1984 74
- Division PYRROPHYTA
 Class DINOPHYCEAE
 Order THORACOSPHAERALES Tangen et al., 1982
 Family SCHIZOSPHAERELLACEAE Deflandre, 1959
 Genus *Prinsiosphaera* Jafar, 1983
P. triassica Jafar, 1983 82
 Genus *Schizosphaerella* Deflandre and Dangeard, 1938
S. punctulota Deflandre and Dangeard, 1938 76
- Family THORACOSPHAERACEAE Schiller, 1930
 Genus *Thoracosphaera* Kamptner, 1927
T. geometrica (Jafar, 1983) comb. nov. 82